AD-A081 962   WYLE LABS EL SEGUNDO CALIF   F/G 20/1
CORRECTION PROCEDURES FOR AIRCRAFT NOISE DATA. VOLUME I. PSEUDO--ETC(U)
DEC 79 R RACKL   DOT-FA78WA-4143
UNCLASSIFIED WR-79-9-VOL-1   FAA/EE-80-1-VOL-1   NL

1 OF 3
AD
A081 962

1.0 1.1 1.25 1.4 1.6 1.8 2.0 2.2 2.5 2.8 3.2 3.6 4.0

MICROCOPY RESOLUTION TEST CHART

NATIONAL BUREAU OF STANDARDS-1963-A

Report No.FAA-EE-80-1, Vol. I

13

ADA081962

CORRECTION PROCEDURES FOR AIRCRAFT NOISE DATA VOLUME I: PSEUDOTONES

WYLE RESEARCH
El Segundo, California

R. Rackl

December 1979

FINAL REPORT

Document is available to the U.S. public through
The National Technical Information Service,
Springfield, Virginia 22161

Prepared for

U.S. DEPARTMENT OF TRANSPORTATION
FEDERAL AVIATION ADMINISTRATION
Office of Environment and Energy
Washington, D.C. 20591

80 3 17 235

NOTICE

Technical Report Documentation Page

1. Report No. FAA-EE-80-1, Vol. I	2. Government Accession No.	3. Recipient's Catalog No.

4. Title and Subtitle
(6) Correction Procedures for Aircraft Noise Data
Volume I. Pseudotones

5. Report Date
(11) Dec[redacted]79

6. Performing Organization Code

7. Author(s)
(10) R. Rackl 12) 221

8. Performing Organization Report No.
(14) WR79-9-VOL-1

9. Performing Organization Name and Address
Wyle Research
El Segundo, California 90245

10. Work Unit No. (TRAIS)

11. Contract or Grant No.
(15) DOT-FA78WA-4143

12. Sponsoring Agency Name and Address
Federal Aviation Administration
Office of Environment and Energy
800 Independence Avenue, SW.
Washington, D.C. 20591

13. Type of Report and Period Covered
(9) Final Report

14. Sponsoring Agency Code
AEE-110

15. Supplementary Notes

16. Abstract

Pseudotones are spectral irregularities due to ground reflections which can cause tone corrections in the calculation of Effective Perceived Noise Level which are not generated by the aircraft itself. Several analytical (reflection theory, lower cutoff frequency for tone corrections) and instrumentation (ground and pole microphones) methods were investigated which remove the pseudotones. In support of this study, a substantial number of aircraft noise measurements were obtained and analyzed in detail; these data are also summarized in the report.

18) FAA/EE 19) 80-1-VOL-1

17. Key Words
Aircraft Noise; Noise Certification; Correction Procedures; Pseudotones

18. Distribution Statement
Document is available to the public through the National Technical Information Service, Springfield, Virginia 22161.

19. Security Classif. (of this report)	20. Security Classif. (of this page)	21. No. of Pages	22. Price
Unclassified	Unclassified	208	

Form DOT F 1700.7 (8-72) Reproduction of completed page authorized 382150

METRIC CONVERSION FACTORS

Approximate Conversions to Metric Measures

Symbol	When You Know	Multiply by	To Find	Symbol
		LENGTH		
in	inches	*2.5	centimeters	cm
ft	feet	30	centimeters	cm
yd	yards	0.9	meters	m
mi	miles	1.6	kilometers	km
		AREA		
in^2	square inches	6.5	square centimeters	cm^2
ft^2	square feet	0.09	square meters	m^2
yd^2	square yards	0.8	square meters	m^2
mi^2	square miles	2.6	square kilometers	km^2
	acres	0.4	hectares	ha
		MASS (weight)		
oz	ounces	28	grams	g
lb	pounds	0.45	kilograms	kg
	short tons (2000 lb)	0.9	tonnes	t
		VOLUME		
tsp	teaspoons	5	milliliters	ml
Tbsp	tablespoons	15	milliliters	ml
fl oz	fluid ounces	30	milliliters	ml
c	cups	0.24	liters	l
pt	pints	0.47	liters	l
qt	quarts	0.95	liters	l
gal	gallons	3.8	liters	l
ft^3	cubic feet	0.03	cubic meters	m^3
yd^3	cubic yards	0.76	cubic meters	m^3
		TEMPERATURE (exact)		
°F	Fahrenheit temperature	5/9 (after subtracting 32)	Celsius temperature	°C

*1 in ≡ 2.54 (exactly). For other exact conversions and more detailed tables, see NBS Misc. Publ. 286, Units of Weights and Measures, Price $2.25, SD Catalog No. C13.10:286.

Approximate Conversions from Metric Measures

Symbol	When You Know	Multiply by	To Find	Symbol
		LENGTH		
mm	millimeters	0.04	inches	in
cm	centimeters	0.4	inches	in
m	meters	3.3	feet	ft
m	meters	1.1	yards	yd
km	kilometers	0.6	miles	mi
		AREA		
cm^2	square centimeters	0.16	square inches	in^2
m^2	square meters	1.2	square yards	yd^2
km^2	square kilometers	0.4	square miles	mi^2
ha	hectares (10,000 m^2)	2.5	acres	
		MASS (weight)		
g	grams	0.035	ounces	oz
kg	kilograms	2.2	pounds	lb
t	tonnes (1000 kg)	1.1	short tons	
		VOLUME		
ml	milliliters	0.03	fluid ounces	fl oz
l	liters	2.1	pints	pt
l	liters	1.06	quarts	qt
l	liters	0.26	gallons	gal
m^3	cubic meters	35	cubic feet	ft^3
m^3	cubic meters	1.3	cubic yards	yd^3
		TEMPERATURE (exact)		
°C	Celsius temperature	9/5 (then add 32)	Fahrenheit temperature	°F

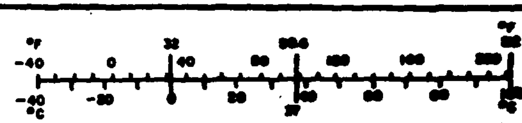

FOREWORD

This report examines several analytical and instrumentation methods for eliminating the interferences caused by reflection of sound waves from the ground surface during FAR Part 36 aircraft noise certification measurements.

The author acknowledges the significant contributions made by C. Bartel for investigating the aircraft position accuracy problem, D. Hoy for researching surface impedance data and programming several key computer modules, R. Helizon and A. Segal for aircraft noise data acquisition at Los Angeles International Airport, L. Sutherland for technical guidance, and J. Parkinson for overall program management.

This work constitutes Technical Areas 1 and 5 under Contract DOT-FA78WA-4143.

TABLE OF CONTENTS

LIST OF TABLES

LIST OF FIGURES

LIST OF FIGURES (Continued)

0. INTRODUCTION

Administration of the rules embodied in FAR Part 36 - Noise Standards: Aircraft Type and Airworthiness Certification, has involved: (1) adherence to specific procedures contained in Appendices to the regulation, and (2) application of administrative processes to approve or define those test procedures not specifically called out in the regulation. It is this latter aspect of administering FAR Part 36 that this report addresses. FAA staff in Washington, and in regional offices, have developed many general and specific guidelines not codified within existing Federal Aviation Regulations. However, the guidelines for noise certification, such as those provided in the handbook on certification procedures published by the FAA Western Regional Office[1] do not include explicit details on a number of procedures such as the following:

- o Methods for correcting measured noise spectra for ground reflection effects
- o Methods for correcting measured levels when ambient noise levels are excessive
- o Methods for correcting propeller aircraft noise data for deviations in aircraft performance from reference conditions

While informal rules have generally been established by the FAA out of necessity for each of these correction procedures, they have not yet been fully documented or validated.

The objective of this document, Volume I of a multiple volume set on correction procedures, is to provide the technical background required to allow FAA to codify ground reflection correction procedures in future revisions to either administrative guidelines handbooks or to FAR Part 36 itself. In the latter case, statements in the existing regulations allowing "approved procedures" or "approved corrections" could be replaced with explicit details.

FAR Part 36 data correction procedures can be categorized into two general classes:

- o Procedures that correct for nonstandard test conditions (e.g., correction for sound attenuation at nonstandard temperature and humidity) or aircraft performance.
- o Procedures that compensate for limitations of the measurement and sound description methods (e.g., correction for aircraft sound levels masked by ambient noise or reflections off the ground).

Corrections for nonstandard performance of propeller aircraft fall in the first category and corrections for ground reflection or ambient noise levels fall in the second class. Table 0-1 identifies the major types of data corrections that are explicitly specified in FAR Part 36. Table 0-2 identifies these data and procedures which are not completely specified and which require FAA approval.

Applicable paragraphs identified as "A," "B," or "C" in Tables 0-1 and 0-2 refer to large subsonic transport airplanes and all turbojet powered aircraft regardless of category. Paragraphs identified as "F" refer to light propeller driven aircraft (A, B, C, and F are Appendices within FAR Part 36). Paragraphs identified with an (*) are associated with the technical correction procedures of this series of volumes. This volume 1 addresses only the pseudotone (ground reflection) problem. At the time of writing, other volumes concerning ambient noise, propeller aircraft performance, and appropriateness of tone correction were either in preparation or being contemplated.

The significant features of this volume are as follows:

- o Analytical methods of pseudotone removal are not practical at this time.
- o The 10 m (pole) microphone position is recommended for certification measurements. This is expected to effectively eliminate pseudotones at takeoff and approach locations without any further correction. However, the 800 Hz low frequency cutoff for tone corrections should be retained for the sideline position only.
- o A substantial number of aircraft flyover noise measurements were obtained in support of this study. These are summarized in this volume.

Table 0-1

Data Corrections Necessary as Part of FAR 36 Certification

	Problem	Acoustical Parameters Needing Adjustment	Applicable Paragraph
Problems Related to Nonstandard Test Conditions	Aircraft Not Flying on Prescribed Flight Track	Propagation Distance	A36.11 F36.111
		Signal Duration	A36.11
	Temperature, Humidity, or Atmospheric Pressure Not at Standard Conditions	Amount of Atmospheric Sound Absorption	A36.5 F36.201(*) A36.9 F36.101
	Engine(s) Not at Prescribed Power Settings	Acoustic Source Noise Level	A36.1 F36.111(*)
	Aircraft Not at Reference Weight	Measured EPNL	A36.1
	Runway Slope $\neq 0$	Noise and Performance	C36.7(3)
	Propeller Aircraft Takeoff Profile	Measured L_A (max)	F36.201(b)
Problems Related to Measurement Limitations	Pseudotones Present in Noise Spectrum	Measured Acoustic Spectrum of Source	A36.1(b), A36.3(f) B36.5(*), F36.107, F36.101
	Ambient Noise Masking Aircraft Noise Levels	Measured Acoustic Noise Level	F36.107(*) A36.5(3) (*)
	Noise Measuring Equipment	Measured Acoustic Noise Level	A36.3(*)

(*) Subject of this document.

Table 0-2

Data or Procedures Requiring FAA Approval
Currently Specified in FAR Part 36 (Change 7)

Category	Data or Procedure	Applicable Paragraph
Aircraft Performance	Aircraft Position Measurement	A36.1(d) A36.11 F36.109(f) (6)
	Sample Rate for Aircraft Performance Data	A36.1(d) (1) A36.3(b) F36.109(g)
	Aircraft Reference Flight Profile, Speed, or Power Setting	A36.11 C36.7(f) C36.9(f) (1) F36.111(b) (1)
	Aircraft Performance Measurement Instrumentation	A36.5 F36.101(b) (6)
Aircraft Noise	Corrections for Non-standard Weight	A36.1 (7)
	Corrections for Non-standard Flight Profile Speed or Power Setting	A36.11
	Noise Measurement Equipment	A36.3 F36.103 F36.105
	Ambient Noise Corrections	A36.5 F36.107(c)
	Overall Data Corrections Procedures	A36.3 A36.5 F36.109(a) F36.203
Atmospheric Parameters	Measurement Facility	A36.3 A36.5

1. GROUND REFLECTION AND PSEUDOTONES

1.1 Nature of Ground Reflection Phenomenon

Technical Area I of this document is concerned with the influence of sound reflection from the ground surface on measured aircraft noise spectra and resulting EPNL values. The word "pseudotone" has become common to describe the spectral irregularities caused by the ground reflections in the lower frequency portion of the spectrum (generally below 1 kHz).

The measurement setup required by FAR Part 36 is sketched in Figure 1-1. In addition to the direct wave from the aircraft to the microphone, the indirect wave reflected from the ground surface is also sensed by the microphone. Direct and reflected waves instantaneously add which leads to an interference pattern, i.e., a succession of constructive and destructive interferences. The nature of this pattern depends on the geometrical relations, the ground surface, and the sound frequencies. Figure 1-2 shows an example of an interference pattern in the form of a theoretical correction chart for the case of source and receiver at the same height over an infinite impedance ground surface. The dB correction is subtracted from a measured spectrum in order to obtain the spectrum that would have been measured under free field conditions. Although this is not typical for a flyover application, the figure shows several features of general interest. At the lower frequency end, the correction approaches 6 dB which corresponds to the well-known doubling of acoustic pressure near a perfectly reflecting surface. At the upper frequency end, the correction for discrete tones consists of very many closely spaced lobes. This is not representative, however, since spectrum analysis of aircraft noise is performed with finite bandwidth filters. The wider the filter bandwidth, the faster the correction will tend towards the stable limit of 3 dB corresponding simply to the energy summation of two uncorrelated signals of equal strength. For the discrete frequency curve, destructive interference leads to an infinitely large dip for a pure tone. For a finite bandwidth of noise, such an infinitely large dip cannot occur; the wider the bandwidth, the less pronounced this dip.

An example of pseudotones observed during a real flyover is shown in Figure 1-3.[2] A series of spectra at regular time intervals are shown. The theory

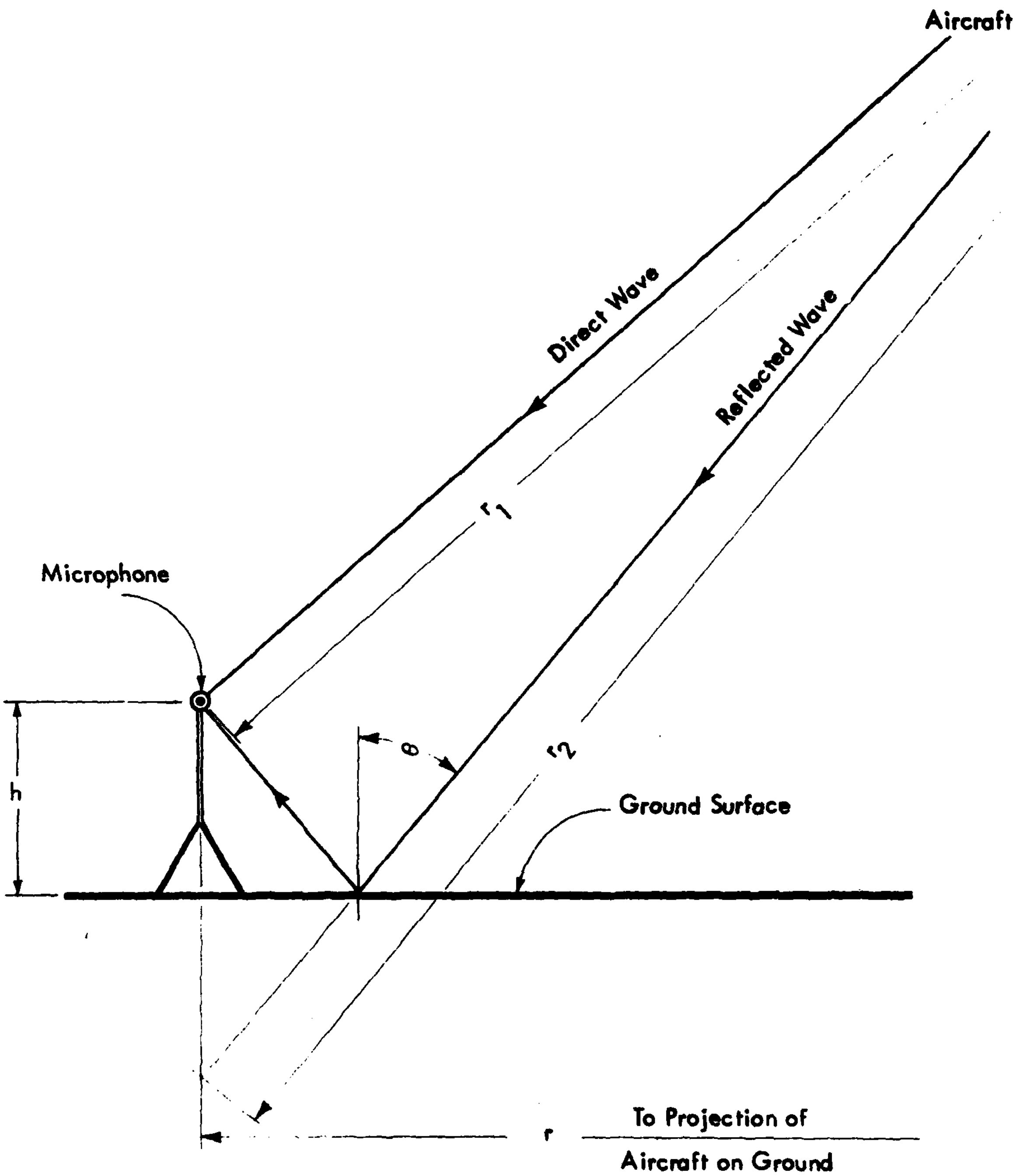

Figure 1-1. Reflection Geometry

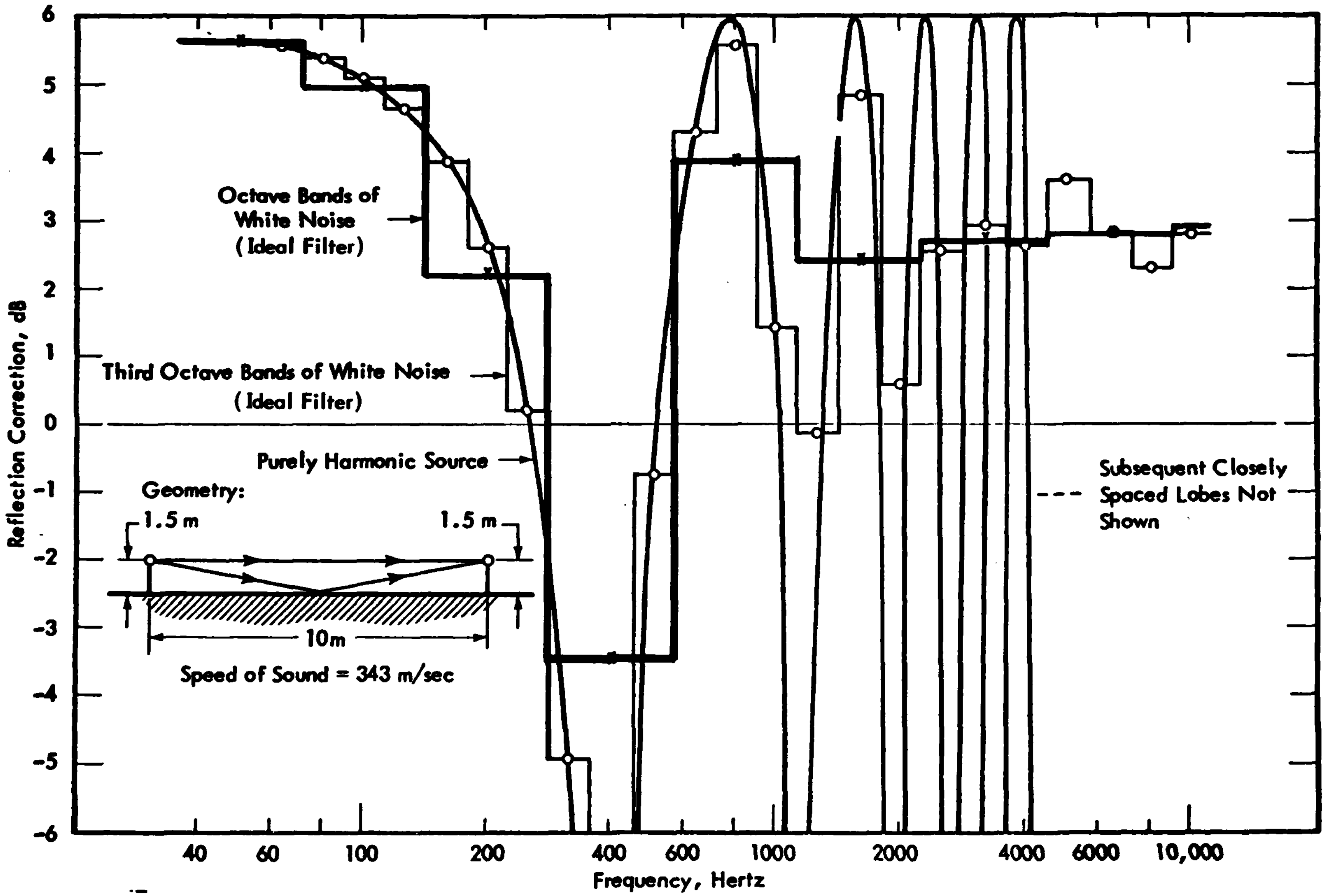

Figure 1-2. Example of a Reflection Correction: Point Source, Infinite Impedance Boundary

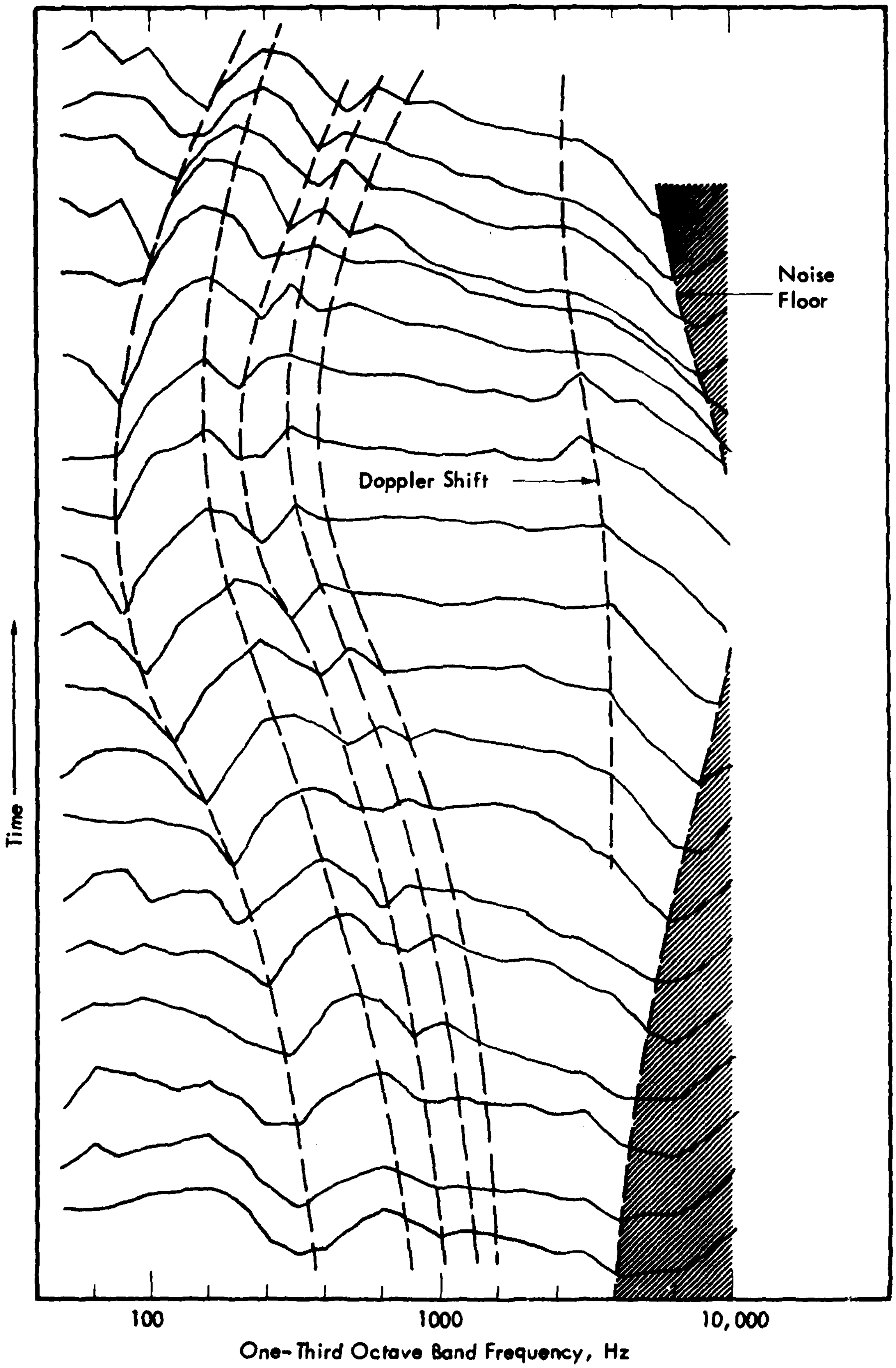

Figure 1-3. Flyover Spectra at 1/2-Second Intervals, 1.2 m High Microphone (from Reference 2)

of ground reflection[5] shows that interference pattern frequencies are inversely proportional to the path length difference between the direct and reflected paths. It is easy to see that this difference is largest when the aircraft is overhead, and decreases as the aircraft is at smaller elevation angles. The pattern in the figure therefore explains itself: pseudotones at higher frequencies during the approach, decreasing to lower frequencies around over head, and increasing again as the aircraft recedes. This is in marked contrast to the behavior of the Doppler shift of true (fan) tone components also indicated in the figure: it starts at an elevated frequency, experiences the most rapid frequency change around overhead, and settles at a lower frequency. This is actually one way of identifying pseudotones for invoking the provision in paragraph B36.3 of FAR Part 36.

Figure 1-3 also shows that pseudotones appearing in real data are never as pronounced as indicated by theoretical simplified considerations. Sharp spectral dips are "washed out" due to: (1) atmospheric turbulence (randomizes propagation speeds and therefore the effective path length difference or the time delay of the reflected relative to the direct wave), (2) surface impedance (may not be constant as the area of the surface that reflects the sound towards the microphone moves with the position of the aircraft), (3) surface randomness (surface is never ideally flat), and (4) the finite bandwidth of the analysis filter.

Pseudotones may have two effects on the Effective Perceived Noise Level (EPNL) calculated from the series of spectra of a flyover. One, the Perceived Noise Level (PNL) at any instant may be different from that of free field conditions. Two, the tone correction to be added to the PNL may be different due to the presence or absence of pseudotones. Concerning the latter, FAR Part 36 allows ignoring the portion of the spectrum containing pseudotones under certain circumstances (see Section 1.2). Nowadays it is common practice (approved by FAA) to ignore tone corrections below 800 Hz, but SPL values must be included in the noy calculation. This procedure has arisen from practical necessity, the 800 Hz cutoff being arbitrary. As shown in Figure 1-3, pseudotones at higher frequencies can occur quite easily.

Subjecting the entire spectrum to tone correction brings up another problem: the tone correction procedure prescribed by FAR Part 36 is considered by many not as advanced as the procedure recommended by SAE ARP 1071.[3] The former represents a stage in the development of ARP 1071 and employs a 10-step

procedure, whereas SAE ARP 1071 employs a 7-step procedure which gives more accurate results in some cases which are of importance when considering pseudotones. Both methods usually give very similar tone corrections, except when a tone is shared by contiguous frequency bands: both tone correction procedure require that the given spectrum be smoothed so that the difference due to the tone can be determined. The 10-step procedure does not result in a spectrum smoothed as well as by the 7-step method. This results in a smaller tone correction for the 10-step method. Considering that pseudotone frequencies continually vary during an aircraft flyover (Figure 1-3), cases when tones are shared by contiguous bands will almost certainly occur. Therefore, if the 7-step procedure were incorporated into FAR Part 36 in place of the 10-step procedure, the pseudotone problem could be accentuated because the 7-step procedure recognizes "tones" more readily.

Another influence of pseudotones on EPNL is as follows: Some aircraft noise spectra contain real tones (for example, buzz-saw noise from supersonic tip speed fan engines without inlet guide vanes IGV) in the frequency region where pseudotones are strongest. These would be ignored if the 800 Hz cutoff is blindly applied. They can be distorted by pseudotones and inaccurate pure tone corrections applied.

It could be argued that pseudotones are really heard by a person standing or sitting outdoors and that, therefore, they should not be eliminated from measured spectra. However, in urban and suburban areas, people spend most of their time indoors.[4] The response of buildings to acoustical excitation generally favors the lower frequencies, the region where pseudotones are found. Therefore, accuracy of the spectrum of the sound as seen by the <u>building</u> is desirable particularly in the lower regime. Inside a building, pseudotones may also occur but will be of a totally different nature due to the presence of so many internal reflecting surfaces in close proximity. In any event, such effects are not pertinent to aircraft noise certification under current rules.

Without specifying in detail the reflecting surface for a certification measurement, the applicant for an aircraft noise type certificate is free to choose a fairly absorbing surface such as lush grass land (FAR Part 36's stipulation of "no excessive sound absorption characteristics" is not quantitative and therefore not enforceable) in order to minimize the influence of the reflected wave resulting in

slightly lower noise levels than with a harder surface. Another applicant may not be able to locate such favorable conditions so that aircraft would be compared under different reference conditions which is unfair. Many of the subsequently discussed methods of dealing with pseudotones automatically carry with them the benefit of removing this inequity.

1.2 Current FAR Part 36 Requirements on Ground Reflections

Applicable excerpts from the current version of FAR Part 36 are:[29]

- Paragraph A36.1(b):

  "Locations for measuring noise from an aircraft in flight must be surrounded by relatively flat terrain having no excessive sound absorption characteristics such as might be caused by thick, matted, or tall grass, shrubs, or wooded areas."

- Paragraph A36.3(f):

  "The microphones must be placed so that their sensing elements are approximately 4 feet above ground."

- Paragraph B36.5 (tone correction procedure):

  "For any i-th one-third octave band, at any k-th increment of time, for which the tone correction factor is suspected to result from something other than (or in addition to) an actual tone (or any spectral irregularity other than aircraft noise), an additional analysis may be made using a filter with a bandwidth narrower than one-third of an octave. If the narrow band analysis corroborates that suspicion, then a revised value for the sound pressure level, SPL" (i, k), may be determined from the analysis and used to compute a revised tone correction factor, F(i, k), for that particular one-third octave band."

From these inclusions, it is seen that FAR Part 36 recognizes spectral irregularities other than those from the source (the aircraft), allows that they be ignored for calculating tone corrections to the Perceived Noise Level, but otherwise does not require any procedures that would avoid or compensate for

pseudotones. It is probably safe to say that pseudotones are present to some extent in all certification tests because FAR Part 36 requires that the microphone be 1.2 m (4 feet) above a ground that is not overly absorptive, i.e., quite capable of reflecting sound and thereby generating pseudotones. The nature of the ground cover need only be reported qualitatively.

In view of the many other corrections to the measured data required by FAR Part 36 (airplane position, weather, ambient noise) which are generally applied with a relatively high degree of accuracy, it appears very desirable to also minimize the influence of the ground surface and correct to free field conditions (i.e., simulating the absence of the ground) because the nature of the ground surface strongly determines the magnitude of its influence. Particularly in the low frequency regime, ground reflections may distort spectra to a much larger degree than other factors (weather, ambient noise, airplane position). An option, not considered further in this report, would restore a +3 dB correction to "free field" data to achieve a level which accounts only for a uniform energy addition of the ground reflected wave at all frequencies.

1.3 Analytical Corrections

We define analytical correction procedures as those procedures which attempt to reconstruct free field flyover spectra from measured spectra contaminated by surface reflection.

Table 1-1 lists the analytical pseudotone correction techniques that were identified as candidates for thorough investigation. Each technique is briefly discussed in the following paragraphs.

1. Spectrum Smoothing

   This technique would apply a calculation procedure to the lower frequency portion of the spectrum that would even out the peaks and troughs caused by the pseudotones. One way would be to assume that the lower portion contains only jet noise for which the spectrum shape is very well known. The spectrum could then be extrapolated on that basis. Another way would be to postulate a simple polynomial expression for the lower spectrum which could then be least squares fitted. The danger would of course be that real tones emitted by the aircraft would also be

Table 1-1

Analytical Pseudotone Correction Procedures

			Advantages	Disadvantages
Empirically Based	1	Spectrum Smoothing	- Attractive simple concept	- Accuracy questionable if based on empirical approach - May smooth over real tones
	2	Cutoff (ignore lower frequency spectrum for tone correction)	- Very simple	- Cutoff frequency arbitrary - May ignore real tones in lower frequency spectrum - PNL still based on raw spectrum
Theoretically Based	3	Classical specular reflection theory	- Theoretically defensible	- Needs certain parameters (aircraft position, ground impedance) very accurately - Parameters change with time - Assumes often unrealistic idealized conditions
	4	Cepstral Techniques	- Quite independent of details of measurement setup	- Very little experience - Needs narrow band analysis - "Comb filtering" sensitive to proper echo time delay selection
Combination	5	Reflection Theory plus empirical adjustments	- Same as (3) plus: - Works well if spectrum exhibits interference pattern containing the first three extrema	- Limited confidence for spectra containing tones in very low frequency range - Empirical adjustments need refinement

smoothed over. Thus, this technique could probably only be used reliably for jet and fan jet aircraft which do not exhibit strong spectral variations for frequencies where pseudotones occur (below 1 kHz or so), such as is the case with multiple pure tones generated by transonic tip speed fans on some older wide body aircraft. In particular, the technique could not be applied to general aviation propeller and rotary wing aircraft which emit most of their acoustic energy in the frequency region strongly influenced by pseudotones.

2. Frequency Cutoff for Tone Correction

This is the technique now sanctioned by FAR Part 36 in Appendix B, Paragraph B36.5(m) (see Section 1.2 in this report). Below a certain frequency (800 Hz), any spectral peaks giving rise to a tone correction to PNL may be ignored in the calculation of the tone correction. This provision arose out of practical necessities in aircraft noise certification. The rigorous theoretician might label this technique a "band-aid approach" since it only avoids a problem rather than solves or eliminates it. Also, the calculation of PNL is still based on the contaminated spectra. Nevertheless, the method has proven useful in practice so that it would deserve more detailed investigation. The cut-off technique actually departs from the definition of an "analytical" correction technique given at the beginning of this section since a correction to free field is not attempted.

3. Specular Reflection Theory

The theory that describes the superposition of the direct and obliquely reflected wave is invoked to calculate correction coefficients to transform the contaminated spectra to the spectra corrected to free field. The value of this technique depends on how faithfully the theory models the real world. Provided the modeling is faithful enough, this approach is very defensible, although the data and computational requirements are rather significant. To a large extent, the success of the technique depends on the accurate knowledge of the acoustic surface impedance. Although substantial progress has been made in this area,[7, 12-14, 16, 19] it remains to be shown that, except for certain special conditions such as

a very hard surface, the impedance of any practical surface can be adequately specified for application to "approved" noise certification procedures.

4. Cepstral Techniques

The measured ("contaminated") spectrum in terms of SPL (in dB) versus frequency is subjected to a Fourier transformation from frequency space into quefrency space (quefrency = echo delay time). In quefrency space, the "spectral" function is called the "cepstrum."[21] If the spectrum subjected to the Fourier transform was contaminated by surface reflections, the cepstrum will show peaks at the quefrencies corresponding to the echo delay time of the reflected signal, and to multiples of that delay. In other words, the influence of reflections may be more readily recognized in the cepstrum than in the spectrum whence it is more easily removed.

Figure 1-4 depicts the process described in the previous paragraph applied to the reflection correction only. The cepstrum was obtained by numerical discrete Fourier transformation of the finite record shown at the top of the figure (128 points on the frequency axis). Sharp peaks (or valleys) do indeed occur in the cepstrum at the integer multiples of the true echo delay time. In the method described in Reference 21, the cepstrum of the measured spectrum is subjected to "comb" filtering, i.e., the cepstral values at the echo delay time quefrency (and/or in its vicinity) are set to zero. Subsequent inverse transformation to the frequency domain results in a "smoothed" spectrum.

Setting certain cepstral values to zero introduces an error in the cepstrum (and the spectrum after inverse transformation) because, strictly speaking, only the cepstrum of the reflection should have been removed, and not also the cepstral values contributed by the direct (free field) sound. If the bands are spaced closely enough, the error is not expected to be significant for broad band noise sources. However, many noise sources (propeller, rotary wings, multiple pure tones from transonic fans) have tones which may give rise to cepstra which look quite similar to the reflection cepstrum. During the processing of 0.5-second flyover

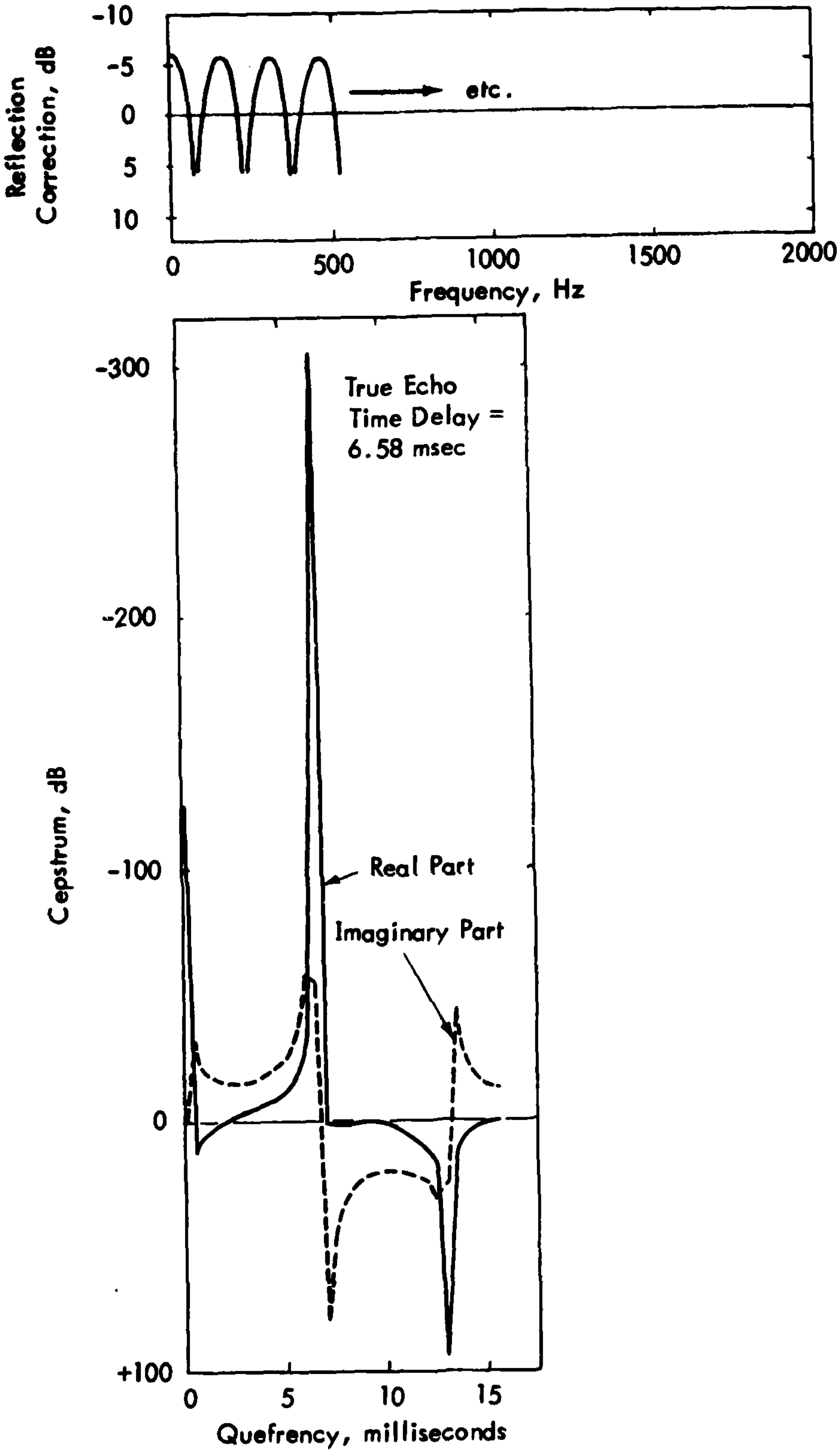

Figure 1-4. Narrow Band Reflection Correction and Its Cepstrum. Angle of Incidence 20°, Microphone Height 1.2 m, Speed of Sound 343 m/sec, Surface Flow Resistivity 300 cgs rayls/cm.

data, the probability is high that the two cepstra (reflection and source) will or almost will coincide so that comb filtering will remove the greater part of the acoustic energy in the signal.

This phenomenon could be corrected by removing only the reflection cepstrum. However, the advantage of using the simple comb filter is lost and the amount of computing work is very similar to (or even greater than) calculating the reflection correction directly.

5. Combination Techniques

These consist of some combination of theoretical and empirical techniques. Where theory is unable to provide a realistic enough mathematical model, empiricism is employed to complement the modeling process.

One combination technique has been developed by SNECMA (Appendix A of Reference 22) which examines each spectrum in the flyover series and identifies the nulls (troughs) presumed to be due to pseudotone phenomena. The location of these on the frequency axis is used to "tune" a theoretical reflection correction curve. As already pointed out for other techniques, this technique is not applicable to spectra containing discrete frequency components in the pseudotone area (propellers, rotors, transonic fans) as they have their own peaks and troughs. On a one-third octave band spectrum, these true spectral peaks and valleys are difficult to distinguish even by the trained eye, or require much more sophisticated analysis of the data in the time domain (i.e., autocorrelation, etc.).

To some extent, many so-called theoretical methods incorporate a certain measure of empiricism. So does the reflection correction technique described later in Section 1.3.2.1 (Step 6) where the atmospheric and surface inhomogeneities and irregularities are accounted for by a correlation coefficient which depends on an empirically determined constant.

1.3.1 Selection of Techniques

For this study, the following criteria were applied during selection of pseudotone correction techniques:

- o Technical feasibility and accuracy,
- o Economic reasonableness,
- o Enforceability(i.e., suitable for "approval" by regulatory agencies),
- o Time frame for implementation.

The direct spectrum smoothing technique is technically feasible, but its accuracy is questionable because it would smooth over source generated tones. It is economically reasonable; its application would be straightforward and therefore cheap. It should be enforceable if a standard technique were adopted. It is immediately implementable.

The frequency cutoff for the tone correction technique has a demonstrated technical feasibility. The criterion of accuracy is not directly applicable because the reflections are not removed (errors are indirectly evaluated in Section 1.3.4). The technique's application is very easy and therefore economically reasonable. It is enforceable if a certain cutoff frequency (800 Hz in the current FAR Part 36) is chosen; if it varies (say, depending on elevation angle), enforceability may suffer. In any event, this technique is already implemented by FAA.

The theoretical reflection correction technique is technically feasible. Its accuracy is great if the assumptions made in the derivation of the theoretical formulas are reasonably well approached. Concerning the assumptions of a perfectly still and homogeneous atmosphere and of a completely plane surface, this assumption is practically never satisfied. This deficiency can be compensated for by an empirical method. The required calculations for this theoretical technique are not straightforward but would not add an undue burden to certification noise processing. One-time development and testing of the necessary computer program code should take, at the most, several man-weeks.

The cepstral technique may be technically feasible but difficult, practically, since it requires narrow band analysis. Whereas the currently implemented one-third octave band analysis requires obtaining 24 values every 0.5 second, narrow band analysis would require at least five times as much if not more. If narrow band (i.e., fixed bandwidth filter) analysis was not used, the data points would not be equispaced in the frequency domain and Fast Fourier Transform techniques could not be applied which would make the process more time-consuming and therefore more expensive. Accuracy is acceptable for smooth

source spectra (such as jet noise), but may not be if tones with harmonics are present. Because of the problems with technical feasibility, the technique would probably be expensive in its implementation. An acceptable, codified and enforceable cepstral pseudotone correction technique would probably take several years to implement.

SNECMA's combined theoretical and empirical technique is not always technically feasible as it breaks down in the presence of spectral irregularities due to the source. If it is applicable, it is probably very accurate. Its economics, enforceability and time frame of implementation are comparable to the theoretical reflection correction technique.

As has already been mentioned above, the latter may be enhanced by empirical adjustments. This technique shows the most promise of providing a rigorous, accurate, and not too complicated pseudotone correction. It is therefore selected as the primary technique to be investigated in this study.

As a secondary technique, the frequency cutoff for tone correction is selected in order to investigate the relative accuracy of an already codified provision.

The other techniques (direct spectrum smoothing, cepstrum, SNECMA) are rejected for the purposes of this study primarily because of their inability to properly deal with spectral irregularities emanating from the source which superimpose themselves over the pseudotones.

1.3.2 Ground Reflection Correction

1.3.2.1 Theory

Recently, an easy-to-use and effective, yet theoretically well founded procedure has been published for calculating ground reflection effects.[5,6] This method is adopted here and briefly summarized in the following paragraphs. The theory is based on the following assumptions:

- Ground surface is flat with a clearly identifiable interface between air and ground (over a lush grassy surface it is often unclear where this boundary is).
- Ground surface is "locally reacting" (i.e., sound waves transmitted into the ground propagate only perpendicularly to the surface).
- Atmosphere is uniform (no wind, no temperature gradients).

- o Spectrum levels vary slowly over any one third-octave band (this condition may well be violated in practice where single tones are present but very narrow band analysis would be required to resolve this problem).
- o Ground impedance is large relative to that for air (more details on this assumption are given later).

The geometry of the situation to be modelled is shown in Figure 1 - 1. The calculation framework for arriving at the ground reflection correction is given in the following steps. This correction must be added to a measured signal in order to remove the ground reflection effect.

Calculation Framework:

Step 1: Determine Ground Complex Impedance or Admittance = 1/impedance as a function of frequency: A separate section (1.3.2.2) is devoted to this subject.

Step 2: Determine Ambient Speed of Sound c_0.

a. Approximate Method:

$$c_0 = 331.6\,(1 + t_c/273.15)^{1/2} \text{ in meters/second,}$$

where t_c is the temperature in degrees Celsius.

b. Thermodynamic Method (includes effect of humidity):

The method employed here for accounting for effects of humidity on the ambient speed of sound is chosen for computational convenience. An alternative, semiempirical method, based on measured data, is also available in Appendix A of Reference 30. The two methods differ by less than 0.1%.

$t_k = t_c + 273.15$, temperature in degrees Kelvin;

$t_r = t_k/273.16$, triple point ratio;

Determine water vapor partial pressure divided by total pressure:

$$VP = \frac{RH}{100}\,\frac{1}{p_o}\,10^{\text{exponent}}$$

where: RH = relative humidity in percent,

characters denote vector quantities), the unit vector $\mathbf{u}$ in direction of the flightpath, and aircraft speed S. With time denoted by t, t_a indicating the time at the apparent location, points on the flightpath are given by $\mathbf{A} + \mathbf{u} S (t - t_a)$. With t_e denoting the time at emission the following relationship holds for the emission location $\mathbf{E}$ (see Figure 1-4.5):

$$\mathbf{E} = \mathbf{A} + \mathbf{u} S (t_e - t_a)$$

Also, $t_a - t_e$ must equal the sound travel time along $\mathbf{E}$:

$$t_a - t_e = |\mathbf{E}|/c_o$$

which may be substituted into the previous equation yielding:

$$\mathbf{A} = \mathbf{E} + \mathbf{u} M |\mathbf{E}|$$

where M is the flight Mach Number S/c_o.

This equation may be solved for $\mathbf{E}$. The solution is obtained as follows (for the derivation see Appendix B):

Given: $\mathbf{A} = (A_1, A_2, A_3,)$, M, $\mathbf{u} = (u_1, u_2, u_3,)$ (1- and 2-direction in ground plane, 3-direction vertical)

Calculate:

$$B_2 = A_2 - A_1 u_2/u_1, \quad B_3 = A_3 - A_1 u_3/u_1$$

$$C_1 = A_1 + u_1 u_2 B_2 M^2 + u_1 u_3 B_3 M^2$$

$$C_2 = A_1^2 - u_1^2 M^2 (B_2^2 + B_3^2)$$

$$E_1 = (C_1 - \text{sign}(u_1)(c_1^2 - C_2 (1 - M^2))^{1/2})/(1 - M^2)$$

$$E_2 = B_2 + E_1 u_2/u_1$$

$$E_3 = B_3 + E_1 u_3/u_1$$

where

$$\text{sign}(u_1) = \begin{cases} 1 \text{ for } u_1 > 0 \\ -1 \text{ for } u_1 < 0 \end{cases}$$

The case of $u_1 = 0$ (or almost zero) needs special consideration because it is a devisor in the above calculations, and an argument of the sign

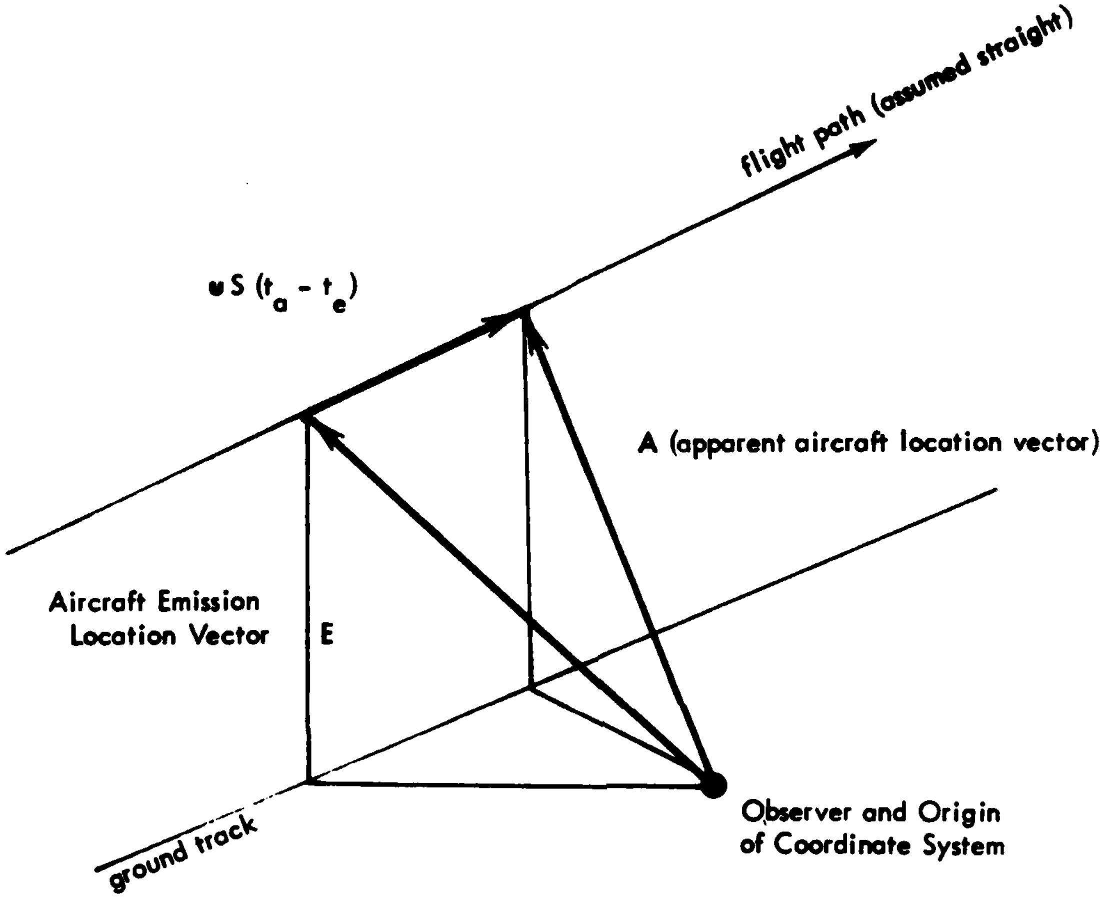

Figure 1-4.5. Illustration of Apparent and Sound Emission Aircraft Location Vectors

p_o = atmospheric pressure in units of atmospheres

(1 atmosphere = 1.01325×10^5 N/m^2)

exponent = $8.58 - (10.8/t_r) - 5.03 \log_{10}(t_r) + 23 \times 10^{-4.77/tr}$

Determine moisture content X in kg of water per kg of dry air:

$$X = 0.6220\ VP/(1-VP)$$

where 0.6220 is the ratio of the air and water vapor gas constants.

Determine the gas constant of the air-water vapor mixture:

$$R_M = (47.06\ X + 29.27)/(1 + X)$$

where 47.06 is the water vapor gas constant, and 29.27 is the air gas constant, both in units of meters/degrees Celsius.

Determine the ratio of specific heats k for the vapor- air mixture:

$$k = 1.402\ (X + 0.868)/(1.0526\ X + 0.868)$$

where 0.868 is the air-to-water ratio of specific heat at constant pressure, and 1.0526 is the air-to-water ratio of the ratios of specific heats (= 1.402/1.332).

Determine the ambient speed of sound c_o:

$$c_o = (k\ g\ R_M\ t_k)^{1/2} \text{ in meters/second,}$$

where $g = 9.81$ m/sec^2 = gravitational acceleration.

Step 3: Determine the Aircraft Emission Location. The time when a sound emitted by the aircraft is heard (apparent location) and the time when this sound was emitted differ by the sound travel time from the emission location to the observer. Almost all of the time, we are given the apparent location and the aircraft speed so that the emission location must be determined in order to know the correct angle of sound incidence.

Without loss of generality, the origin of the coordinate system may be assumed to coincide with the observer. The flightpath is assumed to be a straight line specified by the apparent aircraft location **A** (bold

function which is undefined if the argument equals zero. Since we can safely exclude the case $u_1 = u_2 = 0$ (vertical flight path) it is only necessary to rotate the coordinate system around the 3-direction by 90 degrees for the duration of the emission location calculation.

Knowing the components of **E**, sound travel distance R and elevation angle b are easily calculated:

$$R = (E_1{}^2 + E_2{}^2 + E_3{}^2)^{1/2}$$

$$b = \sin^{-1} (E3/R)$$

The angle of incidence θ is:

$$\theta = 90^o - b$$

<u>Step 4:</u> Determine the Path Length Difference.

The path length difference d between direct and reflected wave is $r_2 - r_1$. However, since $r_2 \doteq r_1$, which is much greater than h, d is more conveniently calculated from

$$d = 2\ h \cos \theta$$

<u>Step 5:</u> Determine Complex Reflection Coefficient. Define a complex variable t as follows:

$$t = (\cos \theta + n)\ (k\ R/2i)^{1/2} \quad , i = + (-1)^{1/2}$$

where: n = complex admittance (from Step 1)

k = wavenumber = $2\ \pi\ f/c_o$ (π = 3.141592...)

f = frequency

Then calculate

$$F(t) = 1 - \pi^{1/2}\ t\ W\ (it)$$

where W is the complex error function. Appendix C gives a detailed calculation procedure for the function F(t), including a computer program.

The plane wave complex reflection coefficient is:

$$G_p = (\cos \theta - n)/(\cos \theta + n)$$

The general complex reflection coefficient is:

$$G_c = G_p + (1 - G_p) F(t) = G e^{ia}$$

where: $G = \left| G_c \right|$, $a = \tan^{-1} (\text{Im } G_c/\text{Re } G_c)$

Step 6: Determine Correlation Coefficient Adjustment to account for Band Averaging of Finite Bandwidths of Noise

The band averaging factor B is given by:

$$B = (\sin (c\,k\,d/2))/(ckd/2)$$

where c is the filter bandwidth relative to the band (geometric) center frequency. For one-third octave bands (using the approximate equivalent of one-tenth decade bands):

$$c = 10^{0.05} - 10^{-0.05} = 0.23077$$

Step 7: Determine Correlation Coefficient (correction for non-ideal atmosphere).

Inhomogeneities in the atmosphere and the reflecting surface cause amplitude and phase differences between direct and reflected signals to vary randomly. A correction factor to the correlation coefficient is used to account for this phenomenon empirically. Higher frequencies (wave numbers) will be affected more strongly than lower ones and coherence between the signals should also be expected to decrease with path length difference d. Reference 6 suggests the following form for this correlation correction factor C which is adopted here:

$$C = \exp^{-(f_{inc}\, kd)^2}$$

where f_{inc} is an incoherence factor with a recommended value of 0.01 (subject to empirical adjustment). Application of this correlation coefficient relaxes some of the assumptions made in the beginning of this section.

Step 8: Determine Reflection Correction

The reflection correction, in decibels, that must be added to a band level in order to remove the ground reflection effect becomes:

$$P_c = -10 \log_{10} (1 + G^2 + 2\,G\,B\,C \cos(a + k\,d))$$

An additional correction factor should, theoretically, be included in the argument of the cosine term in this expression; however, it is essentially equal to unity for one-third octave bands and is neglected here. The effects of source correction due to the finite averaging of the source spectra have been neglected here. It has been shown that averaging times of 0.5 seconds produce a difference of only 0.2 dB by including this extra term,[17] at least at high angles of incidence.

1.3.2.2 Complex Ground Impedance

The accurate prediction of outdoor ground impedance on the basis of measured data and/or theoretical models is generally difficult due to the heterogeneous, anisotropic nature of most surfaces. Impedance (or its reciprocal, admittance) is a complex quantity generally varying as a function of both frequency and angle of incidence. Numerous studies have attempted to evaluate the effect of finite ground impedance indirectly by experimental or analytical studies of horizontal sound propagation or have measured impedances for various surfaces directly or using an assortment of elaborate measurement techniques.[11-19] Invariably, certain assumptions must be made in order to simplify the modeling process: all surfaces are assumed to be homogeneous, isotropic, and "locally reacting."

Delany and Bazley[12] were the first to define normalized impedance (normalized with respect to air) as a function of frequency, f, and flow resistivity, s, for fibrous absorbent materials (cotton, fiberglass, etc.). Both of these quantities are easily obtained for many materials of interest. Indeed, the power law relations developed by Delany and Bazley:

$$R/\rho_o c_o = 1 + 9.08\,(f/s)^{-.75}$$
$$X/\rho_o c_o = 11.9\,(f/s)^{-.73} \;*$$

agree well with the measured data for the materials tested. Here R represents the real part and X the imaginary part of the surface impedance, and $\rho_o c_o$ the specific impedance of air at standard atmospheric conditions.

*In the present formulation of the theory, the imaginary part of the impedance must have a positive sign. Some references give it as negative. See Reference 31 for a discussion.

More recently, other studies have shown that these power law relations agree fairly well with measurements taken over grass,[15, 18] hard ground,[16] spaded soil,[17] and snow.[18] Although measured and extrapolated values of impedance were found to be in excellent agreement with the above model for values of (f/s) between 0.5 and 1000 cgs rayls/cm,[15] caution should be used when applying the model to <u>any</u> surface. Moisture content, root structure, and the geological characteristics of the subsoil (and topsoil) play an important role in describing the flow resistivity of the surface material. For values of s for common surface materials, see Refererence 20.

1.3.2.3 Application of Ground Reflection

A computer program was written to apply the calculation of ground impedance and reflection correction described in the previous sections. In order to demonstrate the dependance of the reflection correction on ground impedance, Figures 1-5 through 1-8 were created by the computer program. In all four cases, the reflection correction (i.e., the amount in dB that is to be added to measured spectra in order to remove the ground effect) is plotted as a function of frequency (a point at each 1/3 - octave band center frequency) and time (a spectrum every 1½ seconds). An aircraft is assumed to execute a level flyover (altitude 1000 feet (304.8 m)) at a constant speed of 160 knots (82.3 m/s). Visual overhead occurs at 10 seconds into the 20 sec display window (actual or emission overhead occurs about 1 second later). The incoherence factor (f_{inc}) was set to 0.01, temperature to 20° Celsius, humidity to 70%, and pressure to 1 atmosphere. The following four extreme values of normalized impedance were evaluated to illustrate the general influence of this parameter.

Figure	Complex Impedance	
1-5	1 - i	constant for all frequencies
1-6	1 + i	constant for all frequencies
1-7	1000 + i0	constant for all frequencies
1-8	frequency dependent with flow resistivity s = 100 cgs rayls/cm	

The normalized impedances used in Figure 1-8 are listed in Table 1-2.

All four spectral time histories of the reflection correction exhibit the expected shift of the peaks-valleys pattern towards lower frequencies in the vicinity of the overhead position. Figure 1-7 is most easily interpreted since it represents very nearly the case of a perfect reflector. As should be expected, the reflection correction tends towards -6 dB for low frequencies (acoustic pressure doubling near perfect reflector), and towards -3 dB at high frequencies (acoustic intensity doubling). The impedance used in Figure 1-5 (1-i) is that of a very absorbent and compliant surface. Because of the high absorption, pressure and intensity do not increase nearly as much as near a hard surface. Changing the sign of the reactance (impedance = 1 + i, Figure 1-6 causes a radical change in the reflection correction pattern; that is, however, not a realistic case as practical surfaces have a positive real part and a negative (i.e., stiffness) imaginary part of

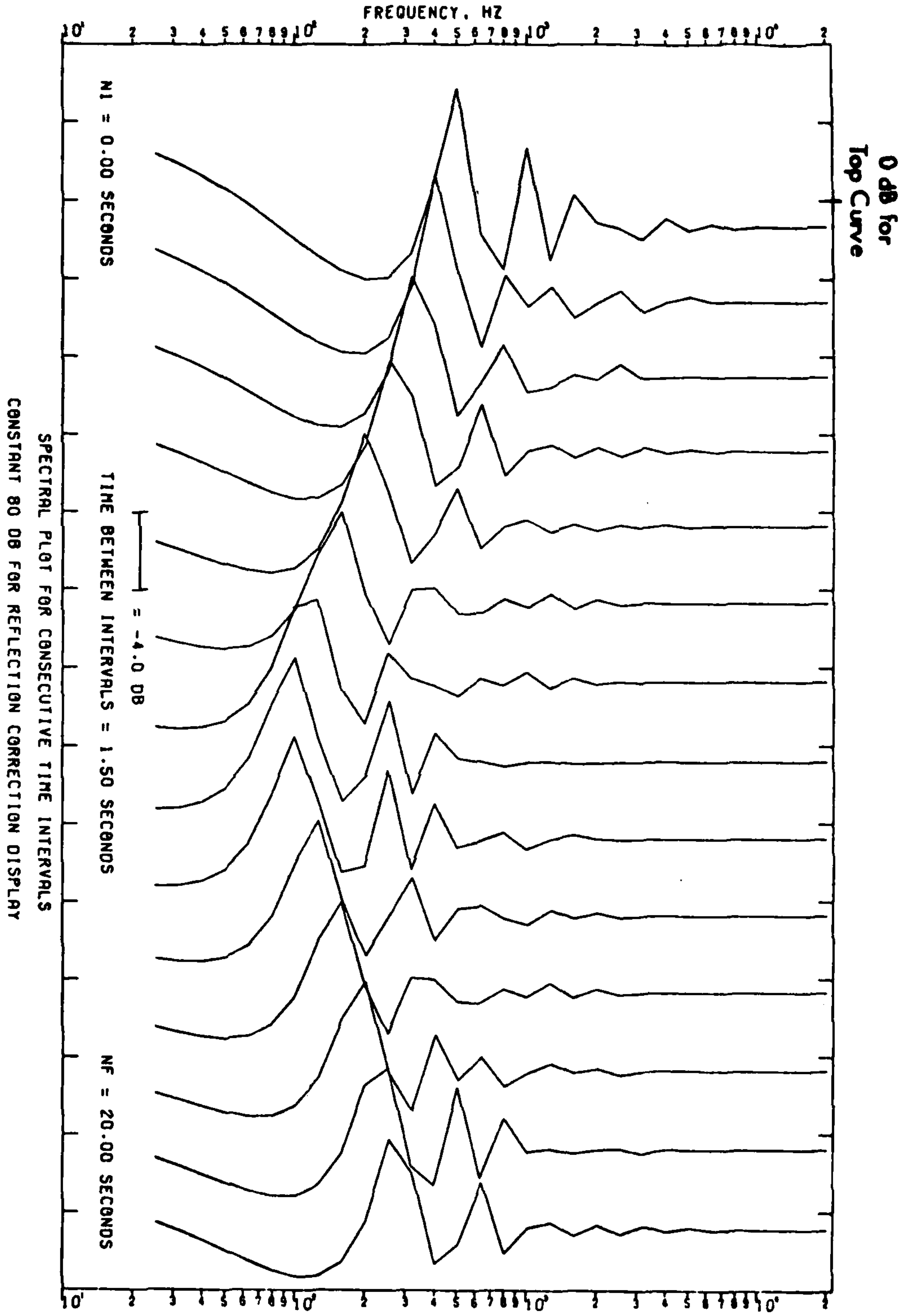

Figure 1-5. Plot of Spectral Time History of Reflection Correction: Level (304.8 m) Constant Speed (82.3 m/sec) Flyover, Visual Overhead at 10 Seconds, Constant Normalized Impedance = 1 - i.

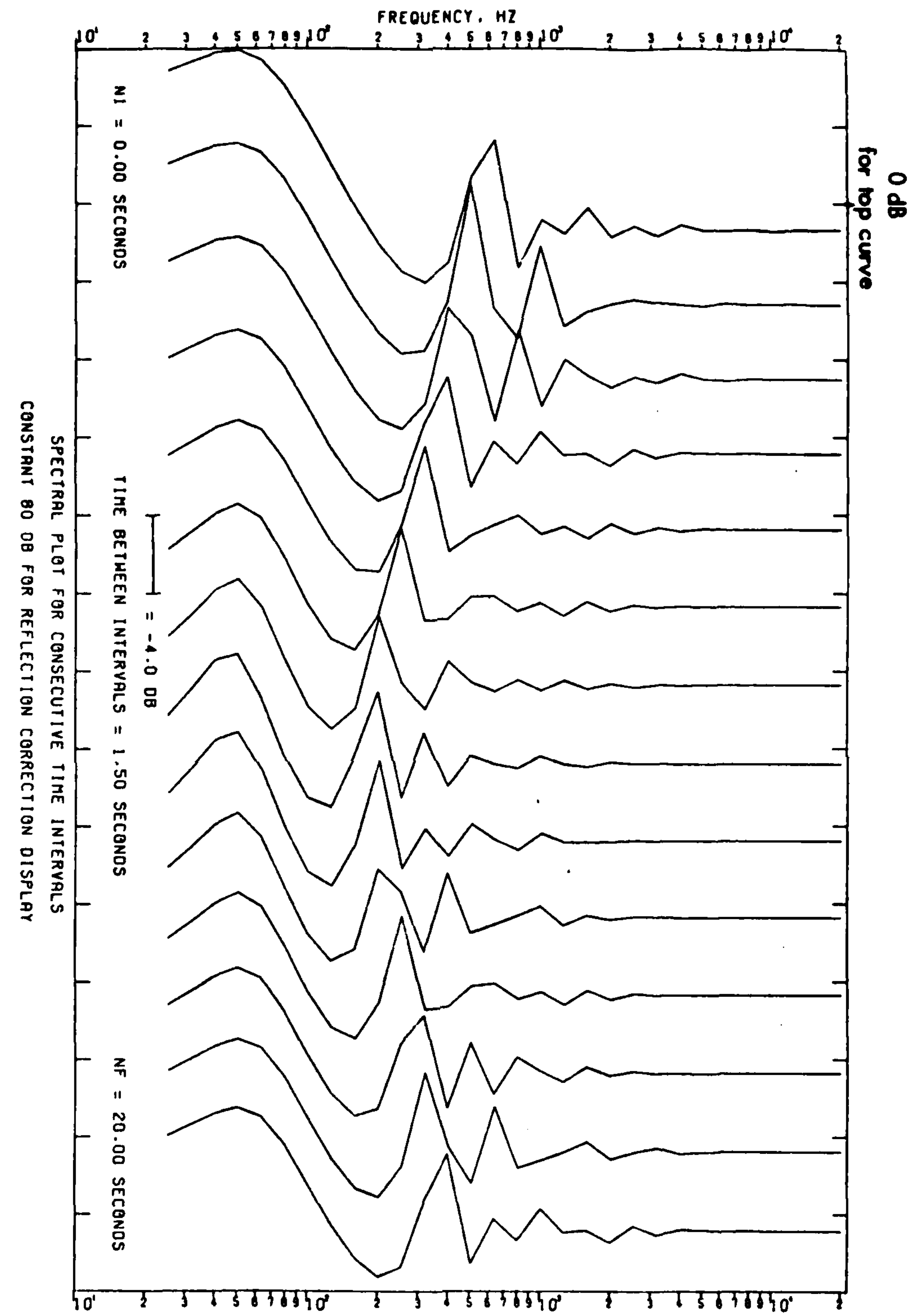

Figure 1-6. Plot of Spectral Time History of Reflection Correction: Level (304.8 m) Constant Speed (82.3 m/sec) Flyover, Visual Overhead at 10 Seconds, Constant Normalized Impedance = 1 + i.

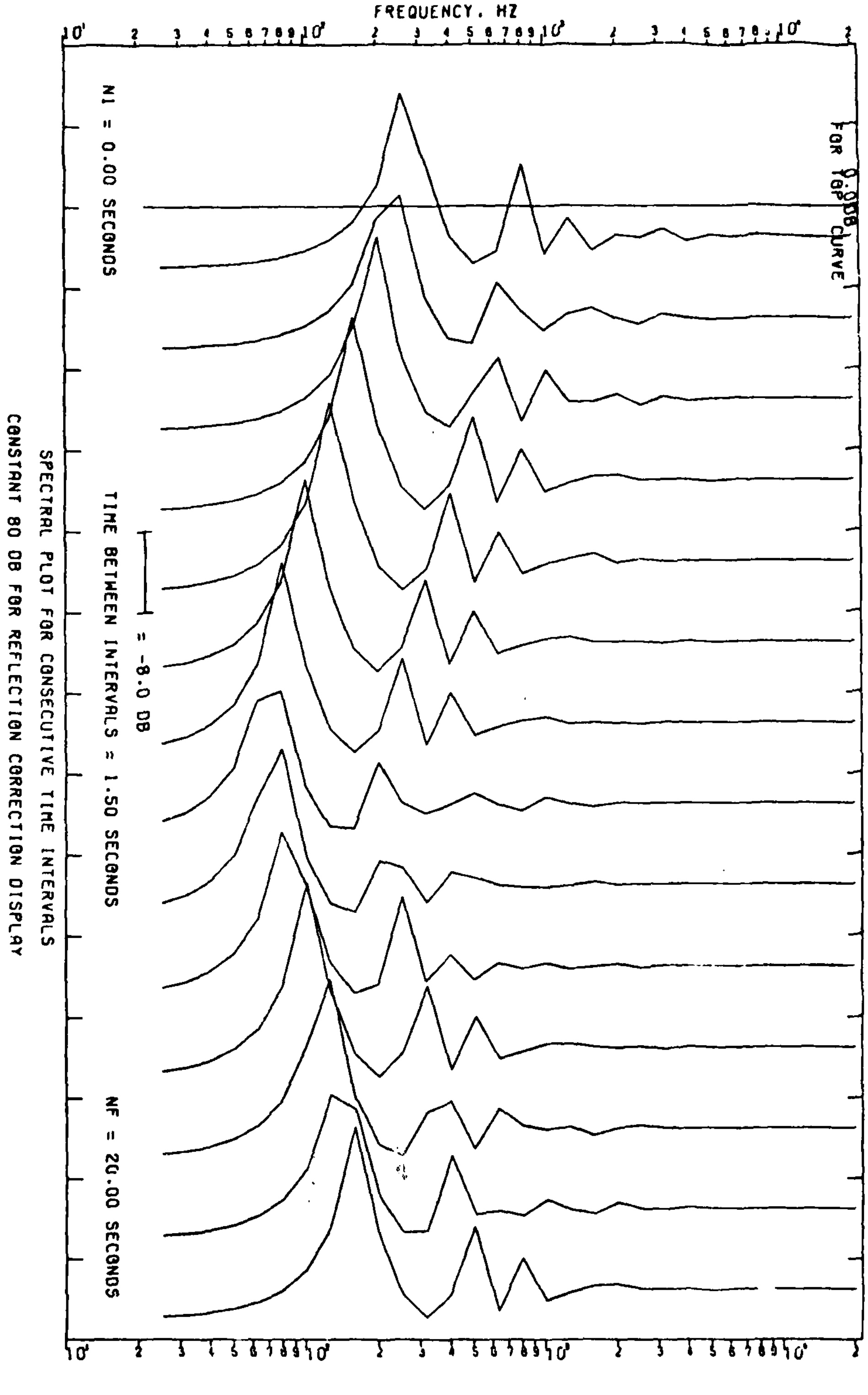

Figure 1-7. Plot of Spectral Time History of Reflection Correction: Level (304.8 m) Constant Speed (82.3 m/sec) Flyover, Visual Overhead at 10 Seconds, Constant Normalized Impedance = 1000 + i0.

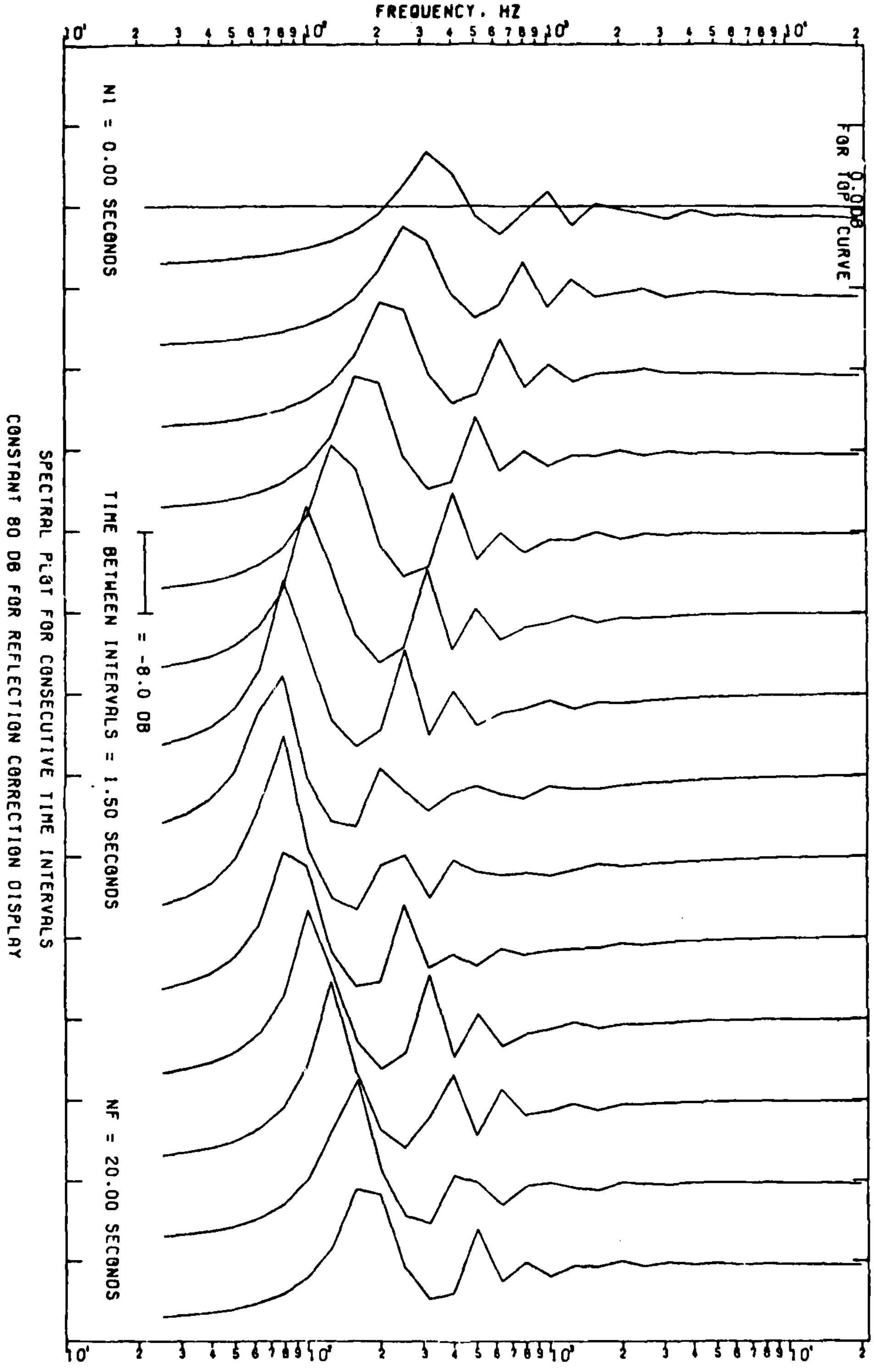

Figure 1-8. Plot of Spectral Time History of Reflection Correction: Level (304.8 m) Constant Speed (82.3 m/sec) Flyover, Visual Overhead at 10 Seconds, Normalized Impedance Depends on Frequency (Calculated with Flow Resistivity = 100 cgs rayls/cm). Imaginary Part of Ground Impedance is Negative. See Footnote on Page 1-22.

Table 1-2

Normalized Impedance and Admittance as a Function of Frequency as Used in Figure 1-8, with Ground Surface Flow Resistivity = 100 cgs rayls/cm
Imaginary Part of Complex Impedance is Negative (See Footnote on Page 1-22)

(Computed from Equation at Beginning of Section 1.3.2.2)

FREQ.,KHZ	IMPEDANCE Real	IMPEDANCE Imag.	ADMITTANCE Real	ADMITTANCE Imag.
.025	26.5909	-32.6247	.150108-01	.164170-01
.032	22.5321	-27.5770	.177672-01	.217452-01
.040	19.1170	-23.3103	.210348-01	.256467-01
.050	16.2435	-19.7037	.249101-01	.302165-01
.063	13.8258	-16.6551	.295080-01	.355463-01
.079	11.7916	-14.0782	.349653-01	.417456-01
.100	10.0800	-11.9000	.414446-01	.489276-01
.126	8.63987	-10.0568	.491384-01	.572066-01
.158	7.42815	-8.50251	.582737-01	.667020-01
.200	6.40861	-7.16699	.691156-01	.775102-01
.251	5.55078	-6.07501	.819704-01	.897119-01
.316	4.82900	-5.15508	.971859-01	.103346
.398	4.22171	-4.34057	.115148	.118590
.501	3.71073	-3.66699	.136268	.134736
.631	3.28079	-3.10152	.160967	.152161
.794	2.91905	-2.62148	.189655	.170303
1.000	2.61468	-2.21568	.222589	.188639
1.259	2.35656	-1.87304	.260006	.206482
1.585	2.14310	-1.58324	.301665	.223006
1.995	1.96180	-1.33828	.347856	.237298
2.512	1.80926	-1.13122	.397371	.248452
3.162	1.68090	-.955195	.449470	.255005
3.981	1.57291	-.808252	.502958	.258449
5.012	1.48204	-.685199	.556487	.256532
6.310	1.40559	-.577445	.608696	.250066
7.943	1.34126	-.488143	.658304	.239607
10.000	1.28713	-.412617	.704519	.225648
12.589	1.24159	-.348776	.746509	.209702
15.849	1.20328	-.294813	.784002	.192087
19.953	1.17104	-.249199	.816950	.173649

the impedance. By contrast, Figure 1-8 presents the reflection correction for a practical surface with a flow resistivity of 100 cgs rayls/cm which is probably representative of lush grass over a very porous and dry soil. These corrections tend toward -6 dB at low frequencies as should be expected due to the relatively high impedance there (Table 1-2). At high frequencies, the corrections tend toward 0 dB due to the associated low impedances. Comparison with Figure 1-7 shows that there is, apart from the high frequency 3 dB shift, little difference between the corrections for a soft grassy surface and a hard surface in the vicinity of the overhead positions (small angle of incidence). Significant differences appear upwards on the figure (earlier in time) at the fifth curve from the top (corresponding to an angle of incidence of 55 to 60°) and downward to the second or third curve from the bottom (corresponding to the same approximate angle of incidence). This would indicate that it is not vital to know the exact surface impedance, as long as some reasonable value is used, for near overhead flyovers since the greatest contribution to single event metrics (such as EPNL) comes from the noise emitted near overhead. For sideline measurements, the angle of incidence (Θ in Figure 1-1) will hardly ever be less than 30° (for a light B727) and often not go below 55° (for a heavy B747). Accurate knowledge of ground impedance then becomes important.

When we attempted to apply the reflection correction to measured data, serious problems were encountered. Before these problems are discussed in detail, the results of several correction attempts are presented. Appendix A contains graphical representations of almost all the measured aircraft noise events utilized in this study: the spectral time histories between the 10-dB-down points are shown. The following flights were selected for attempting the reflection correction:

A B727 on approach (Flight I in Appendix A)

A DC-10 on approach (spectral time history plot not in Appendix A but in this section);

A B727 on takeoff (Flight G in Appendix A).

(a) B727 on Approach

Figure A-13 (Appendix A, page A-30) shows the spectral time history for the 10-dB-down interval as measured by a microphone 1.2 m

over soft ground. The pattern created by reflection interference is easily discernible. The frequency shift of the pattern with time can also be gleaned from the figure. The general position of the aircraft was not measured except that the time of exact overhead was noted. It was then assumed that the aircraft was on the 3° ILS glide slope. The altitude at overhead could then be calculated knowing the distance of the microphone from the runway threshold. The speed of the aircraft was not measured; a nominal speed of 72 m/sec (140 knots) was used. With an incoherence factor of 0.1 and a surface flow resistivity of 100 cgs rayls/cm the correction was then carried out. The result of Figure 1-9 shows that the attempt was to a large extent successful. The characteristic pseudotone pattern is removed. One should expect that the corrected STH will be very similar to the ones measured for the same flight at 10 m and on the ground. Comparison with Figures A-11 (page A-28) and A-15 (page A-32) bears out this similarity except for some "waves" in Figure 1-9 in the 5th and 6th spectrum from the top in the lower frequency portion which are not present in Figure A-11 and A-15.

(b) DC-10 on Approach

In this case, the aircraft flew on an approach path for which the ground projection's perpendicular distance to the measuring station was 230 m (750 ft). The elevation angle was about 30° (it is 90° for overhead flights). The measured STH with pseudotones is shown in Figure 1-10. The attempt to remove pseudotones is shown in Figure 1-11. There is only one spectrum (the 4th from the bottom) for which pseudotones are almost removed. For the rest of the STH, the attempt is a failure for which there are these possible explanations:

- o The exact time of closest approach was not known with sufficient accuracy. This may cause a shift in the correction pattern and result in the "out-of-phase" appearance of Figure 1-11.
- o The aircraft's speed was substantially different from the one assumed for the correction attempt (speed was not measured during the acoustic data acquisition).

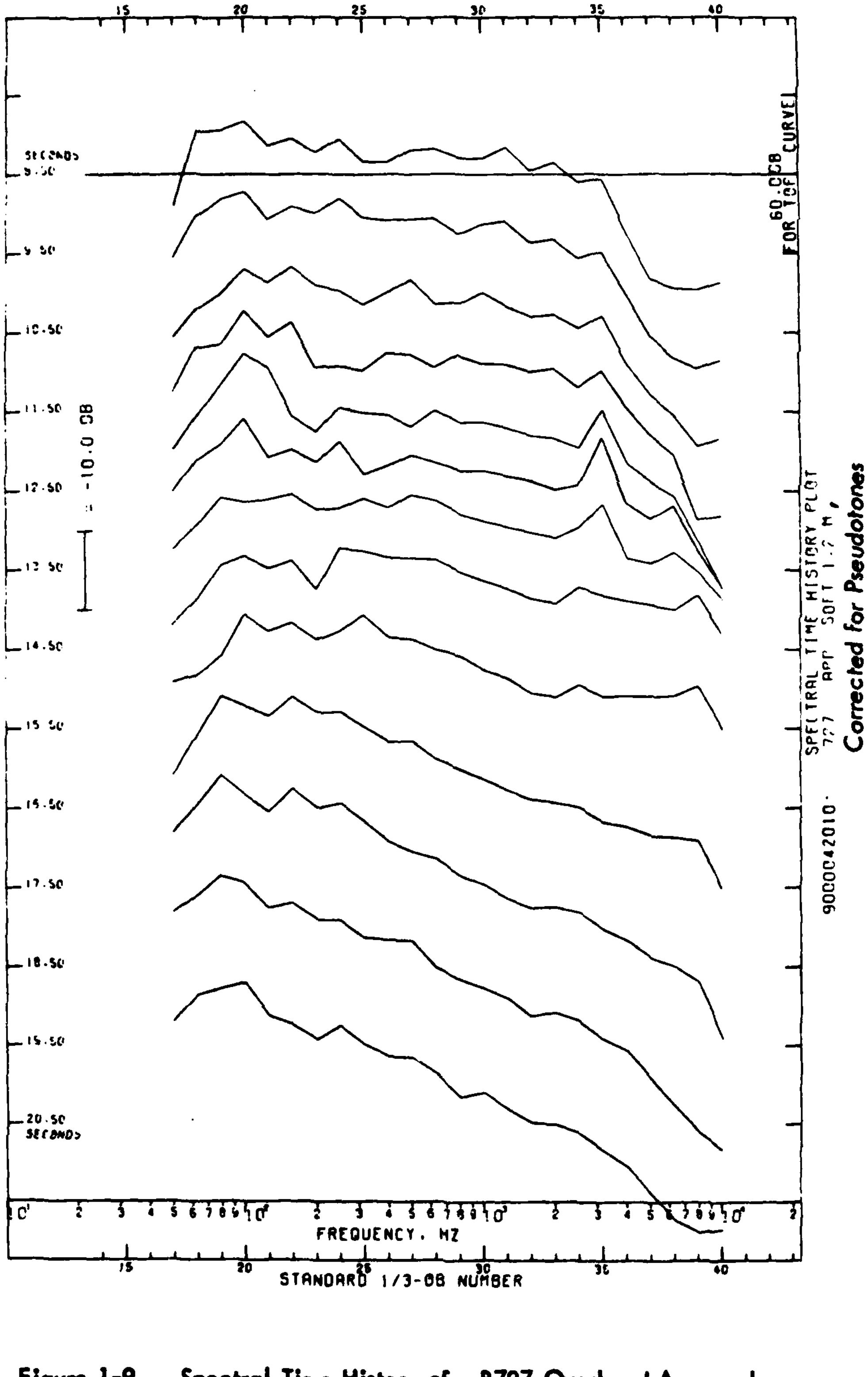

Figure 1-9. **Spectral Time History of a B727 Overhead Approach after Reflection Correction; Flow Resistivity 100 cgs rayls/cm, Incoherence Factor 0.1**

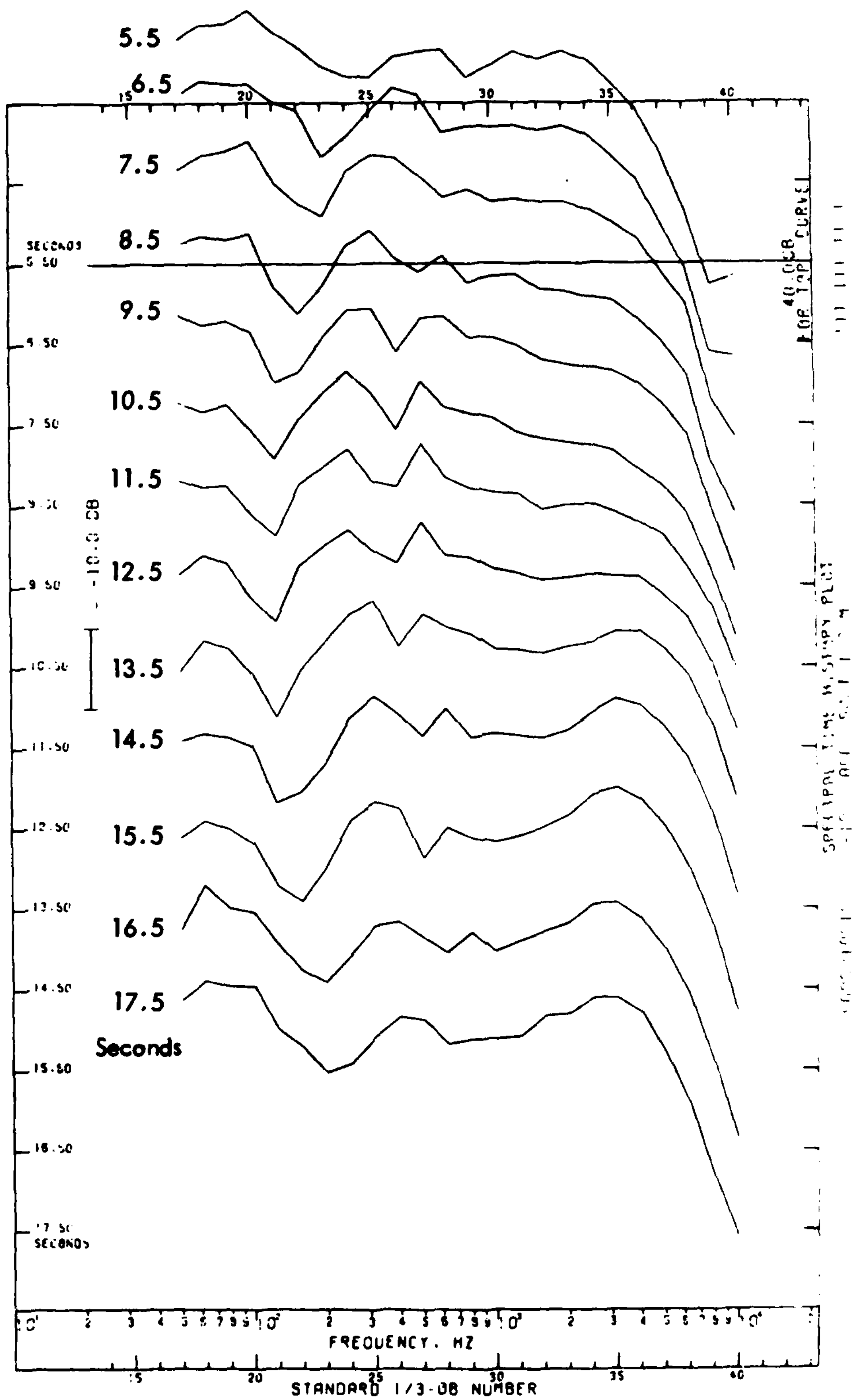

Figure 1-10. Spectral Time History for the 10-dB-down Interval of a DC-10 on a Sideline Approach, Microphone 1.2 m over Soft Ground, Measured Data Smoothed in the Time Domain. Dataset Sentinel 9000010010.

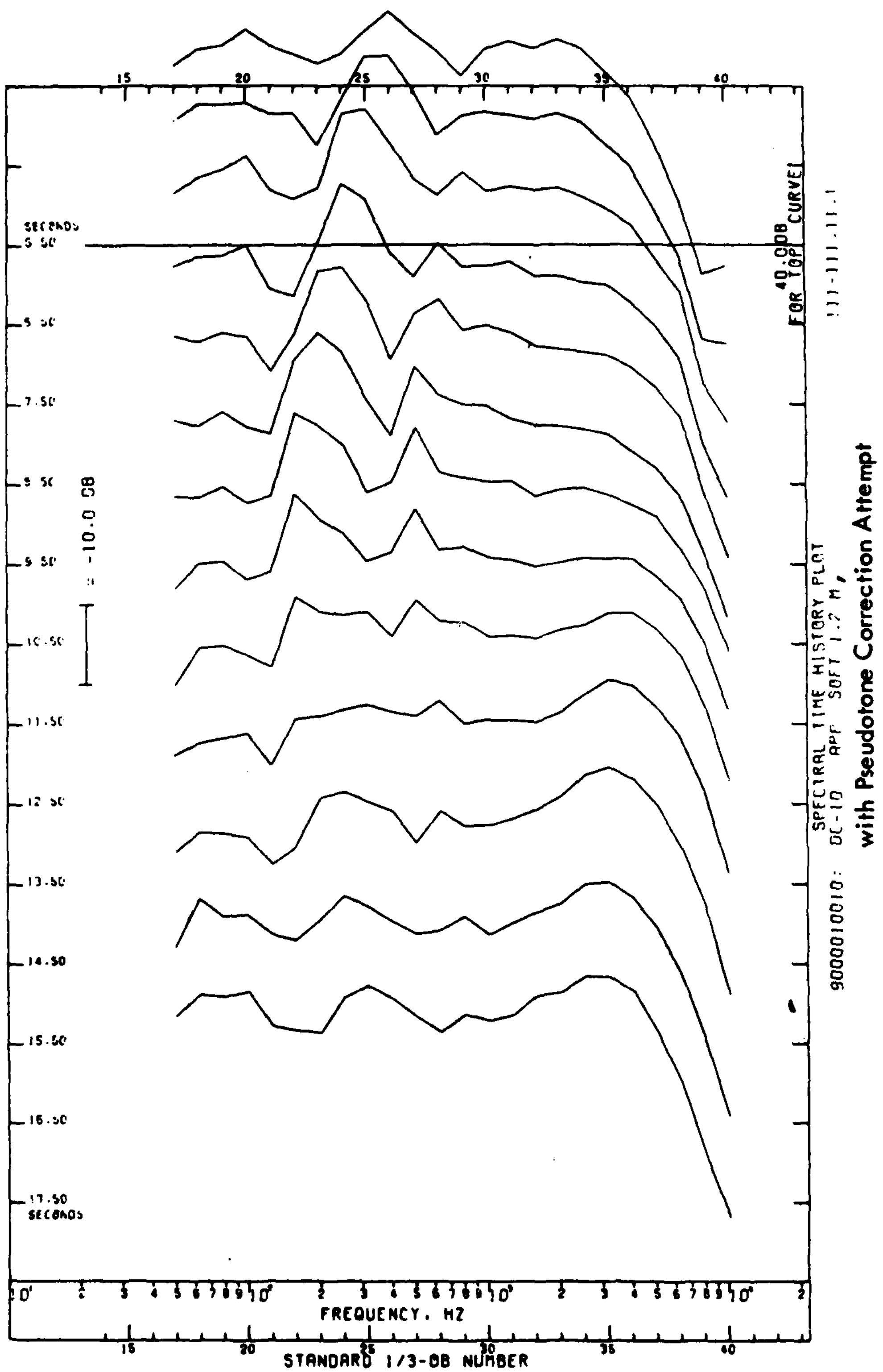

Figure 1-11. Spectral Time History of a DC-10 Sideline Approach after Reflection Correction

(c) B727 on Takeoff

Figure A-G2 (page A-80) shows the spectral time history for the 10-dB-down interval as measured by a microphone 1.2 m over hard ground. The reflection interference pattern is easily discernible. Aircraft position was obtained through the FAA's Aircraft Radar Tracking System (ARTS) at LAX (Los Angeles International Airport). The result of the correction attempt is shown in Figure 1-12. It may be seen that there was moderate success in the lower (i.e., later) part of the spectral time history in removing the interference pattern. However, in the early portion (top part of Figure 1-12) the correction is, so to speak, "out of phase," i.e., increasing the peaks and troughs rather than removing them. The lower part's moderate success indicates that the correction's magnitude was about right, and that aircraft position was known with sufficient accuracy for the part of the time history when the aircraft was receding from the microphone. The failure in the early part was probably caused by inaccuracies in aircraft position data: the ARTS radar provides position data at intervals of somewhat less than 5 seconds; in the critical area (top of Figure 1-12) several ARTS points were missing so that the aircraft's flight path was not known with sufficient accuracy. However, other problems as discussed for the DC-10 approach may also play a role.

Discussion of Problems

In the present form, the analytical reflection correction procedure does not perform satisfactorily. While we believe that there is no fundamental error in the analytical procedures, they do not take account of several physical phenomena which may, singly or together, cause significant departures from the assumed idealized conditions of the analysis:

- Refraction of sound waves due to vertical temperature and wind gradients in the atmosphere may change (both increase or decrease) the actual angle of incidence, which results in a pathlength difference different from that of the idealized condition; hence a

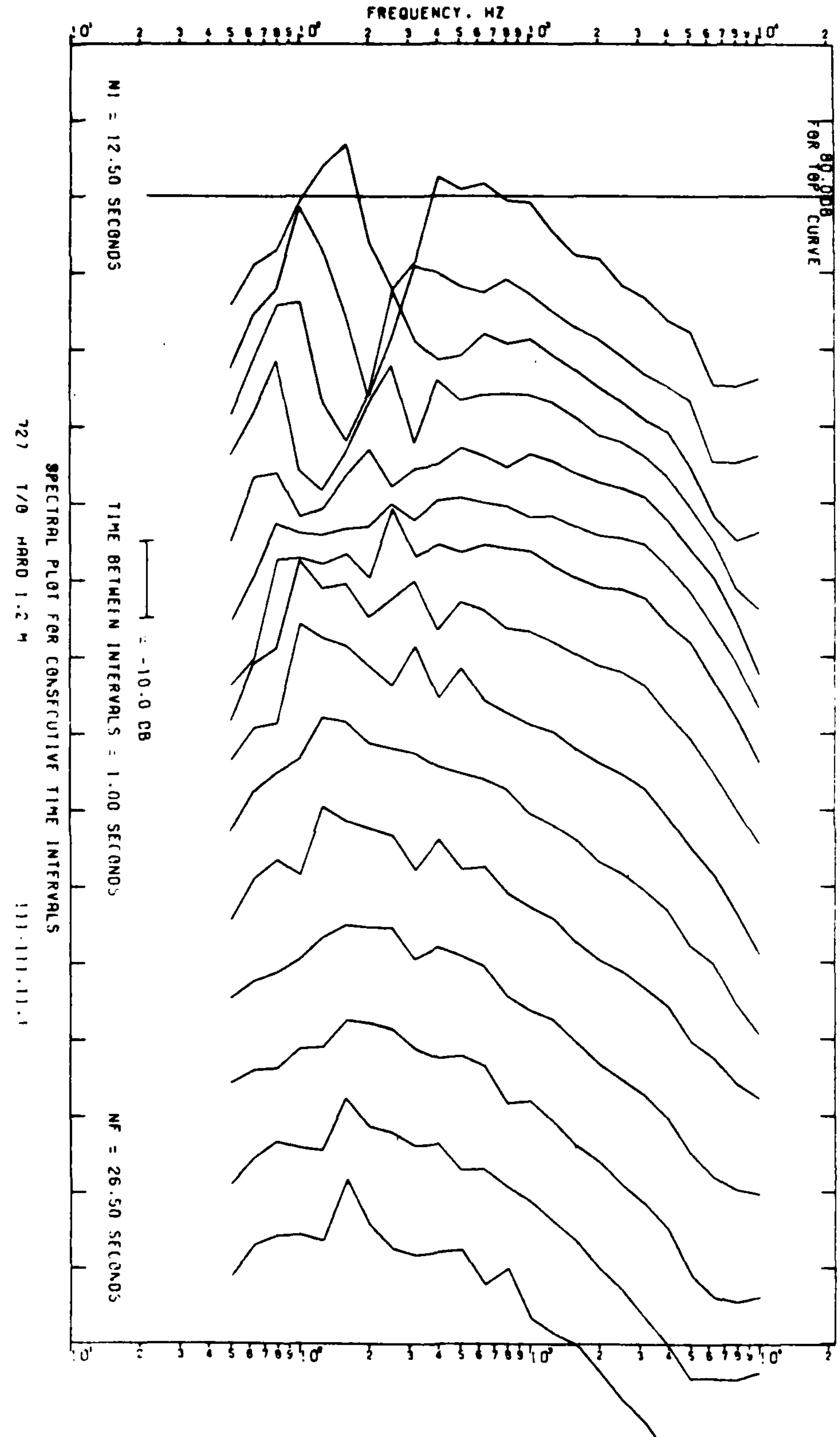

Figure 1-12. Attempted Reflection Correction of a B727 Takeoff Spectral Time History.

shift on the frequency axis of the interference pattern might be observed. This phenomenon is only effective at large incidence angles, i.e., near grazing incidences, so that it would not account for any frequency shifts near the overhead position.

- The finite extent of the sound source would tend to even out the interference pattern's peaks and troughs since sound arrives simultaneously from a range of incidence angles. This might account for the often observed overcorrection of the pseudotone pattern. Note that for the case of the DC-10 on approach the distance between engines is about 1/4 of the aircraft's altitude.

- Microphone height: for hard ground (asphalt, concrete) there is no doubt about how to measure microphone height. For soft ground, there usually is no clearly defined boundary. What is the "effective" height over grass? At its tips, or at the roots? Notice that the B727 takeoff correction attempt (hard ground) was marginally more successful than that for the DC-10 (grass surface). However, this is in contrast to the success of the B727 correction (soft ground).

- Incorporation of the so-called "surface wave" in the theoretical model for ground reflection effects. This refinement is expected to be significant at low grazing angles (i.e., sideline positions).

By contrast, we believe that ground admittance need not be known with great accuracy because both "soft" and "hard" grounds appear "hard" to the relatively low frequencies at which pseudotones commonly occur. At high incidence angles, however (i.e., low elevation angles), the interference pattern moves to higher frequencies whence more accurate knowledge of ground admittance would be required. This may be another explanation for the failure of the DC-10 "sideline" approach correction. Finally, it should be pointed out that the only previously known attempt to analytically predict ground reflection effects for aircraft flyover signals also found that predictions were frequently not in agreement with observations (Reference 17). The one success (the B727 approach), however, encourages further future work on the subject. Refinements which will lead to more successes include:

- More accurate knowledge of source position with time;

- Finite source extent effects taken into account.

- Incorporate the effect of surface waves in the theoretical model.

1.3.3 Position Accuracy Requirements for Ground Reflection Correction

The analysis of the previous sections demonstrates that ground reflection strongly depends on the angle of incidence which continuously varies during a flyover. To a lesser extent, the correction also depends upon actual distance and surface impedance. In this section, we examine the accuracy with which the angle of incidence should be known in order to perform a reliable correction for PNLT calculation purposes. In practical terms, we examine the accuracy with which the noise emission location of the aircraft should be determined, i.e., without explicit mention of the angle of incidence.

The formula for the reflection correction is given in Step 8 of Section 1.3.2.1:

$$P_c = -10 \log_{10} (1 + G^2 + 2GBC \cos (a + kd))$$

Let p be any position coordinate of the aircraft. The error in P_c due to an error p in determining p may be expressed as:

$$e_{P_c} = \left| \frac{dP_c}{d\,p} \right| \quad p$$

In the worst case, the largest error happens to occur at a frequency with a sound level that dominates the PNL calculation. In that case, the final error e_f would equal e_P . However, we must also consider the tone correction to PNL which, again in the worst case, can be as much as one-third of the amount that the band level exceeds some average of the neighboring bands. An upper bound for the magnitude of the final PNLT error therefore is assumed to be:

$$e_f = \frac{4}{3} e_{P_c}$$

This is used in the subsequent discussions.

Introducing the incidence angle θ as an intermediate variable, the error e becomes:

$$e = \frac{4}{3} \left| \frac{d\,P_c}{d\,\theta} \frac{d\,\theta}{d\,p} \right| \Delta\,p$$

$dP_c/d\theta$ was derived formally from the equations in Section 1.3.2.1 with one simplifying assumption: the complex function F(t) (Step 5) equals 1. The details of these derivations are not presented here. The resulting formulas and equations were cast into a computer program which determined $dP_c/d\theta$ as a function of angle θ and frequency. For many values of θ (1 degree increments from 1° to 85°) the maximum absolute value Q of $dP_c/d\theta$ was determined. For a typical acoustically soft surface (surface flow resistivity of 300 cgs rayls/cm), this is plotted in Figure 1-13, and was fitted by least squares by the following function:

$$Q = 10^{-1.37602 + 0.682675 \times 10^{-1}\,\theta - 0.117608 \times 10^{-2}\,\theta^2 + 0.787710 \times 10^{-5}\,\theta^3}$$

(where θ is in degrees).

The same procedure was applied to an acoustically hard surface (surface flow sensitivity of 10^5 cgs rayls/cm) resulting in the following fit:

$$Q = 10^{-1.41795 + 0.731505 \times 10^{-1}\,\theta - 0.135248 \times 10^{-2}\,\theta^2 + 0.980011 \times 10^{-5}\,\theta^3}$$

Rearranging the above equation for e and choosing particular values for a tolerable e, we may write

$$\Delta p = \frac{\frac{3}{4}\,e}{Q \left| \frac{d\theta}{dp} \right|}$$

Choosing the position variable p to indicate either vertical or horizontal directions, graphs like the ones shown in Figures 1-14 and 1-15 result. The data in these figures were actually obtained directly from the computer listings from which the above Q-θ relations were derived. The arrangement on these graphs was chosen such as to be able to choose any maximum error e (numbers in dB on top of middle section) and immediately find the vertical and horizontal position tolerances for a particular angle of incidence. These tolerances can then be compared with the vertical and horizontal position resolution of an aircraft tracking system.

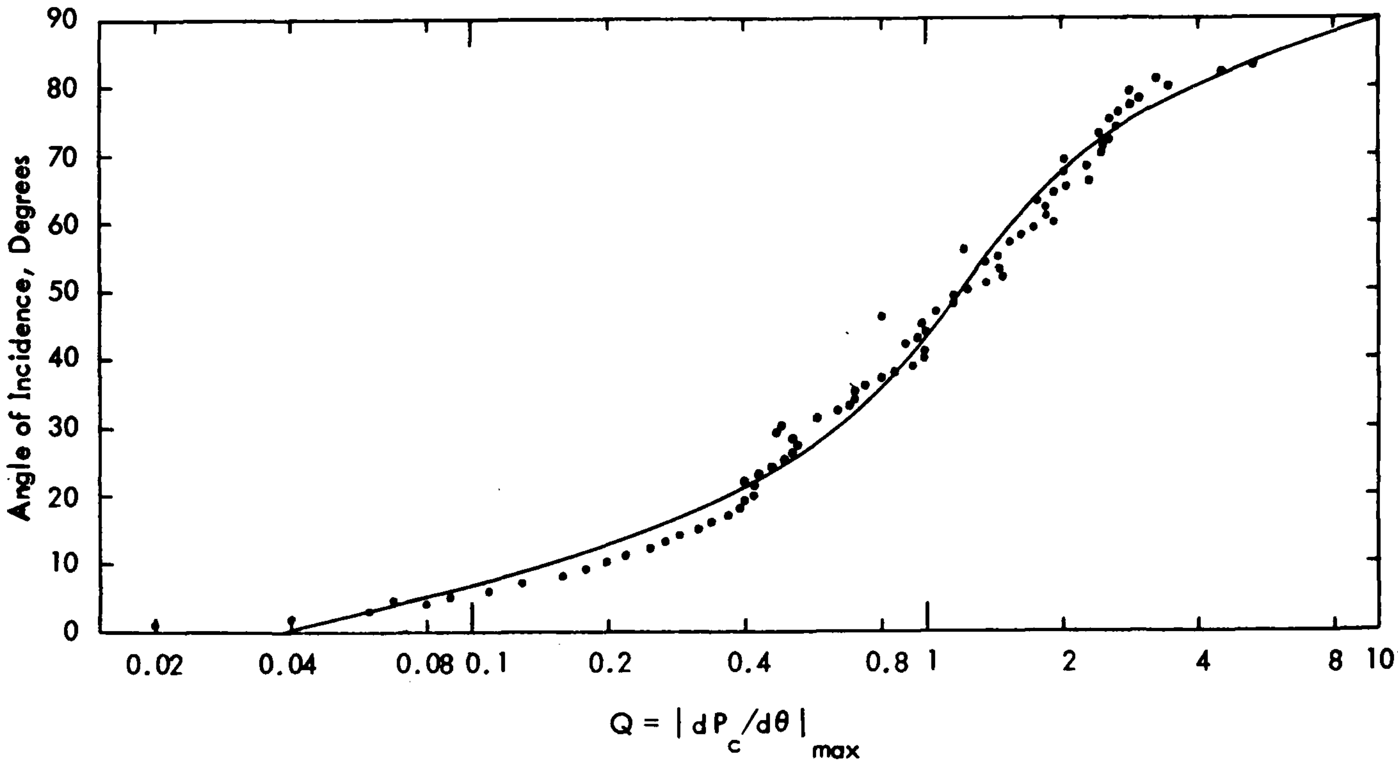

Figure 1-13. Relation Between Maximum Absolute Value of $dP_c/d\theta$ and Angle of Incidence θ for Soft Ground. Dots: Calculated from Reflection Theory. Full Line: Fitted Polynomial.

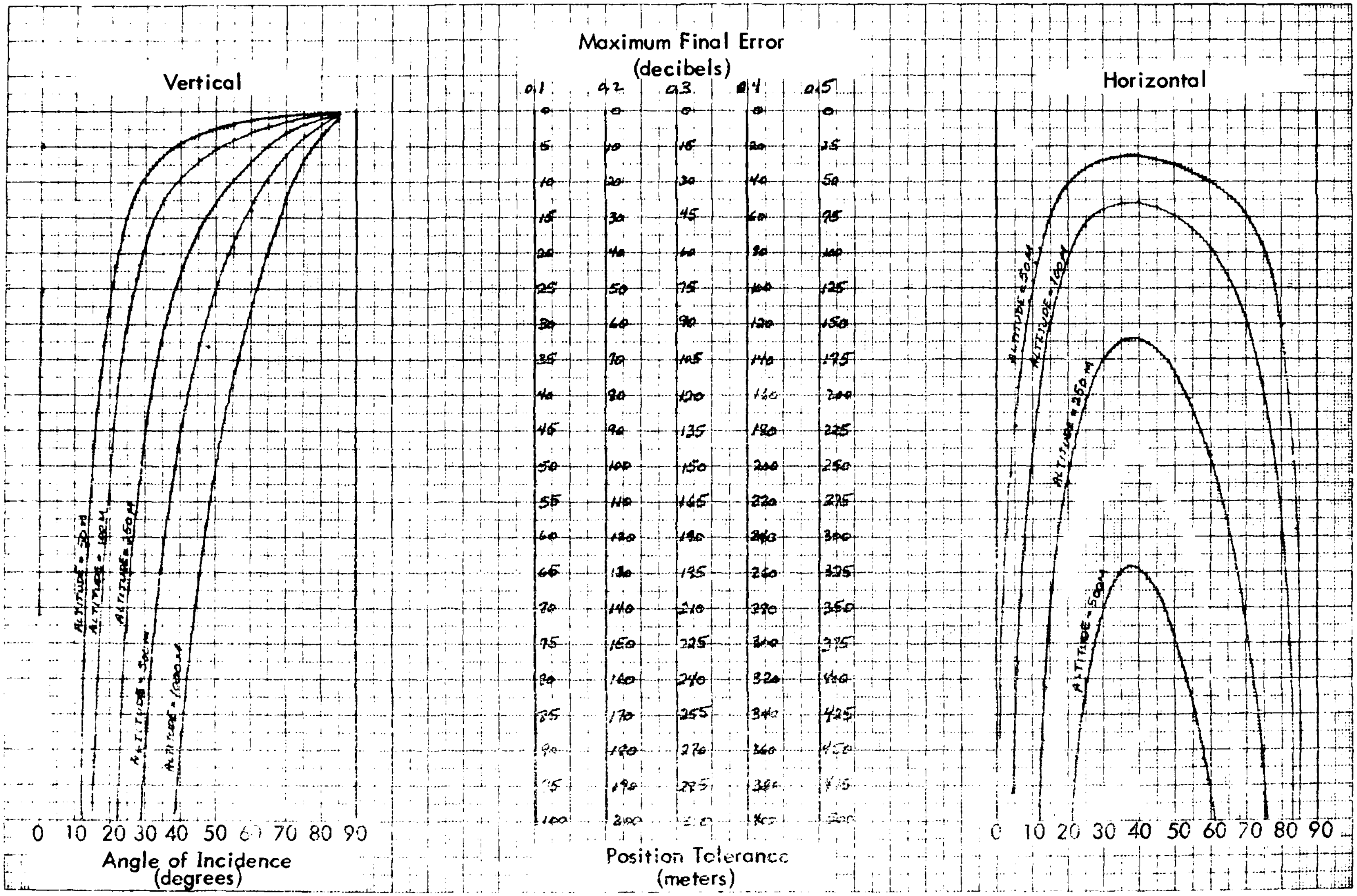

Figure 1-14. Nomogram for Determining Position Tolerance for Reflection Correction as a Function of Angle of Incidence and Altitude, Soft Ground.

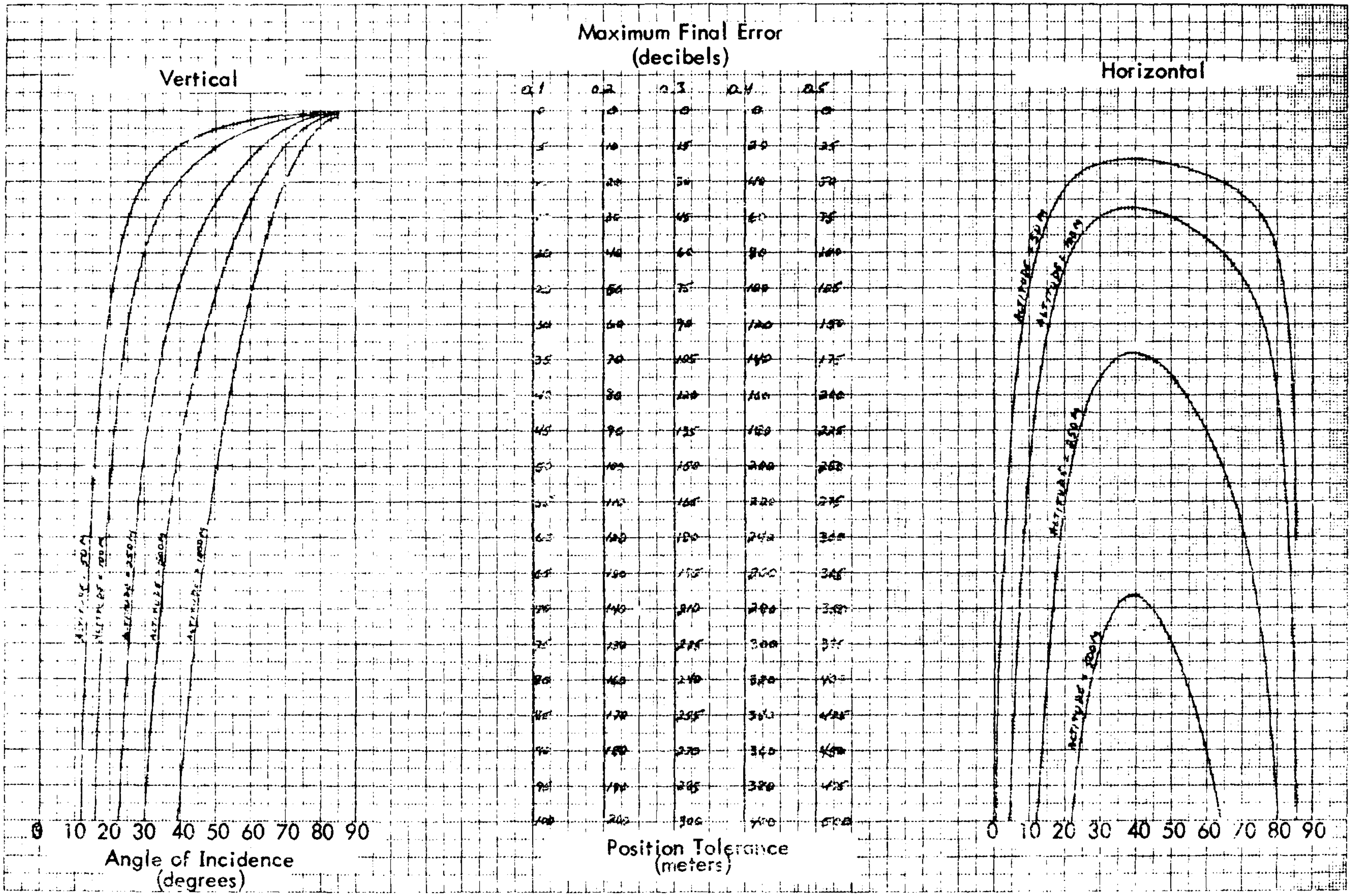

Figure 1-15. Nomogram for Determining Position Tolerance for Reflection Correction as a Function of Angle of Incidence and Altitude, Hard Ground.

Inspecting Figures 1-14 and 1-15, the following observations may be made:

- Near overhead (zero angle of incidence) position tolerances are large, both for vertical and horizontal deviations.
- For vertical deviations, position tolerance rapidly decreases with increasing angle of incidence, and tends toward 0 at grazing incidence.
- For horizontal deviations, the angles of incidence most sensitive to reflection correction are around 35 $\pm$ (10 to 20) degrees, the interval increasing with decreasing altitude.

As an example, consider the Aircraft Radar Tracking System (ARTS III) used by FAA at many busy airports. Its nominal vertical resolution is $\pm$ 50 feet $\doteq$ 15 meters, its nominal horizontal resolution is $\pm$ 0.005 nautical miles $\doteq \pm 10$ meters. Choosing e = 0.1 dB we can see that for an altitude of 100 m, angles of incidence of $\pm 40^{\circ}$ will have less than the specified error. That angle interval increases to $\pm 65^{\circ}$ for an altitude of 500 m. It appears, therefore, that, at least for overhead flyover, the ARTS system's resolution should be sufficient for defining an aircraft's position for applying the reflection correction. However, there exists other problems concerning application of a reflection correction which are further discussed in Section 1.3.2.3.

1.3.4 Frequency Cutoff Technique

This technique attempts to compensate for the occurrence of pseudotones by restricting the range of frequencies within which tone corrections may be calculated, while PNL itself is calculated over the entire frequency range. Currently, FAR Part 36 allows cutting off any tone corrections below 800 Hz if it can be demonstrated that there are no real tones below that cutoff which might cause a greater tone correction than any tones above the cutoff.

In order to investigate the effect of various cutoff frequencies, many pseudotone contaminated spectral time histories from the aircraft flyovers recorded at LAX were subjected to an EPNL analysis allowing the cutoff to take on the following values: 50 Hz (no cutoff), 400 Hz, 800 Hz, 1600 Hz.

Table 1-3 shows the results listing the differences between EPNL's with and without tone correction cutoff. Nonzero differences indicate that for at least a portion of the spectrum within the 10-dB-down interval, there exist tones in the lower part of the spectrum, may they be pseudotones or real tones. Each individual flyover time history is identified by what is called a dataset sentinel which refers to corresponding spectral time history plots in Appendix A. Note that the datasets there are arranged in a sequence given by Table 1-7 to be found in Section 1.4.3.3. Some approach flights occurred displaced laterally by about 230 m (750 ft) from the overhead position. These are identified as "sideline" in Table 1-3. These flights are not representative of the FAR Part 36 approach measurement conditions, but they are included as a matter of interest.

With very few exceptions, the EPNL difference magnitudes are less than 0.5 dB. Since this is within expected measurement errors, one would be tempted to dispense with the subject and conclude that an application of frequency cutoff for tone correction has a negligible influence. However, during certification of large passenger aircraft, minute differences can decide passing or failing of FAR Part 36 requirements. Differences in EPNL values of the order of 0.1 dB are therefore important to the aircraft noise certification process.

Analyzing the results by aircraft type, it may be seen that, for the B707 (representing the four-engine narrow body low engine bypass ratio aircraft category), EPNL difference magnitudes are mostly zero or very small. This indicates the presence of strong tones above any tone correction cutoff, even for the takeoff condition where one might expect jet noise to dominate and mask tones. However, even if such masking did occur, the tone correction as presently prescribed by FAR Part 36 would still be added at full value (this appears to be a weakness of the tone correction procedure).

Table 1-3

Differences Between EPNL's Calculated with Various Tone Correction Lower Cutoff Frequencies
Ground Surface Hard Unless Otherwise Noted
EPNL Subscript Indicates Lower Cutoff Frequency (Hz) for Tone Correction

Microphone Location	Aircraft	Dataset Sentinel	$EPNL_{50}$ - $EPNL_{400}$ dB	$EPNL_{50}$ - $EPNL_{800}$ dB	$EPNL_{50}$ - $EPNL_{1600}$ dB
Approach 1.2 m	B727 (Soft Surface)	19010	0.04	0.04	0.04
	B727	21010	0.00	0.00	0.00
	B727 (Soft Surface)	42010	0.06	0.06	0.06
	B727	50010	0.08	0.10	0.16
	B707 (Soft Surface)	41010	0.00	0.00	0.00
"Sideline"	B707 (Soft Surface)	43010	0.00	0.00	0.00
	B707	49010	0.00	0.00	0.00
"Sideline"	B707	51010	0.00	0.00	0.00
"Sideline"	DC-10	14010	0.00	0.28	0.31
"Sideline"	DC-10 (Soft Surface)	17010	0.00	0.34	0.38
	DC-10	48010	(0.24)*	(0.83)	(1.06)
Sideline, 1.2 m	B727	29010	0.02	0.24	0.26
	B727	64020	0.07	0.24	0.43
	B707	65020	0.00	0.00	0.00
	B707	26010	0.00	0.00	0.00
	B707	27010	0.02	0.06	0.11
	DC-10	66010	(0.02)	(0.03)	(0.04)
	DC-10	67010	0.07	0.11	0.11

Table 1-3 (Continued)

Microphone Location	Aircraft	Dataset Sentinel	$EPNL_{50} - EPNL_{400}$ dB	$EPNL_{50} - EPNL_{800}$ dB	$EPNL_{50} - EPNL_{1600}$ dB
Sideline, 10 m	B727	28010	0.08	0.08	0.13
	B727	60020	0.36	0.37	0.38
	B707	24010	0.00	0.00	0.20
	B707	25010	0.08	0.08	0.29
	B707	61020	0.00	0.00	0.00
	DC-10	62020	(0.08)	(0.08)	(0.08)
	DC-10	63020	0.09	0.16	0.16
Takeoff, 1.2 m	B727	36010	0.20	0.54	0.54
	B727	92020	0.01	0.20	0.25
	B707	94020	0.00	0.00	0.00
	B707	95020	0.00	0.00	0.00
	DC-10	96020	0.06	0.12	0.12
	DC-10	97020	0.13	0.23	0.24
	B747	91020	0.00	0.00	0.00
	B747	93020	0.00	0.00	0.00

* Numbers in parentheses are derived from EPNL values calculated from incomplete spectral time histories (i.e, at least one of the 10-dB-down points of the PNLT time history was not reached).

The B727 represents the JT8D-powered aircraft. The trend for the EPNL differences here is: very small for approach, larger for sideline and takeoff. This is more of an expected trend: on approach the high-pitch fan tones dominate the tone correction; on takeoff, pseudotones may cause greater tone corrections than real tones.

The DC-10 and B747 represent the wide body high bypass ratio aircraft. The B747 takeoffs are obviously tone correction dominated at higher than the cutoff frequencies. For the DC-10, EPNL differences are generally larger than for other aircraft types. This could either be because there exist real tones in the lower part of the spectrum, or due to pseudotones. Knowing the noise emission characteristics of a high bypass ratio engine, the likely situation is a combination of both real and pseudotones. However, inspection of the spectral time history plots of Appendix A indicates that pseudotones are mostly responsible for low frequency tone corrections.

It is difficult to derive general recommendations from the above results. For overhead flyovers (approach, takeoff) the method of restricting the frequency range above of where pseudotones occur does work quite well providing there are no real tones below that range. For sideline, the angle of incidence is usually so large as to push the pseudotones up into the vicinity of real fan, turbine, or compressor tones if the 1.2 m microphone height is used. <u>In this case, a frequency cutoff technique cannot be used</u>. For the 10 m microphone and sideline, pseudotones occur in about the same frequency range as for the 1.2 m microphone for overhead flyovers, so that this technique may again be applied. However, there are other reasons that make this frequency cutoff method unattractive:

- The effects of pseudotones are not corrected for, but simply "evaded" as far as the tone correction is considered. PNL still is calculated in the presence of the pseudotones.
- A narrow band analysis (not done in this study) must be performed to prove the absence of real tones below the cutoff frequency.
- The method cannot be applied generally for all aircraft types such as propeller and rotor aircraft which usually exhibit strong tones in the lower frequency regions.

Section 1.5 attempts to strike a balance between the various pseudotone correction procedures considered in this study, and incorporates the results of this section.

1.4 Instrumentation Correction Techniques

We will define instrumentation correction techniques for pseudotones as those procedures which are applied either by physical arrangement of the measurement setup, or are applied to the instantaneous acoustic signal before it enters a frequency decomposition device. These solutions are attractive because no analytical corrections will be necessary when the data is reduced. The raw data will reflect only noise due to the source (aircraft) and therefore should be less dependent on the measurement site than data contaminated by reflections.

As discussed in Section 1.1, the pseudotones exist due to an interaction of the incident noise with the ground plane. The actual pseudotones which occur are a function of the impedance of the ground plane, the position of the aircraft in relation to the microphone, and the height of the microphone above the ground plane. Alternate measurement techniques could be designed to alter one or more of these parameters in order to reduce or eliminate the effect of pseudotones. Possible techniques are:

- Surface or flush-mounted microphone
- Elevated microphone
- Simulated "anechoic" ground plane
- Highly directional microphone
- Moving microphone array
- Real time electronic cancellation system
- Real time impedance cancellation system

1.4.1 Overview of Methods (See Table 1-4)

a. Surface or Flush-Mounted Microphone

The microphone is either mounted directly into the ground surface so that its diaphragm is in the same place as the surface, or it is laid on the surface with the diaphragm perpendicular to the ground surface, or it is pointed down towards the ground surface and fixed at a very small distance from it (usually 1/2 inch).[2, 8]

Table 1-4

Instrumentation Pseudotone Correction Procedures

	Measurement Technique	Advantages	Disadvantages	Now Used
1	Surface or Flush-Mounted Microphone	- No spectrum-distorting ground reflections - Easy accessibility to microphone for calibration and servicing - Improved resolution of low discrete frequency noise - Data compatibility between sites	- Size and smoothness of reflection plane must be regulated - Adverse effects of transmission path irregularities induced by strong wind and temperature gradients near surface - Possible high frequency losses for angles nearing grazing incidence	In conjunction with other microphones for static testing
2	Elevated Microphone	- Little or no spectral distortion - No correction necessary to raw data - No surface restrictions	- Poor accessibility to microphone for calibration and servicing - Microphone wind noise problem increases with elevation - Awkward to set up and take down equipment	Yes
3	Anechoic Ground	- Little or no ground reflection - No correction necessary to raw data - Federally accepted 1.2 meter microphone height may be used - Easy accessibility to microphone - Data compatibility between sites	- Size and absorption of reflecting surface must be regulated - Not highly portable - Possible damage from weather elements (sun, wind, rain) - Not easily adaptable to flyby tests	For static tests only
4	Highly Directional Microphones	- Ground reflections greatly reduced or eliminated	- Aircraft tracking system required - Side lobes could cause problems - Corrections required for nonuniform frequency response of microphone	No
5	Moving Microphone Array	- Ground reflections could be averaged out of the data - Approximate adherence to 1.2 meter microphone height is maintained	- More complex system – field repairs more difficult - Awkward mechanical system required to move array	Not Widely
6	Real Time Electronic Cancellation System	- 1.2 meter microphone height can be maintained - No corrections to spectral raw data	- Very complex system – field repairs may be impossible - Aircraft tracking system required - Microprocessor development work required	No

This technique nearly eliminates the reflected wave problem (see Section 1.4.3.1 for a further discussion on expected performance of a ground microphone). Pressure doubling occurs at the ground surface (assuming it is rigid) which increases the signal by 6 dB relative to free field. A series of spectra obtained with this technique is shown in Figure 1-16 which should be compared with the earlier Figure 1-3 showing spectra measured simultaneously with a 1.2 m microphone. The absence of pseudotones for the flush-mounted microphone is striking.

This is a very attractive technique because it is relatively simple to set up and the microphone is easy to get at for calibration. In addition, data should be compatible between measurement sites. However, the effects of surface smoothness and size as well as the often strong refractive effects of wind and temperature gradients very near the surface are not well understood.

b. <u>Elevated Microphone</u>

The pseudotones which are observed in aircraft flyover noise signatures are a function of the height of the microphone above the reflecting surface. If the height of the microphone is increased to 10 meters or so, pseudotones are pushed down in frequency to a range we are not interested in (except for sideline; see Figure 1-25 in Section 1.4.3.1). This technique would allow measurements to be taken over almost any ground surface. The main drawback of this technique is that access to the microphone is awkward. Calibration and setup are less convenient, although manageable. In addition, a 10 meter or higher structure could be undesirable near an airport. Nevertheless, one major aircraft engine manufacturer strongly advocates this technique.[9, 23, 27]

c. <u>Anechoic Ground</u>

This technique is now being used for some static aircraft engine testing and it involves applying absorptive material or an anechoic section consisting of sound-absorbing wedges on the ground surface where the reflections would occur.[15] This method eliminates the reflected wave and hence the pseudotones and also maintains the 1.2 meter microphone height which is convenient for access and above the strongest flow and thermal gradients near the ground. However, for flyover measurements, the amount of absorptive material required may be prohibitive, or the anechoic section would have to move with the aircraft position.

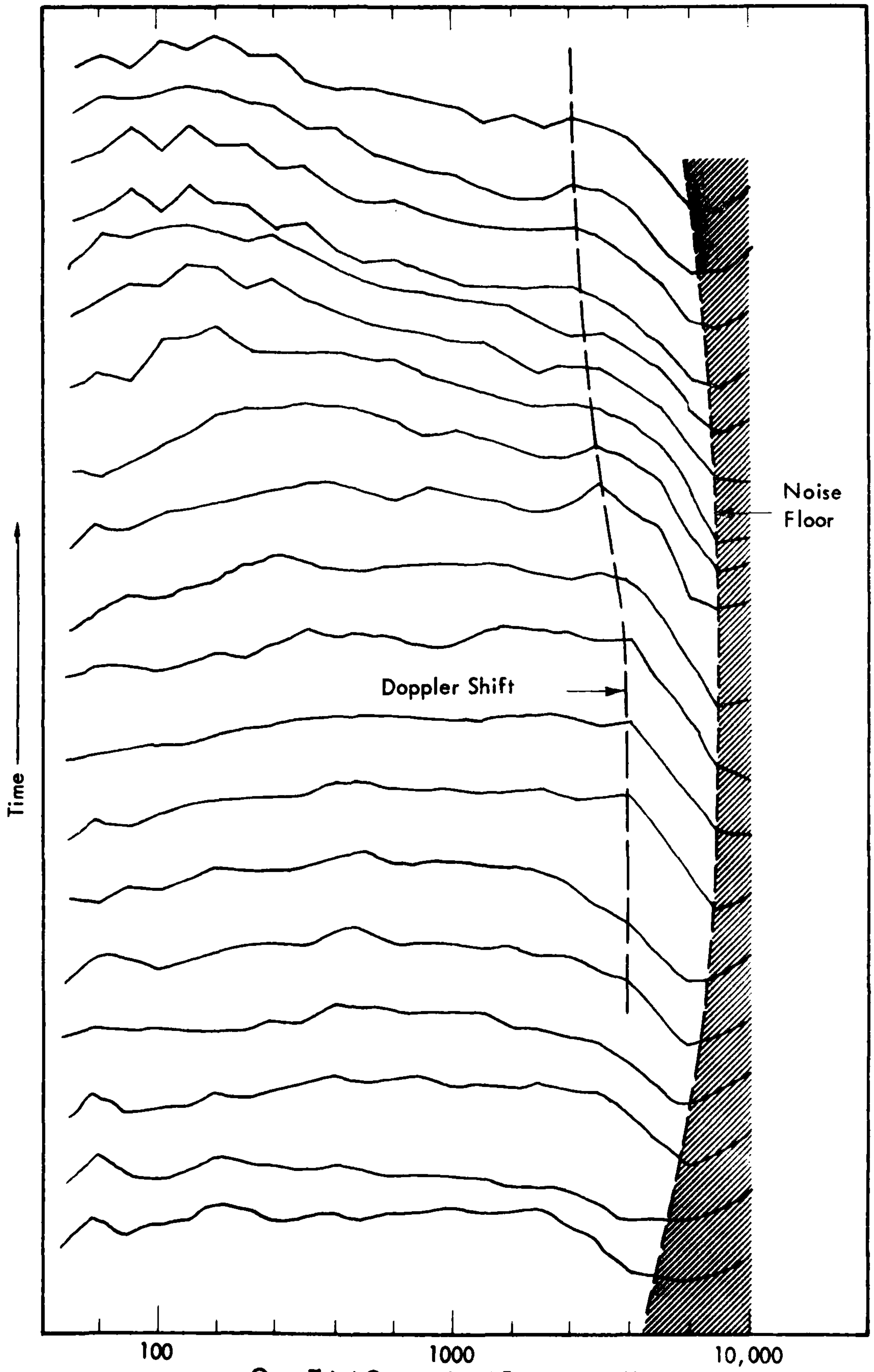

Figure 1-16. Flyover Spectra at 1/2 Second Intervals, Ground Level Microphone (from Reference 2)

d. Highly Directional Microphone

If a highly directional microphone is pointed at the aircraft during the flyover, all but the direct sound will be virtually eliminated. This technique has an additional benefit in that acoustic ambient noise will be reduced. A method of tracking the aircraft with sound travel time delay would be necessary, and since the frequency response of directional microphones is usually nonuniform, a frequency correction would have to be applied during data reduction. Although current technology is available for implementing this approach, including the use of electronically steerable arrays, it is not a practical approach for general application at this time.

e. Moving Microphone Array

Microphones at differing heights which are multiplexed to obtain an average sound level will produce results in which the pseudotones are averaged and hence greatly reduced. Moving the microphones will reduce the probability that a pseudotone at a given frequency will continue to occur. This method would reduce the influence of ground reflections and make data more repeatable between measurement sites. There are several development problems associated with this method, one of which is designing a mechanical system which will move the microphones without producing mechanical noise or developing an electronic equivalent noise. Neglecting this substantial problem, considerable effort would also be required to standardize the dimensions and effective motion of the array.

f. Real Time Electronic Cancellation System

This method would include a microprocessor which would be fed data on the distance and position of the aircraft in order to calculate instantaneous reflection corrections and thereby suppress pseudotones at the input. This highly sophisticated system would be difficult to develop. However, once developed, it would produce very repeatable data. The system could be conveniently calibrated by feeding it a simulated, reflected wave only and checking that the output is zero. Since it would use reflection theory, this technique suffers from some of the drawbacks listed for the analytical reflection correction technique; in particular, surface impedance should be known as accurately as possible. Furthermore, the general lack of success in this program of applying an analytically-derived

correction in the data processing phase argues against use of this similar but real time approach.

1.4.2 Selection of Instrumentation Correction Techniques

The same criteria as listed at the beginning of Section 1.3.1 are used for selection of an instrumentation technique to eliminate or minimize pseudotones.

The technical feasibility of the surface microphone has been demonstrated. The accuracy of the method needs to be investigated. It is cheaply implemented, easily enforceable because appropriate specifications can be written straightforwardly, and it could be implemented on relatively short notice.

The technical feasibility of the elevated microphone technique has been demonstrated; its accuracy is controversial. It is not cheaply implemented because of the tower requirement and the awkward access to the microphone. The technique would be easily enforceable and could be implemented on relatively short notice.

The anechoic ground technique is technically feasible and very accurate if practically all reflections can be eliminated. It would be quite expensive as an outdoor rig would be required which effectively absorbs sound over most of the audible range and which would have to be very large (or moving with aircraft position) to cover all possible reflection points. Enforcement of this technique could turn into an administrative nightmare considering that the absorptive qualities of the surface would need to be demonstrated. The time frame of implementation would probably be several years including the development and construction of a suitable surface.

The use of a highly directional microphone would be technically feasible and probably very accurate. The technique would be expensive as the microphone would have to be pointed in the direction of sound arrival which is different from the optical aircraft position; some kind of computerized pointing system is probably required. Because of this complicated system, enforcement would be difficult, and it would take a long time to implement.

The real time electronic cancellation system may be technically feasible with a state-of-the-art digital processor modeling the time-domain transfer

function of the reflection process. It would be very expensive, probably difficult to enforce, and would take a long time to implement.

The above discussion clearly shows that there are two rather straightforward instrumentation correction techniques for pseudotones which show good promise of being successfully applied in routine aircraft noise certification measurements. These techniques are the flush-mounted and elevated microphones. These techniques are investigated in more detail in the subsequent sections of this report.

1.4.3 Surface and Elevated Microphones

Smith (Reference 23) and McKaig (Reference 2) have given excellent reviews of the uses and effects of surface and elevated microphones, both also reporting measured data. Here, their results, conclusions and recommendations are combined with theoretical considerations and with experimental evidence collected under this study.

1.4.3.1 Theoretical Considerations

It is instructive to study first some theoretical results obtained by applying the reflection algorithm given in Section 1.3.2.1 to the surface and elevated microphones. A simple way to mount a surface microphone is to invert it and position the diaphragm at a very small distance, say, 1/2 inch, from the ground surface. Under the assumption of an infinitely large and plane surface of large impedance (flow resistivity 10^5 cgs rayls/cm), and a point microphone, Figure 1-17 shows what correction would need to be added to the measured signal in order to obtain free field conditions. It is seen that, particularly near the overhead position (small angle of incidence), that correction is not even near the expected -6 dB for high frequencies (4 kHz and up) often strongly contributing to PNL.

This problem could be circumvented by mounting the microphone truly flush with the ground surface. This usually necessitates mounting the microphone through a board or panel. The minimum size requirements for such a panel can be estimated from diffraction theory. Figure 1-18 is taken from Reference 24. It indicates that the product of wave number K and disc radius a should be at least 10 in order to acoustically simulate an infinite plane. This translates into the following requirement:

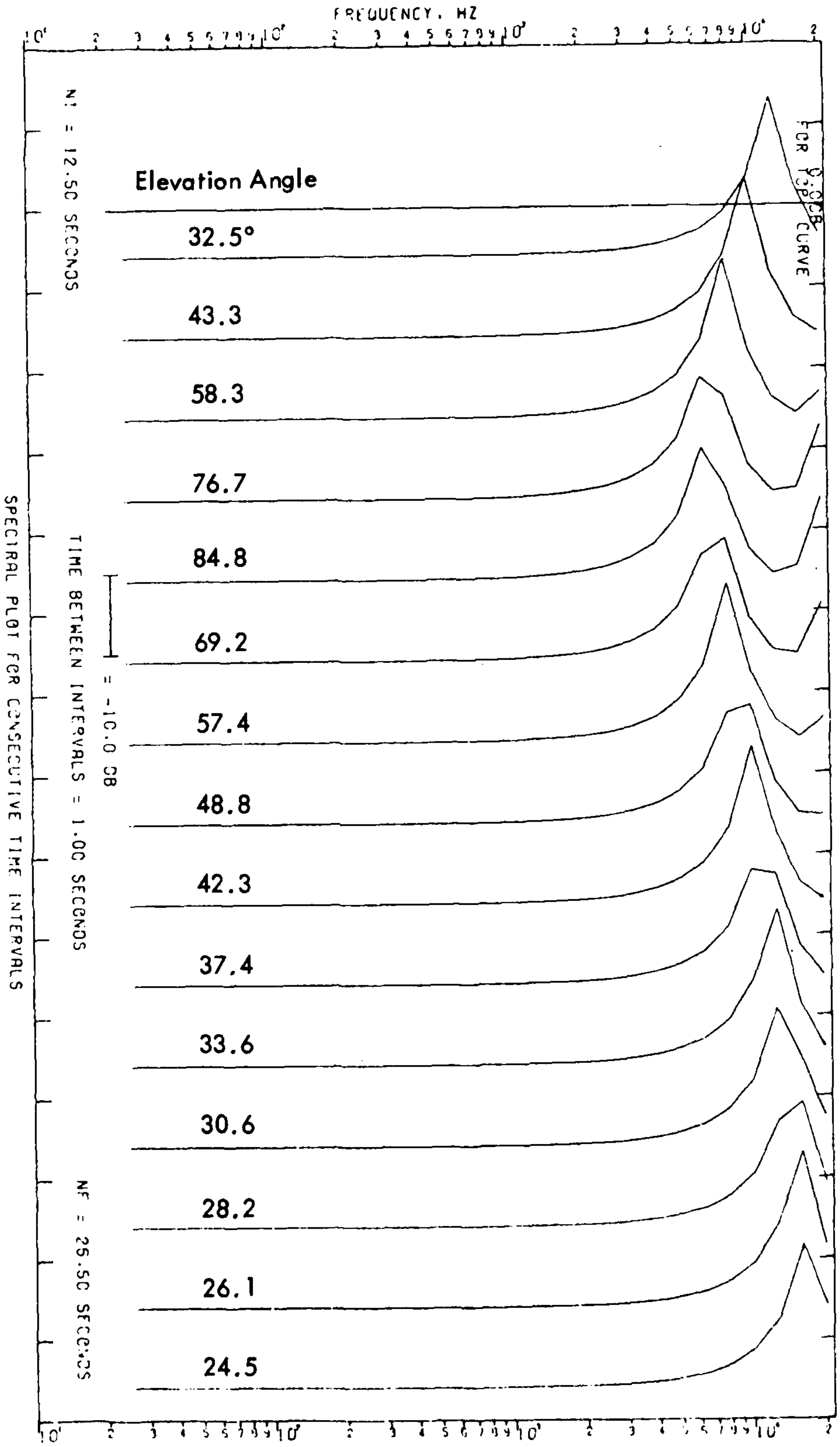

Figure 1-17. Plot of Spectral Time History of Reflection Correction for a Simulated Takeoff Condition: Climb Angle 6°, Altitude at Overhead 244 m, Speed 80 m/sec, Microphone Height 1/2 inch.

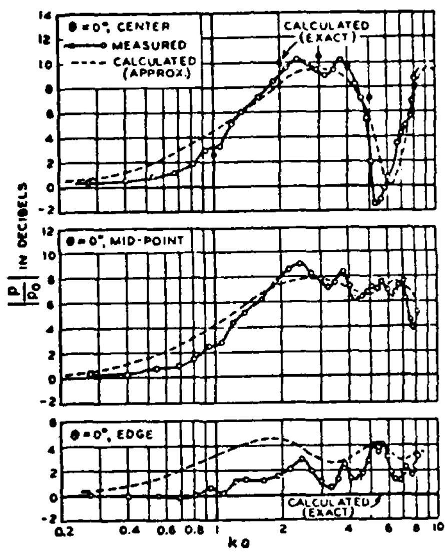

Figure 1-18. Showing |p/p0| in Decibels vs Frequency for three Points on the Disk and $\theta = 0$, Together With the Theoretical Values (from Reference (24).

disc radius should be greater than (10 times speed of sound) / ($2\pi f$)

where f is frequency. The lowest frequencies of interest are around 50 Hz. With 343 m/sec for the speed of sound, the minimum disc diameter becomes about 22 m (about 70 feet), a very large disc indeed. Even if requirements could be relaxed by a factor of 2 or 3 (by strategically placing the microphone on the panel, giving the panel a noncircular shape, raising the lowest frequency of interest), the panel size would still be quite large. At permanent stationary test installations this may quite easily be accomplished by imbedding a small panel flush into a larger hard surface (asphalt or concrete). A portable system seems indeed difficult to realize.

Turning towards the elevated microphone, let us compare Figures 1-8, 1-19, and 1-20, which demonstrate (for a soft surface) how the interference pattern moves to lower frequencies as the microphone height is increased from 1.2 m to 5 m and 10 m. The pattern in the vicinity of the overhead position is of course most important since noise levels are greatest there. Whereas the 5 m location still shows significant corrections above 50 Hz (8-th and 9-th spectra from left of Figure 1-19 are closest to overhead), the effect at 10 m can be termed almost negligible at overhead and is conditionally acceptable further away from overhead; the word "conditionally" is inserted because the reflection effects may be unacceptable in the case of a very directional source where the strongest flyover noise level occurs away from overhead, possibly in a region where even the pseudotones for a 10 m microphone height may not have a significant influence on EPNL.

Figure 1-21 portrays the same case as Figure 1-20 except that the acoustic surface impedance is very large simulating a rigid surface. At low frequencies there is hardly any difference between soft and hard ground, i.e., soft grass acts like a hard surface. At higher frequencies the soft surface absorbs much or most of the sound (approximately 0 dB correction) whereas the hard surface reflects it (about -3 dB correction to free field).

The preceding discussion applied to overhead flyovers. Both the ground microphone and elevated microphone are reasonably free of pseudotones. The elevated microphone also avoids possible panel diffraction problems which may occur with a casual ground microphone installation. At sideline conditions, the

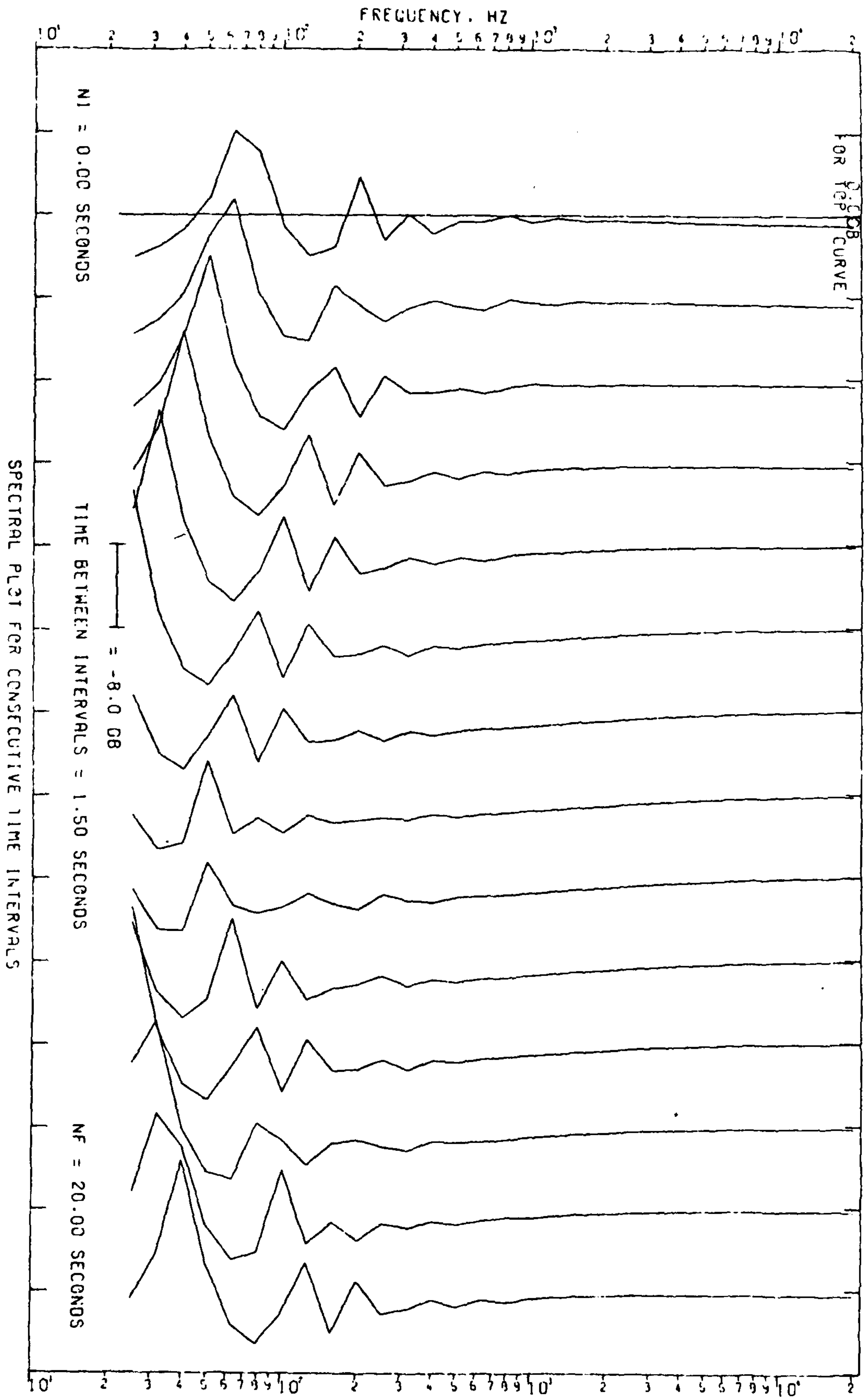

Figure 1-19. **Reflection Correction Spectral Time History. Microphone Height 5 m, Specific Impedance Calculated from Surface Flow Resistivity = 100 cgs rayls/cm. Imaginary Part of Impedance Is Negative.**

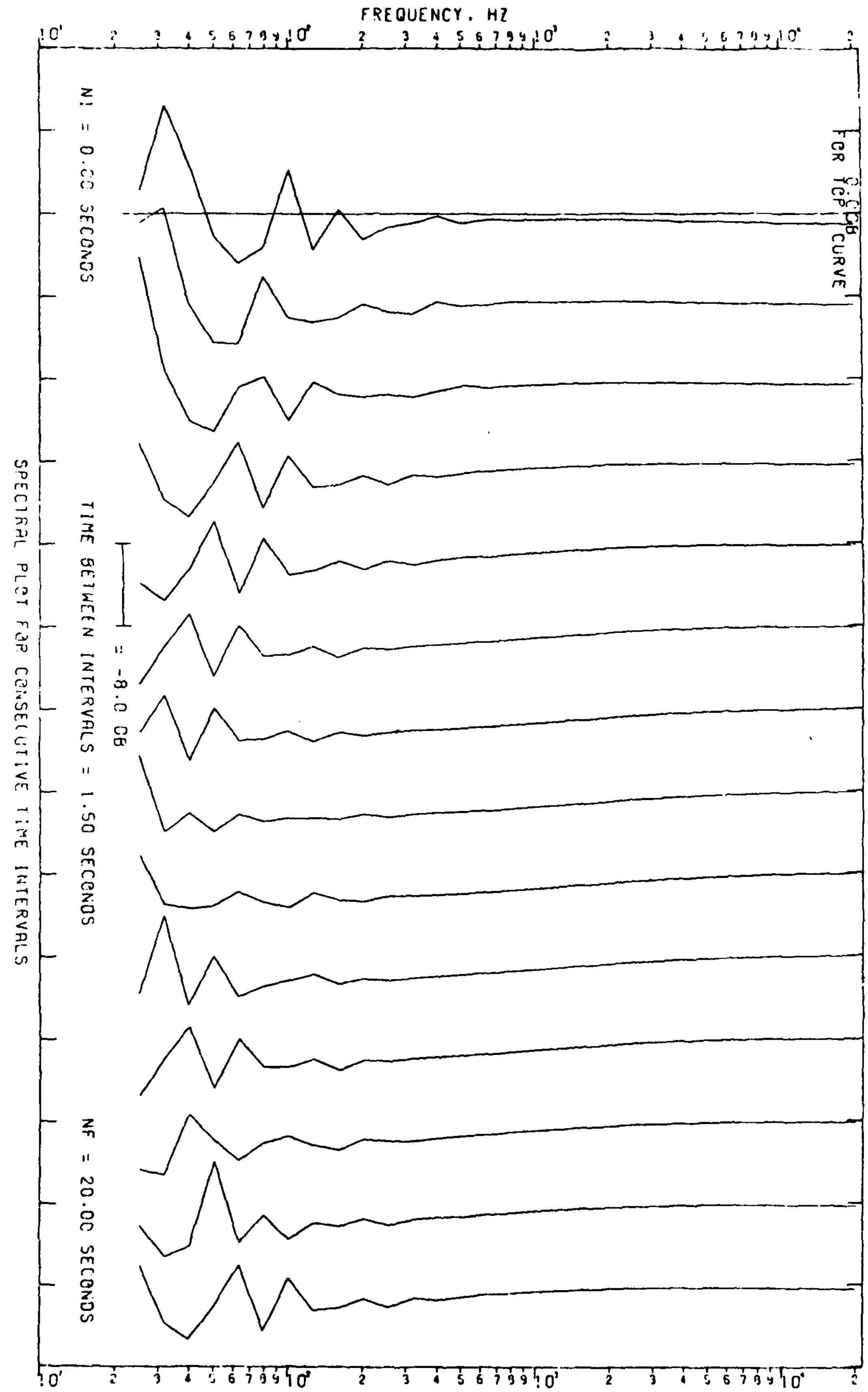

Figure 1-20. **Reflection Correction Spectral Time History. Microphone Height 10 m, Specific Surface Impedance Calculated from Surface Flow Resistivity = 100 cgs rayls/cm. Imaginary Part of Impedance is Negative.**

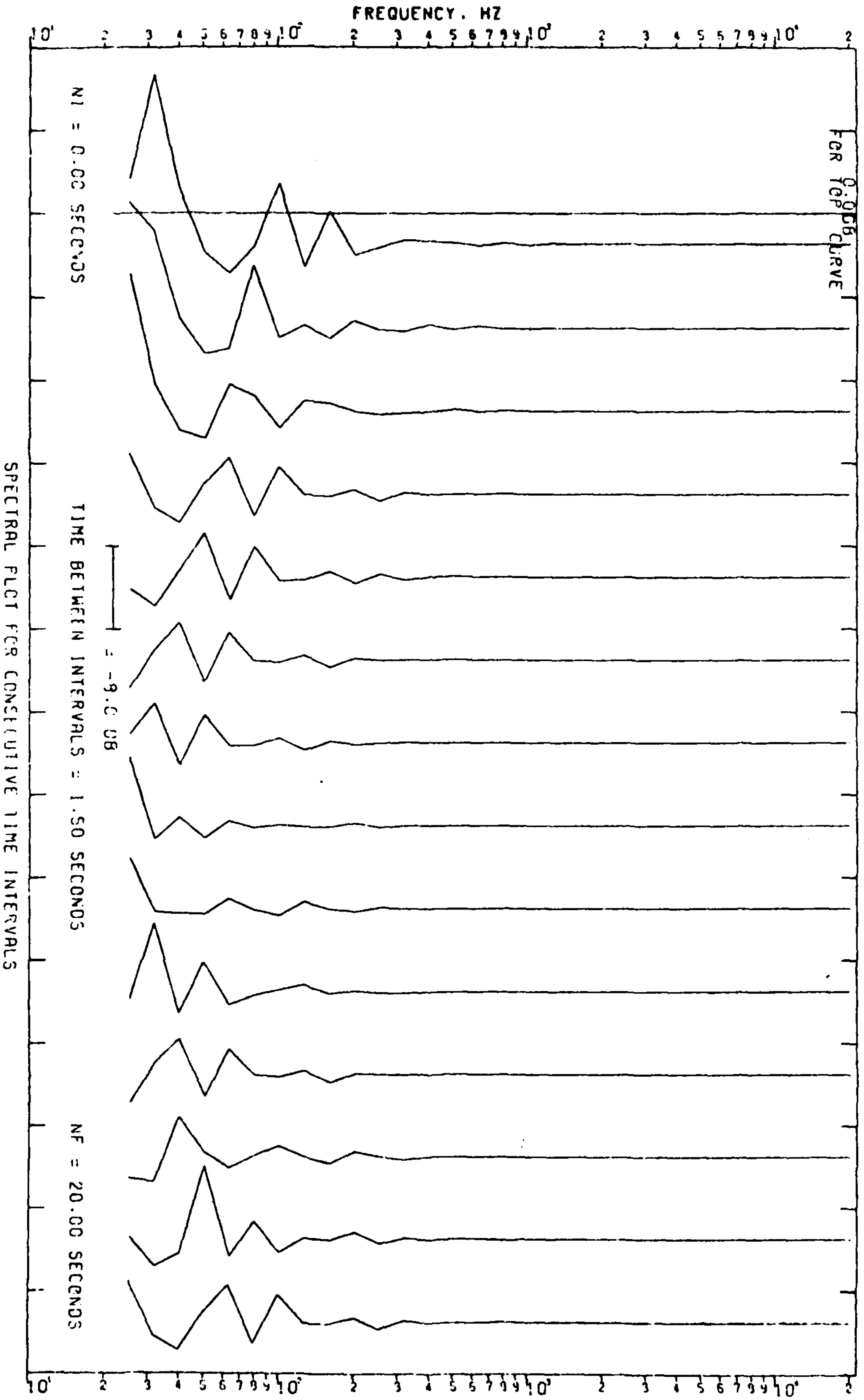

Figure 1-21. **Reflection Correction Spectral Time History. Microphone Height 10 m, Constant Specific Surface Impedance = 1000 + 0i**

theoretically predicted interference patterns look very different. Figure 1-22 shows the reflection correction for a simulated takeoff: climb angle is 9^{o}, at the sideline measurement point, the elevation angle is 20^{o} and the aircraft altitude and speed are 200 m and 80 m/sec, respectively. Ground was assumed soft with a flow resistivity of 300 cgs rayls/cm; the associated impedances/admittances as a function of frequency are shown in Table 1-5. Microphone height is 1.2 m. Near grazing incidence (90^{o} angle of incidence, 0^{o} elevation angle), the correction shows a broad hump centered around 400 Hz. This hump begins to clearly develop at elevation angles of about 5^{o} and below. Such behavior can be observed in measured spectra which show a marked deficiency in the same frequency region for sound which has traveled horizontally over acoustically soft ground. The latter part of the spectral time history of Figure 1-2 shows the pseudotone interference pattern as has been observed before. The pattern in the early part, however, moves up to higher frequencies as should be expected from the reduced path length difference between direct and reflected waves (note that this implies that the analytical pseudotone correction technique consisting of disregarding tone corrections to PNL below a certain frequency may fail on sideline).

The input to Figure 1-23 differs from that of Figure 1-22 merely by the nature of the ground which is assumed hard with a flow resistivity of 10^{5} cgs rayls/cm. The resulting impedances/admittances are shown in Table 1-6. Note that the grazing incidence hump develops at much higher frequencies. This case is, however, hardly of practical significance as sideline propagation will most frequently occur over acoustically soft ground.

The spectral time history plot for the reflection correction at sideline conditions for the surface microphone (assumed to be truly flush mounted in an infinite acoustically soft surface) does not, of course, show any pseudotone pattern, but it also is not, by any means, constant. A correction to free field would have to account for ground absorption which is what Figure 1-24 displays. If one were to place a large hard disc (10 m diameter or so) around the microphone, the theoretical handling of the case of near grazing incidence would be made very difficult or impossible since sound waves traveling horizontally (or almost so) will encounter a surface impedance discontinuity. This analysis therefore suggests that, if a surface microphone is at all used for sideline measurements, it be placed right on the soft surface. An attempt could then be made to correct for ground absorption.

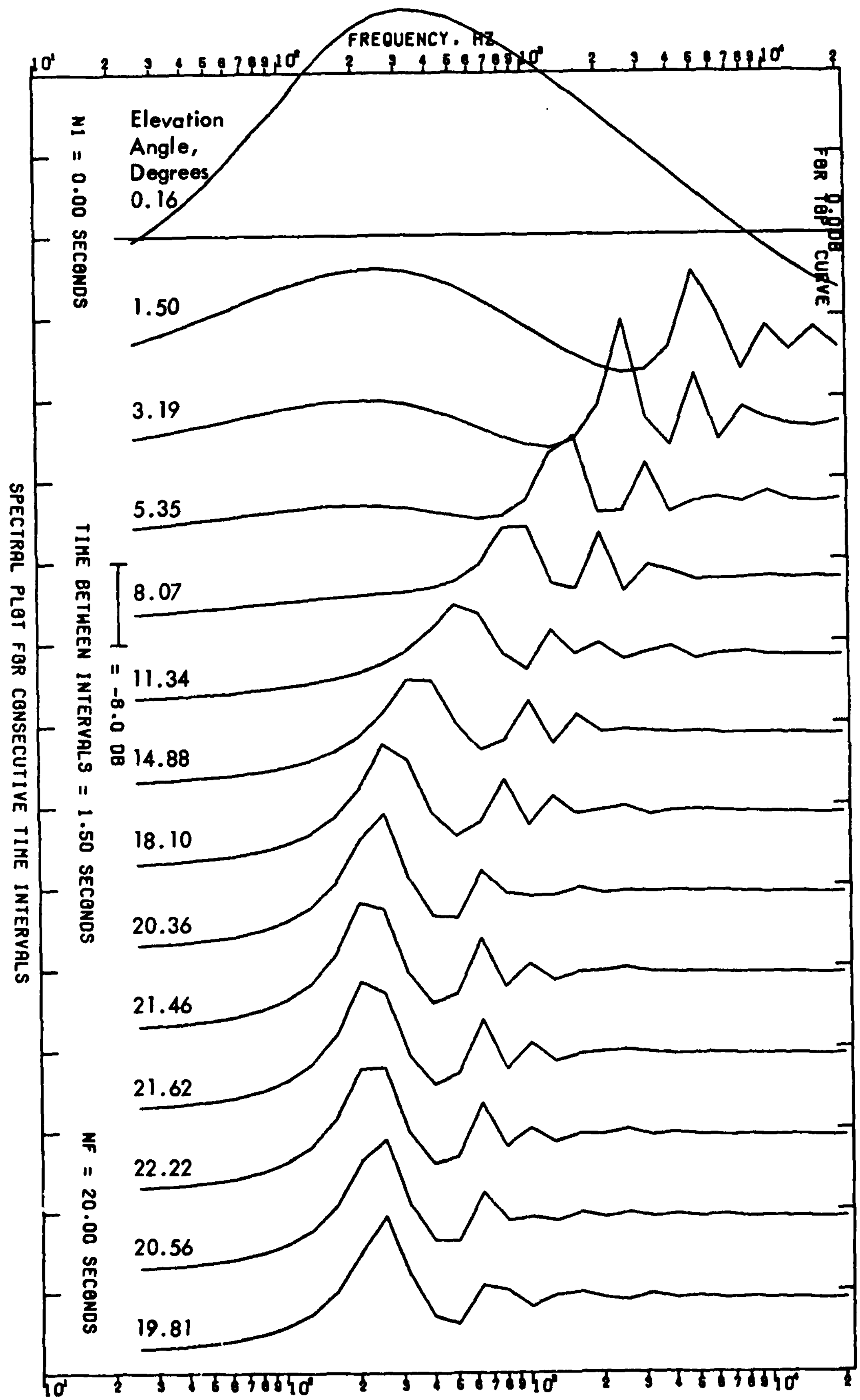

Figure 1-22. Theoretical Reflection Correction for Sideline, Soft Ground, 1.2 Microphone

Table 1-5

Impedance/Admittance for a Surface Flow Resistivity of 300 cgs rayls/cm
Imaginary Part of Impedance Is Negative (See Footnote on Page 1-22)

FREQ.,KHZ	IMPEDANCE		ADMITTANCE	
.025	59.3347	-72.7521	.673227-02	.825465-02
.032	50.0825	-61.4958	.796225-02	.977677-02
.040	42.2976	-51.9811	.941806-02	.115741-01
.050	35.7478	-43.9385	.111416-01	.136944-01
.063	30.2366	-37.1403	.131827-01	.161926-01
.079	25.5995	-31.3939	.156008-01	.191320-01
.100	21.6979	-26.5366	.184664-01	.225845-01
.126	18.4151	-22.4308	.218640-01	.266317-01
.158	15.6530	-18.9605	.258937-01	.313648-01
.200	13.3290	-16.0268	.306753-01	.368840-01
.251	11.3735	-13.5471	.363511-01	.432979-01
.316	9.72824	-11.4511	.430901-01	.507210-01
.398	8.34390	-9.67935	.510923-01	.592696-01
.501	7.17912	-8.18174	.605932-01	.690555-01
.631	6.19908	-6.91585	.718671-01	.801767-01
.794	5.37448	-5.84582	.852299-01	.927044-01
1.000	4.66067	-4.94135	.101039	.106666
1.259	4.09690	-4.17682	.119686	.122021
1.585	3.60571	-3.53058	.141589	.138638
1.995	3.19244	-2.98432	.167162	.156265
2.512	2.84470	-2.52258	.196787	.174504
3.162	2.55213	-2.13229	.230753	.192793
3.981	2.30595	-1.80238	.269199	.210411
5.012	2.09882	-1.52351	.312040	.226506
6.310	1.92454	-1.28779	.358904	.240158
7.943	1.77791	-1.08854	.409102	.250477
10.000	1.65453	-.920122	.461632	.256725
12.589	1.55071	-.777760	.515252	.258424
15.849	1.46337	-.657424	.568596	.255444
19.953	1.38968	-.555707	.620324	.248021

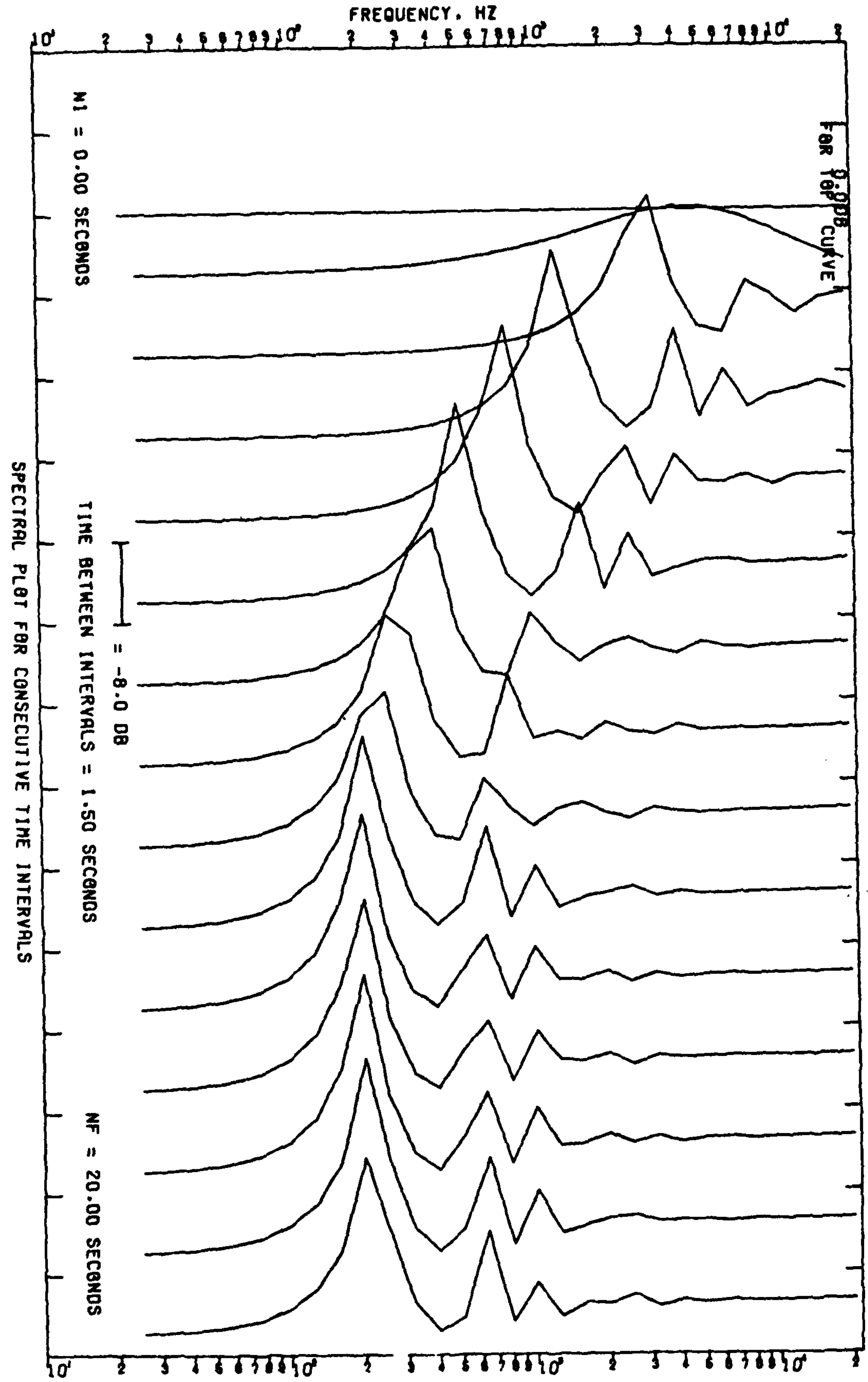

Figure 1-23. Theoretical Reflection Correction for Sideline, Hard Ground, 1.2 Microphone

Table 1-6

Impedance/Admittance for a Surface Flow Resistivity of 10^5 cgs rayls/cm
Imaginary Part of Impedance Is Negative (See Footnote on Page 1-22)

FREQ.,KHZ	IMPEDANCE		ADMITTANCE	
.025	4551.78	-5052.97	.984142-04	.109251-03
.032	3830.00	-4271.17	.116372-03	.129776-03
.040	3222.71	-3610.33	.137603-03	.154154-03
.050	2711.73	-3051.74	.162705-03	.183105-03
.063	2281.79	-2579.57	.192382-03	.217488-03
.079	1920.05	-2180.45	.227468-03	.258316-03
.100	1615.68	-1845.09	.268948-03	.306603-03
.126	1359.58	-1557.93	.317980-03	.364376-03
.158	1144.10	-1316.88	.375960-03	.432736-03
.200	962.802	-1113.13	.444496-03	.513699-03
.251	810.256	-940.908	.525519-03	.610257-03
.316	681.904	-795.329	.621301-03	.724646-03
.398	573.909	-672.275	.734533-03	.860429-03
.501	483.043	-568.260	.868392-03	.102159-02
.631	406.569	-480.338	.102664-02	.121266-02
.794	342.260	-406.020	.121371-02	.143962-02
1.000	288.135	-343.200	.143486-02	.170910-02
1.259	242.594	-290.100	.169635-02	.202653-02
1.585	204.276	-245.215	.200546-02	.240740-02
1.995	172.035	-207.275	.237097-02	.285664-02
2.512	144.908	-175.205	.280312-02	.338919-02
3.162	122.064	-148.097	.331414-02	.402031-02
3.981	102.879	-125.183	.391846-02	.476798-02
5.012	86.7207	-105.815	.463319-02	.565333-02
6.310	73.1250	-89.4431	.547862-02	.670119-02
7.943	61.6850	-75.6044	.647881-02	.794069-02
10.000	52.0606	-63.9068	.760230-02	.940583-02
12.589	43.9621	-54.0191	.906300-02	.111363-01
15.849	37.1481	-45.6612	.107212-01	.131761-01
19.953	31.4149	-38.5904	.126848-01	.155646-01

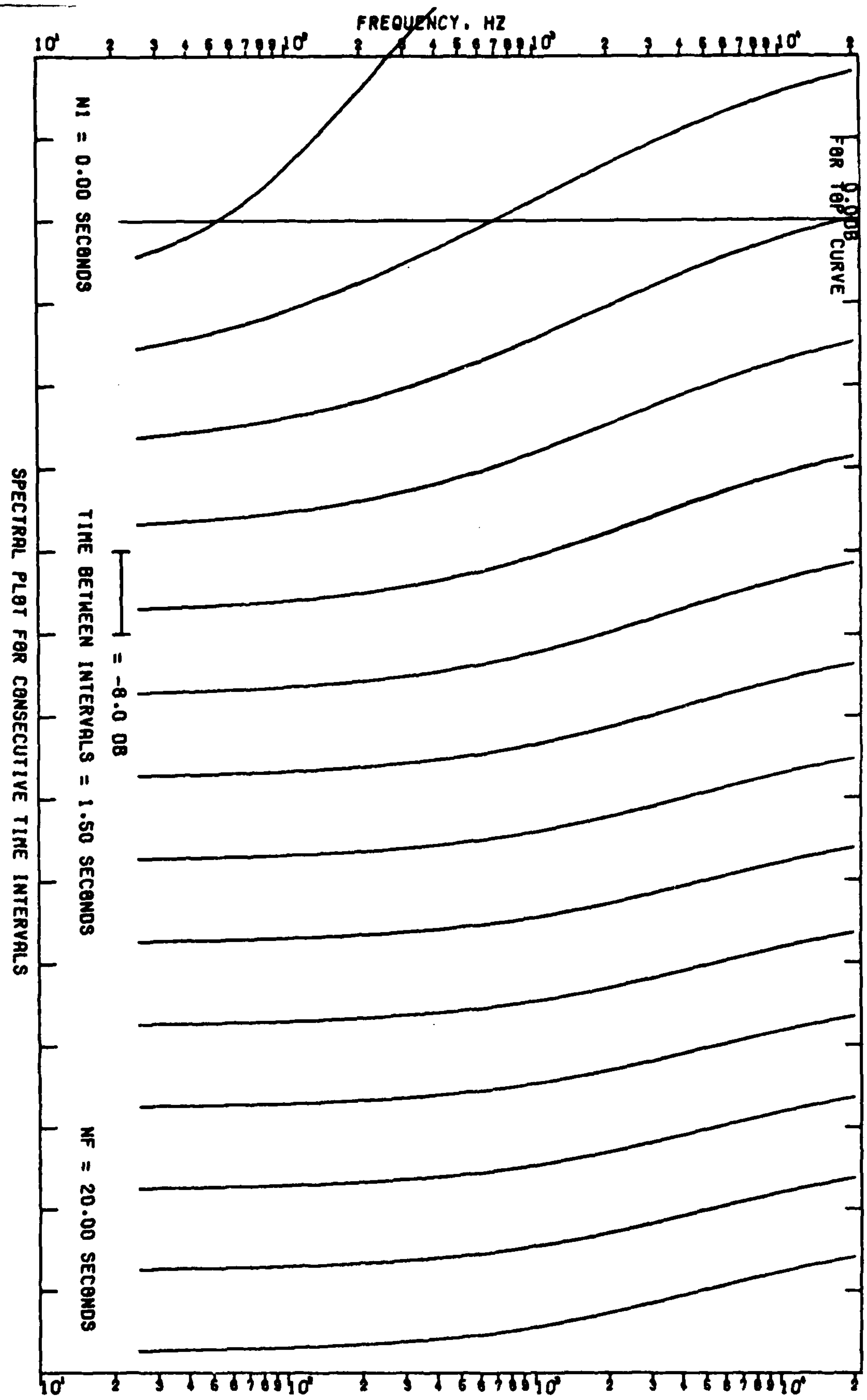

Figure 1-24. Ground Effect Correction for Sideline, Soft Ground, Ground Microphone. Elevation Angles Same as on Figure 1-22.

Figure 1-25 shows the calculated ground interference pattern for sideline with an elevated microphone (10 m above ground). The figure shows that pseudotone phenomena occur near the closest approach portion of the flyby (middle of plot). In particular, the inverted peak at 100 Hz in the six lower-most spectra could give rise to a spurious tone correction. At very low elevation angles (top portion of plot) the pattern shifts to higher frequencies and the above mentioned "hump" appears at lower frequencies.

The above paragraphs on sideline measurements indicate that it is very difficult to obtain free field spectra from sideline measurements considering only the presence of an idealized ground. This is compounded by several other effects which introduce largely unpredictable variations:

- Terrain irregularities and obstacles (diffraction)
- Temperature and wind gradients (refraction)
- Atmospheric turbulence which is strongest near the ground (scattering)

Sideline measurements are much more susceptible to the above influences than approach or overhead takeoff measurements since the propagation path is much closer to the ground (much smaller elevation angles during high-noise portion of flyby) for the sideline condition than for the other two measurement locations.

1.4.3.2 Short Literature Review

McKaig (Reference 2) states that "...it appears hopeless, or at least extremely risky, to try to compensate analytically for the presence of ground reflection." He reports on the use of surface microphones 1/2 inch from the surface saying that at about 14 kHz there will be at most a 0.2 dB error from the 6 dB perfect reinforcement case with the difference being less at lower frequencies. This is not at all in agreement with the results shown in Figure 1-17 even considering that the finite microphone size will reduce the theoretical corrections of that figure. McKaig also found that near-grazing incidence angles did not produce any loss of high frequency signal strength so long as the angle of incidence was less than 87^o (elevation angle greater than 3^o). He recognizes that the ground microphone technique may not be at all applicable to sideline

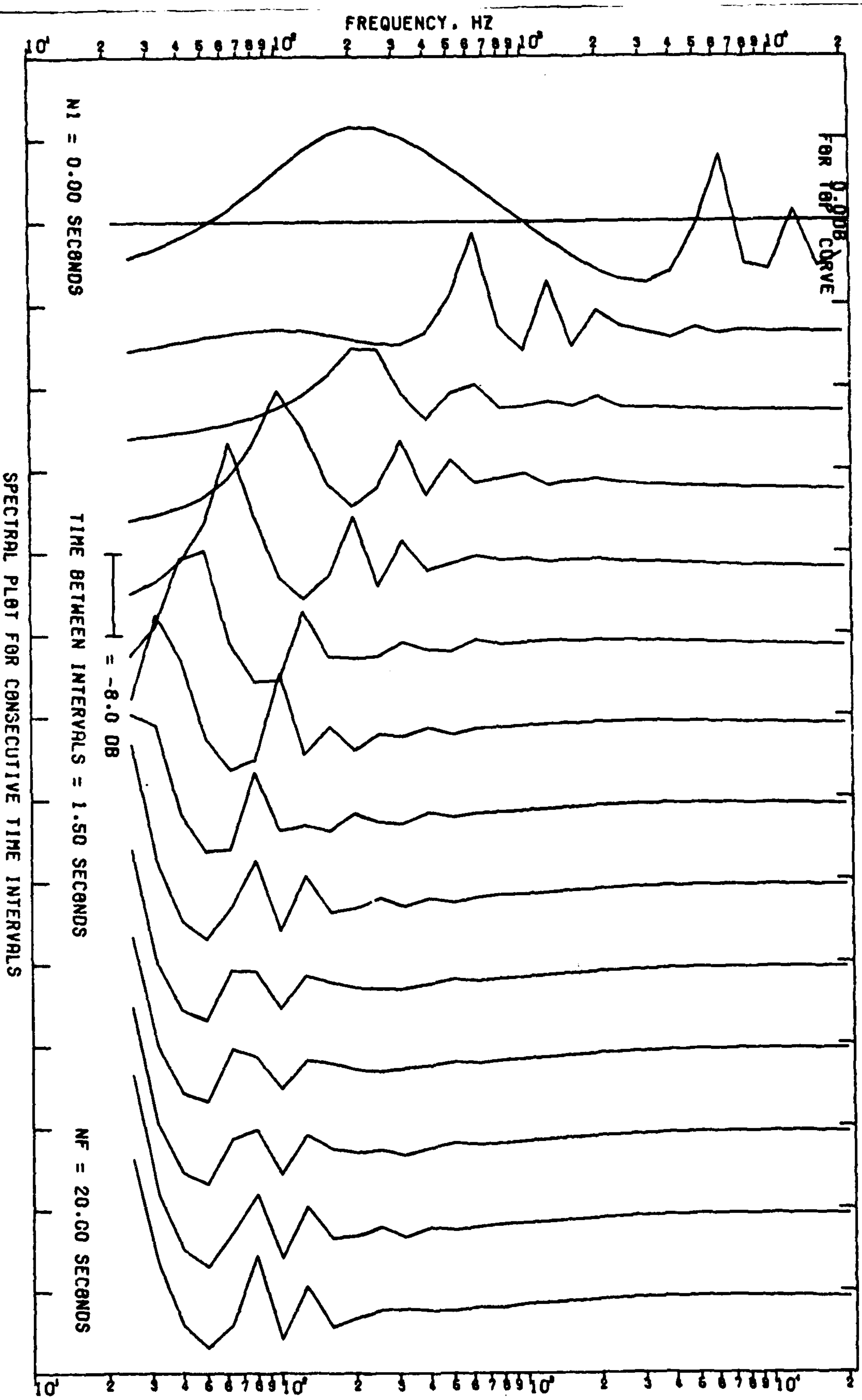

Figure 1-25. Theoretical Reflection Correction for Sideline, Soft Ground, 10 m Microphone. Elevation Angles Same as on Figure 1-22.

measurements. Use of flush-mounted microphones in acoustic scale model tests does not permit the customarily casual full-scale mounting techniques; good results were obtained only with extreme care. Figures 1-3 and 1-16 presented earlier were taken from McKaig's paper.

In Reference 23, Smith makes an excellent case against the 1.2 m microphone height, and in favor of the elevated microphone as opposed to the ground microphone. Some pertinent quotations from Smith's paper:

- "1.2 and 10 meter locations produce virtually the same absolute levels over varied surfaces, except at low angles to the flight line where the 1.2 meter results are totally distorted. A flush system shows amplification relative to the other systems, 3 dB to 5 dB.

- Surface conditions have a similar effect on the 1.2 and 10 meter systems. The impedance change from board to grass with the flush system appears to produce some spectral change relative to an infinite hard surface, which would be difficult to allow for in practical tests.

- At 1.2 meters, ground interference effects produce extreme spectral distortion, causing loss of several 1/3 octave bands at shallow angles of incidence. 10 meter and flush systems minimize or eliminate interference effects.

- Recognizable source characteristics are well displayed by both a flush system in a hard surface and by 10 meter systems over both hard and soft surfaces. Source character is unacceptably distorted by a 1.2 meter system.

- A system mounted 10 meters above ground produces less scatter due to ground surface conditions, less destructive impact from ground reflection and a more faithful portrayal of source character. In a certification context this virtually eliminates "pseudo tone" corrections, avoids the effect of localized temperature and humidity gradients and does not introduce any increased background/wind noise. Such a system also minimizes the problem of 1/3 octave "drop out" at the fringes of the time history.

- o A change to a 10 meter location would put the measuring systems at the same position that is currently used to define ground level atmospheric conditions."

A surprising statement is that the use of the elevated microphone does not introduce any increased background/wind noise since the opposite might be expected as wind speed generally increases with height above ground. The explanation probably is that 10 m is usually just above the atmospheric viscous boundary layer with its turbulence adversely affecting lower microphones whereas the 10 m microphone is more likely to be exposed to a steady stream whose speed may be less than the peak velocities in the turbulence below.

Smith has also drafted an Appendix to a proposed SAE AIR (Reference 27)which is based on the same measurements as Reference 23, but presents some additional relevant details and observations:

- o Solar heating and small scale turbulence above a surface mounted microphone cause high frequency loss; the turbulence also generates "comparatively high levels of ambient noise."
- o Diffraction ripples induced by the edge of an 8 feet diameter board used for mounting the microphone are generally within 3 to 4 dB.
- o At the 10 m microphone location, there are some small "augmentational/cancellation" effects, i.e., recognizable reflection interference patterns, in the very low frequencies. This corroborates the theoretical prediction of Figure 1-20.

Smith recommends that microphones mounted 10 m above a hard ground be used. The surface should be painted a light color to avoid solar heating effects. If the measurements are taken over acoustically soft terrain, he proposes a correction curve (shown in Figure 1-26) replacing the constant -3 dB correction to be applied for hard surfaces.

Reference 25 demonstrated that at a height of 137 m (450 feet) above the ground, aircraft noise spectra are completely free of ground reflections. Reference 26 found that a reflection signal comparable to the direct signal can be found at heights of up to 60 m (200 feet) above the ground for frequencies of less than 1000 Hz.

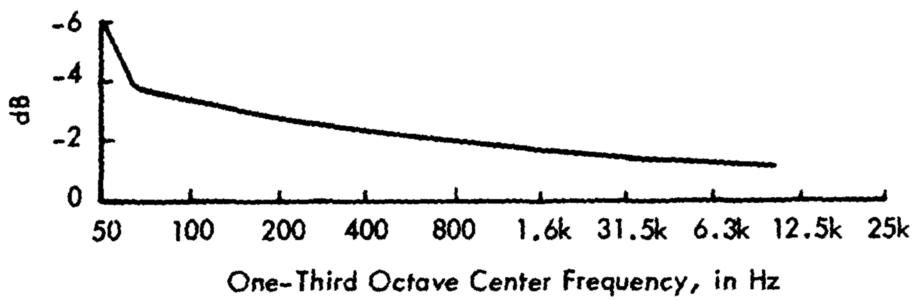

Figure 1-26. Correction to Free Field for Aircraft Flyover Measurements Taken with 10m Microphones Over Soft Ground (from Reference 34)

1.4.3.3 Evaluation of Data Measured at LAX

Appendix A contains Spectral Time History (STH) plots (spectra at successive time intervals) and for various microphone locations and ground surfaces employed during the measurement of over 20 flights from Los Angeles International Airport. Table 1-7 summarizes the observations which may be made on inspection of these STHs. The table also lists numerical values for each flight. The "waviness" is defined for a single spectrum as follows:

$$W = \sum_{i=18}^{32} (L_{i+1} - 2L_i + L_{i-1})^2$$

where L_i is the level of the i-th third-octave band, with i indicating standard third-octave band numbers. W is a measure of how much the spectrum fluctuates in the frequency domain. Mathematically, W is the sum of squares of numerical approximations to the second derivative of the spectrum with respect to the logarithm of frequency. This calculation is limited to the lower portion of each spectrum (below 2 kHz) where pseudotones commonly occur since W is used as a numerical indicator of the power of correction methods to remove pseudotones. Two waviness values are listed in Table 1-7, one for the spectrum at $PNLT_{max}$, and the other is the mean $\pm$ one standard deviation over the 10-dB-down interval.

The noise levels listed in Table 1-7 were computed in the standard manner. The integral of the A-weighted time history is the sound exposure level L_S for which the integration time interval was taken as the 10-dB-down interval. The latter may be different from the one used for EPNL since the 10-dB-down are measured from L_{Amax} or $PNLT_{max}$, respectively. Levels in parentheses are "incomplete" levels in the sense that the 10-dB-down point was not reached within the measured interval. Appendix D describes how the data was treated before the noise metric calculations.

In the identification section of Table 1-7, the aircraft type is followed by a letter which uniquely identifies a flight for which several simultaneous measurements at various microphone positions were made. The data in Appendix A are organized in the same sequence as in Table 1-7. The "sentinel" uniquely identifies a flyover spectral time history (STH) for computerized retrieval from a databank. This sentinel, prefixed by "90000," appears on the STH data plots of

Table 1-7

Measured Noise Data: Comments, Waviness, Noise Levels

Identification					Comments			Waviness		Noise Levels [1]			
Micro-phone Location	Aircraft/ Flight	Sentinel	Nominal Micro-phone Height m	Ground Surface	Pseudotones	Real Tones	Other Spectral Features	Mean ±Std. Dev.	At $PNLT_{max}$	EPNL dB	$PNLT_{max}$ dB	L_S dB	L_{Amax} dB
Approach "Sideline"	DC-10/A	15010	0	Grass on sand with 4' x 4' board	None	One at about 4 kHz occurring after overhead	Possibly a true dip at about 200 Hz	127±52	92	99.37	103.74	(93.63)	87.01
		16010	0	Asphalt	None		High instrumentation noise	121±85	66	99.18	104.30	(93.65)	87.03
		17010	1.2	Grass on sand	Pronounced		Low instrumentation noise	286±84	342	95.08	99.52	(90.30)	82.72
		14010	1.2	Asphalt	Pronounced			245±87	291	96.30	100.28	(91.08)	84.17
		11010	10	Grass on sand	Possibly some at low frequencies		Quite constant overall slope	161±77	238	(95.67)	100.39	(90.48)	83.83
		12010	10	Asphalt				157±93	93	98.69	103.16	(92.75)	86.45
Approach	727/B	22010	0	Grass on sand with 4' x 4' board	None	One at about 3 kHz occurring throughout, but somewhat "washed out"	Jet noise easy to see	107±53	89	107.19	111.59	101.42	96.56
		23010	0	Asphalt	None			97±20	90	105.73	110.66	100.04	95.46
		19010	1.2	Grass on sand	Pronounced	One at about 3 kHz occurring throughout	Jet noise obliterated	356±155	282	104.50	108.56	98.24	93.33
		21010	1.2	Asphalt	Pronounced and irregular			303±129	405	104.54	109.42	98.72	93.76
		18010	10	Grass on sand	Very little if any		Jet noise easy to see	65±32	53	104.23	108.39	98.15	92.81
		20010	10	Asphalt	Very little if any			81±35	117	106.73	111.55	100.78	95.86
Approach	707/H	53010	0	Grass on sand with 4' x 4' board	None	One at about 3 KHz decreasing to 2 KHz (Doppler effect), harmonic at 6 Khz	Flat in lower lower position	122±39	171	116.29	121.19	109.02	104.14
		57010	0	Asphalt	None			136±51	146	114.76	119.21	107.67	102.40
		41010	1.2	Grass on sand	Pronounced		Absorption by soft ground is apparent	349±99	499	112.89	116.95	105.49	99.75
		49010	1.2	Asphalt	Very clear			330±106	372	114.01	118.55	106.88	101.28
		38010	10	Grass on sand	None			147±56	122	112.14	115.71	104.63	97.83
		45010	10	Asphalt				159±65	111	115.78	119.57	108.45	102.32

Table 1-7 (Continued)

Identification					Comments			Waviness		Noise Levels			
Microphone Location	Aircraft/ Flight	Sentinel	Nominal Microphone Height m	Ground Surface	Pseudotones	Real Tones	Other Spectral Features	Mean ±Std. Dev.	At $PNLT_{max}$	EPNL dB	$PNLT_{max}$ dB	L_S dB	L_{Amax} dB
Approach	727/I	54010	0	Grass on sand with 4' x 4' board	None	One directional weak tone at 3 KHz, harmonic at about 6 KHz	Source Spectrum exceptionally free of irregularities	65±23	57	103.90	107.85	99.95	95.02
		58010	0	Asphalt	None			81±51	38	103.30	107.66	99.43	94.53
		42010	1.2	Grass on Sand	Very clear		Very sharp rise and fall with time at high frequencies	178±71	171	101.17	105.57	96.35	91.66
		50010	1.2	Asphalt	Very clear			180±70	284	101.91	106.50	97.27	92.57
		39010	10	Grass on sand	Maybe some at low freq.			72±38	56	101.54	106.20	96.53	92.03
		46010	10	Asphalt	Maybe some at low freq.			76±28	89	103.73	108.70	98.52	94.37
Approach "Sideline"	707/J	55010	0	Grass on sand with ' x 4' board	None	One at 3 KHz decreasing to 2 KHz (Doppler), weak harmonic; one weak tone at 1.6 KHz	Lower portion is flat	199±46	178	113.22	116.81	106.34	100.06
		59010	0	Asphalt	None			168±72	145	111.87	116.66	105.06	99.38
		43010	1.2	Grass on sand	Pronounced			324±87	380	109.61	113.65	102.80	96.57
		51010	1.2	Asphalt	Pronounced			392±78	416	109.79	114.37	103.14	97.65
		40010	10	Grass on sand	Possibly some at low freq.		Lower portion is flat	233±83	197	110.07	114.30	103.16	97.25
		47010	10	Asphalt				238±95	197	111.42	116.66	104.47	99.35
Approach "Sideline"	DC10/K	52010	0	Grass on sand with 4' x 4' board	None	None	Very smooth spectrum	89±40	47	101.05	102.91	96.60	88.40
		56010	0	Asphalt	None	None		108±36	117	101.49	105.00	97.23	90.72
		48010	1.2	Asphalt	Pronounced	None		277±78	264	(97.96)	100.61	(93.24)	85.98
		44010	10	Asphalt	Weak ones at low frequencies	None	Very smooth spectrum	155±85	82	98.98	101.70	94.66	87.14
		37010	10	Grass on sand	None	None		123±73	35	96.90	98.68	92.18	83.91

Table 7-1 (Continued)

Identification					Comments			Waviness		Noise Levels			
Micro-phone Location	Aircraft/ Flight	Sentinel	Nominal Micro-phone Height m	Ground Surface	Pseudotones	Real Tones	Other Spectral Features	Mean ±Std. Dev.	At $PNLT_{max}$	EPNL dB	$PNLT_{max}$ dB	L_S dB	L_{Amax} dB
Sideline	707/C	26010	1.2	Concrete	Pronounced, at higher frequencies as expected for sideline	One at 3 to 4 kHz, Doppler shift obvious	-	189±67	177	111.54	114.40	105.09	97.25
		24010	10		Maybe a little		Strong jet noise	153±101	92	107.50	111.04	100.92	93.33
Sideline	707/D	27010	1.2		Pronounced	Surprisingly none (aircraft with quiet nacelle?)	-	181±87	98	113.22	115.51	111.15	104.30
		25010	10		Marked drop-off at lower end		Strong jet noise	123±32	134	108.32	109.85	106.28	97.44
Sideline	707/E	30010	0	Grass on sand with ' x 4' board	None		Demonstrates noise floor nicely. Some irregularities due to diffraction?	94±43	59	109.17	112.93	107.06	101.76
		32010	0	Concrete	None		Jet noise pronounced	87±48	37	112.37	115.61	110.12	103.74

Table 1-7 (Continued)

Identification					Comments			Waviness		Noise Levels			
Micro-phone Location	Aircraft/ Flight	Sentinel	Nominal Micro-phone Height m	Ground Surface	Pseudotones	Real Tones	Other Spectral Features	Mean ±Std. Dev.	At $PNLT_{max}$	EPNL dB	$PNLT_{max}$ dB	L_S dB	L_{Amax} dB
Sideline	727/F	31010	0	Grass on sand with 4' x 4' board	None	Directional 4 kHz tone	Jet noise pronounced	96±25	50	97.66	100.29	92.74	84.40
		33010	0	Concrete	None			102±39	76	97.59	99.68	93.38	85.98
		29010	1.2	Concrete	Pronounced but tend to disappear at low elevation angle	4 kHz tone hard to see		700±89	302	97.14	99.48	93.06	85.65
		28010	10	Concrete	None	Directional 4 kHz tone	Can really see jet noise directivity	135±72	157	95.57	96.77	91.80	83.88
Sideline	B727/L	68020	0	Grass on Sand with 4' x 4' board	None	One weak low frequency tone at about 100 Hz		103±43	149	100.69	101.70	98.60	90.13
		72020	0	Concrete	None			84±32	91	105.49	108.12	103.66	96.13
		64020	1.2	Concrete	Pronounced in middle frequencies about 900 Hz			198±78	149	105.33	106.66	103.38	95.81
		60020	10	Concrete	Low frequency pseudotones, enhancing weak real tone			268±132	305	101.63	102.36	99.27	90.52
Sideline	B707/N	69020	0	Grass on Sand with ' x4' board	None	One tone occurring at 3 kHz, possible low frequency tone around 800 Hz		65±29	45	104.33	108.41	97.85	90.68
		73020	0	Concrete	None			75±27	49	107.34	111.81	100.18	93.41
		65020	1.2	Concrete	Hard to see			106±43	108	107.89	111.99	101.32	94.99
		61020	10	Concrete	Some in low frequencies			110±63	158	105.18	106.38	99.26	90.51

Table 1-7 (Continued)

Identification					Comments			Waviness		Noise Levels			
Micro-phone Location	Aircraft/ Flight	Sentinel	Nominal Micro-phone Height m	Ground Surface	Pseudotones	Real Tones	Other Spectral Features	Mean ±Std. Dev.	At $PNLT_{max}$	EPNL d	$PNLT_{max}$ dB	L_S d	L_{Amax} dB
Sideline	DC10/Q	70020	0	Grass on Sand with 4' x 4' board	None	Weak directional tone around 3kHz	No obvious diffraction effects	101±35	81	97.86	98.19	94.78	85.60
		74020	0	Concrete	None			129±66	162	101.95	103.47	99.18	91.13
		66020	1.2	Concrete	Pronounced in mid-frequency			160±74	163	(101.37)	101.67	(97.40)	87.71
		62020	10	Concrete	Pronounced in low frequency			155+74	306	(98.21)	98.26	(94.87)	85.56
Sideline	DC10/R	71020	0	Grass on Sand with 4' x 4' board	None	Weak tone around 3 kHz		94±52	43	93.43	96.22	88.77	82.03
		75020	0	Concrete	None			88±43	39	(95.62)	99.69	(90.50)	84.58
		67020	1.2	Concrete	Irregular pseudotones in mid-frequencies merging w/ real tone			105±53	86	96.12	99.09	91.30	85.65
		63020	10	Concrete	Pronounced in low frequencies			169±65	129	94.31	95.40	89.75	82.08

Table 1-7 (Continued)

Identification					Comments			Waviness		Noise Levels			
Micro-phone Location	Aircraft/ Flight	Sentinel	Nominal Micro-phone Height m	Ground Surface	Pseudotones	Real Tones	Other Spectral Features	Mean ±Std. Dev.	At $PNLT_{max}$	EPNL dB	$PNLT_{max}$ dB	L_S dB	L_{Amax} dB
Takeoff	727/G	34010	0	Asphalt	None	None	Mostly jet noise	74±25	134	116.92	120.18	115.06	108.59
		36010	1.2	Asphalt	Very pro-nounced	None	Difficult to identify jet noise	434±205	790	114.94	118.42	112.24	105.70
		35010	10	Asphalt	Maybe a little	None	Mostly jet noise	101±68	102	115.01	118.82	112.61	106.47
Takeoff	B727/M	77020	0	Asphalt	None	Real tone around 4 to 5 kHz		56±30	27	111.85	114.60	109.08	102.57
		92020	1.2	Asphalt	Pronounced low & mid-frequency pseudotones			349±147	443	110.14	113.09	106.63	99.90
		85020	10	Asphalt	Possibly little in low frequencies			96±71	98	110.18	114.41	106.72	100.31
Takeoff	B707/O	79020	0	Asphalt	None	Real tone around 3 to 4 kHz	"Textbook" Record	86±34	66	113.27	117.76	107.65	101.09
		94020	1.2	Asphalt	Pronounced			389±144	246	121.74	126.97	115.55	109.30
		87020	10	Asphalt	None			98±54	63	112.79	117.85	106.20	99.91
Takeoff	B707/P	80020	0	Asphalt	None	Real tone around 3 to 4 kHz		91±43	148	113.97	118.00	107.95	99.73
		95020	1.2	Asphalt	Pronounced			414±135	417	112.79	116.60	105.78	98.32
		88020	10	Asphalt	None			105±50	151	112.93	117.24	105.83	98.52

Table 1-7 (Continued)

Identification					Comments			Waviness		Noise Levels			
Micro-phone Location	Aircraft/ Flight	Sentinel	Nominal Micro-phone Height m	Ground Surface	Pseudotones	Real Tones	Other Spectral Features	Mean ±Std. Dev.	At $PNLT_{max}$	EPNL dB	$PNLT_{max}$ dB	L_S dB	L_{Amax} dB
Takeoff	DC-10/S	81020	0	Asphalt	None	2 directional tones at about 3 and 4 kHz		100±40	134	107.26	110.47	102.62	94.84
		96020	1.2	Asphalt	Pronounced low & mid-frequency pseudotones			285±139	335	105.89	109.84	100.67	94.11
		89020	10	Asphalt	None			115±50	92	106.10	110.05	100.89	94.67
Takeoff	DC-10/T	82020	0	Asphalt	None	Weak tones around 4 kHz		96±37	127	106.91	109.62	103.14	95.33
		97020	1.2	Asphalt	Pronounced			360±185	736	105.52	109.75	100.93	94.29
		90020	10	Asphalt	None			126±62	251	105.79	109.96	100.81	94.45
Takeoff	B747/U	76020	0	Asphalt	None	Weak tones around 3 and 5 kHz	No evidence of multiple pure tones	54±25	20	112.21	116.96	107.24	102.03
		91020	1.2	Asphalt	Pronounced			181±91	136	111.02	116.44	105.44	100.54
		84020	10	Asphalt	None			110±53	95	111.32	117.56	105.32	100.94
Takeoff	B747/V	78020	0	Asphalt	None	Weak tones around 3 and 5 kHz		90±32	134	117.14	123.32	110.87	106.64
		93020	1.2	Asphalt	Pronounced			190±119	323	114.74	120.94	108.61	104.79
		86020	10	Asphalt	Possibly some at low frequencies			123±107	44	112.96	119.36	106.68	102.77

(1) L_S designates sound exposure level, values in parentheses are derived from spectral time histories too short to include the full 10-dB-down interval.

Appendix A. Some approach flights occurred displaced laterally by about 230 m (750 ft) from the overhead position. These are identified as "sideline" in Table 1-7. These flights are not representative of the FAR Part 36 approach measurement conditions, but they are included as a matter of interest.

Discussion of Data in Table 1-7

As must be expected, no pseudotones are discernible in any STH for the ground (0 m) microphone. For the pole (10 m) microphone pseudotone interference patterns are sometimes recognizable in the lowermost 1/3-octave bands. For almost all 1.2 m microphone positions, the pseudotone patterns are readily discernible. From this first overall impression, one might be tempted to prefer the ground over the pole microphone position.

Figure 1-27 shows histograms of the waviness (the mean over the 10-dB-down interval from Table 1-7). Ground and pole microphone positions generally show low waviness, whereas the 1.2 m position exhibits generally greater wavinesses which are also more spread out. This confirms in a numerical way the qualitative observations of the previous paragraph including the residual pseudotones of the pole microphone position: its wavinesses cluster slightly higher than those of the ground position.

Figure 1-28 shows histograms of the EPNL differences between the microphone positions. A clue as to a preferred choice for the microphone height to minimize pseudotones is not apparent except perhaps that the EPNL differences between the 0 m and 1.2 m, and the 0 m and 10 m positions do not cluster around 3 dB as one might expect at least for hard ground, but around 1 or 2 dB. This may well be due to the various causes of high frequency anomalies as observed by Smith for the ground microphone[23] (see Section 1.4.3.2) and as predicted analytically in Figure 1-17. This can also be observed in some of the STH plots of Appendix A. For example, compare Figures A-G1 and A-G3: the 0 m data is above the 10 m data for the lower part of the spectrum, but, as expected according to Figure 1-17, crosses over for the higher frequency portion, especially close to overhead.

In summary, while a complete explanation for all of the anomalies at high frequencies for the surface microphone is not available, it does appear that the basic ground reflection process resulting from the ½-inch elevation of the ground microphone is responsible for a major part of the phenomena.

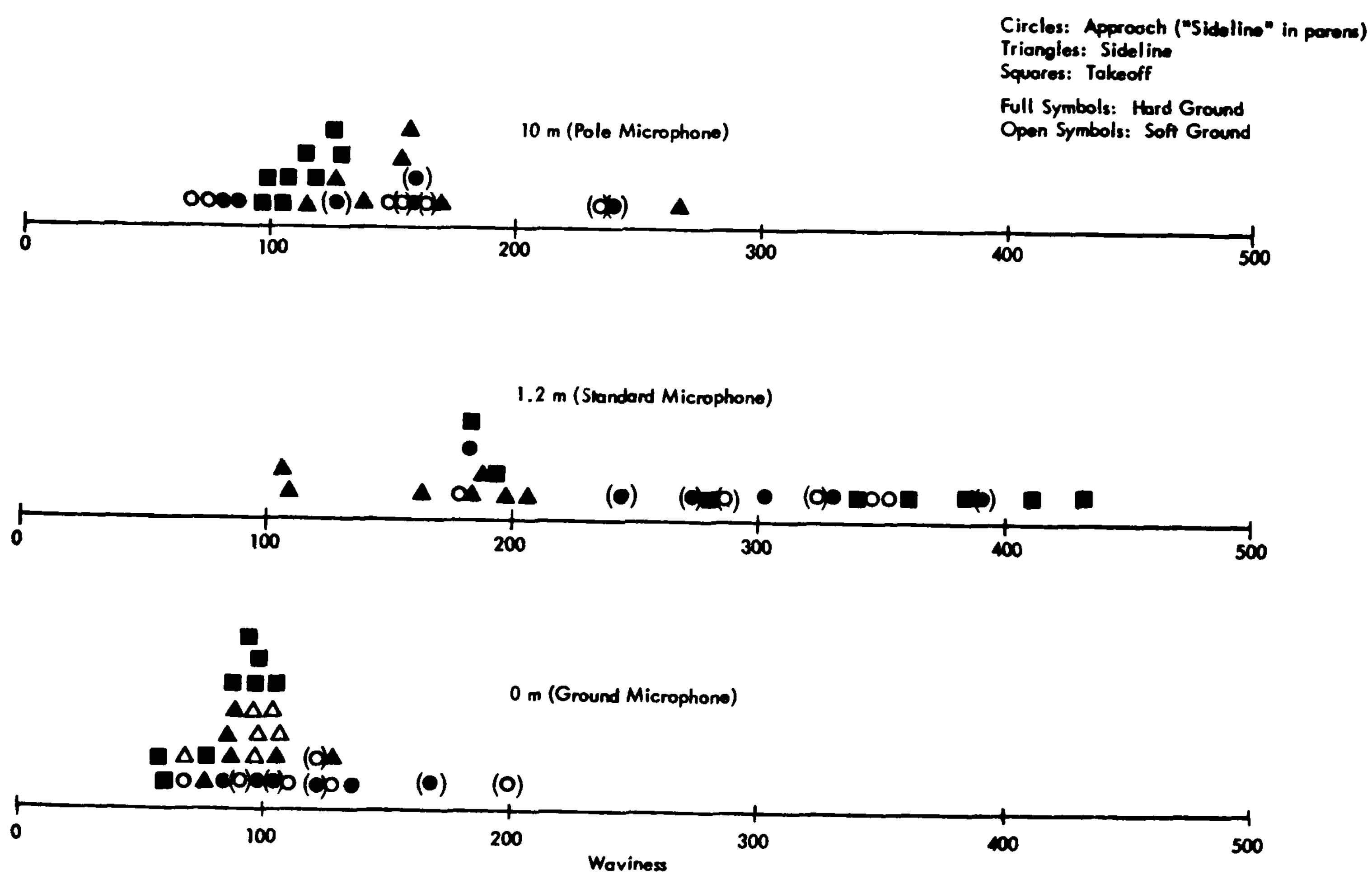

Figure 1-27. Waviness Histograms

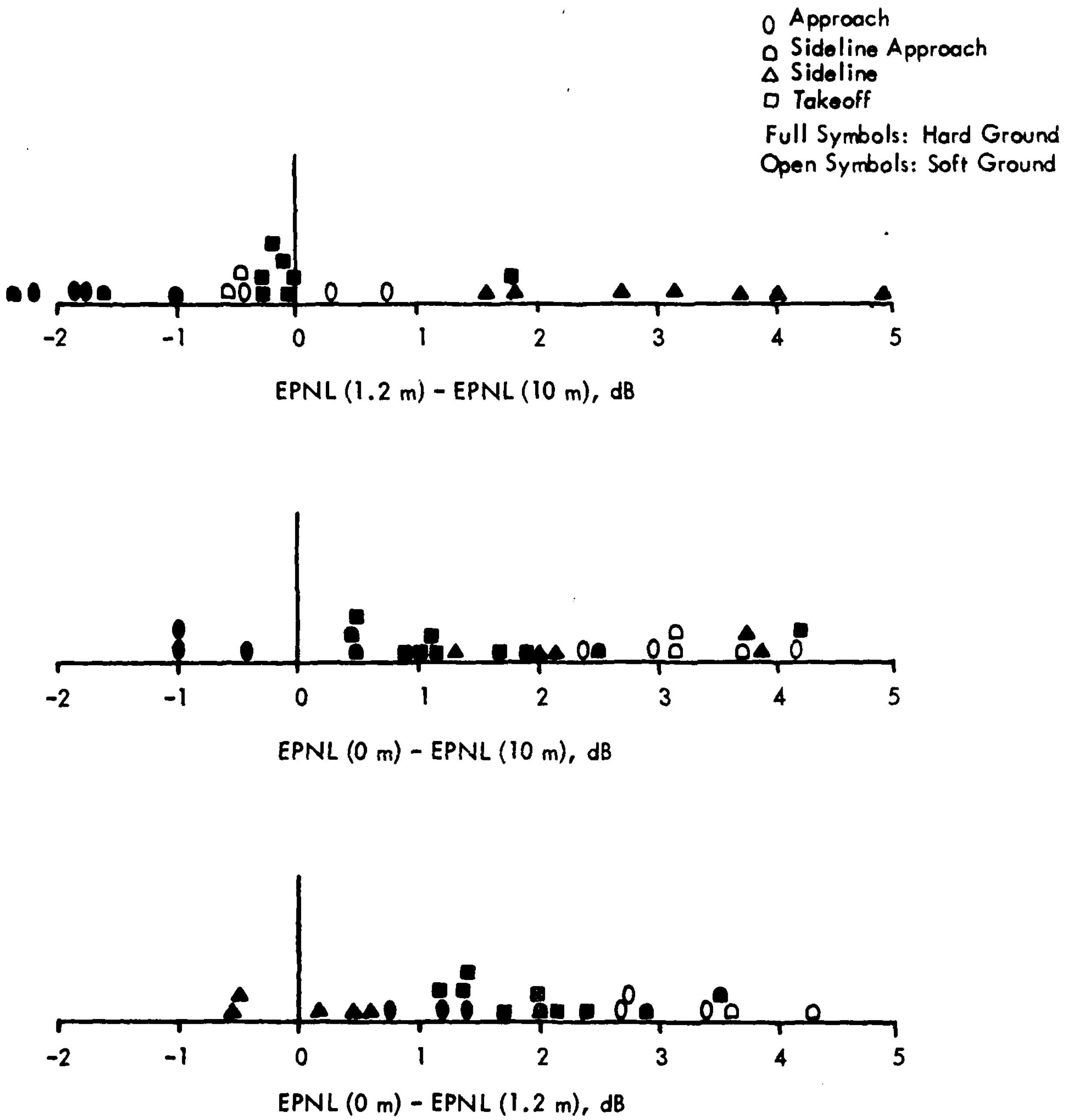

Figure 1-28. EPNL Difference Histogram

Recommended Correction Procedure: Pole Microphone

Table 1-8 lists advantages and disadvantages of the two instrumentation correction procedures considered in this study. Most of those points have been discussed in previous paragraphs. We were able to support Smith's[23] finding that pole mounting does not increase background/wind noise. A cursory analysis of several ambient noise records taken during the LAX measurements (Appendix A) showed differences (L_{ground} - L_{pole}) ranging between -1 and 4.9 dB for A-weighting, and -0.8 and 5.1 dB for the overall level. Presumably, this is true only as long as the maximum wind speed at the pole microphone is below some threshold speed, probably the usual 10 knots (5 m/sec) with the use of a windscreen.

We judge that the pole microphone position is preferable to the ground microphone position for aircraft noise certifiction measurements. The only serious drawback of the pole microphone is that reflection interference patterns (pseudo-tones) do appear on sideline measurements. The ground microphone, however, is equally undesirable for sideline measurements as the sound must travel close to the ground over much larger distances than for the overhead measurements. The sound is thus subjected to both refraction, scattering and excess ground attenuation effects for sideline positions which cannot be satisfactorily removed with the present state of the art.

We do not believe that the use of a 10 m pole for microphone mounting constitutes an undue burden for an applicant for an aircraft type certificate, at least as far as large scale manufacturers are concerned. In the case of small manufacturers or private hobbyists, FAA may consider making such poles and instrumentation available in some of the regional offices.

Although Smith[27] suggests a correction method for 10 m measurements taken over soft ground, only hard ground should be used for certification measurements at this time. More research is required to ascertain a reliable soft ground correction (which depends on frequency) as a function of ground surface impedance. Such research would first have to start with methods for determining ground surface impedance.

AD-A081 962 WYLE LABS EL SEGUNDO CALIF F/G 20/1

CORRECTION PROCEDURES FOR AIRCRAFT NOISE DATA. VOLUME I. PSEUDO--ETC(U)

DEC 79 R RACKL DOT-FA78WA-4143

UNCLASSIFIED WR-79-9-VOL-1 FAA/EE-80-1-VOL-1 NL

2 OF 3

AD
A081 962

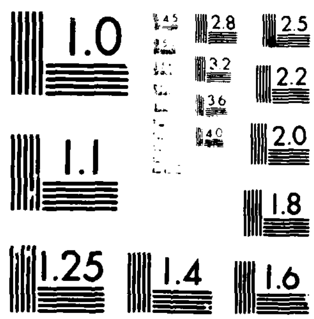

MICROCOPY RESOLUTION TEST CHART

NATIONAL BUREAU OF STANDARDS-1963-A

Table 1-8

Comparison of Ground and Pole Microphone Positions

	Advantages	Disadvantages
Ground Microphone	No reflection interference whatsoever if flush-mounted. Reflection interference negligible if mounted inverted close enough to surface. Easy access if mounted inverted close to surface.	Susceptible to micrometeorological effects (high frequency loss). Flush mounting is awkward (setup and calibration). Must have very large reflecting surface to avoid edge diffraction effects.
Pole Microphone	Reflection interference usually negligible. Measurement System more easily portable than ground microphone with its reflecting surface. Microphone usually just above atmospheric boundary layer. No increased background/wind noise as compared to 0 m and 1.2 m positions.	On sideline, reflection interference may not be negligible. Setup and calibration are cumbersome.

1.5 Recommended FAR Part 36 Actions

Simultaneously with the work on this study, Wyle Laboratories was also working on other aspects of aircraft noise certification under different tasks of the same contract and under a different contract.[28] The recommendations put forward in this section should therefore be viewed as part of a larger set of recommended modifications to FAR Part 36.

We recommend that:

- The current microphone distance from the ground of 1.2 m be changed to 10 m, with a tolerance of plus or minus 0.2 m.
- The 800 Hz cutoff for tone correction calculations be eliminated except for sideline measurements with a 10 m microphone.
- The ground surface condition be more rigorously controlled by requiring that the surface be acoustically hard such as provided by concrete or asphalt. The extent of such a surface should be at least 25 m (82 ft) to either side of the microphone vertical projection on the ground in the flight direction, and 10 m (33 ft) to either side perpendicular to the flight direction.
- The 10 m microphone support be of light weight slender design so as to minimize its interference with the sound field. This can be achieved for example by using one vertical pipe (or several single vertical pipes stacked end to end) held in place by guy wires.

It would also be desirable that the ground surface be of a light color so as to minimize solar heating effects. However, in the absence of more specific evidence of the need for this refinement,it is not put forward as a recommendation.

This change of microphone height should not cause a change in EPNL standards (aircraft noise limits), nor should there be a correction necessary to derive EPNL values measured at 1.2 m from those measured at 10 m. Smith[23] finds that the two positions ". . . produce virtually the same absolute levels over varied surfaces . . ." The limited data of this study finds that the difference EPNL (1.2 m) - EPNL (10 m) straddles zero, ranging from -2 to +5 dB (including sideline), and from -2 to +2 (excluding sideline) (see Figure 1-28). More data should be examined to ascertain this point.

REFERENCES

1. Anonymous, "Type Certification Handbook," Federal Aviation Administration, Western Regional Office, WE AE 8110.4, December 20, 1974 (Revised June 2, 1975.

2. McKaig, M.B., "Use of Flush Mounted Microphones to Acquire Free-Field Data," AIAA Paper 74-92, January 1974.

3. Society of Automotive Engineers, Inc., "Definitions and Procedures for Computing the Effective Perceived Noise Level for Flyover Aircraft Noise," National Physics Laboratory Acoustics Report Ac 77, Great Britain, October 1976.

4. Szalai, A., ed., "The Use of Time - Daily Activities of Urban and Suburban Population in Twelve Countries,"Mouton, The Hague, Paris, 1972.

5. Pao, S.P., et al, "Prediction of Ground Effects on Aircraft Noise," NASA Technical Paper 1104, January 1978.

6. Zorumski, W.E., "Prediction of Aircraft Sideline Noise Attenuation," NASA TM 78717, June 1978.

7. Chessel, C.I., "Propagation of Noise Along a Finite Impedance Boundary," J. Acoust. Soc. Am. 62(4), 825 (1977).

8. Brüel, P.V., "Electroacoustical Performance Requirements for Aircraft Noise Certification Measurements," F23V10, Inter-Noise 73, Copenhagen, August 1973.

9. Smith, M.J.T., "International Standards - Reasons and Proposals for an Alternative to the 1.2 Meters Microphone Height Used in Aircraft Noise Measurement," Rolls Royce, February 1977.

10. Gutin, L.Y., "On the Sound Field of a Rotating Propeller," translated as NACA TM-1195, National Advisory Committee on Aeronautics, 1948.

11. Parkin, P.H.and Scholes, W.E., "The Horizontal Propagation of Sound from a Jet Engine Close to the Ground, at Hatfield," Sound & Vib. 2(4), 353-374 (1965).

12. Delany, M.E. and Bazley, E.N., "Acoustical Properties of Fibrous Absorbent Materials," Applied Acoustics 3(2), 105-116 (1970).

13. Embleton, T.F.W., Piercy, J.E. and Olson, N., "Outdoor Sound Propagation Over Ground of Finite Impedance," J. Acoust. Soc. Am. 59(2), 267-277 (1978).

14. Donato, R.J., "Propagation of a Spherical Wave Near a Plane Boundary with a Complex Impedance," J. Acoust. Soc. Am. 60(1), 34-39 (1976).

15. Moore, C.J., "Sound-Absorbing Pad for Minimizing the Acoustical Effect of the Ground on Noise Test Rigs," Paper 7A11, Acoustical Society of America, November 1969.

16. Bass, H.E. and Bolen, L.N., "Propagation of Sound Through the Atmosphere: Effects of Ground Cover," University of Mississippi, June 19, 1978.

17. Chapkis, R.L. and Marsh, A.H., "Investigation of Ground Reflection and Impedance from Flyover Noise Measurements," NASA CR 145302, February 1978.

18. Lanter, S., M.S. Thesis Paper for University of Utah, 1977, "A Method for Determining Acoustic Impedance of Ground Surfaces."

19. Mansbach, P.A. and Holmer, C.I., "Techniques for the Measurement of Acoustic Impedance of Asphalt," Report No. NBSIR-78-1541, October 1978.

20. Brown, R., Lee, M.C. and Sutherland, L.C., "Flow Resistivity and Porosity Testing of Surface Materials," Wyle Research Report WCR 75-8, for the U.S. Environmental Protection Agency, 1975.

21. Miles, J.H., et al., "Analysis and Correction of Ground Reflection Effects in Measured Narrow Band Spectra Using Cepstral Techniques," NASA TM X-71810, November 1975.

22. Society of Automotive Engineers, A-21 Ground Reflection Measurement Subcommittee, "Proposed AIR: Methods to Account for the Effect of Ground Reflections on Acoustic Measurements," Draft, December 1977.

23. Smith, M.J.T., "International Aircraft Noise Measurement Procedures - Expensive Procedures - Expensive Acquisition of Poor Quality Data," AIAA Paper 77-1371, October 1977.

24. Wiener, F.M., "The Diffraction of Sound by Rigid Discs and Rigid Square Plates," J. Acoust. Soc. Am. 21(4), 334, July 1949.

25. Brooks, J.R., "Flight Noise Studies on a Turbojet Using Microphone Mounted on a 450 Ft. Tower," AIAA Paper 77-1325, October 1977.

26. Kasper, P.K., Pappa, R.S., Keefe, L.R. and Sutherland, L.C., "A Study of Air-to-Ground Sound Propagation Using an Instrumental Meteorological Tower," NASA Report CR-2617, 1975.

27. Smith, M. J. T., "Determination of Freefield Levels from Flight Tests," Draft Appendix C to SAE AIR, February 19, 1979.

28. Contract No. DOT-FA77-WA-3990, awarded August 1977.

29. Federal Aviation Administration, United States Government, "Noise Standards: Aircraft Type Certification," Federal Aviation Regulations, Part 36, November 1969; last Amendment: Number 10, June 1978.

30. Sutherland, L. C., "Review of Experimental Data in Support of a Proposed Method for Computing Atmospheric Absorption Losses," Wyle Research Report for U. S. Department of Transportation, Contract No. DOT-TST-75-87, May 1975 (revised December 1976).

31. Daigle, G. A., et al., "Some Comments on the Literature of Propagation Near Boundaries of Finite Acoustical Impedance," J. Acoust. Soc. Am. 66(3), 918, September 1979.

APPENDIX A

AIRCRAFT NOISE DATA ACQUISITION (LAX)

Measurement sites in the vicinity of Los Angeles International Airport (LAX) were used to obtain samples of measured noise for different types of aircraft at locations representative of FAR Part 36 (takeoff, sideline and approach). The locations are shown in Figure A-1 and described in Table A-1. The takeoff location is much closer to brake release than specified in the Regulation because of airport geography restrictions.

Microphones were placed at ground level, 1.2 m and 10.0 m as shown in Figure A-2 over both a hard surface (concrete/asphalt) and a soft surface (sand/grass) with the two surfaces separated by about 10 m. In all cases, the microphones were oriented with the diaphragm horizontal. Measurement sites were selected to be in open, generally flat areas as free as possible of nearby reflecting obstacles.

Three two-channel Nagra tape recorders were used to record the acoustic pressure signals from the six microphones. Correlation between microphones was maintained by using a common Irig-B time code generator as shown in Figure A-3. The Irig time was noted at aircraft overhead (or sideline) together with airline/flight number/ aircraft type information. A photograph was taken at the aircraft overhead position (or point of closest approach for sideline). The microphones were B&K half inch condenser type 4133. Windscreens were used on each microphone. Calibrations were performed on each tape immediately before the start of measurement using pistonphones (B&K types 4220 and 4230) and a pink noise generator (General Radio 1382). The same three calibrations were recorded at the end of each tape.

The tapes were reviewed in the laboratory by examining the L_A time history (see Figure A-4), and selections made for digitizing. Aircraft powered by different power plants (high by-pass and low by-pass engines) were selected for each of the locations.

Digitization of the selected flyovers was performed with the use of a GR 1926 multichannel rms detector and a GR 1925 one-third octave band filter system.

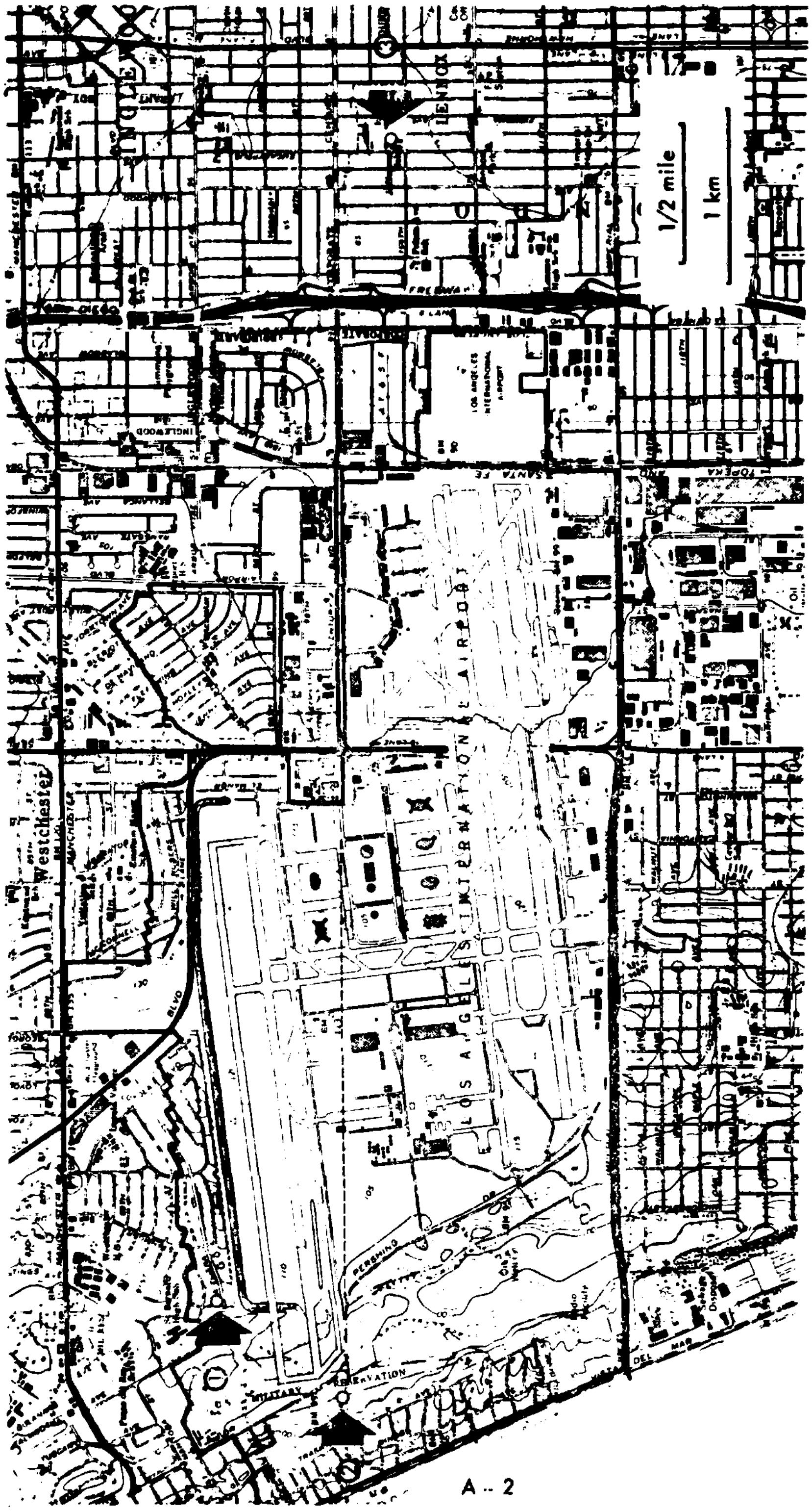

Figure A-1. Location of Measurement Sites Around Los Angeles International Airport

Table A-1

Microphone Locations and Surface Conditions

1. Sideline Location (9000 Feet from Brake Release, 1600 Feet Sideline)

   Microphone Altitude/Surface:

   10 Meters/Sandy Grassland
   10 Meters/Asphalt
   1.2 Meters/Sandy Grassland
   1.2 Meters/Asphalt
   *Ground/4' x 4' x 3/4" Plywood Board over Grass
   *Ground/Asphalt

2. Takeoff Location (11,100 Feet from Brake Release, 200 Feet Sideline)

   10 10 Meters/Concrete
   1.2 Meters/Concrete
   *Ground/Concrete

3. Approach Location (7000 Feet from Threshold, Under Flight Path)

   10 Meters/Grass (Short Cut)
   10 Meters/Asphalt
   1.2 Meters/Grass (Short Cut)
   1.2 Meters/Asphalt
   *Ground/4' x 4' x 3/4" Plywood Board over Grass
   *Ground/Asphalt

*Ground microphones were inverted with 1/2 inch space between diaphragm and ground surface or wooden board.

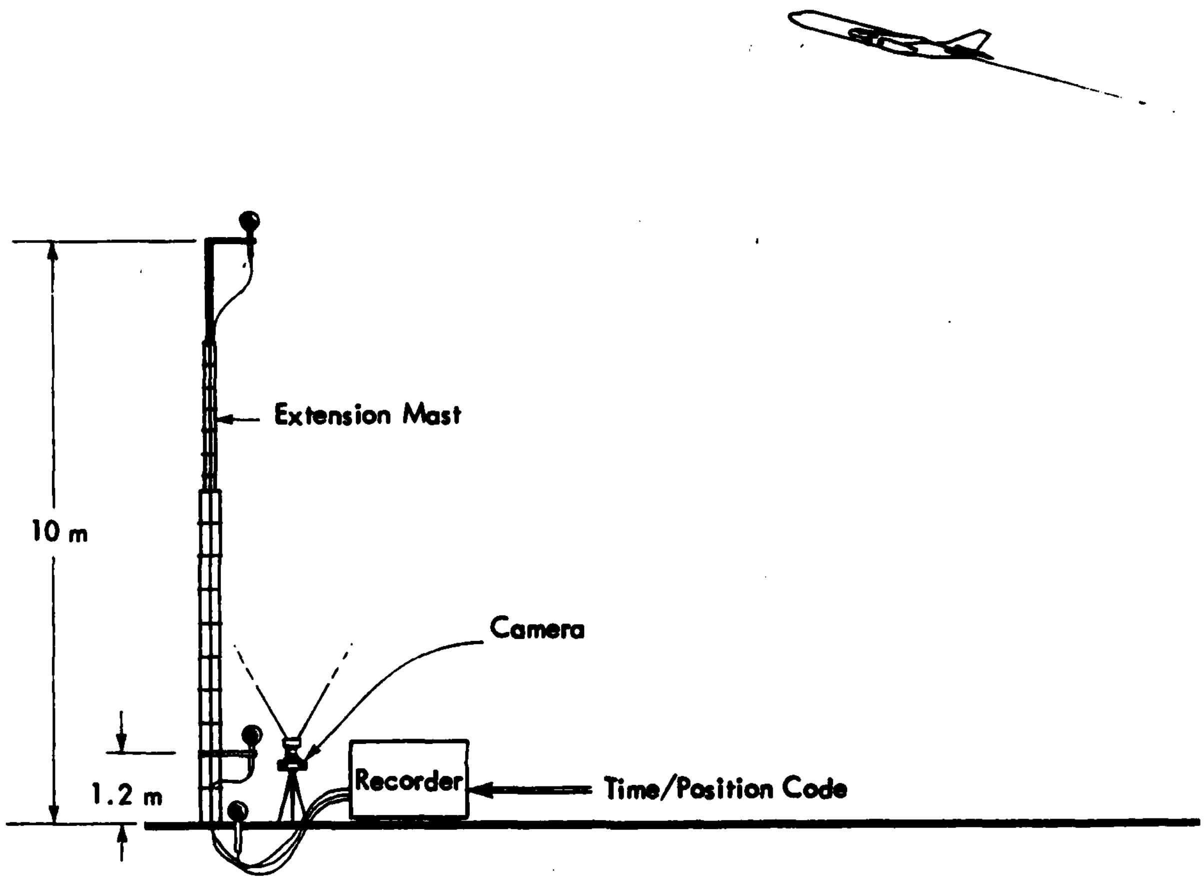

Figure A-2. Three Microphone Array (10 m, 1.2 m and Ground Microphone for Measurement of Aircraft Flyover Noise (Hard and Soft Ground Surface).
Note: Ground microphone was inverted, not embedded into ground as shown.

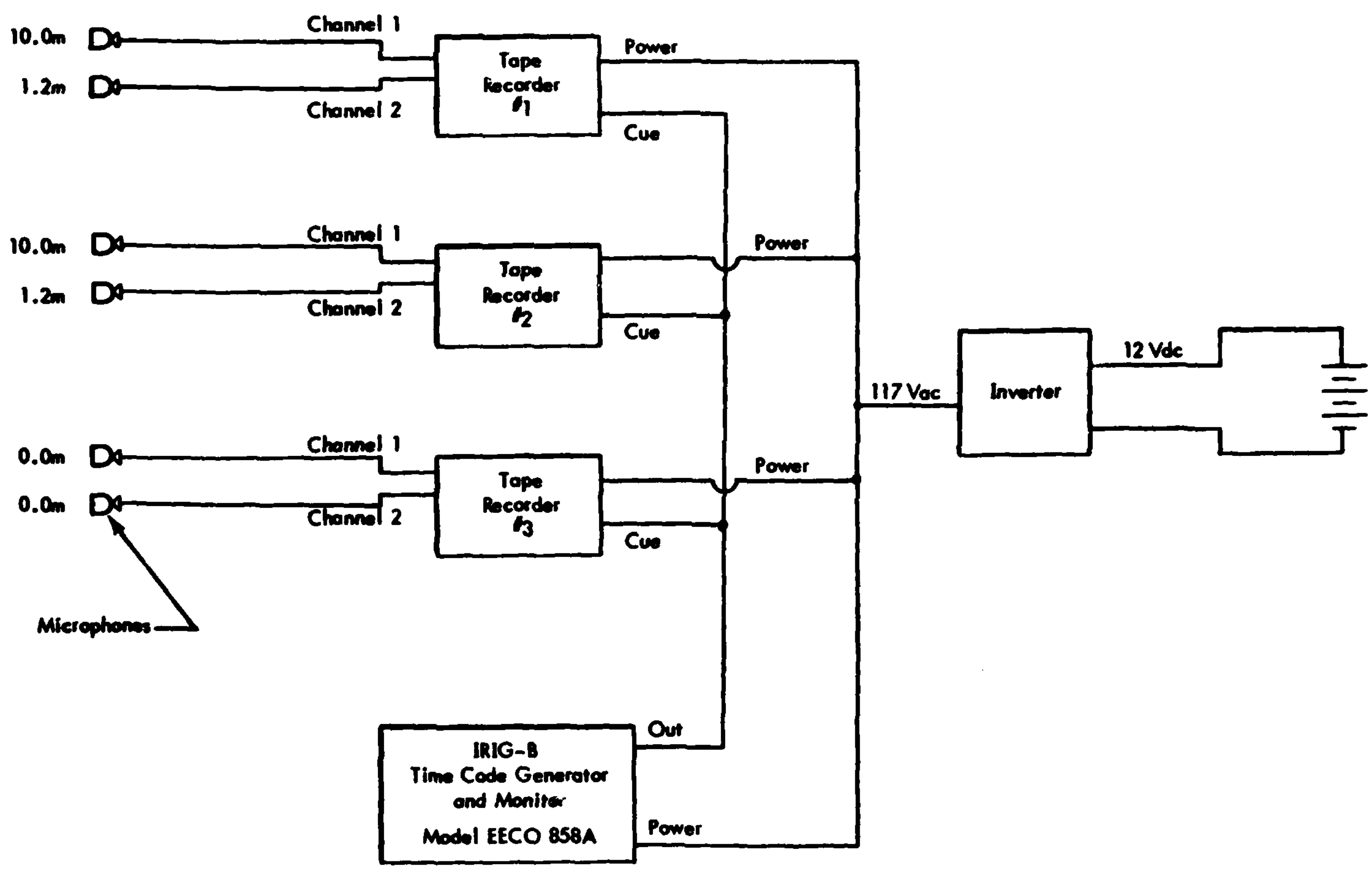

Figure A-3. Instrumentation Block Diagram

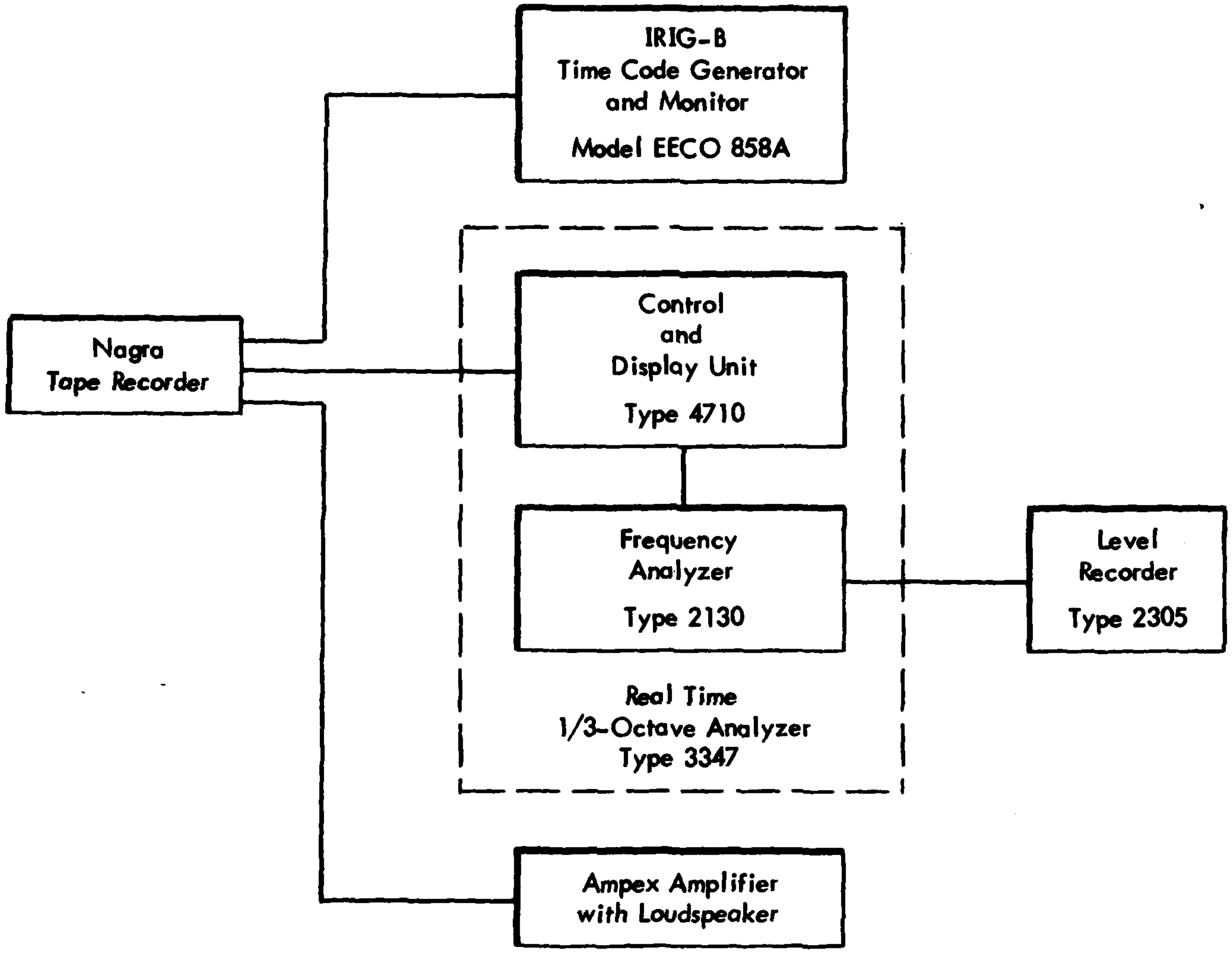

Figure A-4. Flow Diagram of a Preliminary Data Reduction

The average sound pressure level for each half second of each selected flyover for each of the 24 frequency bands was obtained and stored without consideration of time constant requirements, i.e., no temporal weighted averaging was incorporated in the digitization process. A PDP 11 computer was used to write the digitized data on tape and, after reformatting, the data was stored by Wyle Laboratories on a Univac 1108 computer for analysis (one-third octave band sound pressure level data half second time histories referred to as "spectral time histories" or STH).

In order to capture where the aircraft was located relative to the microphone at the time of noise emission corresponding to each half second of recorded data, data from the FAA ARTS (Area Radar Tracking System) were provided (by courtesy of FAA). The aircraft overhead time was used to correlate ARTS time and the Irig-B time code. The ARTS data was used to determine aircraft speed and flight path gradient as well as distance to the microphone.

Meteorological data was recorded before and after each period of noise measurement.

Table 1-7 in Section 1.4.3.3 list the aircraft flyovers selected for digitizing. The remainder of this Appendix consists of spectral time history plots for the selected flyovers. Spectra are shown for the time interval approximately between the 10 dB down points at 1 second intervals (actual data was obtained at 1/2 second intervals). The sequence of these plots is the same as in Table 1-7 (i.e., <u>not</u> ordered by dataset sentinel), and is given again in Table A-2.

Prior to calculation of the various single event metrics, the data were "cleaned," as defined in Appendix D, by applying temporal smoothing and corrections for ambient noise levels.

Table A-2

Contents of Remainder of Appendix A
Spectral Time History Plots)

Microphone Location	Flight	Sentinel (-9000000000)	Page
Approach	DC-10/A	15010	A-10
		16010	A-11
		17010	A-12
		14010	A-13
		11010	A-14
		12010	A-15
Approach	727/B	22010	A-16
		23010	A-17
		19010	A-18
		21010	A-19
		18010	A-20
		20010	A-21
Approach	707/H	53010	A-22
		57010	A-23
		41010	A-24
		49010	A-25
		38010	A-26
		45010	A-27
Approach	727/I	54010	A-28
		58010	A-29
		42010	A-30
		50010	A-31
		39010	A-32
		46010	A-33
Approach	707/J	55010	A-34
		59010	A-35
		43010	A-36
		51010	A-37
		40010	A-38
		47010	A-39
Approach	DC10/K	52010	A-40
		56010	A-41
		48010	A-42
		44010	A-43
		37010	A-44
Sideline	707/C	26010	A-45
		24010	A-46
Sideline	707/D	27010	A-47
		25010	A-48
Sideline	707/E	30010	A-49
		32010	A-50
Sideline	727/F	31010	A-51
		33010	A-52
		29010	A-53
		28010	A-54

Table A-2 (Continued)

Sideline	B727/L	68020	A-55
		72020	A-57
		64020	A-58
		60020	A-59
Sideline	B707/N	69020	A-61
		73020	A-62
		65020	A-64
		61020	A-66
Sideline	DC10/Q	70020	A-67
		74020	A-69
		66020	A-71
		62020	A-73
Sideline	DC10/R	71020	A-75
		75020	A-76
		67020	A-77
		63020	A-78
Takeoff	727/G	34010	A-79
Takeoff	727/G	36010	A-80
		35010	A-81
Takeoff	B727/M	77020	A-82
		92020	A-83
		85020	A-84
Takeoff	B707/O	79020	A-85
		94020	A-86
		87020	A-87
Takeoff	B707/P	80020	A-88
		95020	A-89
		88020	A-90
Takeoff	DC-10/S	81020	A-91
		96020	A-92
		89020	A-93
Takeoff	DC-10/T	82020	A-94
		97020	A-95
		90020	A-96
Takeoff	B747/U	76020	A-97
		91020	A-98
		84020	A-99
Takeoff	B747/V	78020	A-100
		93020	A-101
		86020	A-102

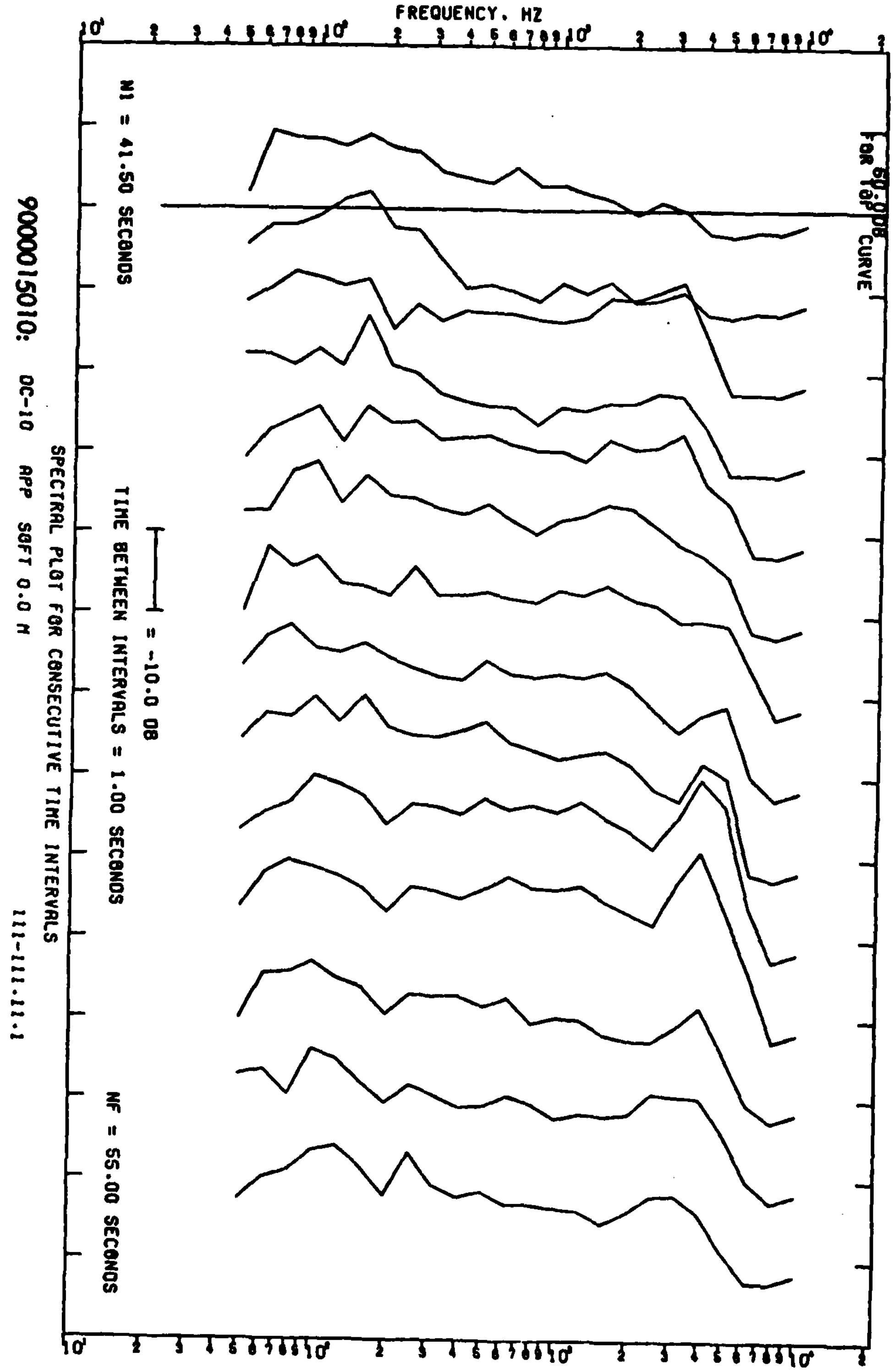
FREQUENCY, HZ
NI = 41.50 SECONDS
60.0 DB FOR TOP CURVE
= -10.0 DB
TIME BETWEEN INTERVALS = 1.00 SECONDS
SPECTRAL PLOT FOR CONSECUTIVE TIME INTERVALS
9000015010: DC-10 APP SOFT 0.0 M
NF = 55.00 SECONDS

Figure A-A1

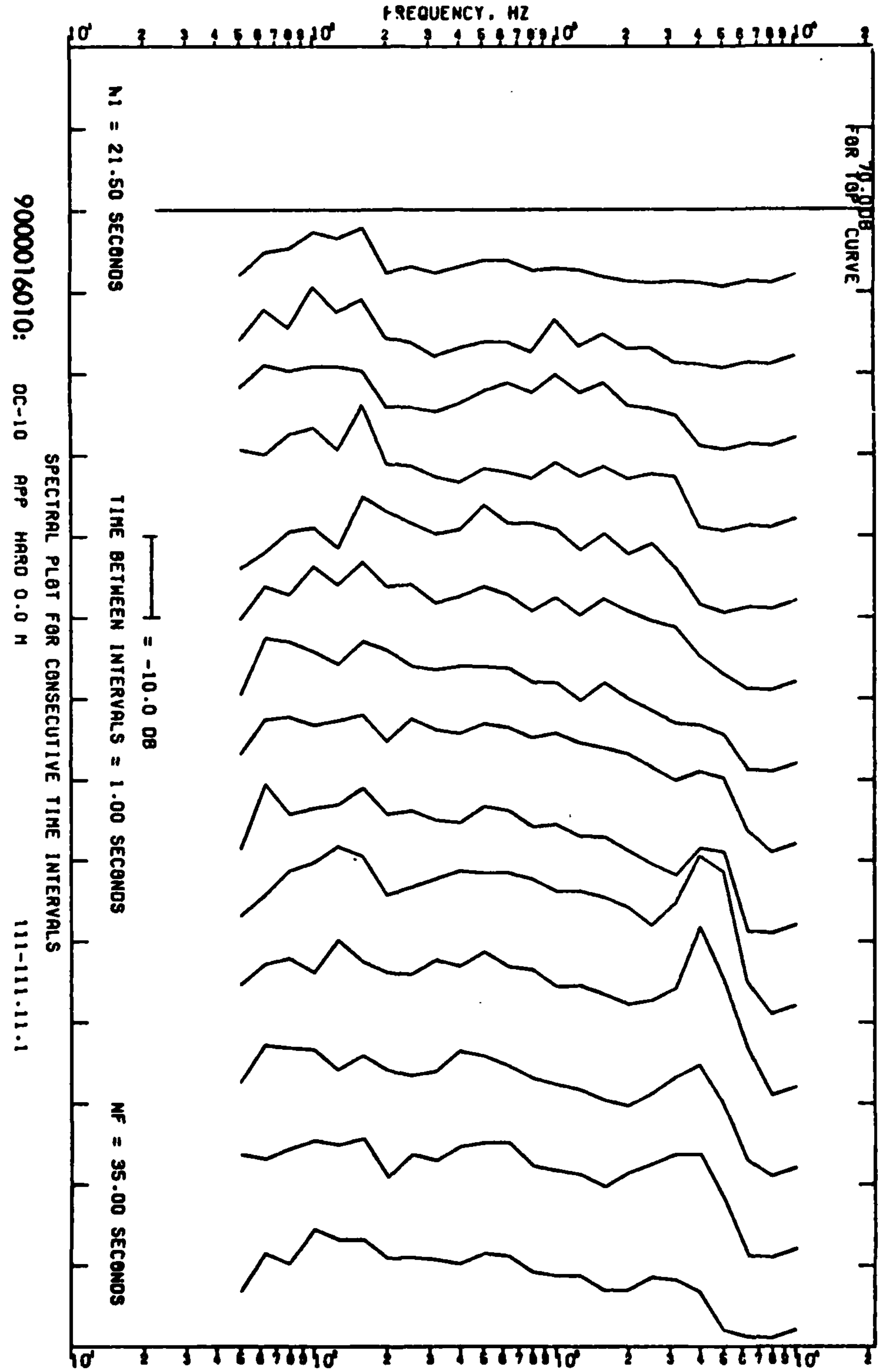
FREQUENCY, HZ
70.0 DB FOR TOP CURVE
NI = 21.50 SECONDS
= -10.0 DB
TIME BETWEEN INTERVALS = 1.00 SECONDS
NF = 35.00 SECONDS
SPECTRAL PLOT FOR CONSECUTIVE TIME INTERVALS
900001601O: DC-10 APP HARD 0.0 M
111-111.11.1

Figure A-A2

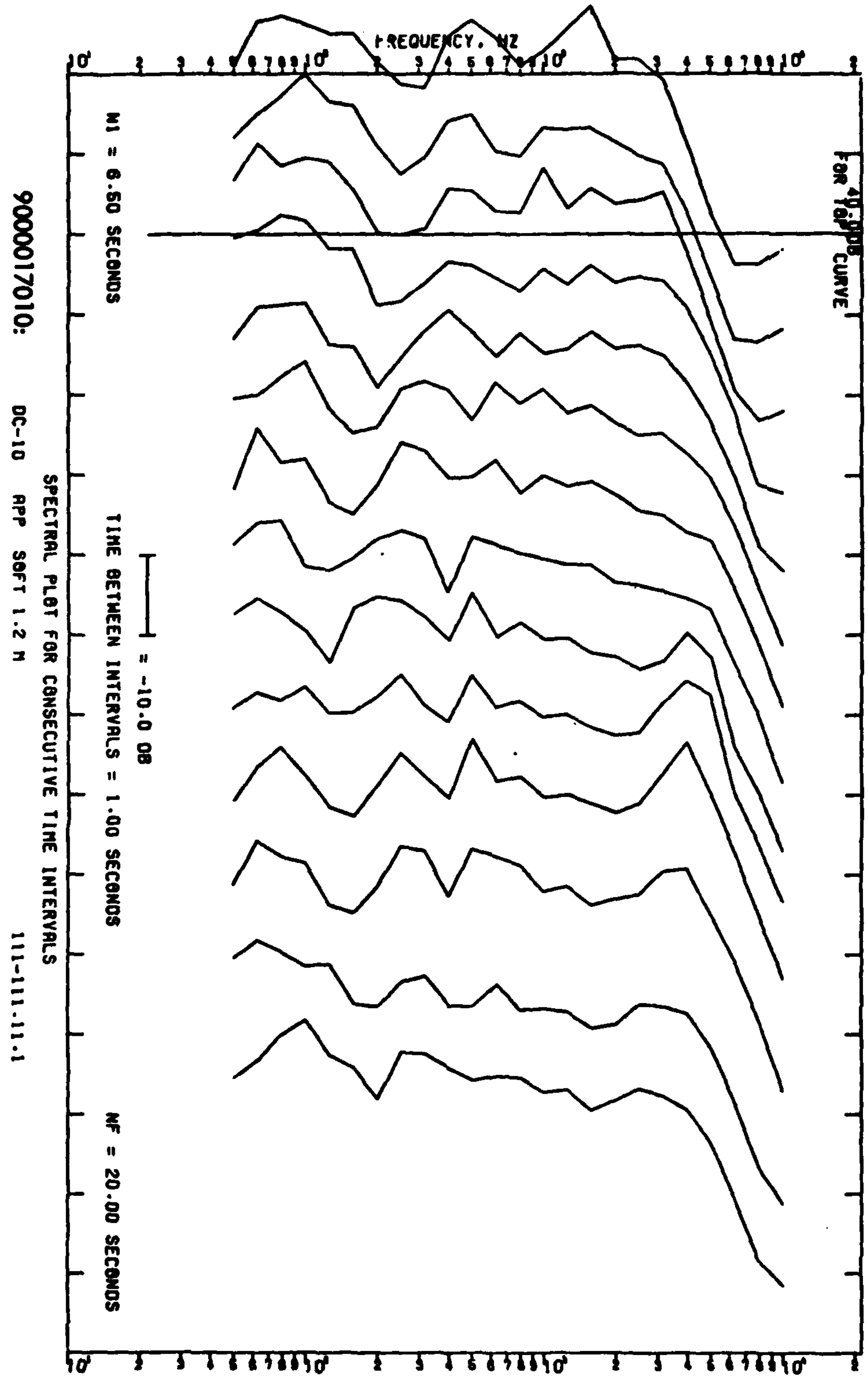
FREQUENCY, HZ
40.0 DB FOR YOP CURVE
NI = 6.50 SECONDS
= -10.0 DB
TIME BETWEEN INTERVALS = 1.00 SECONDS
NF = 20.00 SECONDS
SPECTRAL PLOT FOR CONSECUTIVE TIME INTERVALS
9000017010:
DC-10 APP S0FT 1.2 M
111-111.11.1

Figure A-A3

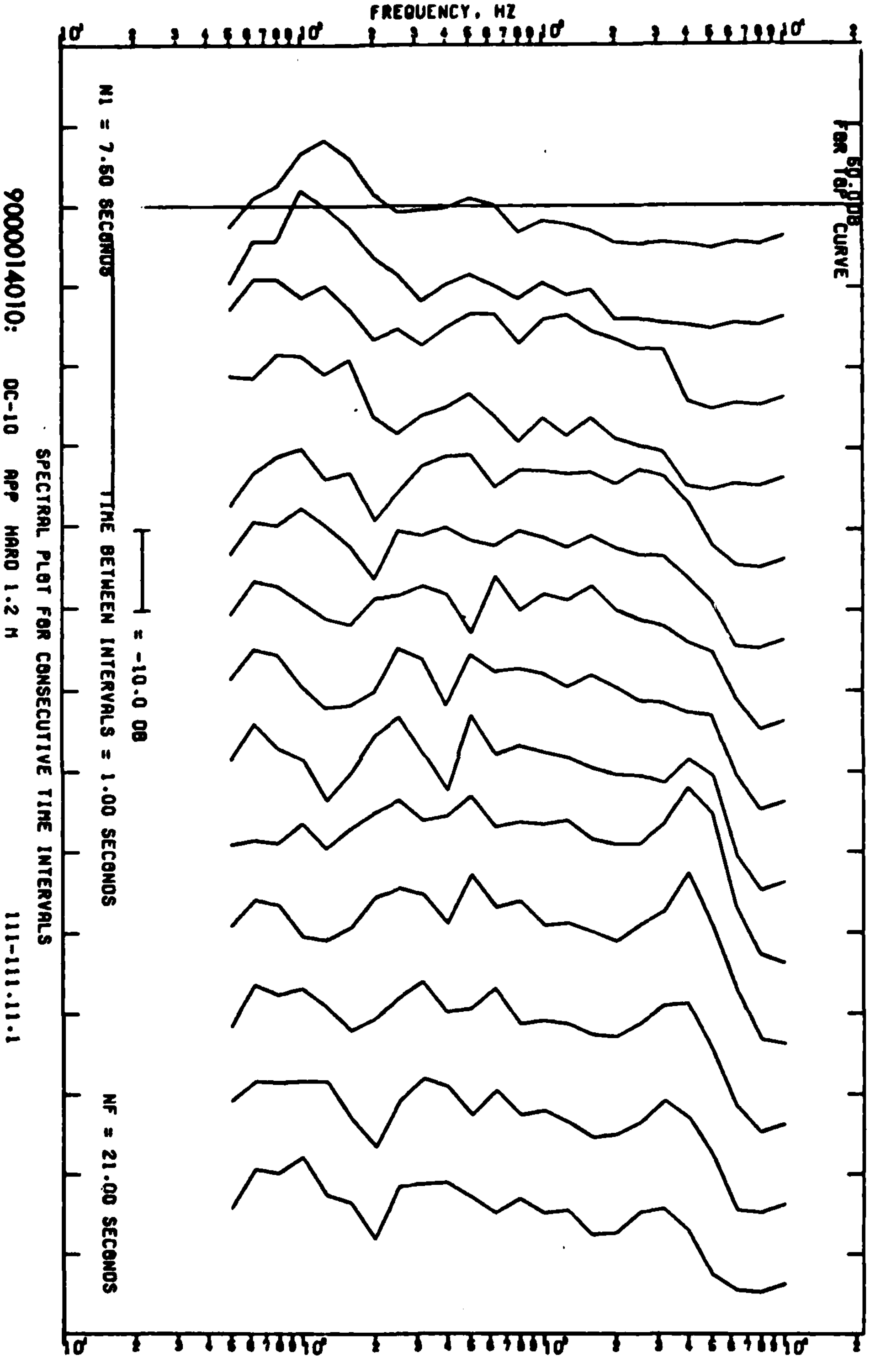
FREQUENCY, HZ
50.0 DB
FOR TOP CURVE
N1 = 7.50 SECONDS
= -10.0 DB
TIME BETWEEN INTERVALS = 1.00 SECONDS
NF = 21.00 SECONDS
SPECTRAL PLOT FOR CONSECUTIVE TIME INTERVALS
111-111.11.1
9000014010: DC-10 APP HARD 1.2 M

Figure A-A4

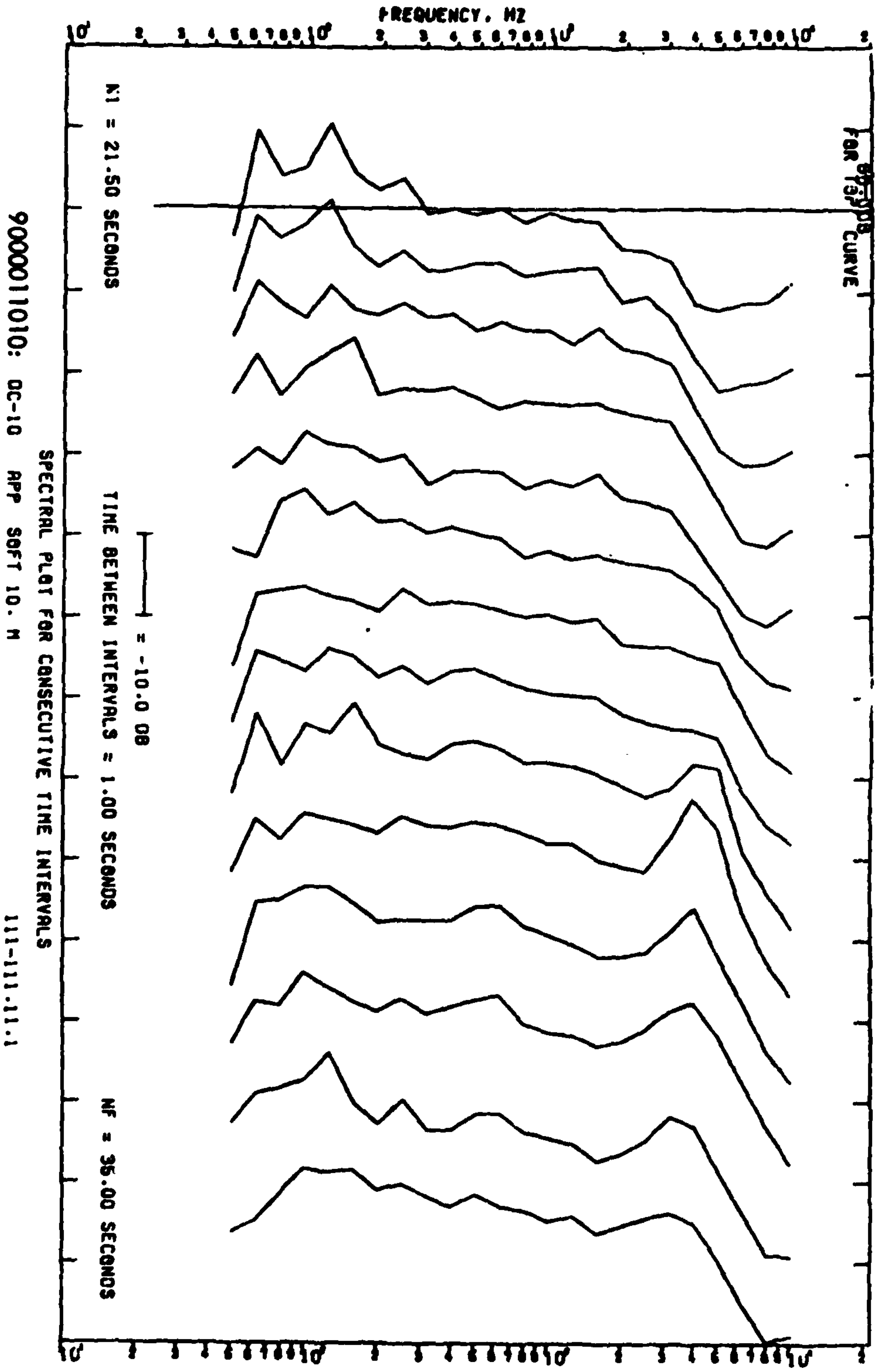
FREQUENCY, HZ
NI = 21.50 SECONDS
TIME BETWEEN INTERVALS = 1.00 SECONDS
= -10.0 DB
NF = 35.00 SECONDS
SPECTRAL PLOT FOR CONSECUTIVE TIME INTERVALS
9000011010: DC-10 APP 50FT 10. M
111-111.11.1

Figure A-A5

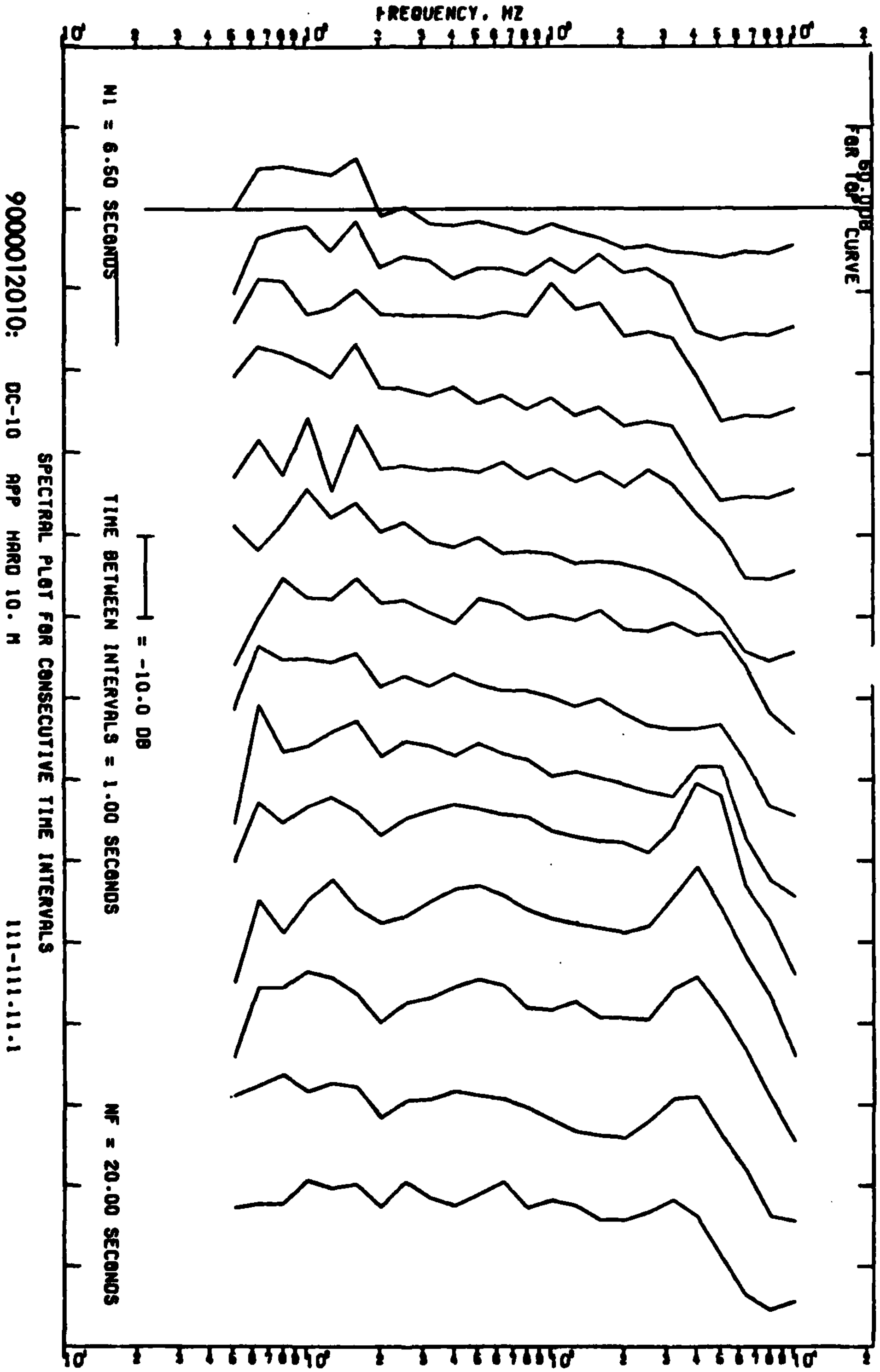
FREQUENCY, HZ
60.0 DB FOR TOP CURVE
NI = 6.50 SECONDS
= -10.0 DB
TIME BETWEEN INTERVALS = 1.00 SECONDS
NF = 20.00 SECONDS
SPECTRAL PLOT FOR CONSECUTIVE TIME INTERVALS
9000012010: DC-10 APP HARD 10. M
111-111-11.1

Figure A-A6

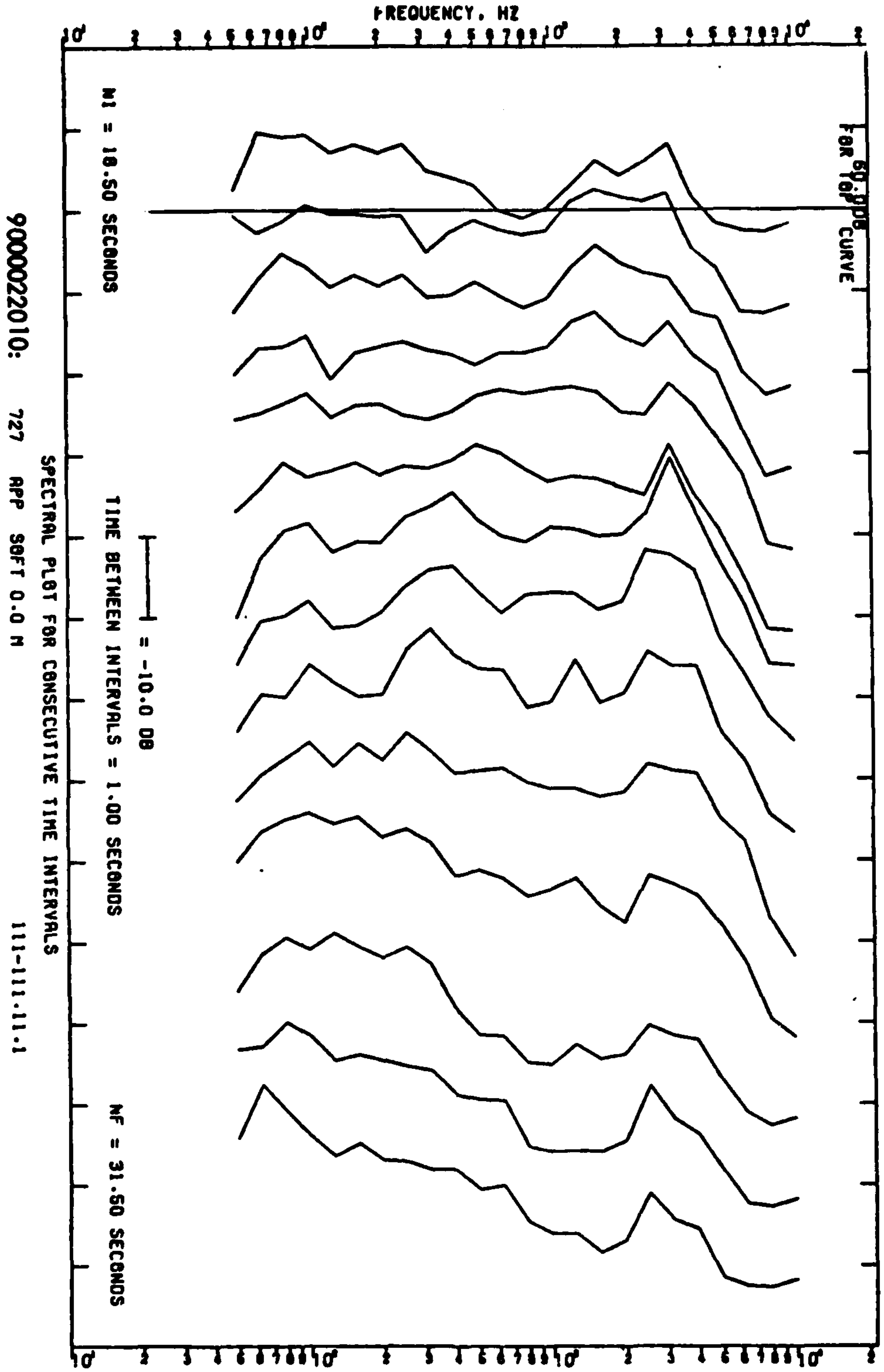
FREQUENCY, HZ
60.0 DB FOR TOP CURVE
NI = 18.50 SECONDS
= -10.0 DB
TIME BETWEEN INTERVALS = 1.00 SECONDS
NF = 31.50 SECONDS
SPECTRAL PLOT FOR CONSECUTIVE TIME INTERVALS
9000022010: 727 APP SOFT 0.0 M
111-111.11.1

Figure A-B1

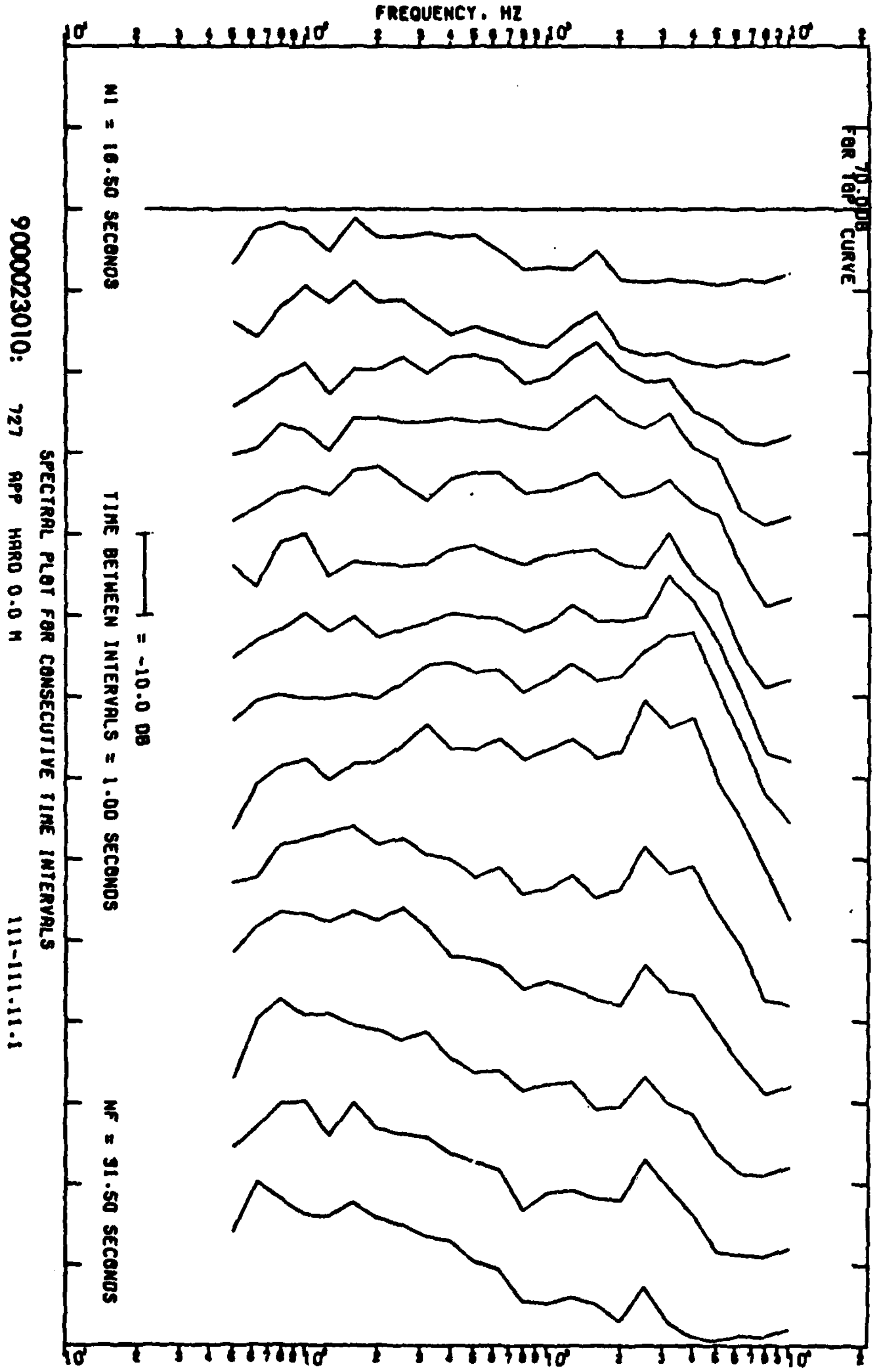
FREQUENCY, HZ
70.0DB FOR TGP CURVE
NI = 18.50 SECONDS
= -10.0 DB
TIME BETWEEN INTERVALS = 1.00 SECONDS
NF = 91.50 SECONDS
SPECTRAL PLOT FOR CONSECUTIVE TIME INTERVALS
9000023010: 727 APP HARD 0.0 M
111-111.11.1

Figure A-82

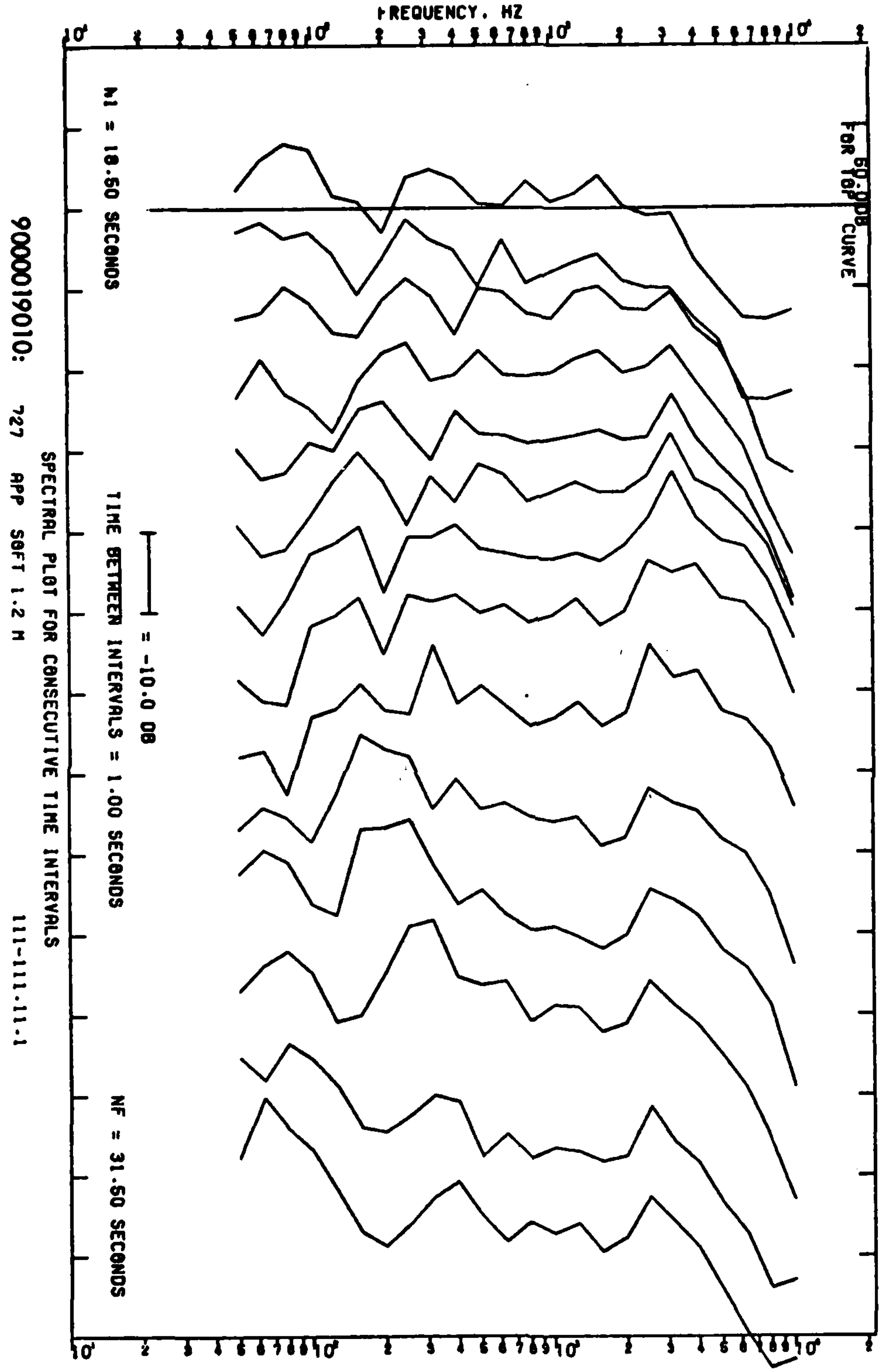
FREQUENCY, HZ
NI = 18.50 SECONDS
60.0 DB FOR TGP CURVE
= -10.0 DB
TIME BETWEEN INTERVALS = 1.00 SECONDS
NF = 31.50 SECONDS
SPECTRAL PLOT FOR CONSECUTIVE TIME INTERVALS
9000019010: 727 APP SOFT 1.2 M
111-111.11.11.1

Figure A-B3

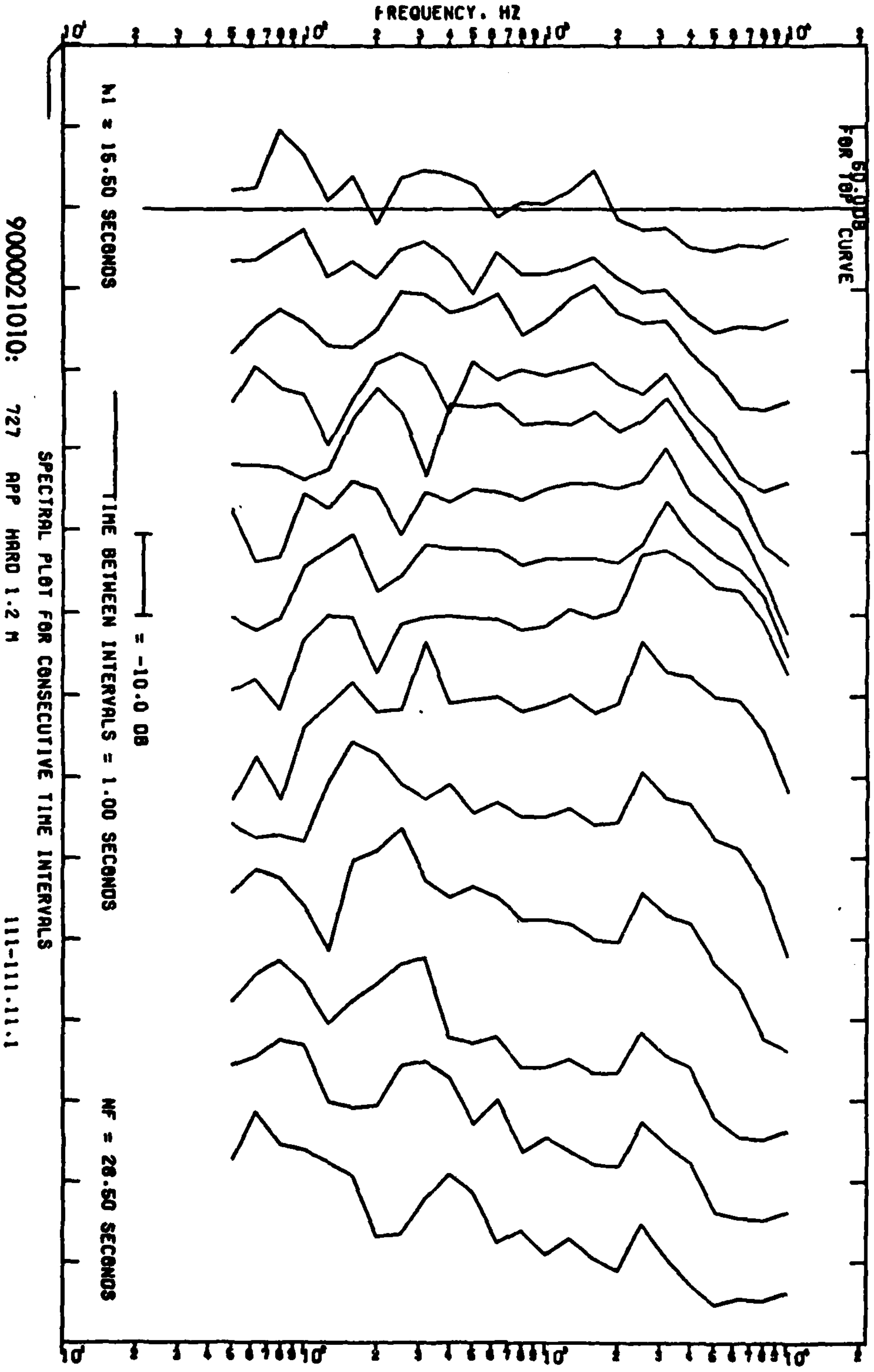
FREQUENCY, HZ
60.0 DB FOR TOP CURVE
NI = 15.50 SECONDS
NF = 28.50 SECONDS
= -10.0 DB
TIME BETWEEN INTERVALS = 1.00 SECONDS
SPECTRAL PLOT FOR CONSECUTIVE TIME INTERVALS
9000021010: 727 APP HARD 1.2 M
111-111.11.11.1

Figure A-B4

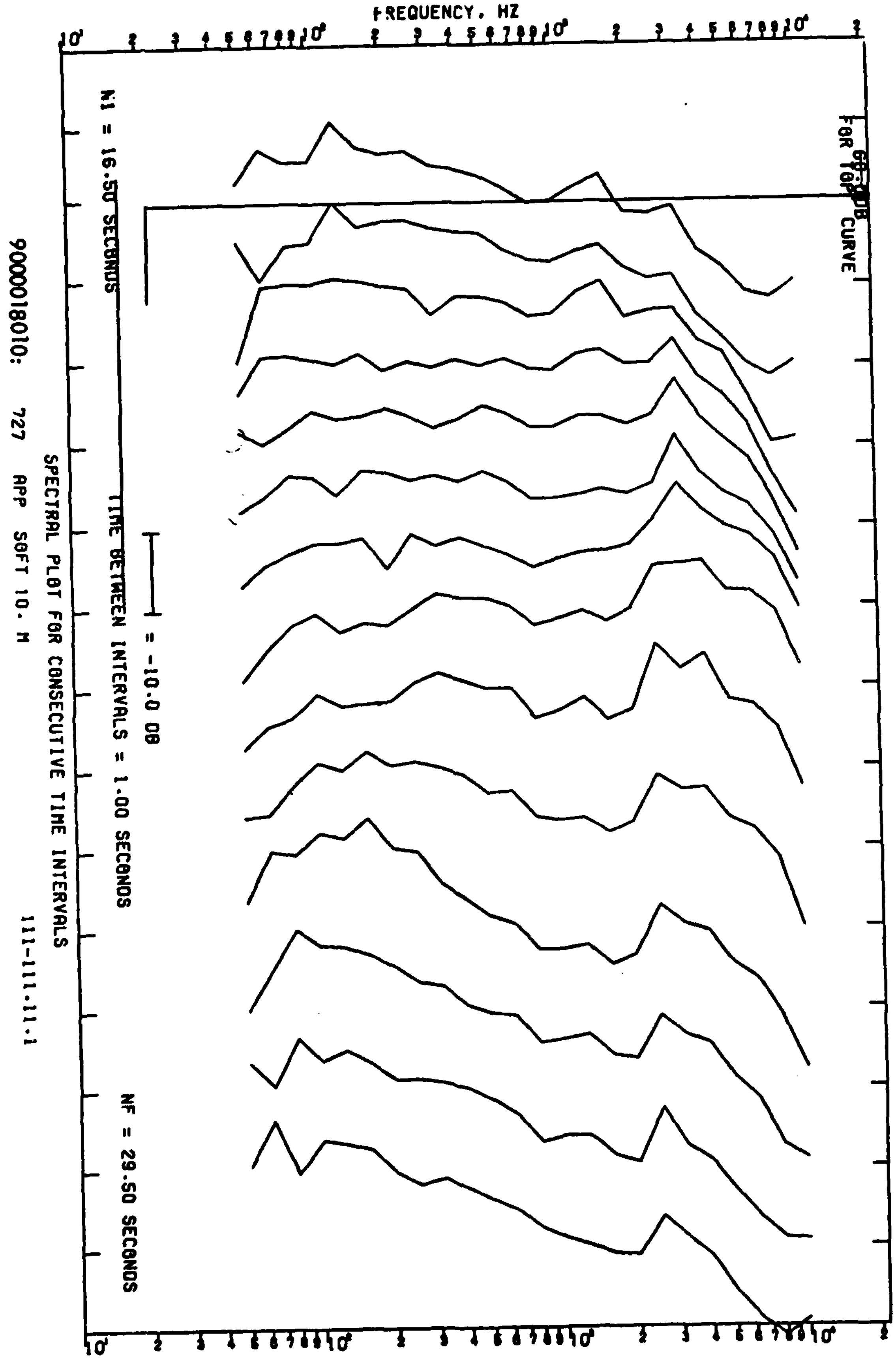

FREQUENCY, HZ
60.0 DB FOR TOP CURVE
N1 = 16.50 SECONDS
= -10.0 DB
TIME BETWEEN INTERVALS = 1.00 SECONDS
NF = 29.50 SECONDS
SPECTRAL PLOT FOR CONSECUTIVE TIME INTERVALS
9000018010: 727 APP SOFT 10. M
111-111.11.1

Figure A-B5

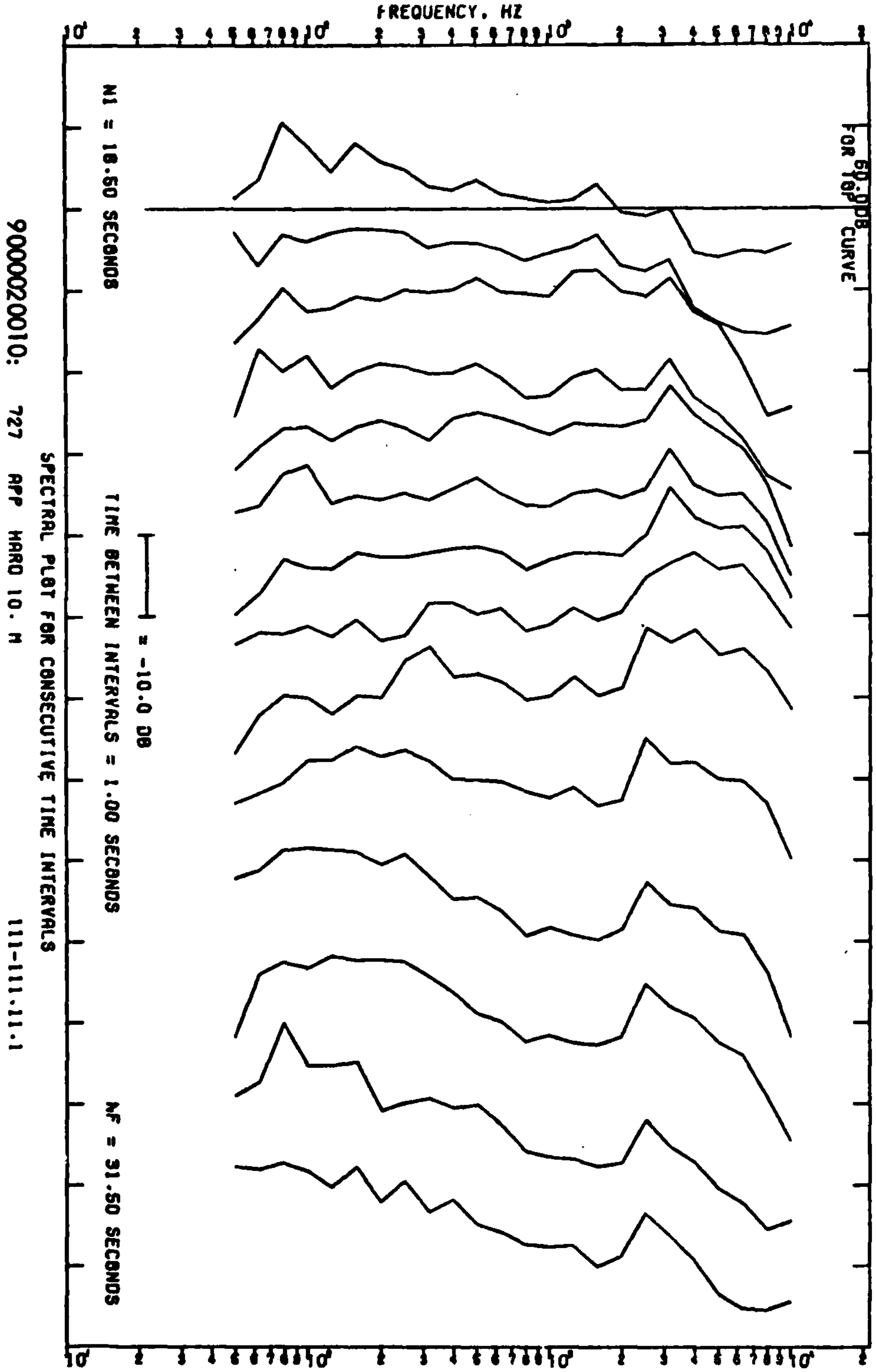
FREQUENCY, HZ
60.0 DB FOR TOP CURVE
NI = 18.50 SECONDS
TIME BETWEEN INTERVALS = 1.00 SECONDS
= -10.0 DB
NF = 31.50 SECONDS
SPECTRAL PLOT FOR CONSECUTIVE TIME INTERVALS
9000020010: 727 APP HARD 10. M
111-111.11.1

Figure A-B6

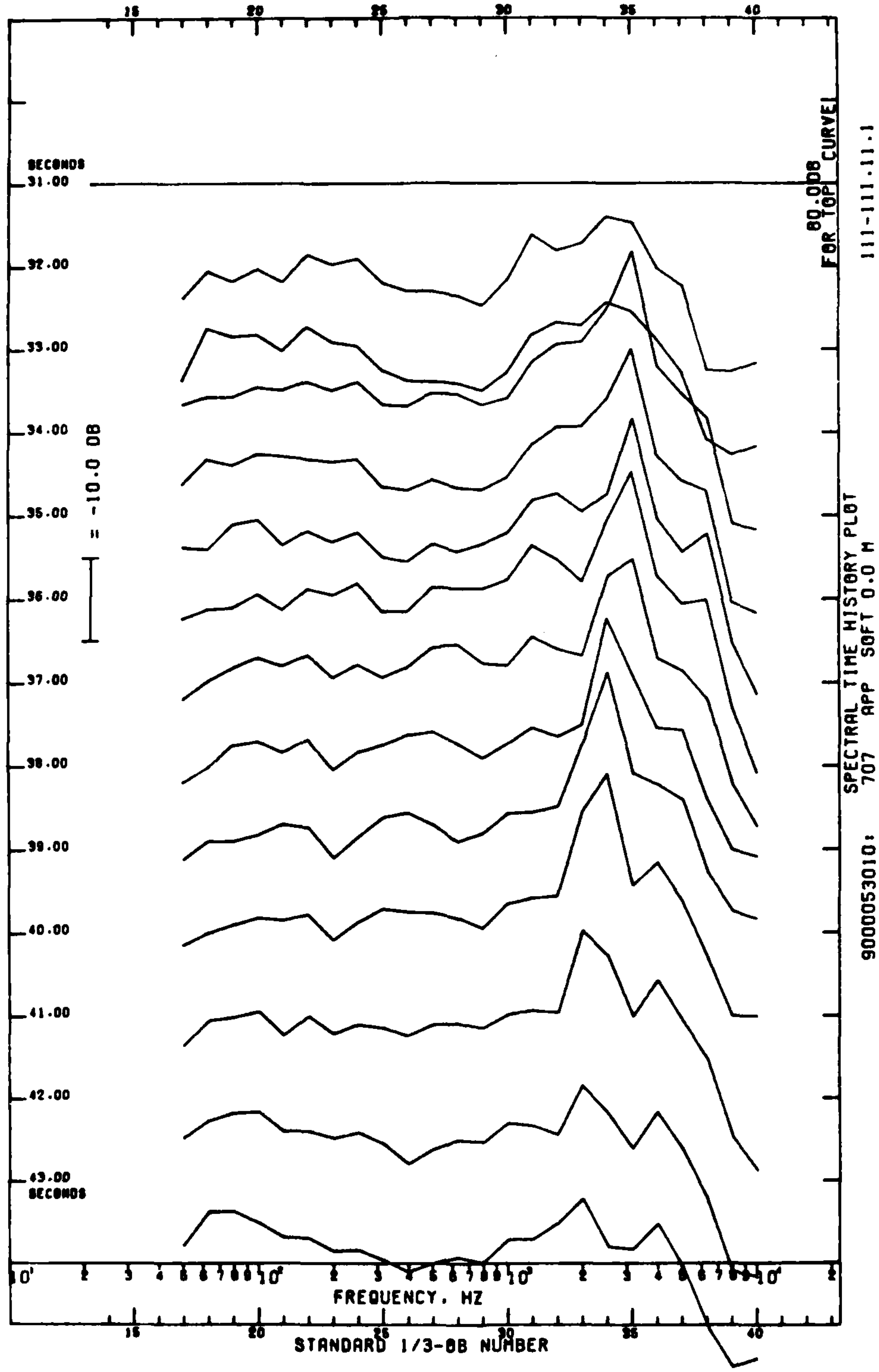
SECONDS
31.00
32.00
33.00
34.00
35.00
36.00
37.00
38.00
39.00
40.00
41.00
42.00
43.00
SECONDS
= -10.0 DB
80.0DB
FOR TOP CURVE
111-111.11.1
SPECTRAL TIME HISTORY PLOT
707 APP SOFT 0.0 M
900005301O:
FREQUENCY, HZ
STANDARD 1/3-OB NUMBER

Figure A-H1

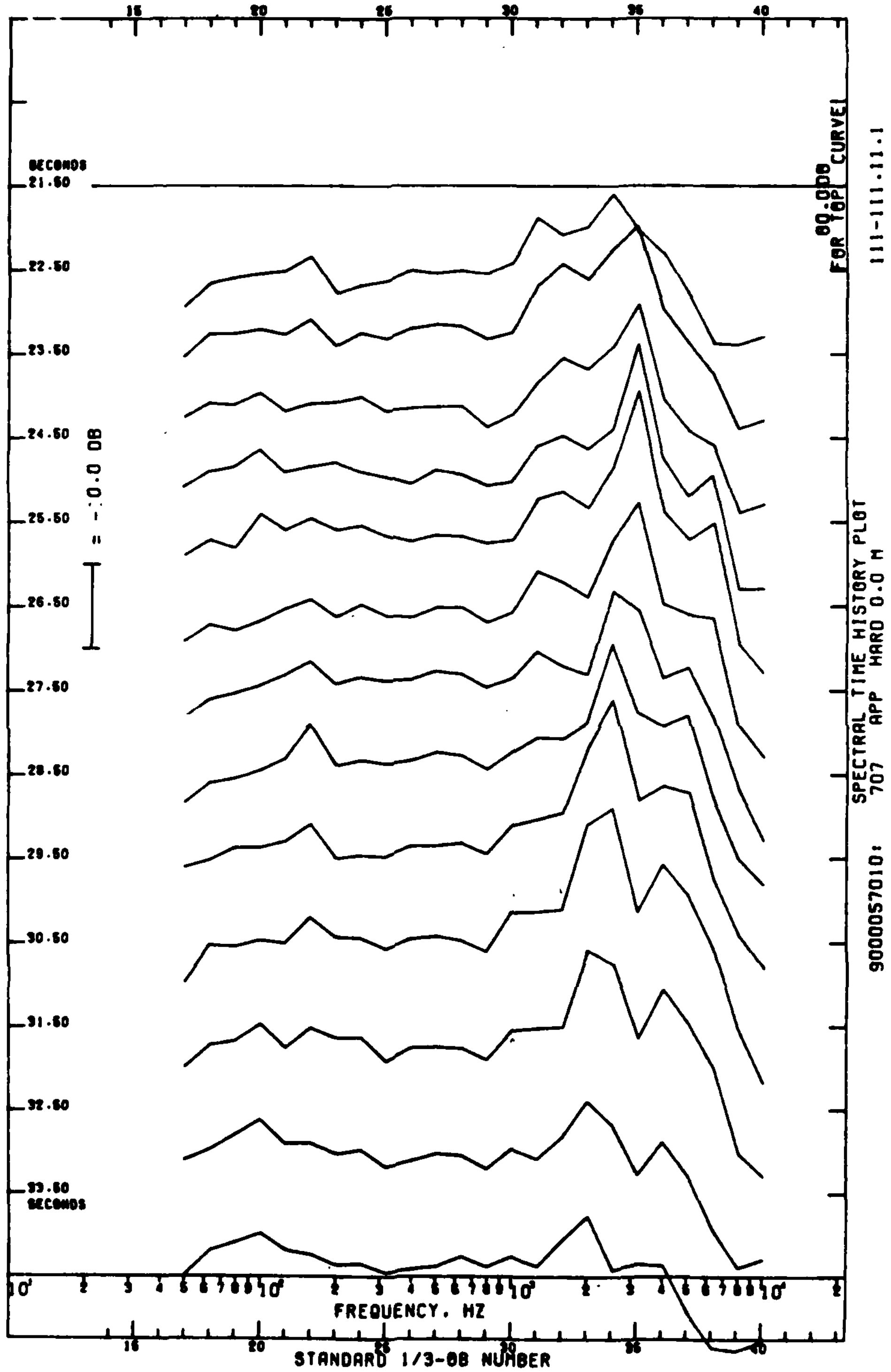

SECONDS
21.50
22.50
23.50
24.50
25.50
26.50
27.50
28.50
29.50
30.50
31.50
32.50
33.50
SECONDS
= -10.0 DB
80.0DB
FOR TOP CURVE)
111-111.11.1
SPECTRAL TIME HISTORY PLOT
707 APP HARD 0.0 M
9000057010:
FREQUENCY, HZ
STANDARD 1/3-OB NUMBER

Figure A-H2

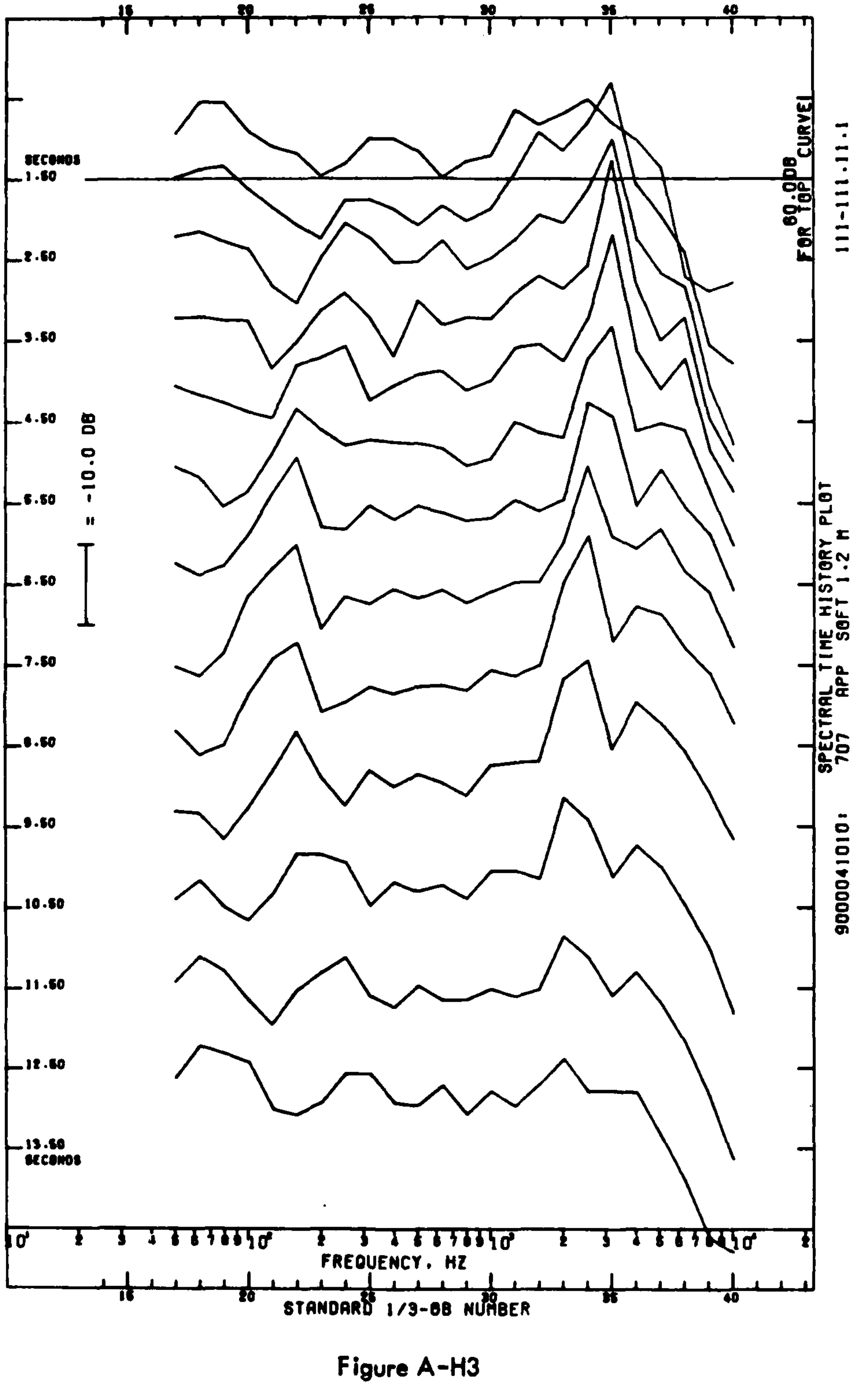
SECONDS
1.50
2.50
3.50
4.50
5.50
6.50
7.50
8.50
9.50
10.50
11.50
12.50
13.50
SECONDS
= -10.0 DB
60.0DB
FOR TOP CURVE)
111-111.11.1
SPECTRAL TIME HISTORY PLOT
707 APP SOFT 1.2 M
9000041010:
FREQUENCY, HZ
STANDARD 1/3-OB NUMBER

Figure A-H3

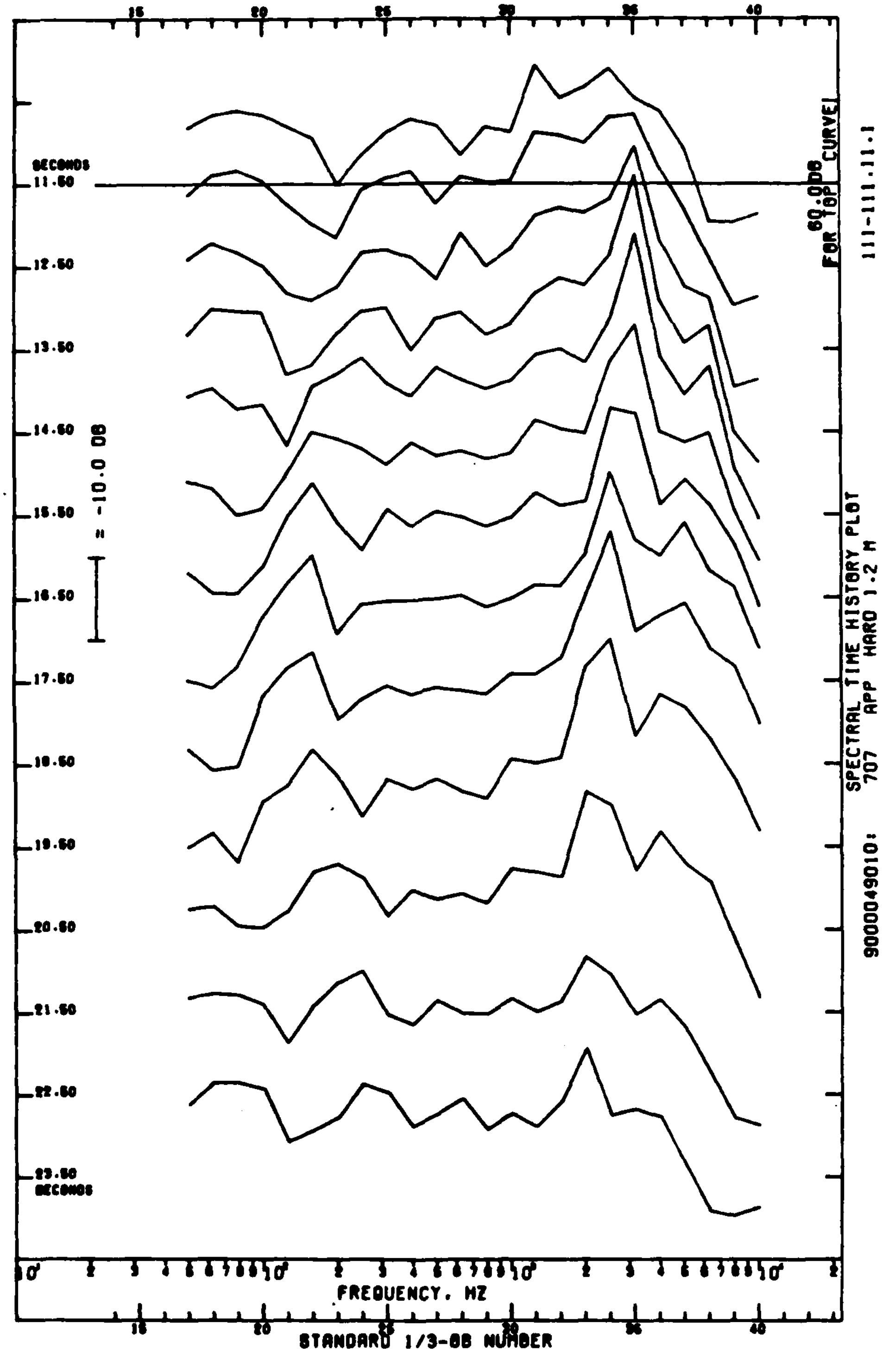
SECONDS
11.50
12.50
13.50
14.50
15.50
16.50
17.50
18.50
19.50
20.50
21.50
22.50
23.50
SECONDS
= -10.0 DB
60.0DB FOR TOP CURVE)
111-111.11.1
SPECTRAL TIME HISTORY PLOT
707 APP HARD 1.2 M
9000049010:
FREQUENCY, HZ
STANDARD 1/3-OB NUMBER

Figure A-H4

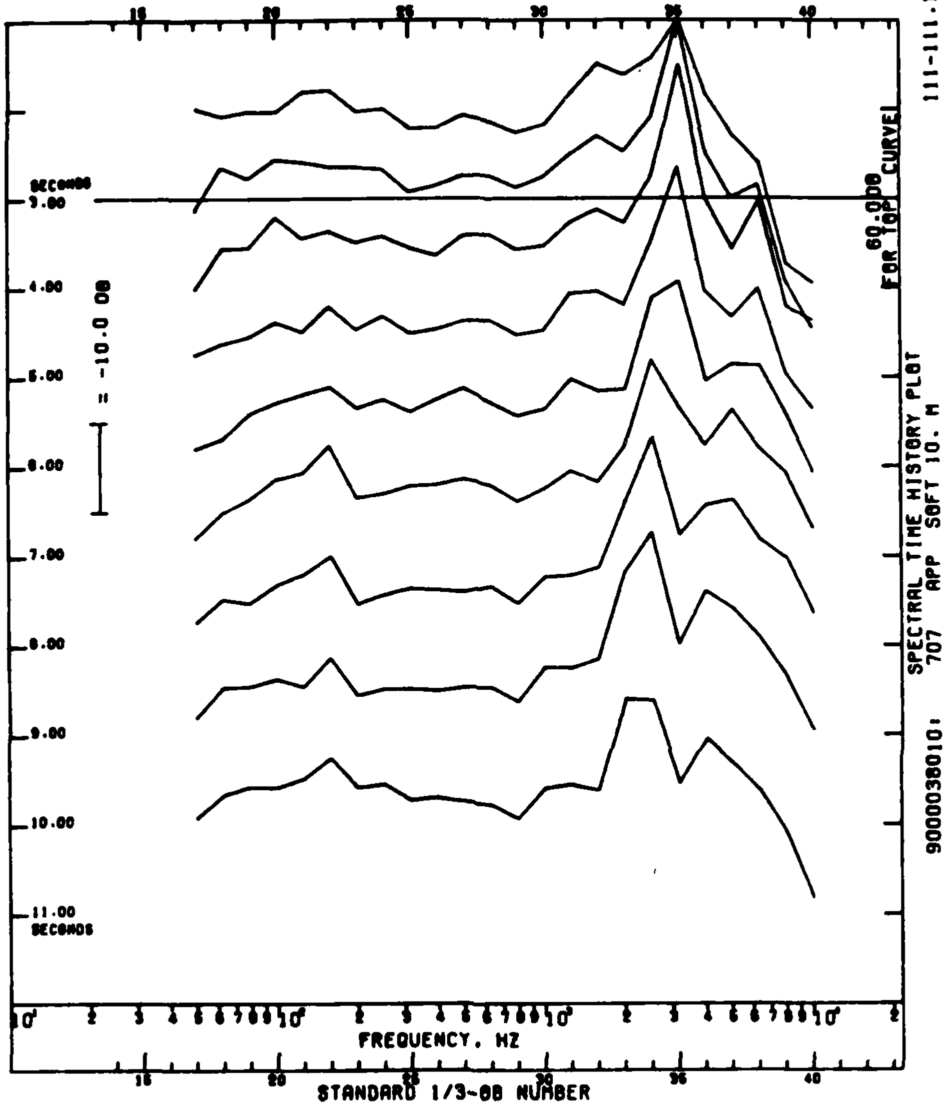
SECONDS
3.00
4.00
5.00
6.00
7.00
8.00
9.00
10.00
11.00
SECONDS
= -10.0 DB
60.000 FOR TOP CURVE
SPECTRAL TIME HISTORY PLOT
707 APP SGFT 10. M
9000038010:
111-111.11.1
FREQUENCY, HZ
STANDARD 1/3-OB NUMBER

Figure A-H5

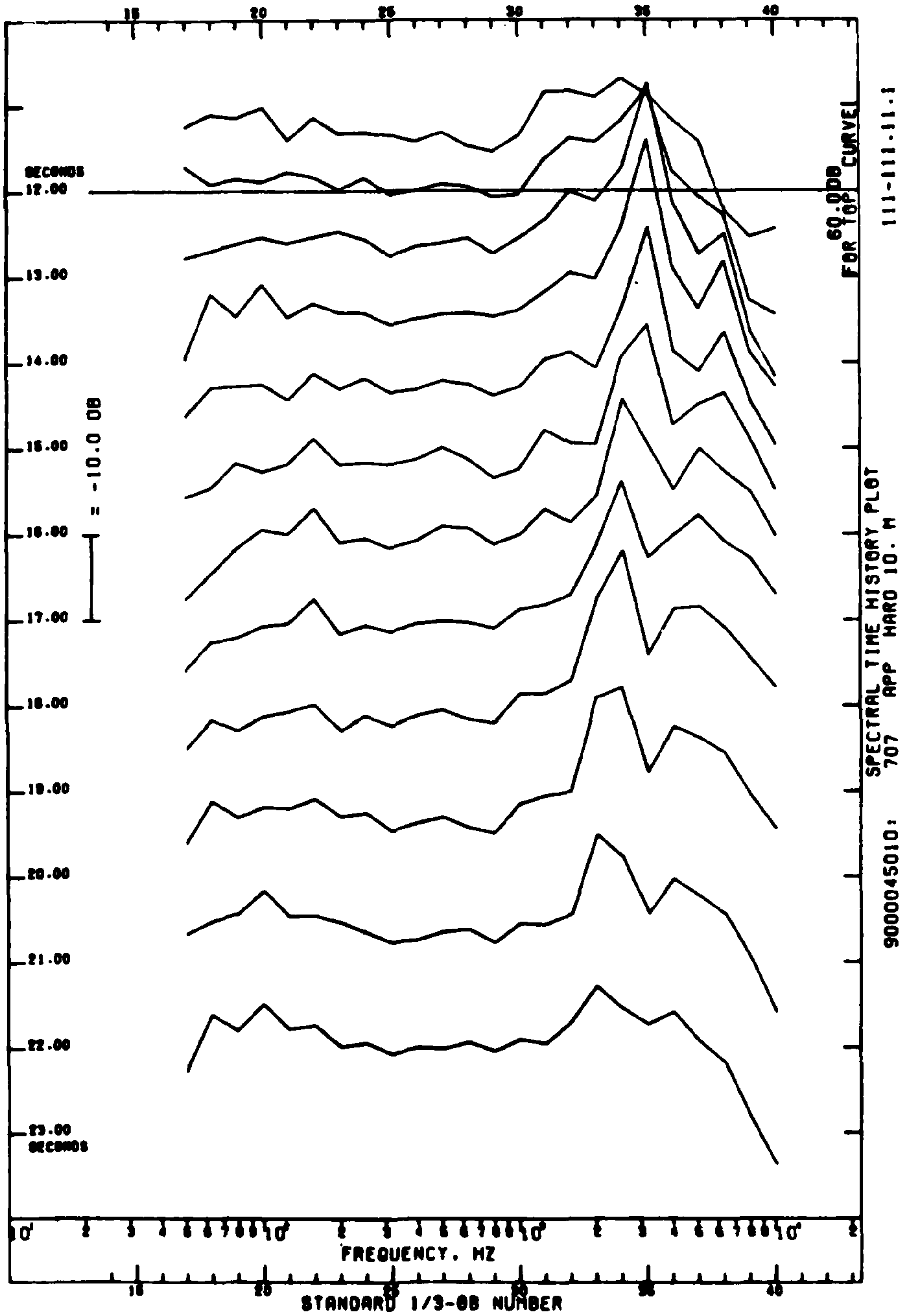

SECONDS
12.00
13.00
14.00
15.00
16.00
17.00
18.00
19.00
20.00
21.00
22.00
23.00
SECONDS
= -10.0 DB
60.0DB FOR TOP CURVE
111-111-11-1
SPECTRAL TIME HISTORY PLOT
707 APP HARD 10. M
900004501O:
FREQUENCY, HZ
STANDARD 1/3-OB NUMBER

Figure A-H6

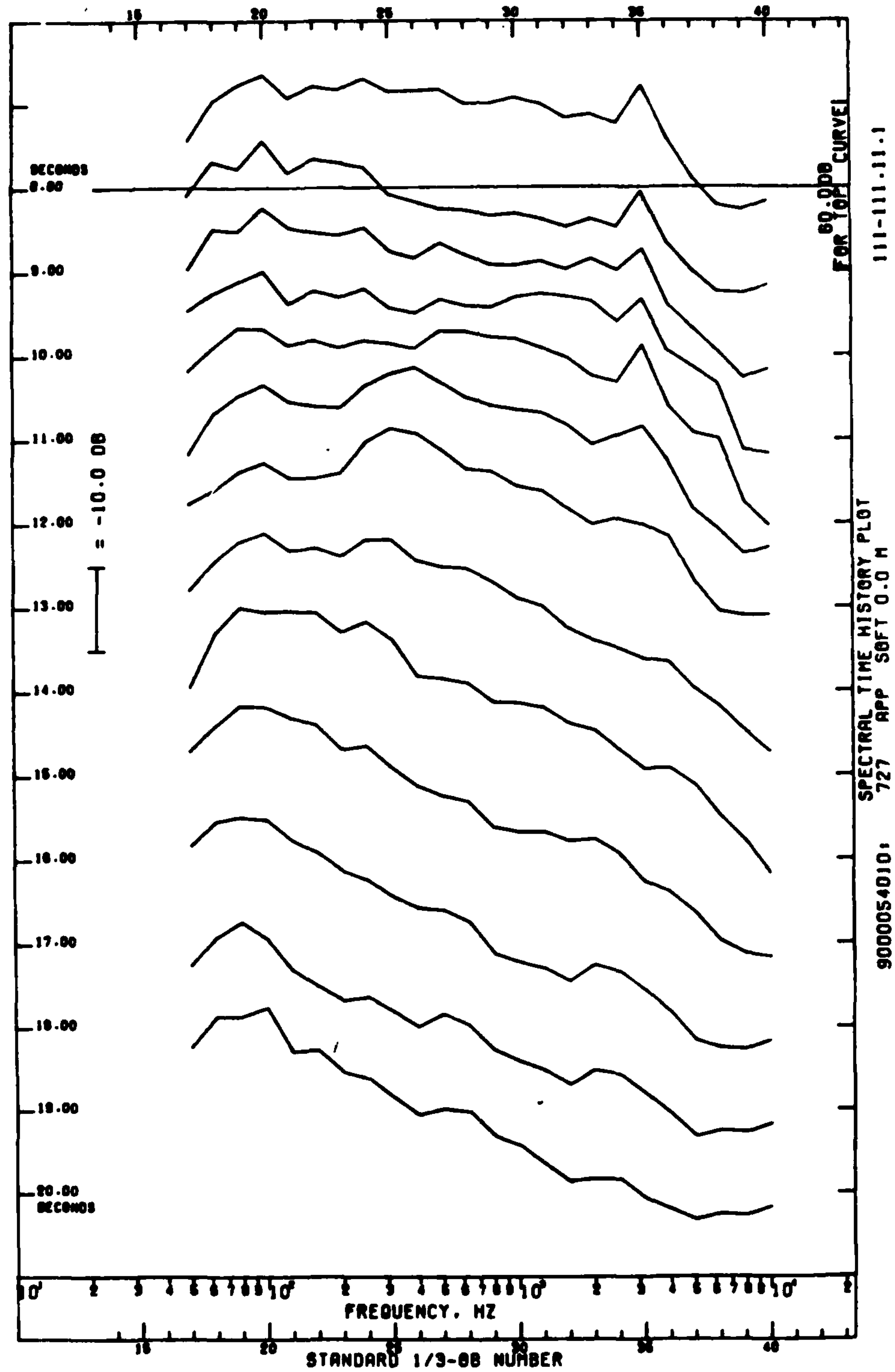
SECONDS
8.00
9.00
10.00
11.00
12.00
13.00
14.00
15.00
16.00
17.00
18.00
19.00
20.00
SECONDS
= -10.0 DB
60.0DB
FOR TOP CURVE
111-111.11.1
SPECTRAL TIME HISTORY PLOT
727 APP 50FT 0.0 M
9000054010:
FREQUENCY, HZ
STANDARD 1/3-OB NUMBER

Figure A-11

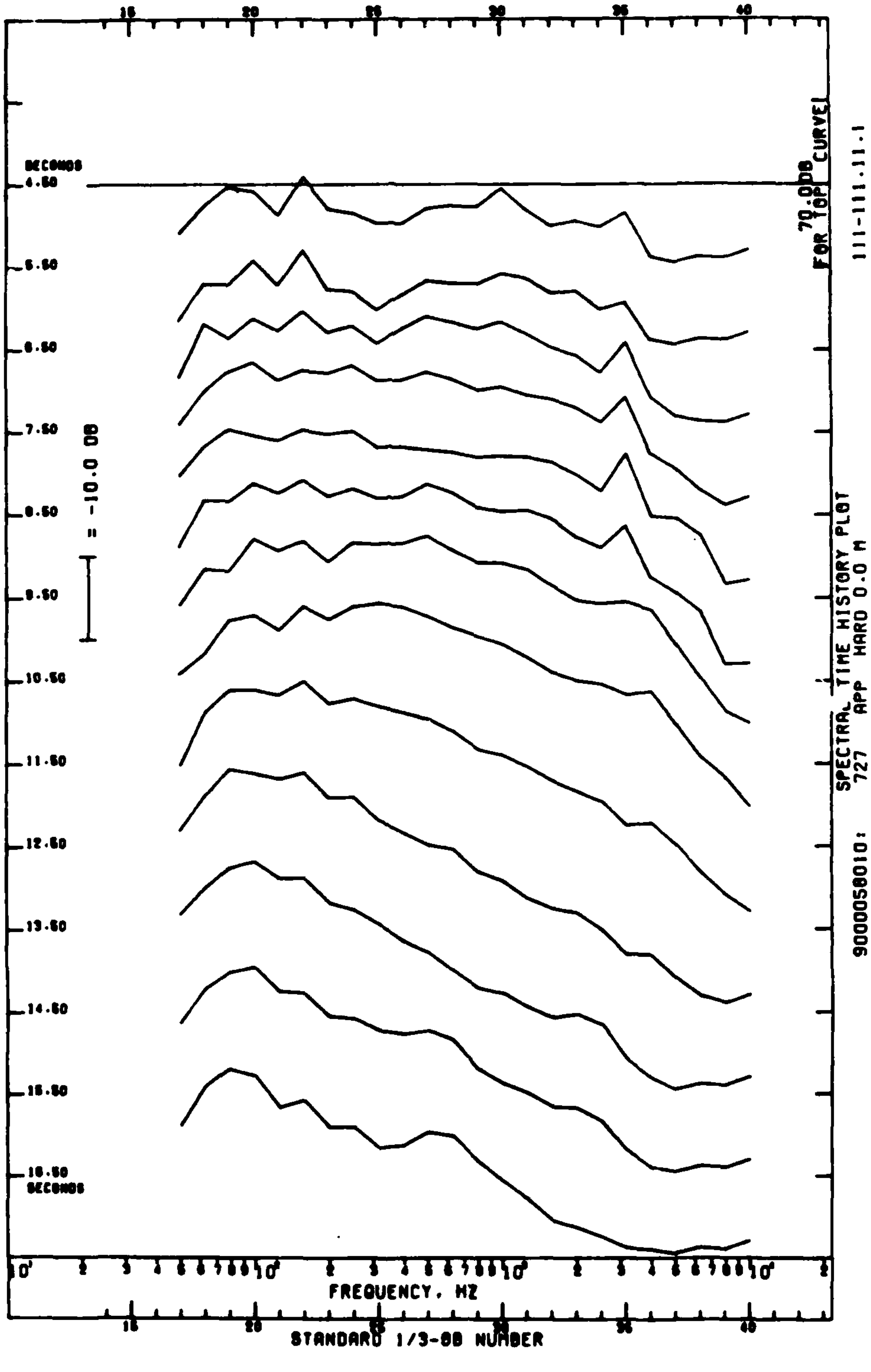
SECONDS
4.50
5.50
6.50
7.50
8.50
9.50
10.50
11.50
12.50
13.50
14.50
15.50
16.50
SECONDS
= -10.0 DB
70.0DB
FOR TOP CURVE
111-111.11.1
SPECTRAL TIME HISTORY PLOT
727 APP HARD 0.0 M
900005801O:
FREQUENCY, HZ
STANDARD 1/3-OB NUMBER

Figure A-12

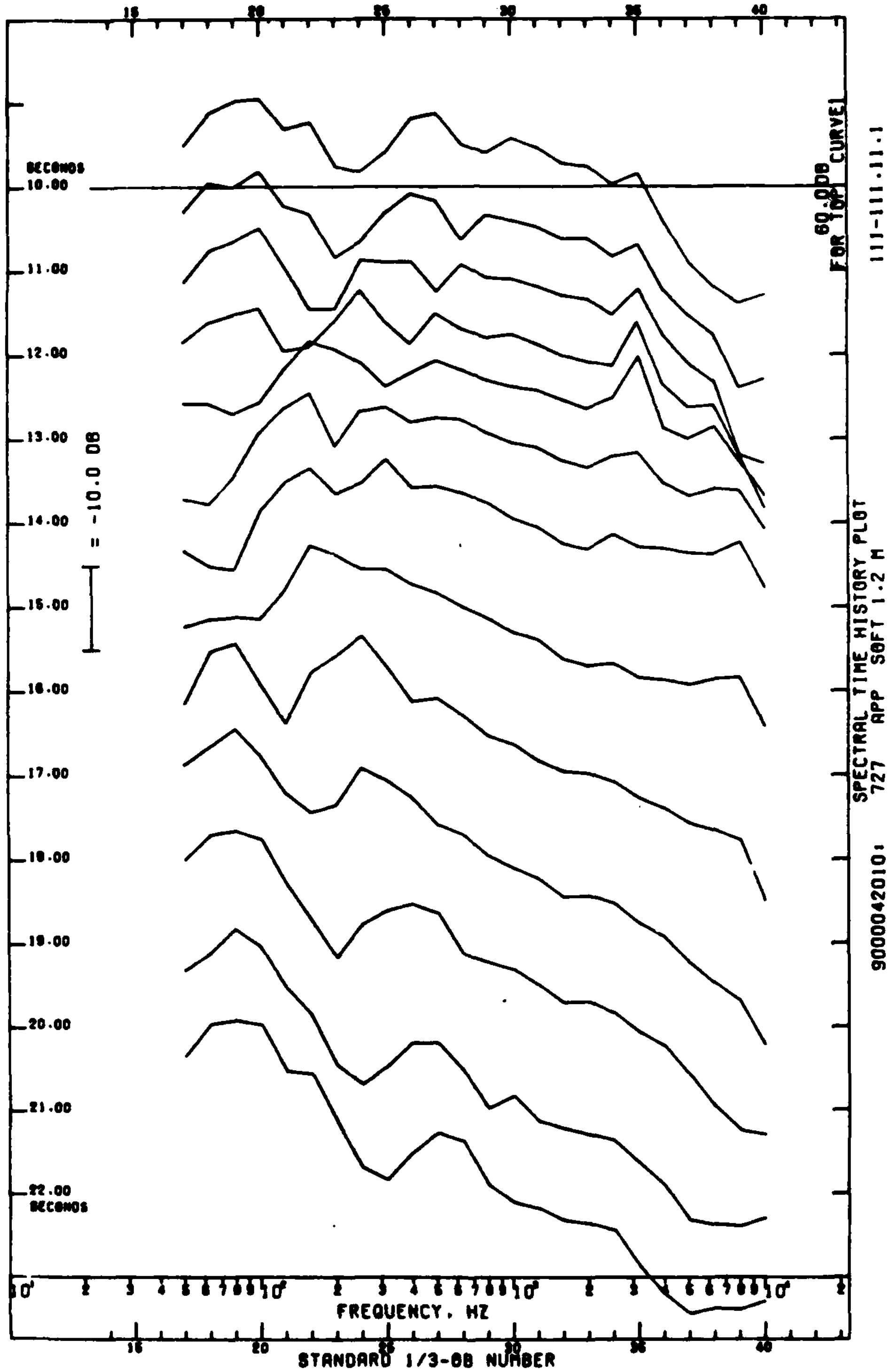
SECONDS
10.00
11.00
12.00
13.00
14.00
15.00
16.00
17.00
18.00
19.00
20.00
21.00
22.00
SECONDS
= -10.0 DB
60.0DB
FOR TOP CURVE
111-111.11.1
SPECTRAL TIME HISTORY PLOT
727 APP SOFT 1.2 M
9000042010:
FREQUENCY, HZ
STANDARD 1/3-OB NUMBER

Figure A-13

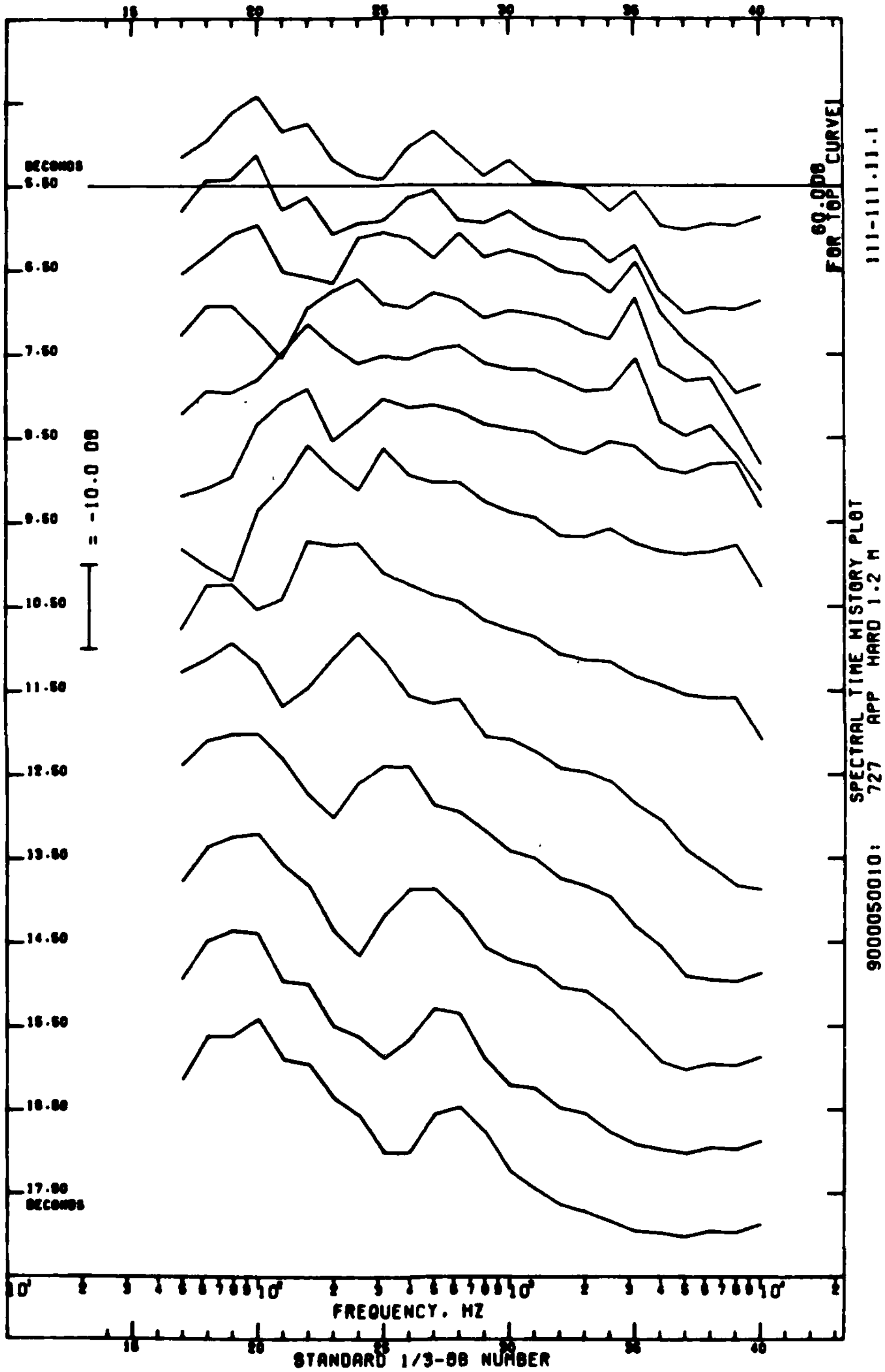

SECONDS
5.50
6.50
7.50
8.50
9.50
10.50
11.50
12.50
13.50
14.50
15.50
16.50
17.50
SECONDS
= -10.0 DB
60.0DB FOR TOP CURVE
111-111.11.1
SPECTRAL TIME HISTORY PLOT
727 APP HARD 1.2 M
900005001O:
FREQUENCY, HZ
STANDARD 1/3-OB NUMBER

Figure A-14

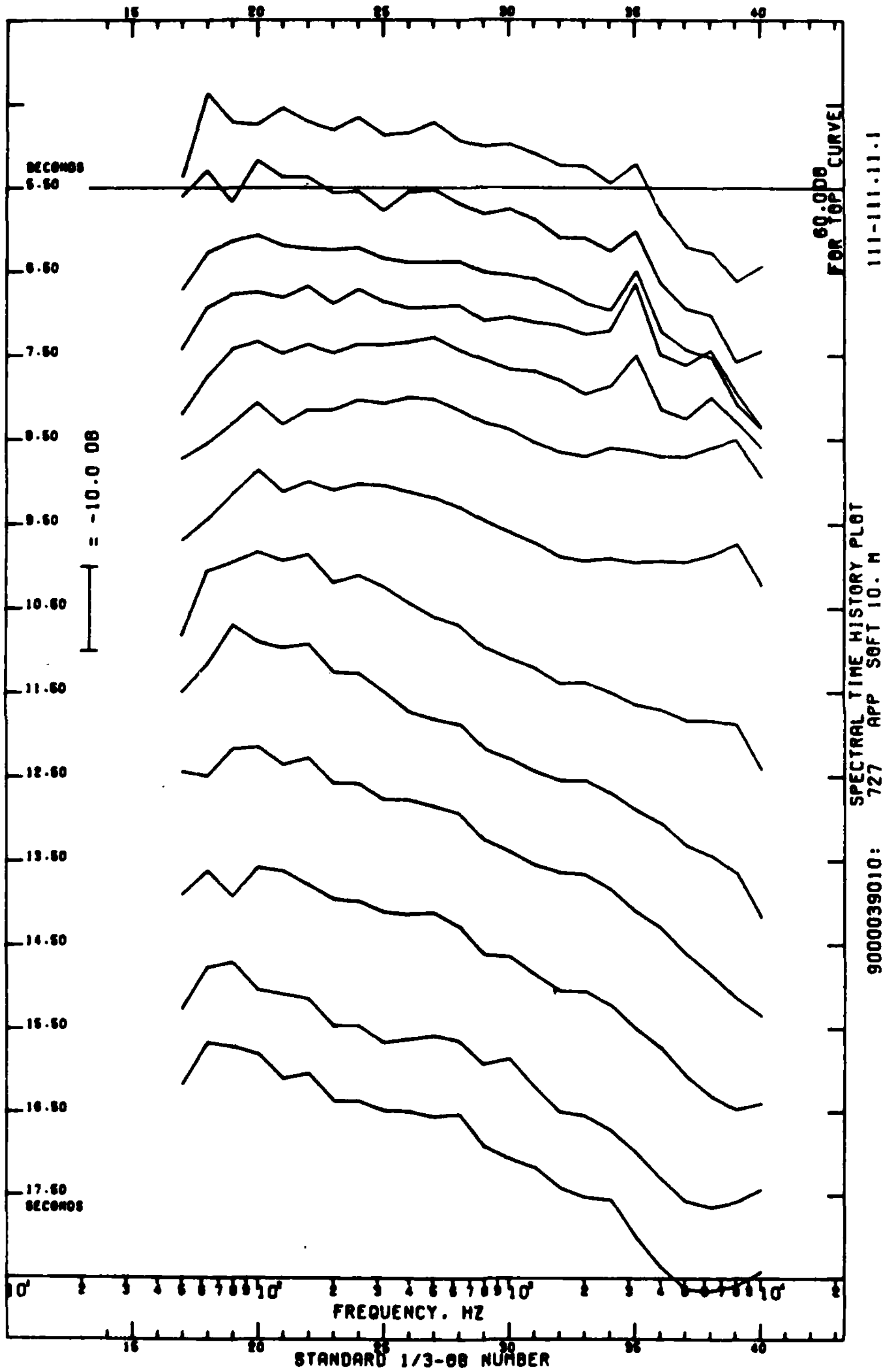
SECONDS
5.50
6.50
7.50
8.50
9.50
10.50
11.50
12.50
13.50
14.50
15.50
16.50
17.50
SECONDS
= -10.0 DB
60.0DB
FOR TOP CURVE
111-111.11.1
SPECTRAL TIME HISTORY PLOT
727 APP SOFT 10. M
9000039010:
FREQUENCY, HZ
STANDARD 1/3-OB NUMBER

Figure A-15

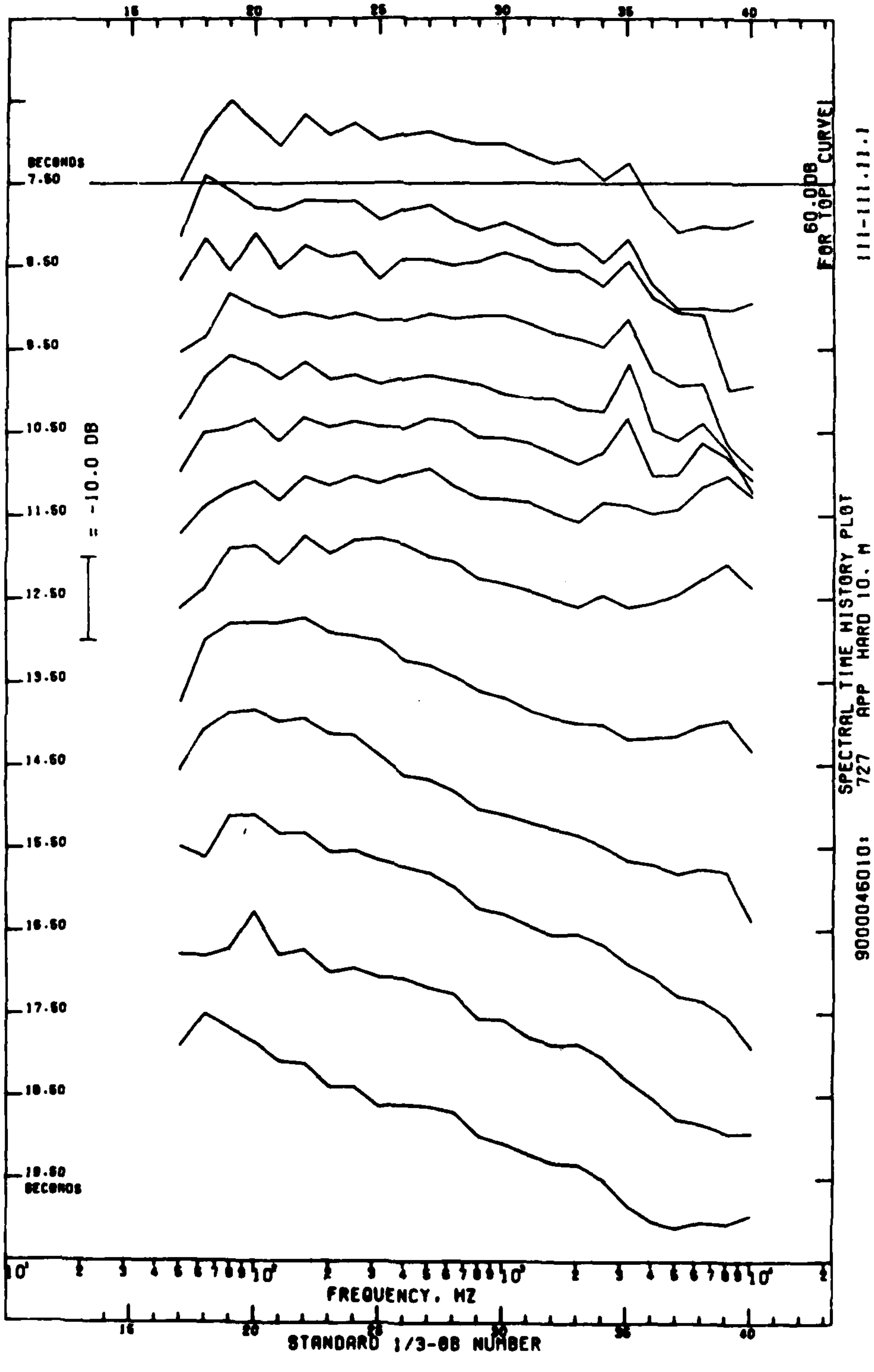
SECONDS
7.50
8.50
9.50
10.50
11.50
12.50
13.50
14.50
15.50
16.50
17.50
18.50
19.50
SECONDS
= -10.0 DB
60.0DB
FOR TOP CURVE
SPECTRAL TIME HISTORY PLOT
727 APP HARD 10. M
900004601O:
FREQUENCY, HZ
STANDARD 1/3-OB NUMBER

Figure A-16

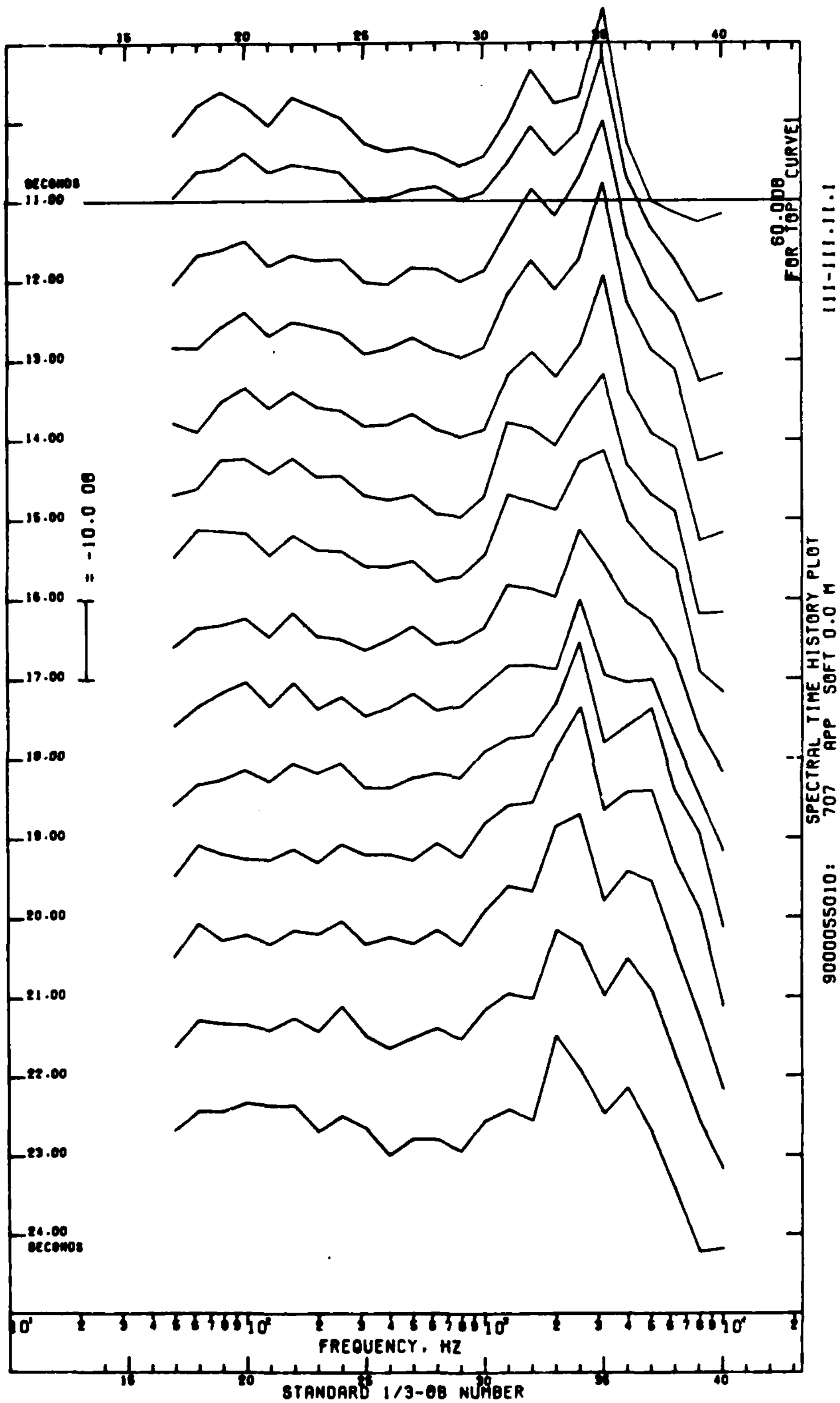
SECONDS
11.00
12.00
13.00
14.00
15.00
16.00
17.00
18.00
19.00
20.00
21.00
22.00
23.00
24.00
SECONDS
= -10.0 DB
60.0DB
FOR TOP CURVE
III-III.II.I
SPECTRAL TIME HISTORY PLOT
707 APP SOFT 0.0 M
900055010:
FREQUENCY, HZ
STANDARD 1/3-OB NUMBER

Figure A-J1

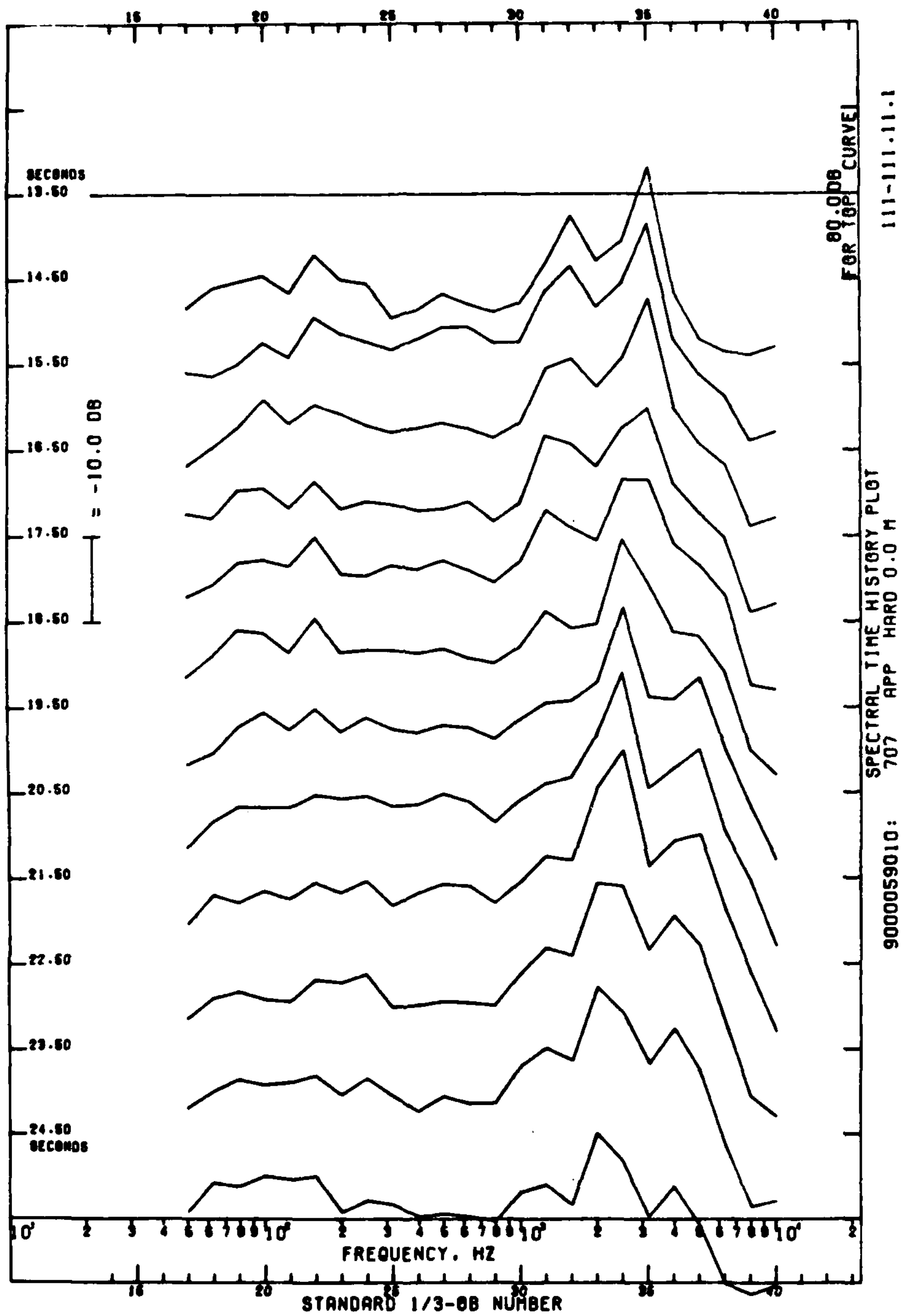
SECONDS
13.50
14.50
15.50
16.50
17.50
18.50
19.50
20.50
21.50
22.50
23.50
24.50
SECONDS
= -10.0 DB
80.0DB
FOR TOP CURVE
SPECTRAL TIME HISTORY PLOT
707 APP HARD 0.0 M
900005901O:
111-111.11.1
FREQUENCY, HZ
STANDARD 1/3-OB NUMBER

Figure A-J2

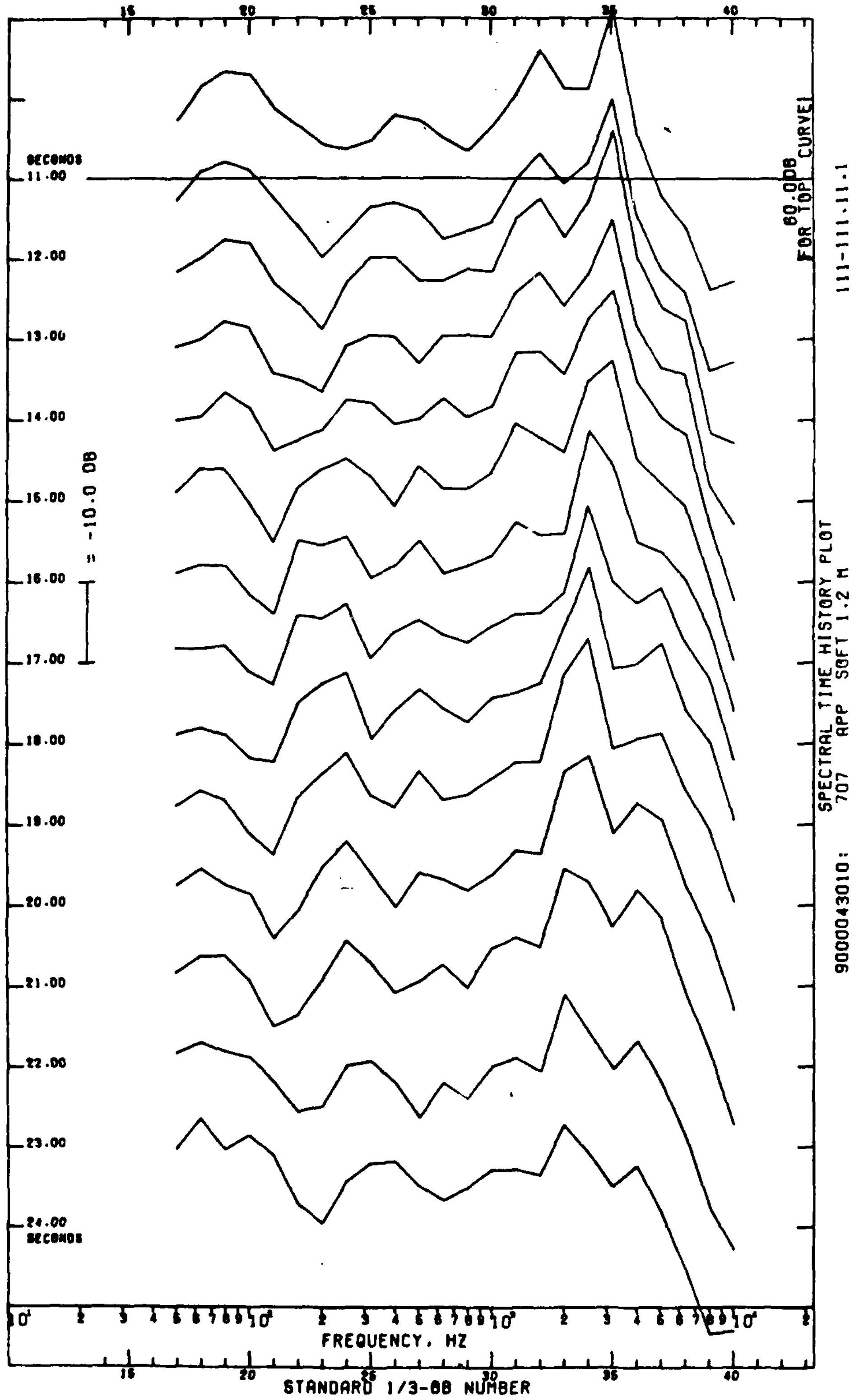

SECONDS
11.00
12.00
13.00
14.00
15.00
16.00
17.00
18.00
19.00
20.00
21.00
22.00
23.00
24.00
SECONDS
= -10.0 DB
60.0DB
FOR TOP CURVE)
111-111.11.1
SPECTRAL TIME HISTORY PLOT
707 APP SOFT 1.2 M
9000043010:
FREQUENCY, HZ
STANDARD 1/3-OB NUMBER

Figure A-J3

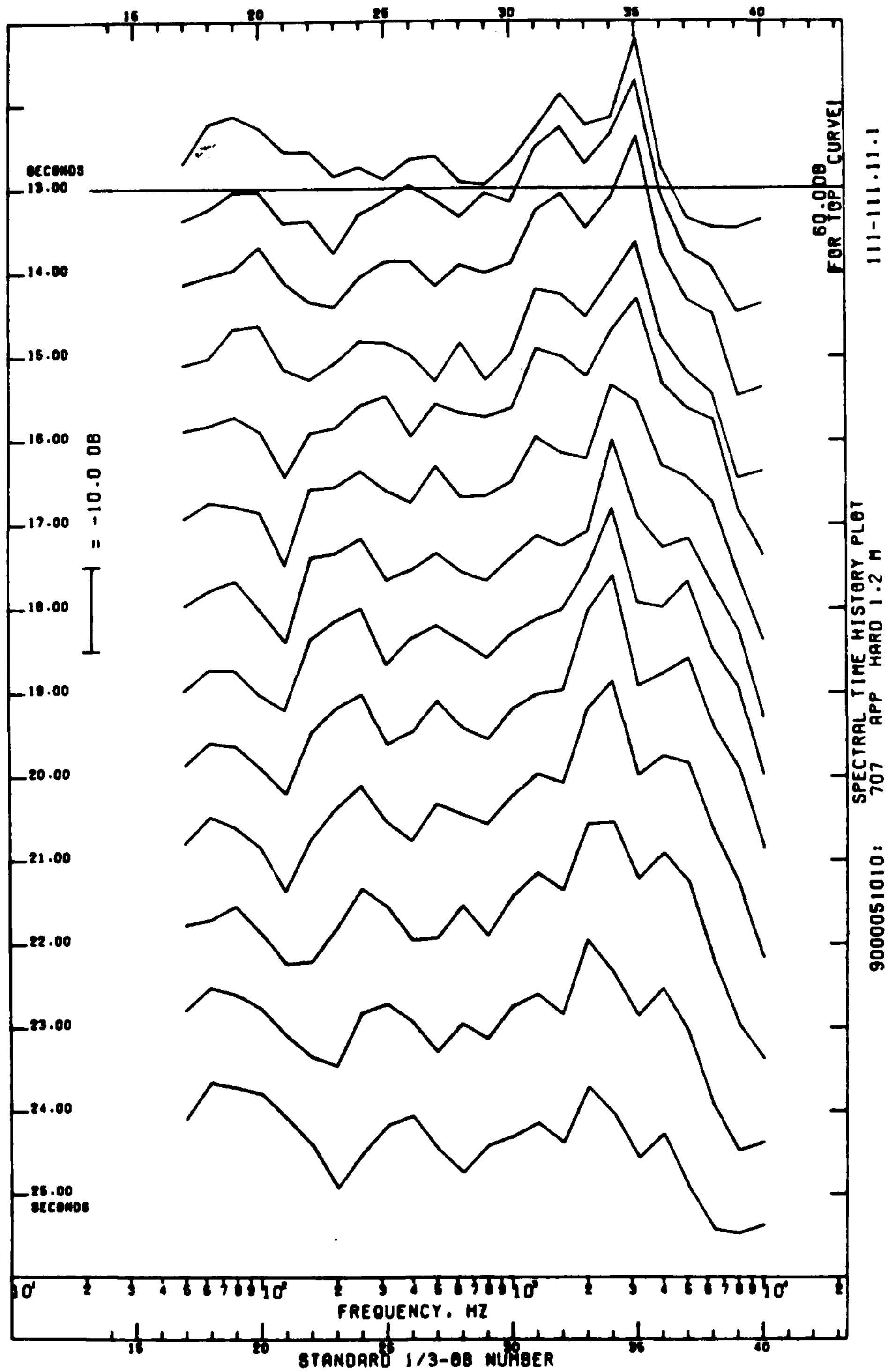
SECONDS
13.00
14.00
15.00
16.00
17.00
18.00
19.00
20.00
21.00
22.00
23.00
24.00
25.00
SECONDS
= -10.0 DB
60.0DB
FOR TOP CURVE
111-111.11.1
SPECTRAL TIME HISTORY PLOT
707 APP HARD 1.2 M
9000051010:
FREQUENCY, HZ
STANDARD 1/3-OB NUMBER

Figure A-J4

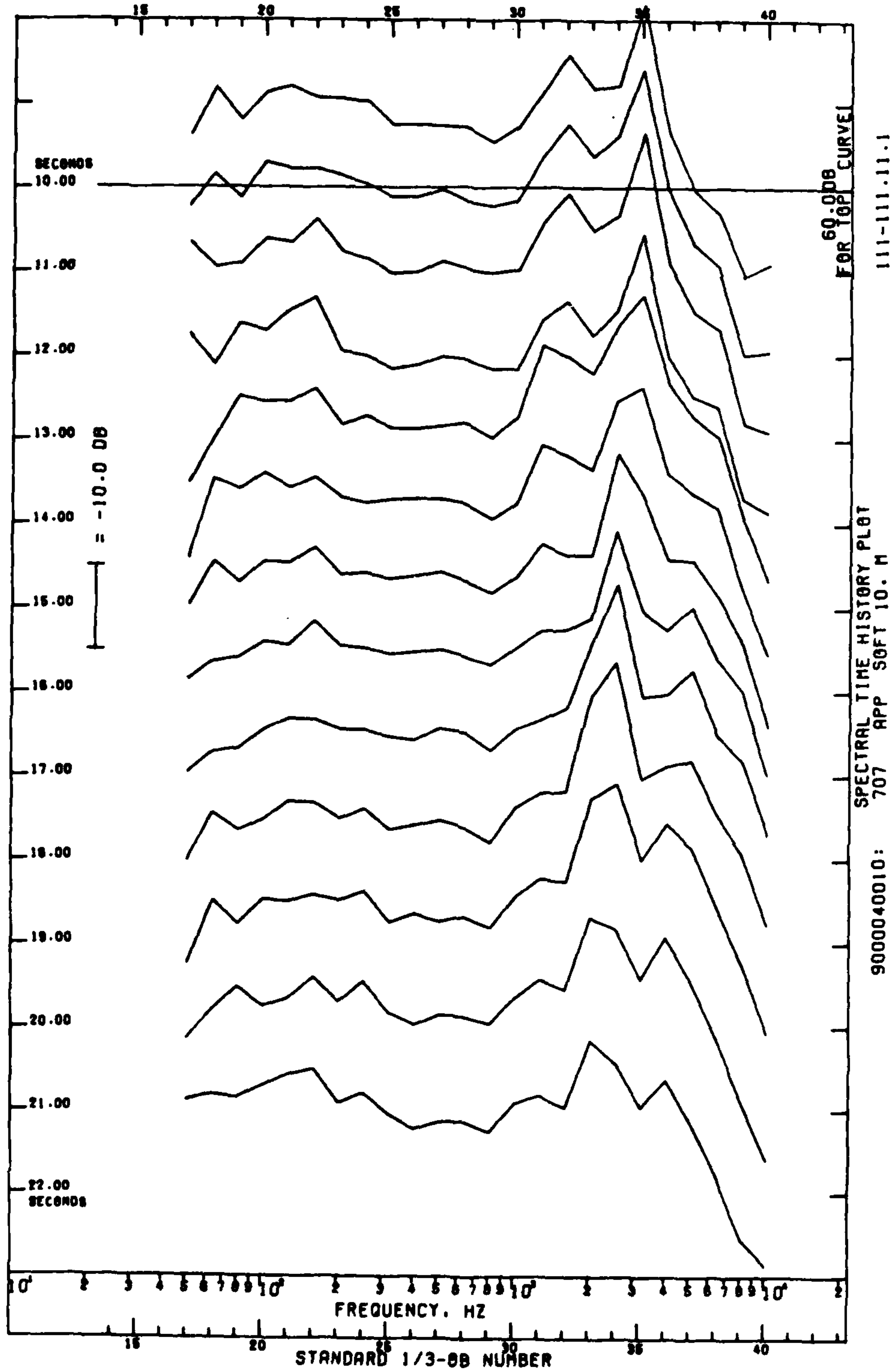
SECONDS
10.00
11.00
12.00
13.00
14.00
15.00
16.00
17.00
18.00
19.00
20.00
21.00
22.00
SECONDS
= -10.0 DB
60.0 DB
FOR TOP CURVE
SPECTRAL TIME HISTORY PLOT
707 APP SOFT 10. M
9000040010:
111-111.11.1
FREQUENCY, HZ
STANDARD 1/3-OB NUMBER

Figure A-J5

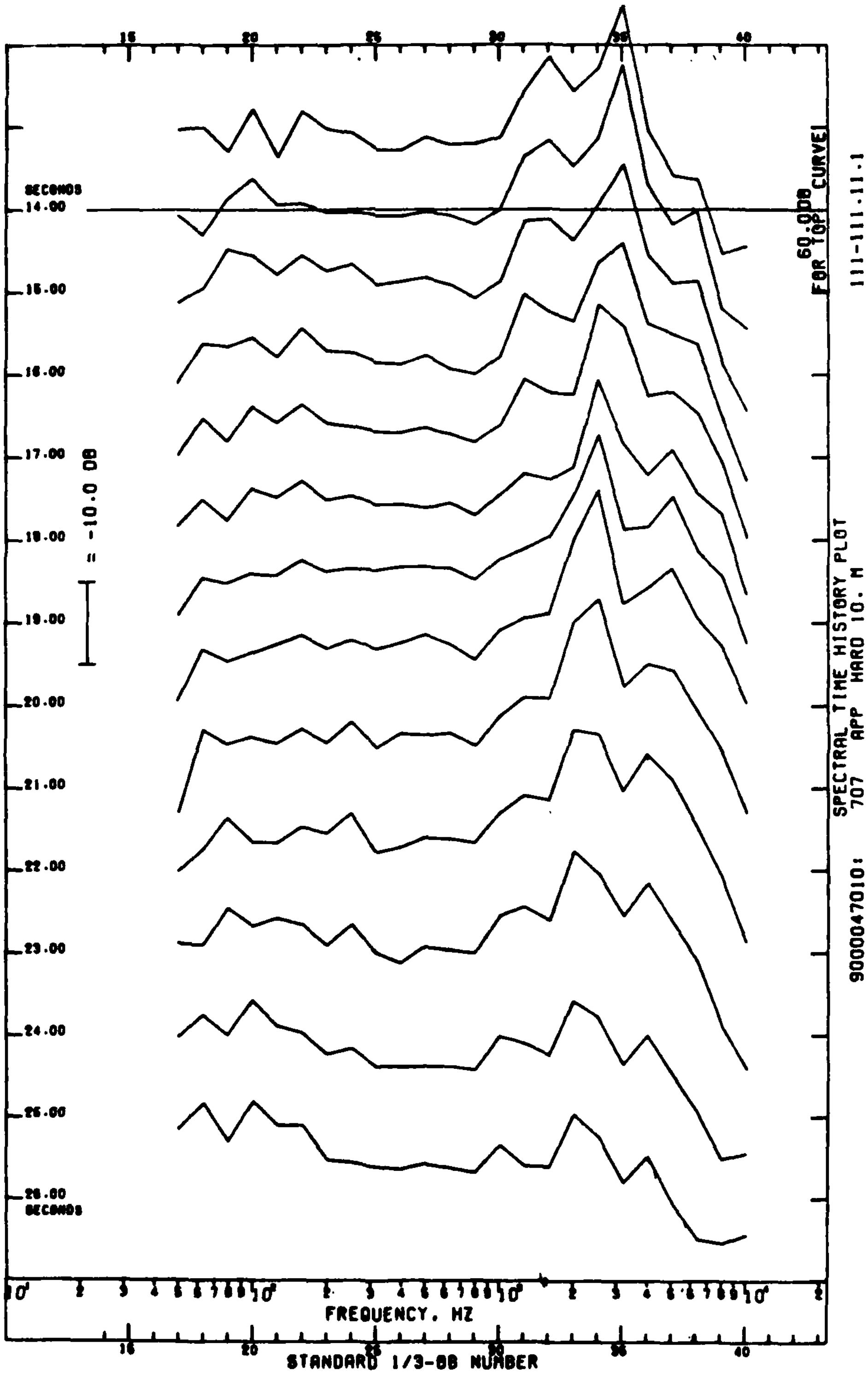
SECONDS
14.00
15.00
16.00
17.00
18.00
19.00
20.00
21.00
22.00
23.00
24.00
25.00
26.00
SECONDS
= -10.0 DB
60.0DB
FOR TOP CURVE
111-111-11-1
SPECTRAL TIME HISTORY PLOT
707 APP HARD 10. M
9000047010:
FREQUENCY, HZ
STANDARD 1/3-OB NUMBER

Figure A-J6

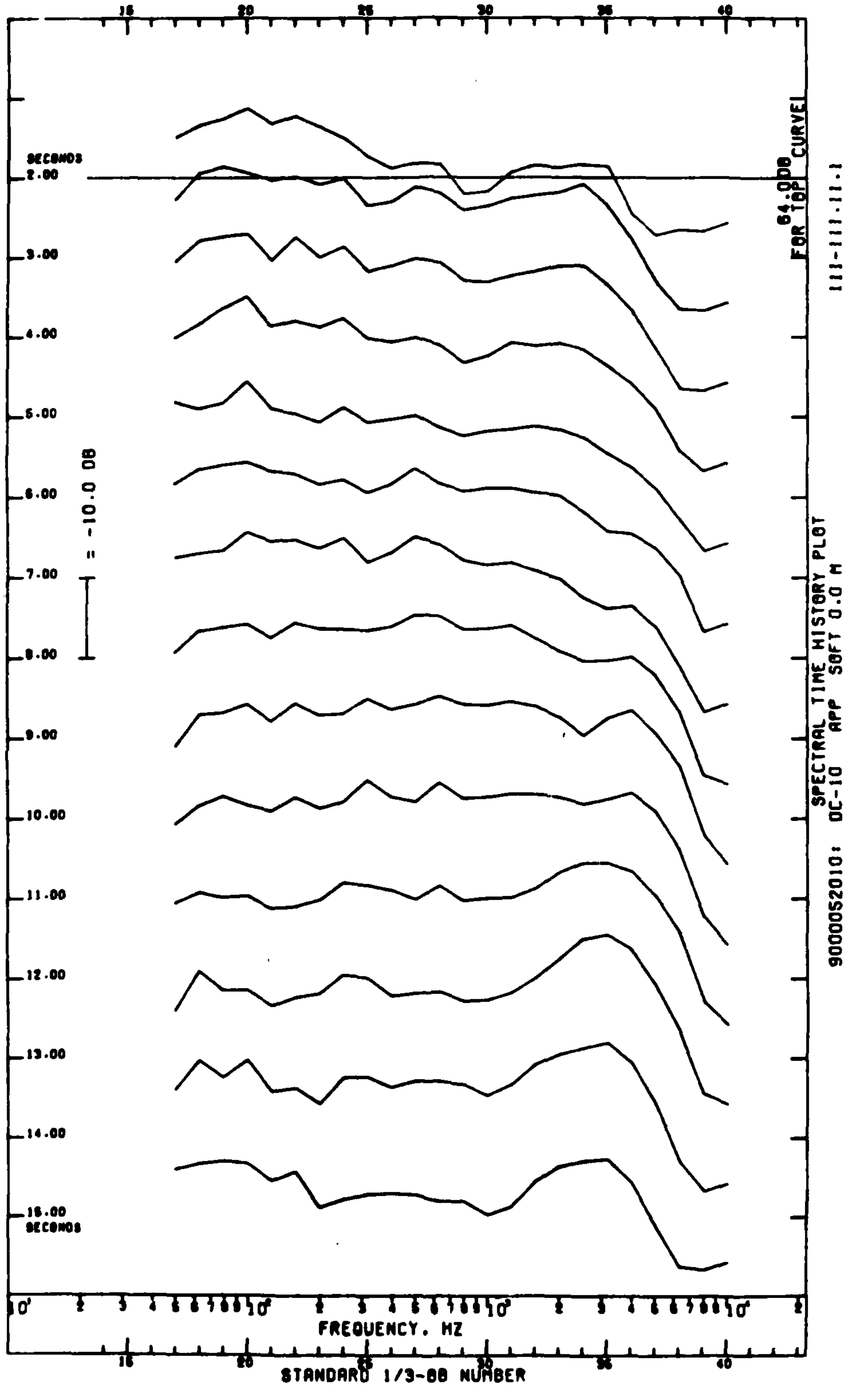
SECONDS
2.00
3.00
4.00
5.00
6.00
7.00
8.00
9.00
10.00
11.00
12.00
13.00
14.00
15.00
SECONDS
= -10.0 DB
64.0DB FOR TOP CURVE
SPECTRAL TIME HISTORY PLOT
9000052010: DC-10 APP SOFT 0.0 M
FREQUENCY, HZ
STANDARD 1/3-OB NUMBER

Figure A-K1

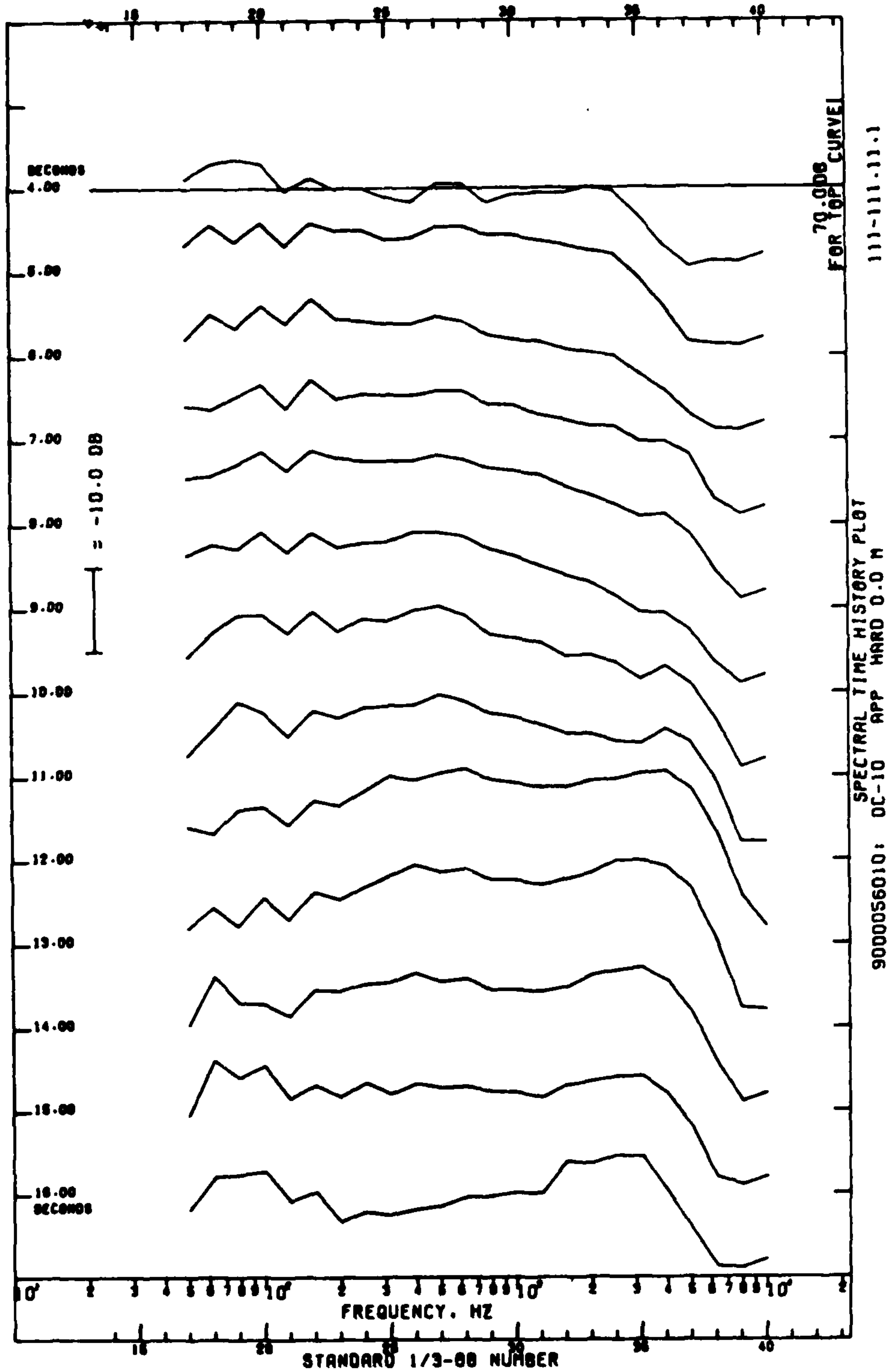
SECONDS
4.00
5.00
6.00
7.00
8.00
9.00
10.00
11.00
12.00
13.00
14.00
15.00
16.00
SECONDS
= -10.0 DB
70.0DB FOR TOP CURVE
111-111.11.1
SPECTRAL TIME HISTORY PLOT
900005601D: DC-10 APP HARD 0.0 M
FREQUENCY, HZ
STANDARD 1/3-OB NUMBER

Figure A-K2

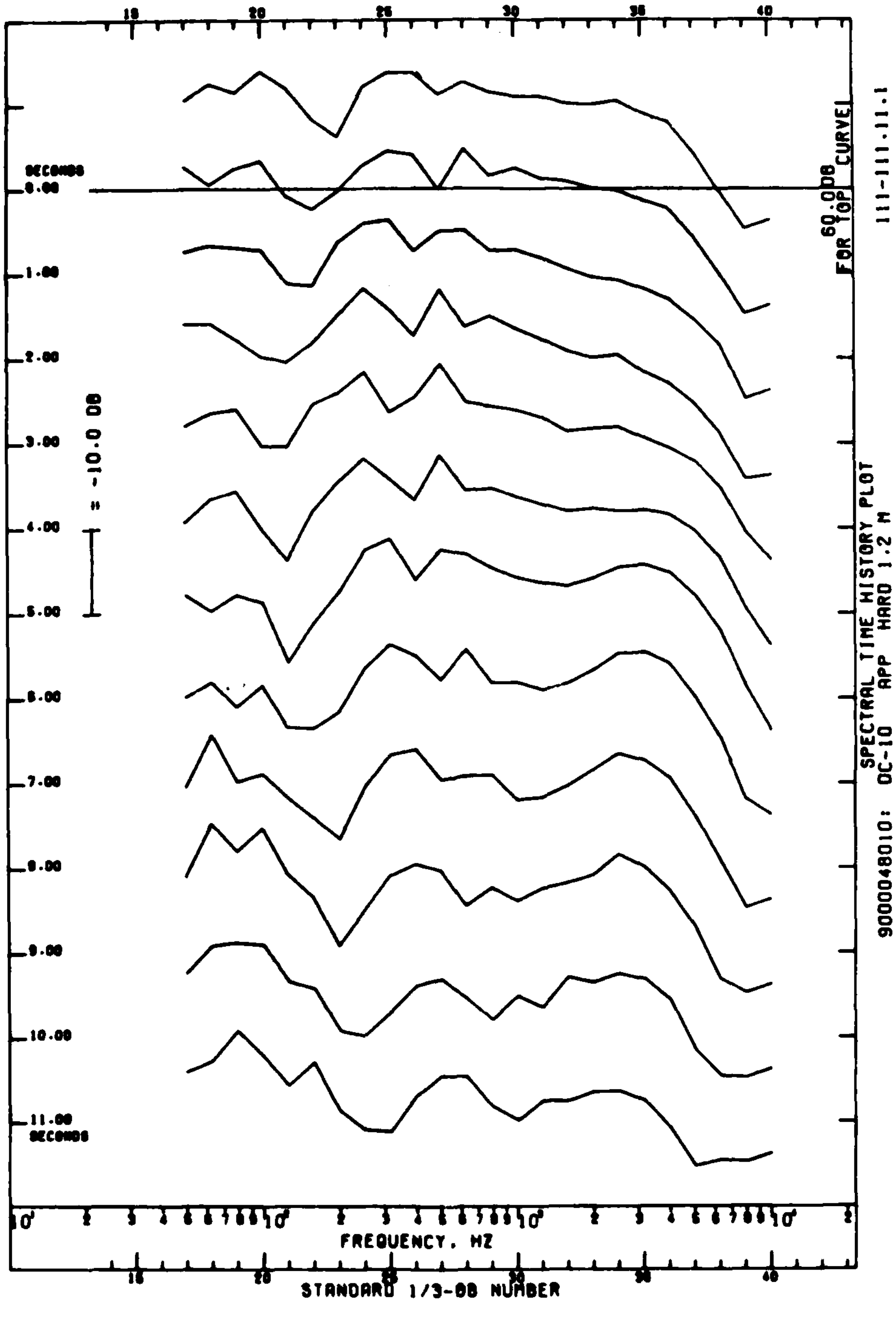
SECONDS
0.00
1.00
2.00
3.00
4.00
5.00
6.00
7.00
8.00
9.00
10.00
11.00
SECONDS
= -10.0 DB
60.0DB
FOR TOP CURVE
111-111-11.1
SPECTRAL TIME HISTORY PLOT
9000048010: DC-10 APP HARD 1.2 M
FREQUENCY, HZ
STANDARD 1/3-OB NUMBER

Figure A-K3

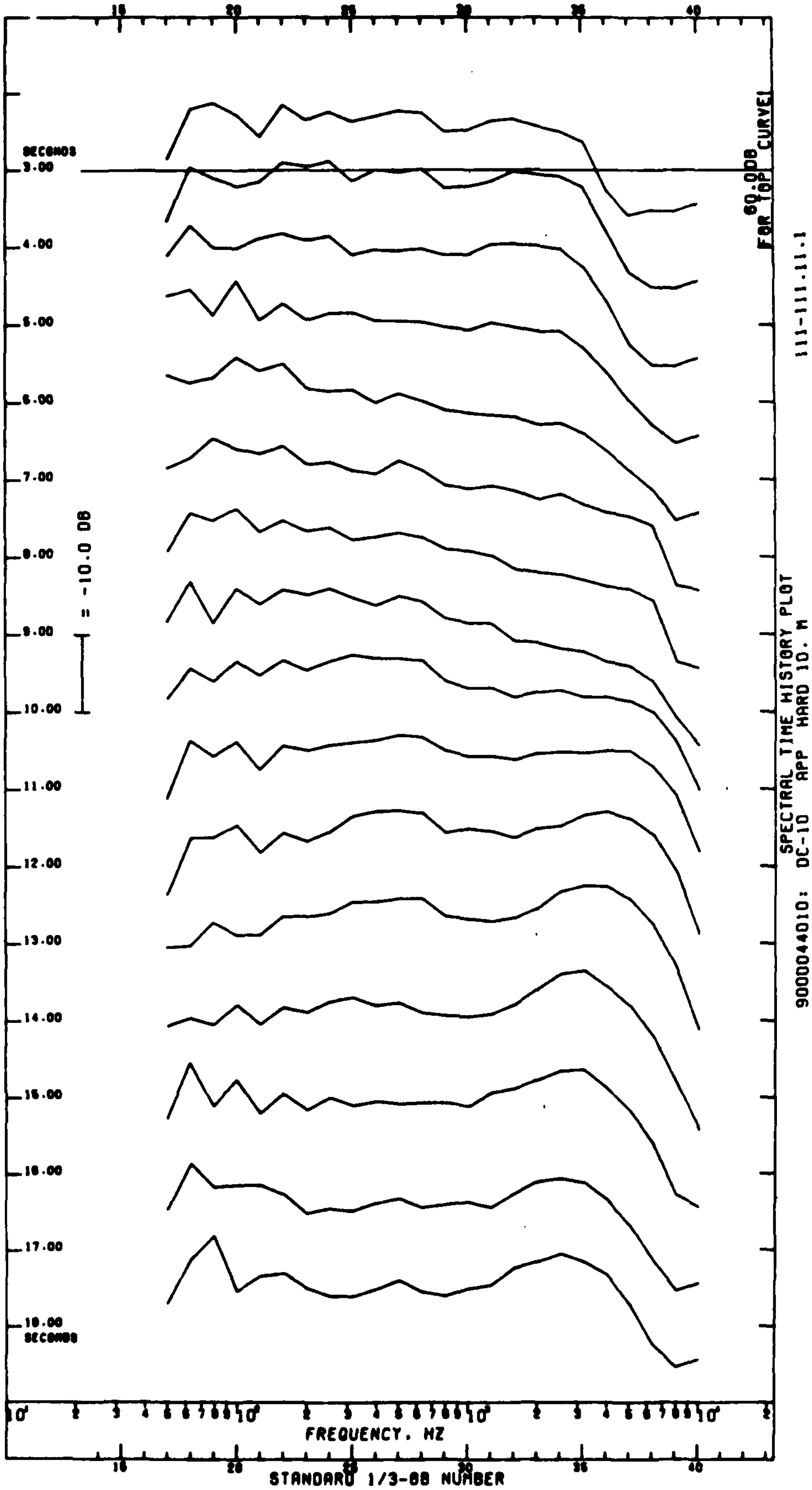

15
20
25
30
35
40
SECONDS
3.00
4.00
5.00
6.00
7.00
8.00
9.00
10.00
11.00
12.00
13.00
14.00
15.00
16.00
17.00
18.00
SECONDS
= -10.0 DB
60.0DB
FOR TOP CURVE
111-111.11.1
SPECTRAL TIME HISTORY PLOT
9000044010: DC-10 APP HARD 10. M
FREQUENCY, HZ
STANDARD 1/3-OB NUMBER

Figure A-K4

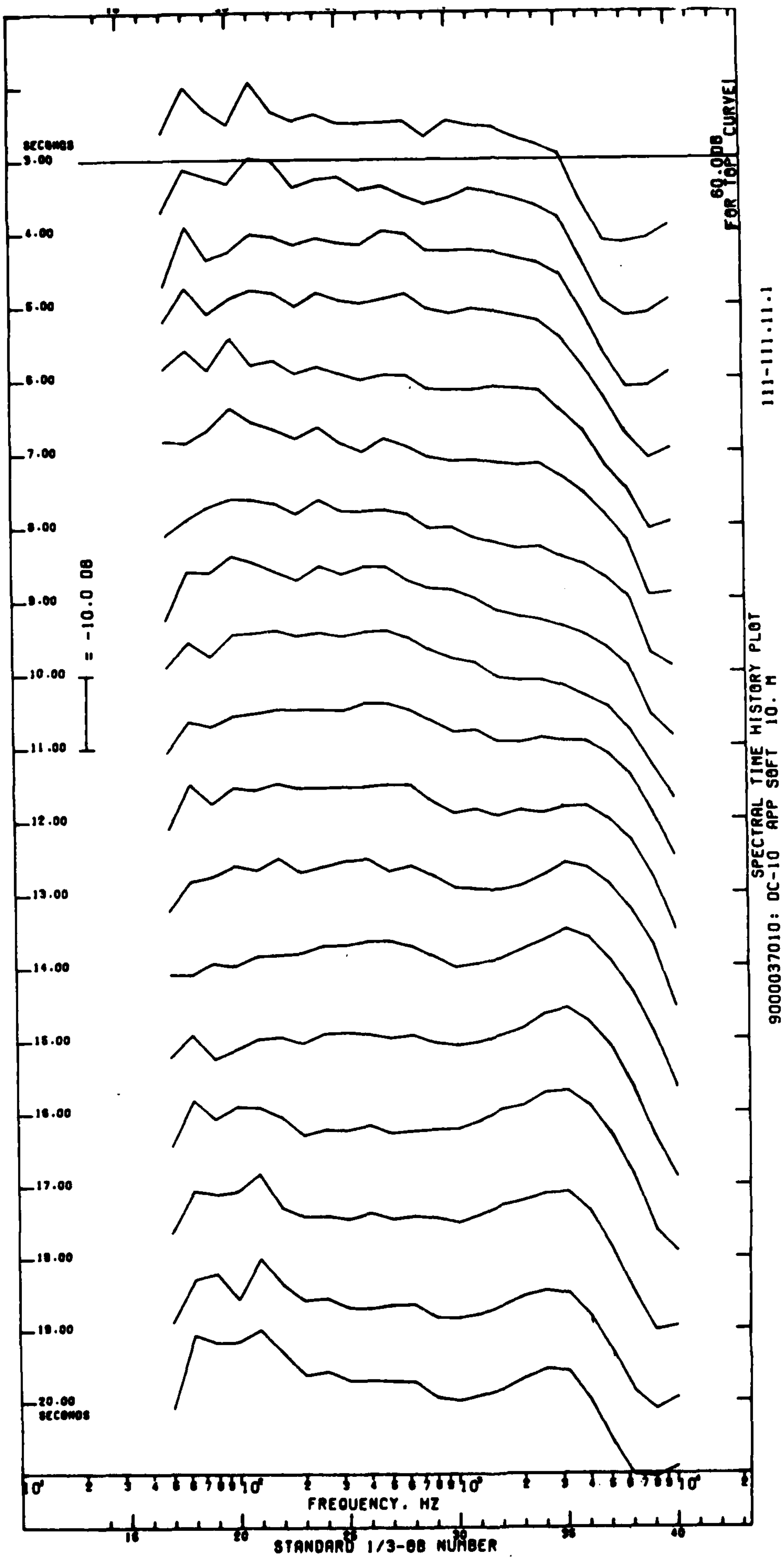
SECONDS
3.00
4.00
5.00
6.00
7.00
8.00
9.00
10.00
11.00
12.00
13.00
14.00
15.00
16.00
17.00
18.00
19.00
20.00
SECONDS
= -10.0 DB
60.0DB
FOR TOP CURVE)
111-111.11.1
SPECTRAL TIME HISTORY PLOT
9000037010: DC-10 APP SOFT 10. M
FREQUENCY, HZ
STANDARD 1/3-OB NUMBER

Figure A-K5

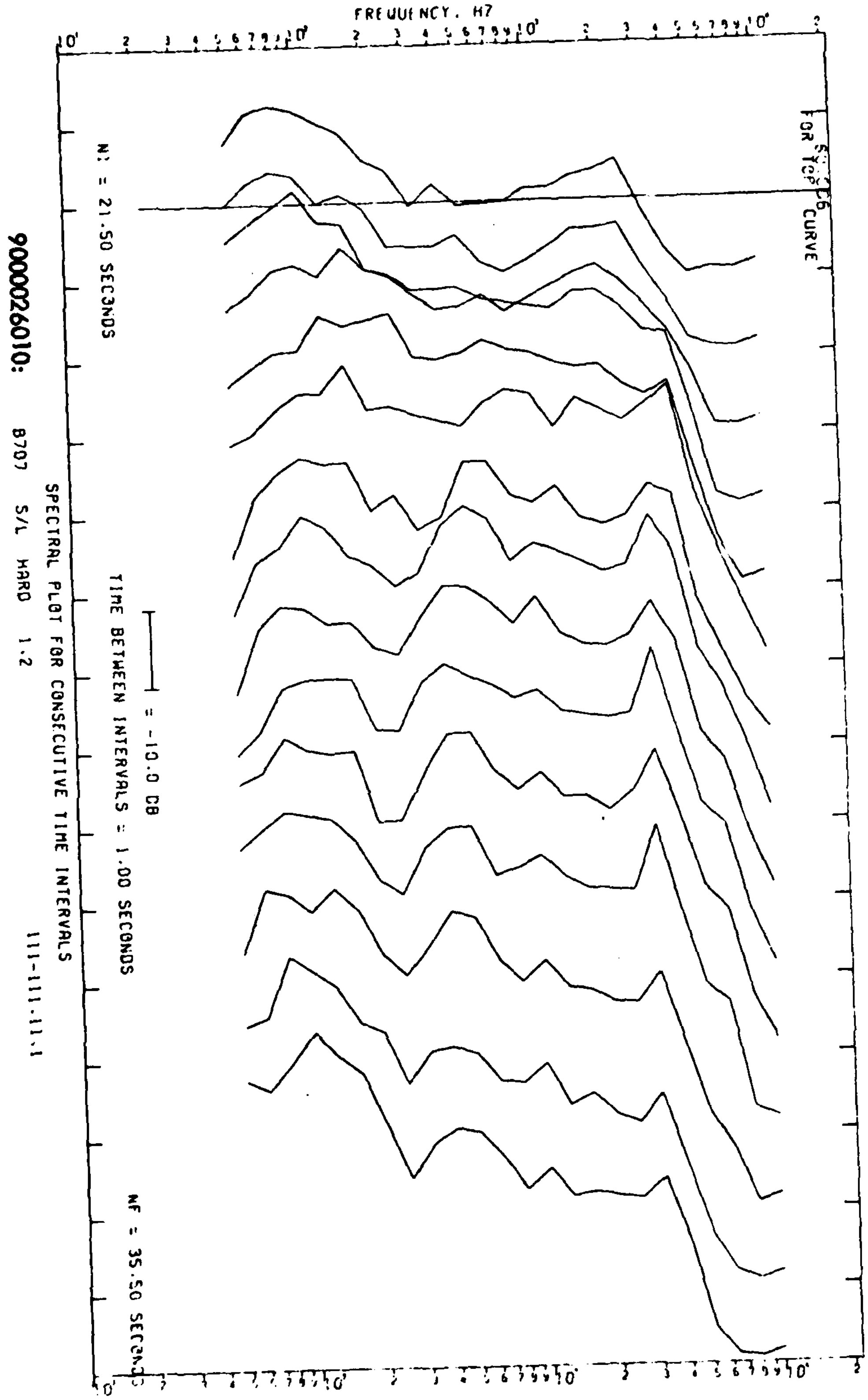
FREQUENCY, HZ
FOR TOP CURVE
NI = 21.50 SECONDS
= -10.0 DB
TIME BETWEEN INTERVALS = 1.00 SECONDS
NF = 35.50 SECONDS
9000026010:
SPECTRAL PLOT FOR CONSECUTIVE TIME INTERVALS
B707 S/L HARD 1.2
111-111.11.1

Figure A-C1

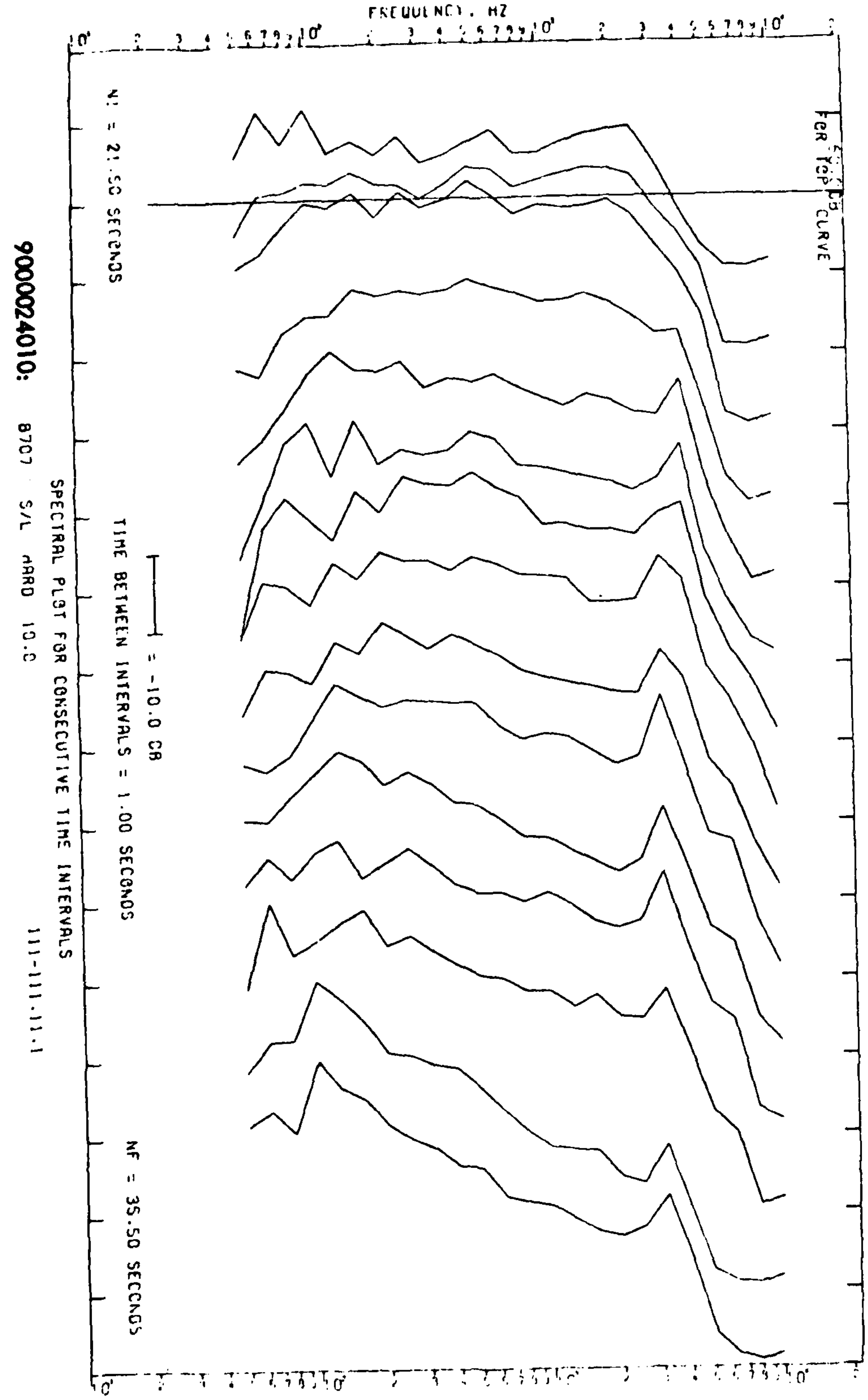
FREQUENCY, HZ
FOR TOP CURVE
NI = 21.50 SECONDS
NF = 35.50 SECONDS
= -10.0 DB
TIME BETWEEN INTERVALS = 1.00 SECONDS
SPECTRAL PLOT FOR CONSECUTIVE TIME INTERVALS
9000024010:
B707 S/L HARD 10.0

Figure A-C2

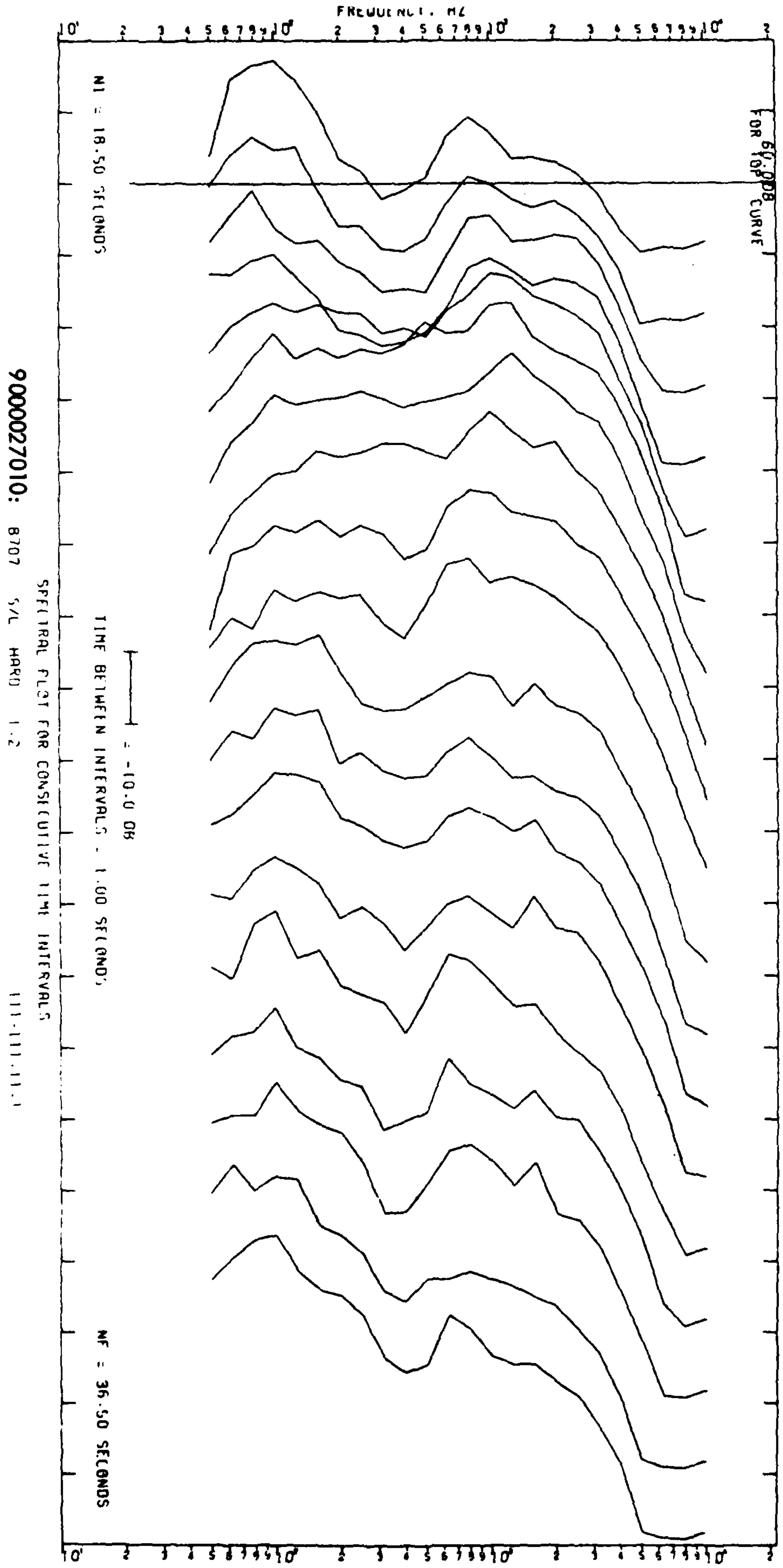

FREQUENCY, HZ
NI = 18.50 SECONDS
60.0 DB FOR TOP CURVE
= -10.0 DB
TIME BETWEEN INTERVALS - 1.00 SECONDS
SPECTRAL PLOT FOR CONSECUTIVE TIME INTERVALS
9000027010: B707 S/L HARD 1.2
NF = 36.50 SECONDS

Figure A-D1

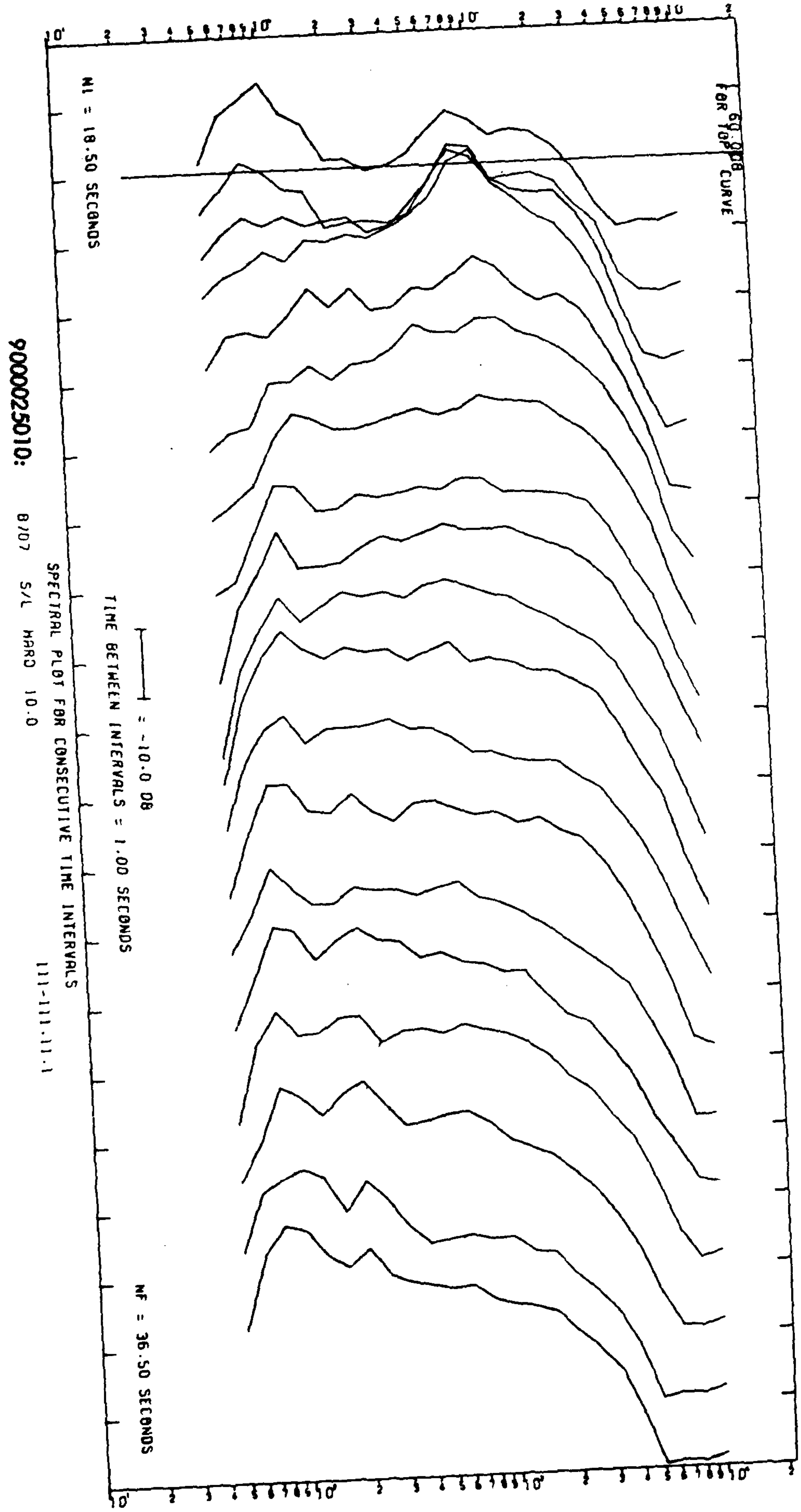
NI = 18.50 SECONDS
60.0 DB FOR TOP CURVE
9000025010:
B/D7 S/L HARD 10.0
SPECTRAL PLOT FOR CONSECUTIVE TIME INTERVALS
TIME BETWEEN INTERVALS = 1.00 SECONDS
= -10.0 DB
111-111.11.1
NF = 36.50 SECONDS

Figure A-D2

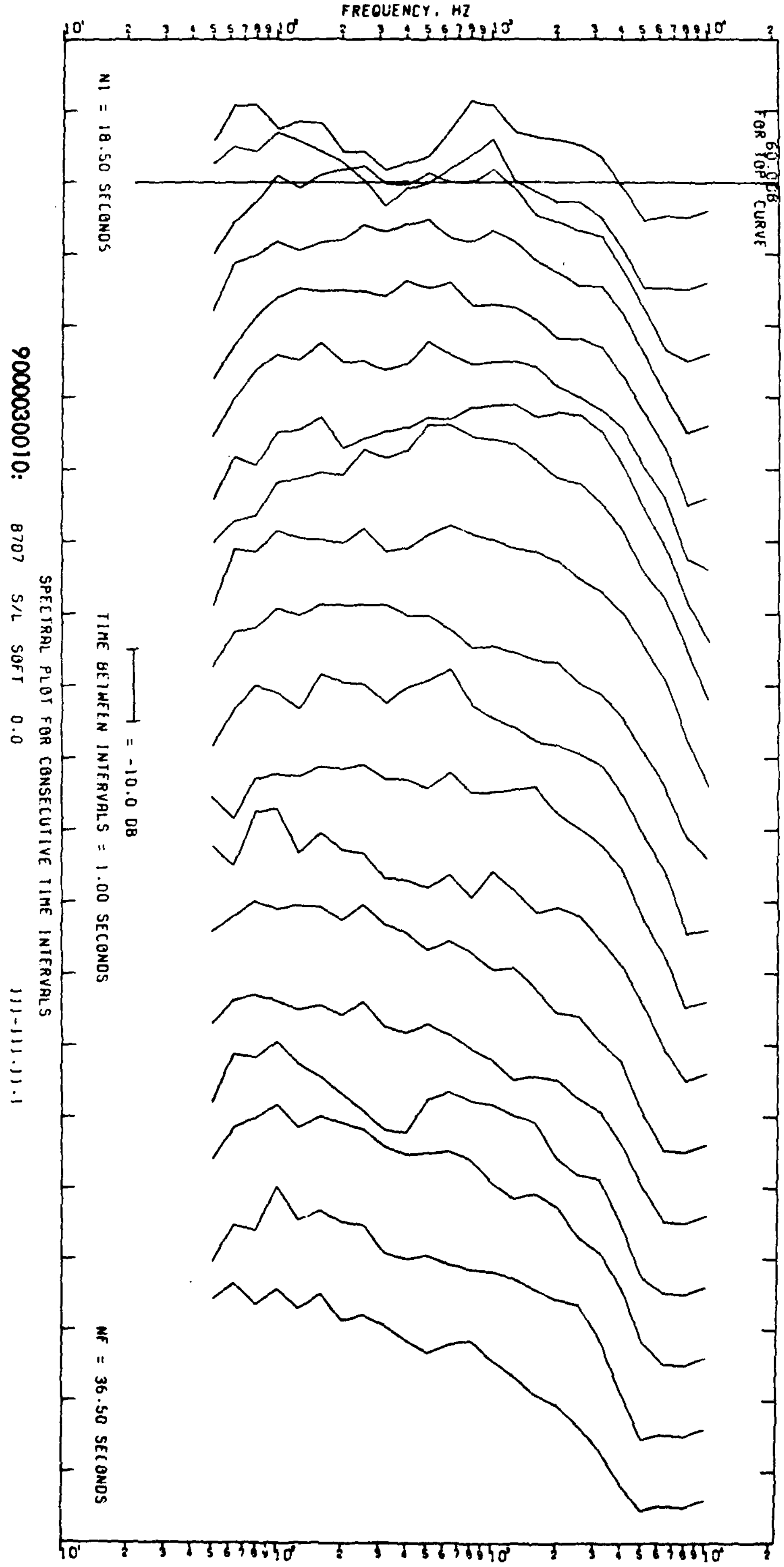
FREQUENCY, HZ
NI = 18.50 SECONDS
NF = 36.50 SECONDS
60.0 DB FOR TOP CURVE
= -10.0 DB
TIME BETWEEN INTERVALS = 1.00 SECONDS
SPECTRAL PLOT FOR CONSECUTIVE TIME INTERVALS
9000030010:
8707 S/L SOFT 0.0

Figure A-E1

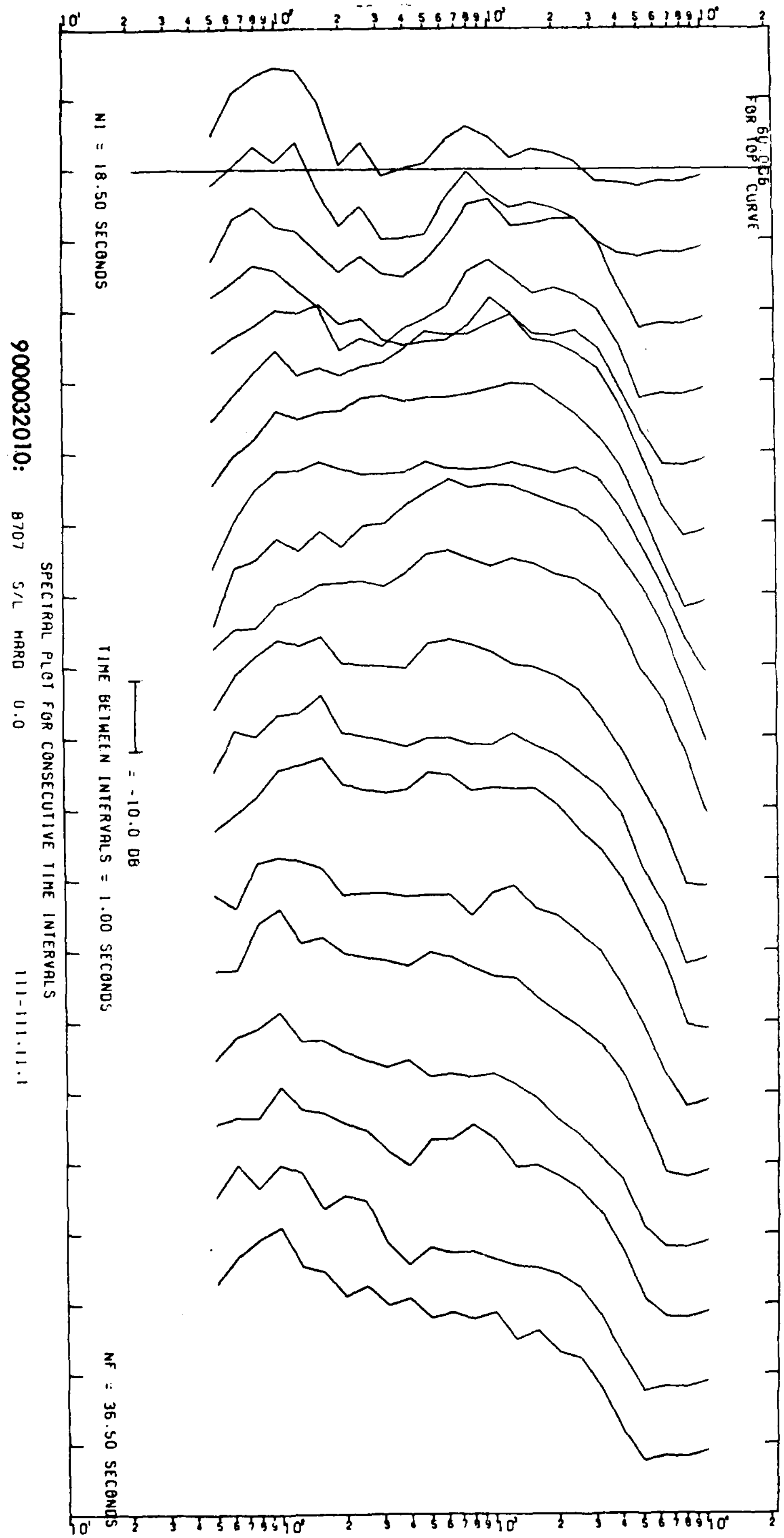
9000032010: B707 S/L HARD 0.0
SPECTRAL PLOT FOR CONSECUTIVE TIME INTERVALS
111-111.11.1
TIME BETWEEN INTERVALS = 1.00 SECONDS
= -10.0 DB
NI = 18.50 SECONDS
NF = 36.50 SECONDS
FOR TOP CURVE

Figure A-E2

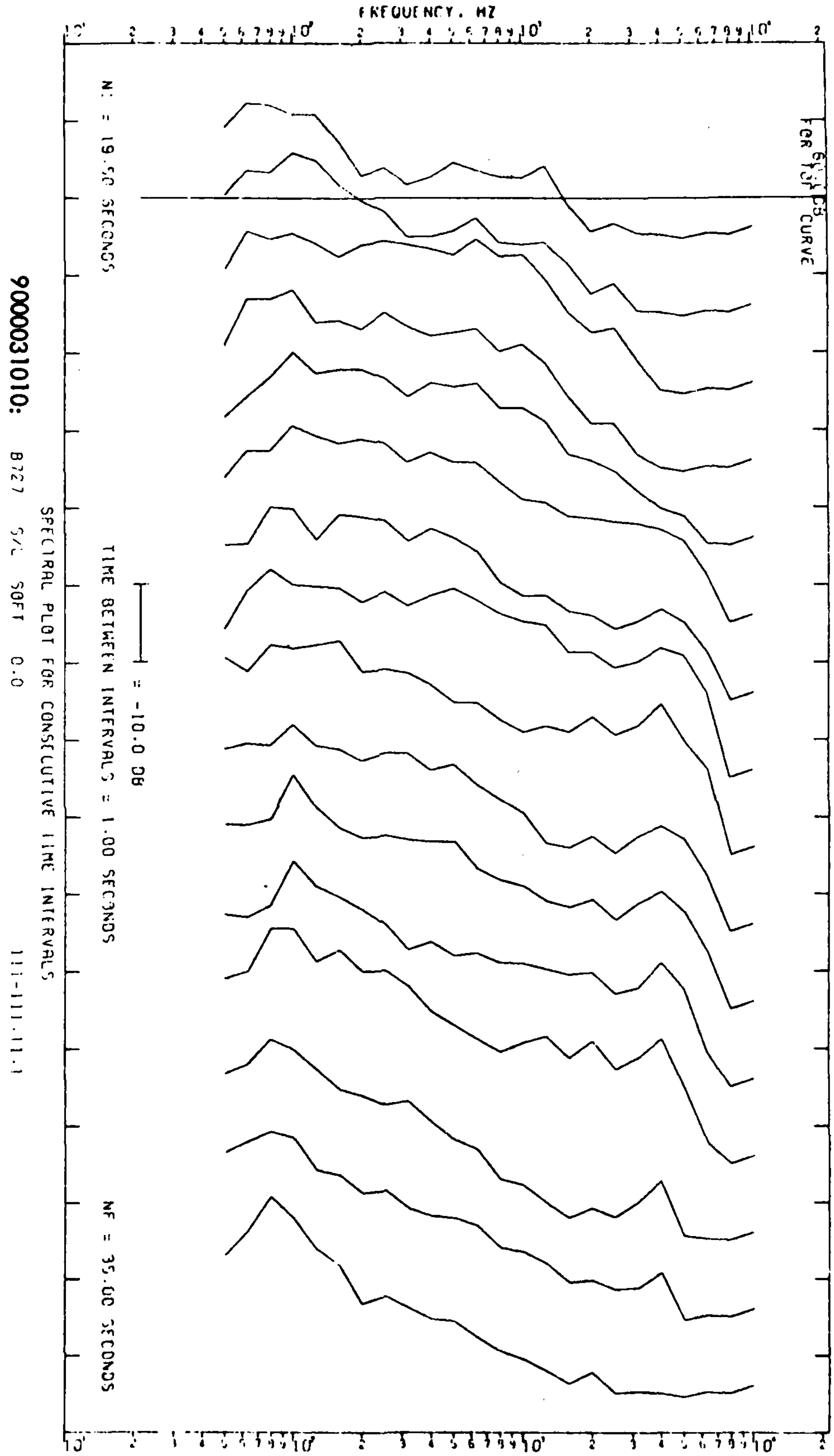
FREQUENCY, HZ
NF = 19.50 SECONDS
NF = 35.00 SECONDS
TIME BETWEEN INTERVALS = 1.00 SECONDS
= -10.0 DB
FOR TOP CURVE
9000031010:
SPECTRAL PLOT FOR CONSECUTIVE TIME INTERVALS
0.0

Figure A-F1

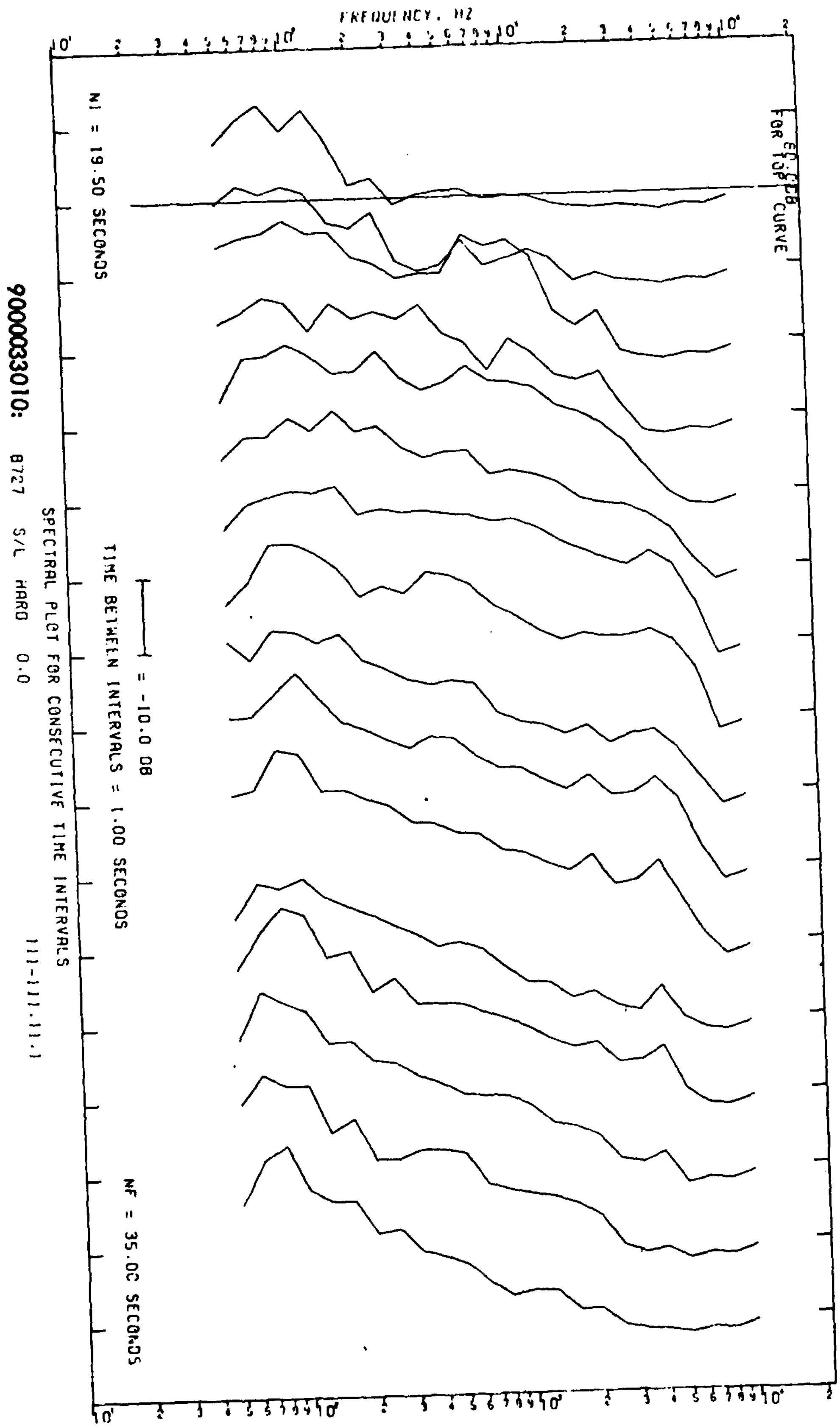
FREQUENCY, HZ
NI = 19.50 SECONDS
9000033010:
B727 S/L HARD 0.0
SPECTRAL PLOT FOR CONSECUTIVE TIME INTERVALS
TIME BETWEEN INTERVALS = 1.00 SECONDS
= -10.0 DB
NF = 35.0C SECONDS
FOR TOP CURVE

Figure A-F2

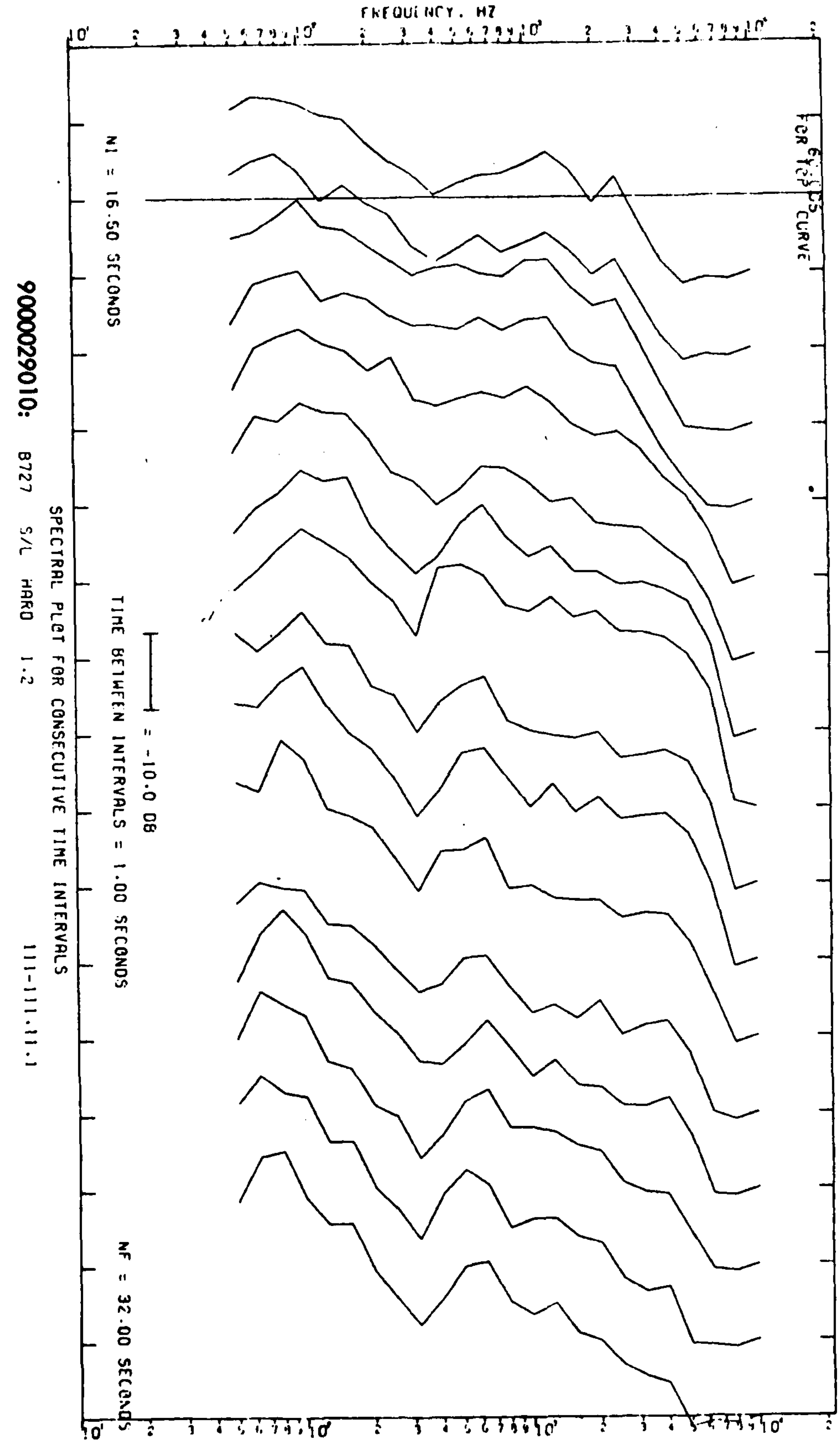
FREQUENCY, HZ
NI = 16.50 SECONDS
= -10.0 DB
TIME BETWEEN INTERVALS = 1.00 SECONDS
NF = 32.00 SECONDS
9000029010: B727 S/L HARD 1.2
SPECTRAL PLOT FOR CONSECUTIVE TIME INTERVALS
111-111.11.1

Figure A-F3

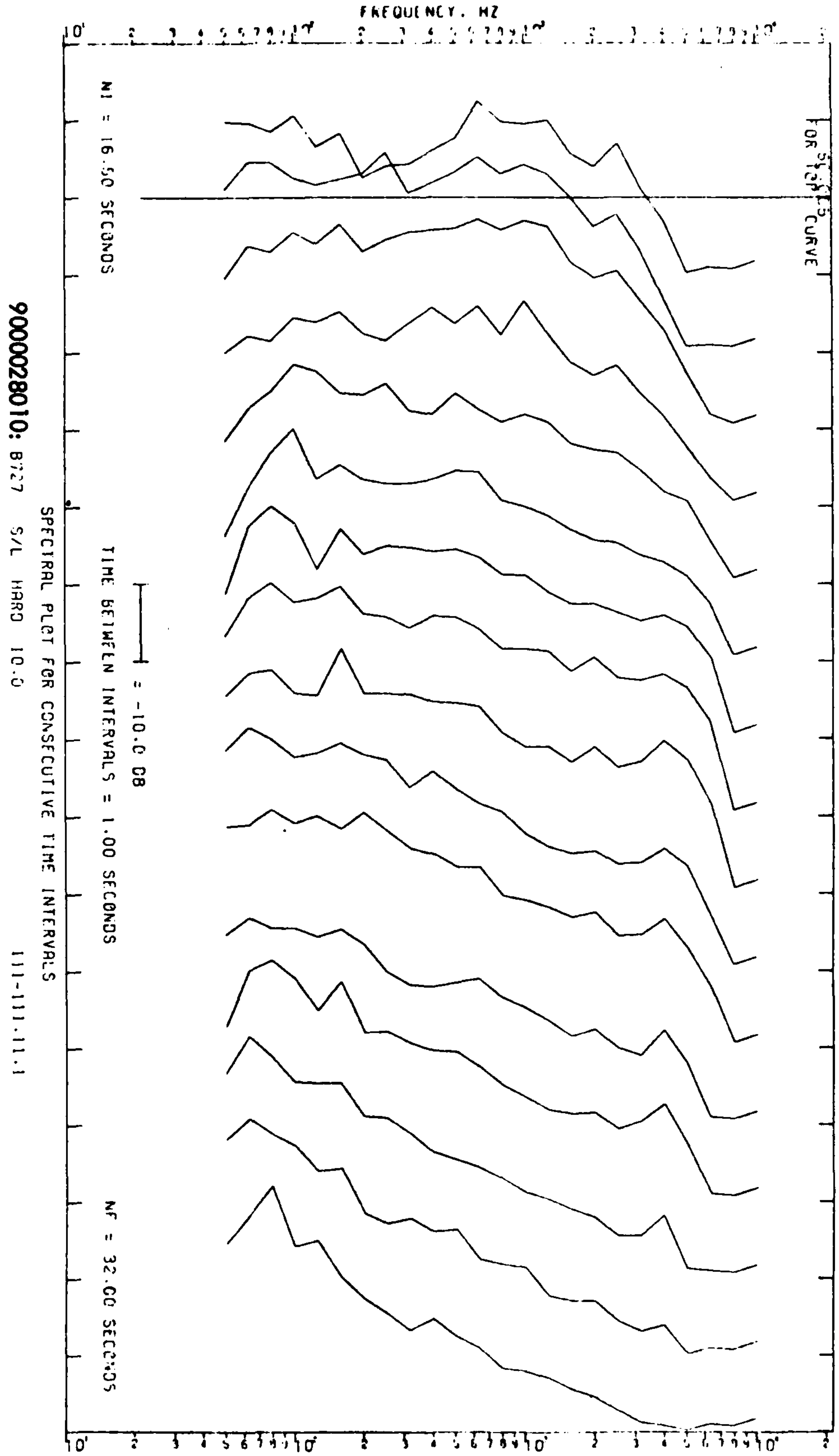
FREQUENCY, HZ
NI = 16.50 SECONDS
FOR TOP CURVE
= -10.0 DB
TIME BETWEEN INTERVALS = 1.00 SECONDS
NF = 32.00 SECONDS
9000028010: B727 S/L HARD 10.0
SPECTRAL PLOT FOR CONSECUTIVE TIME INTERVALS
111-111.11.1

Figure A-F4

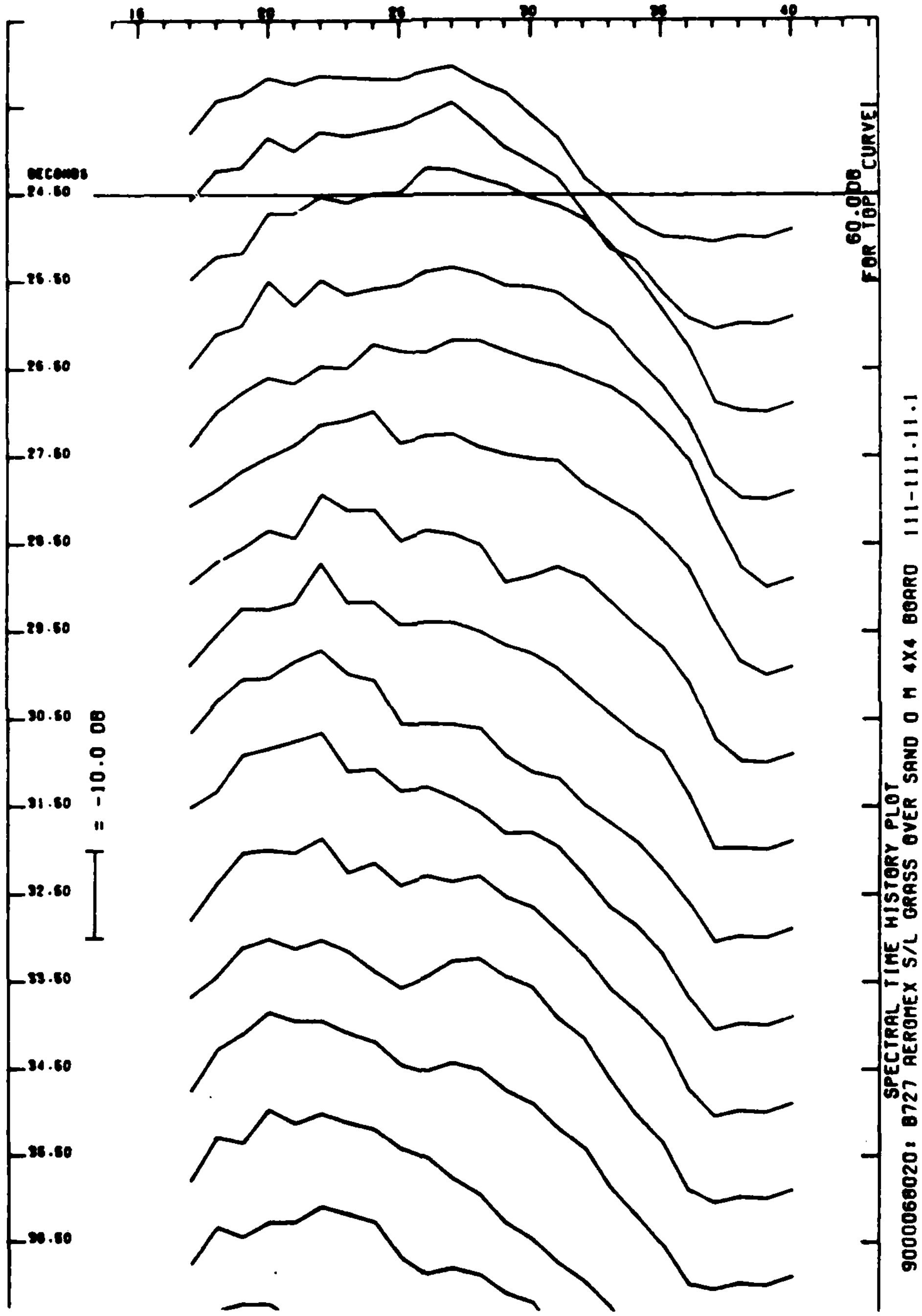

15
20
25
30
35
40
SECONDS
24.50
25.50
26.50
27.50
28.50
29.50
30.50
31.50
32.50
33.50
34.50
35.50
36.50
= -10.0 DB
60.0DB
FOR TOP CURVE
SPECTRAL TIME HISTORY PLOT
900006B020: B727 AEROMEX S/L GRASS OVER SAND 0 M 4X4 BOARD 111-111.11.1

Figure A-L1

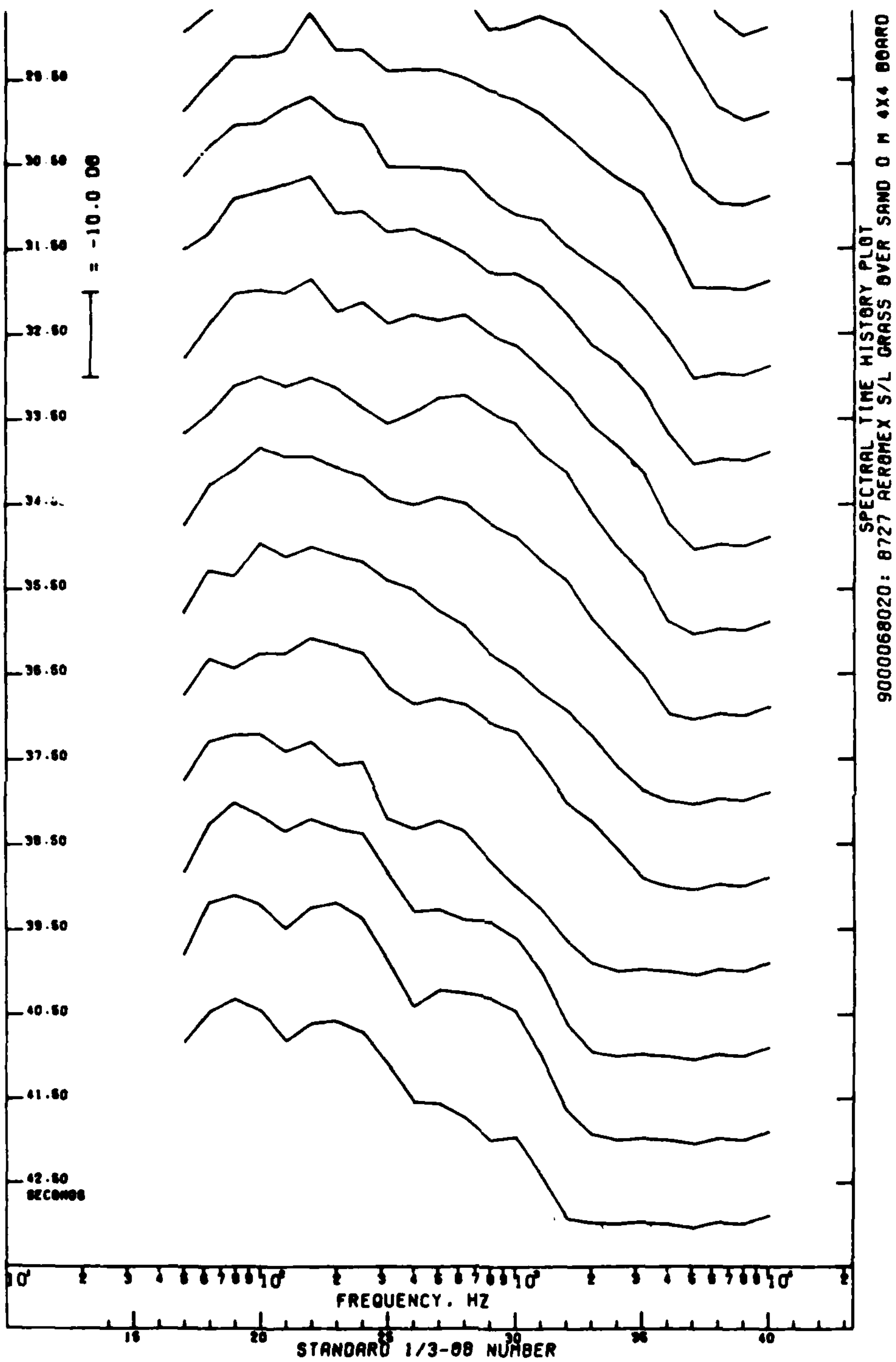

Figure A-L1 (Continued)

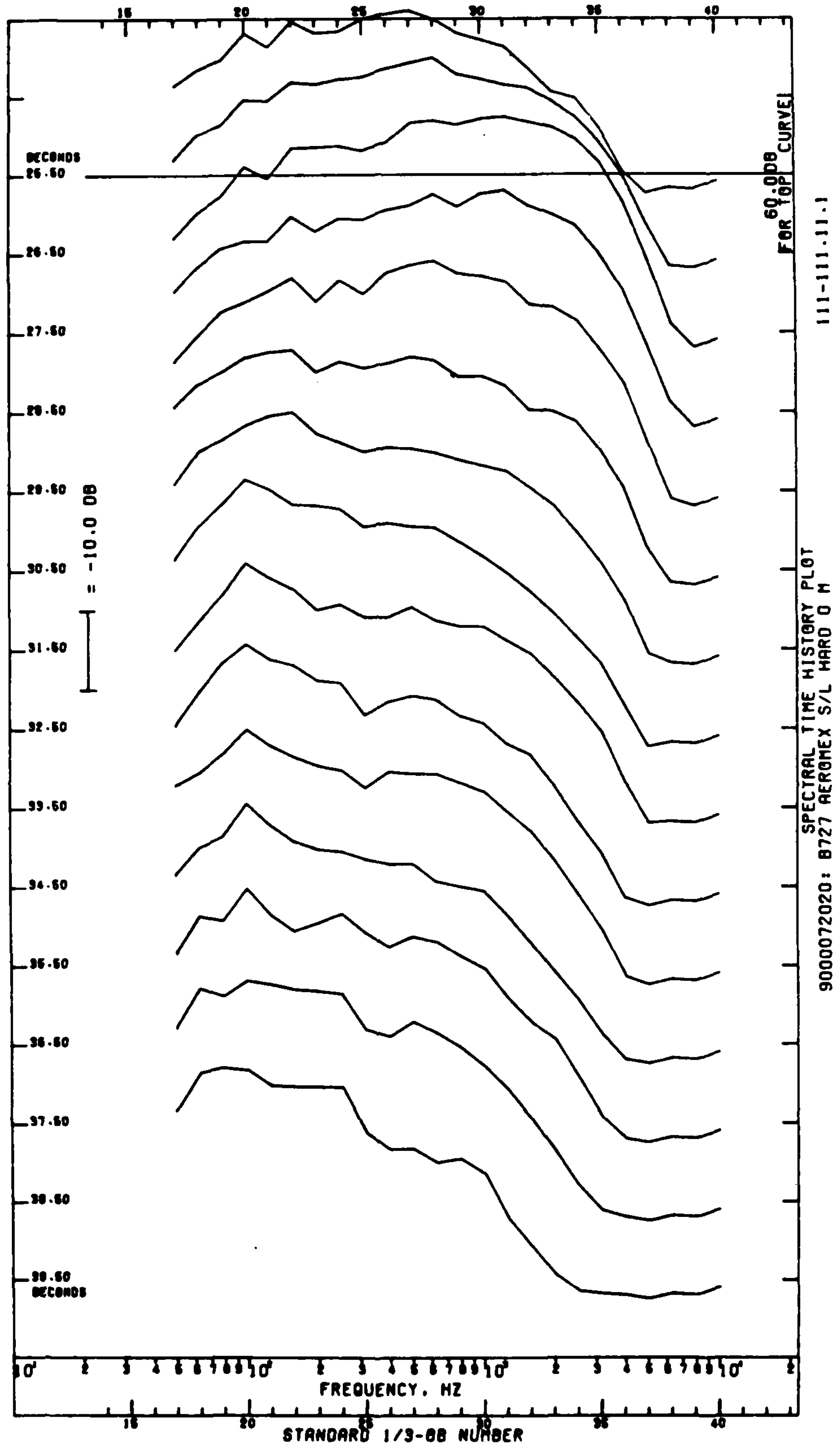
SECONDS
25.50
26.50
27.50
28.50
29.50
30.50
31.50
32.50
33.50
34.50
35.50
36.50
37.50
38.50
39.50
SECONDS
= -10.0 DB
60.0DB
FOR TOP CURVE
SPECTRAL TIME HISTORY PLOT
9000072020: B727 AEROMEX S/L HARD 0 M
111-111.11.1
FREQUENCY, HZ
STANDARD 1/3-OB NUMBER

Figure A-L2

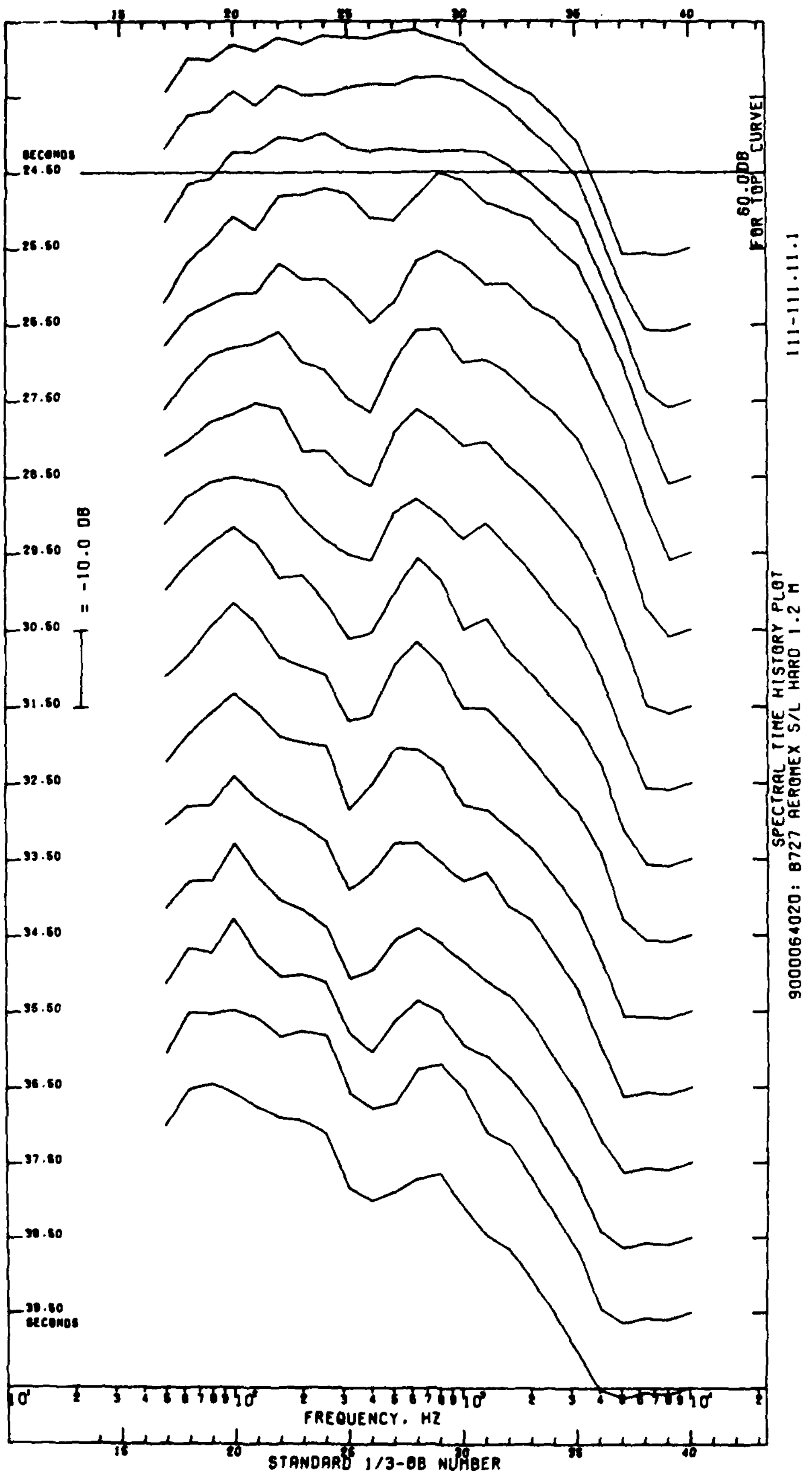
SECONDS
24.50
25.50
26.50
27.50
28.50
29.50
30.50
31.50
32.50
33.50
34.50
35.50
36.50
37.50
38.50
39.50
SECONDS
= -10.0 DB
60.0DB
FOR TOP CURVE
111-111.11.1
SPECTRAL TIME HISTORY PLOT
9000064020: B727 AEROMEX S/L HARD 1.2 M
FREQUENCY, HZ
STANDARD 1/3-OB NUMBER

Figure A-L3

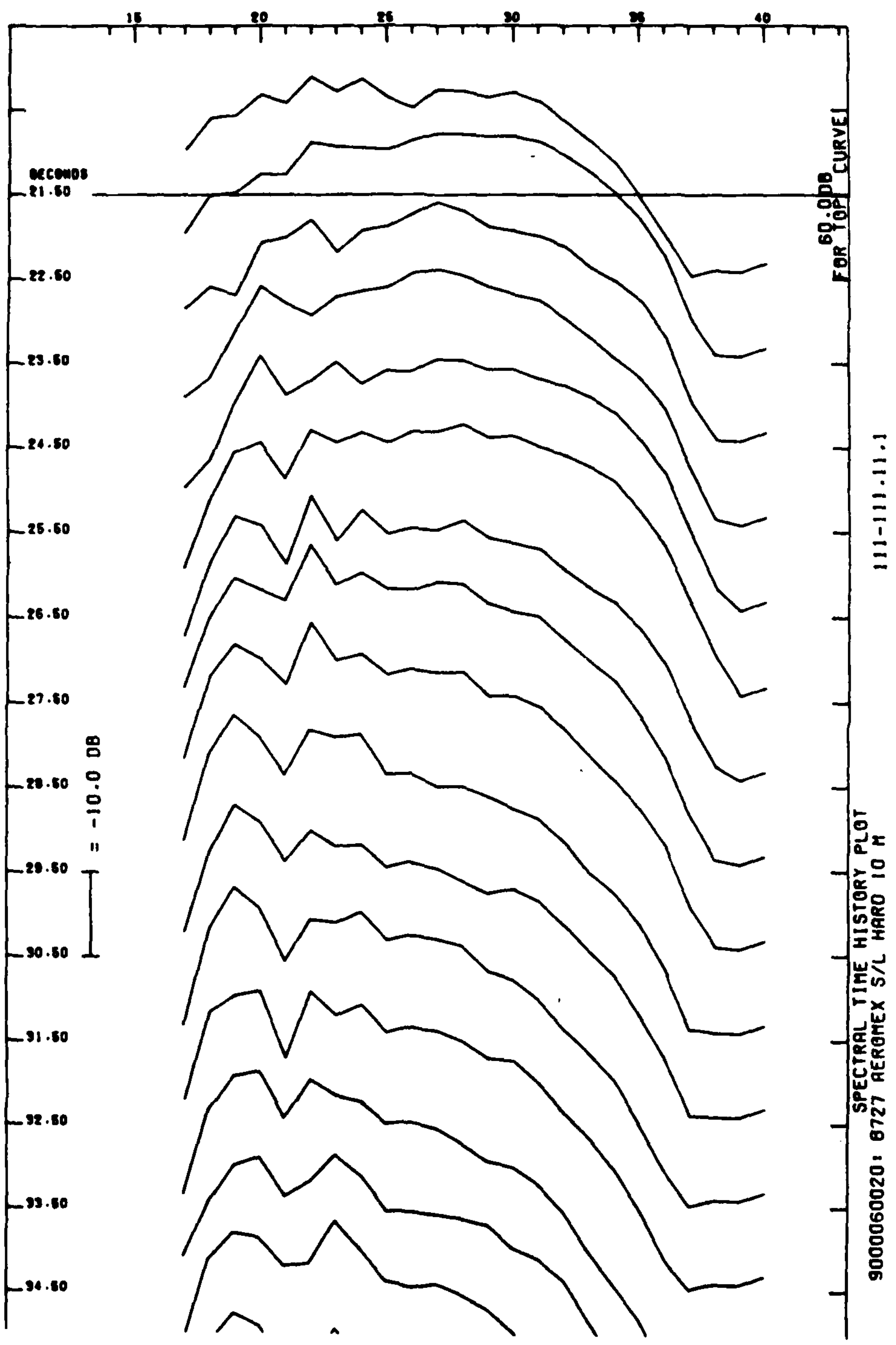
15
20
25
30
35
40
SECONDS
21.50
22.50
23.50
24.50
25.50
26.50
27.50
28.50
29.50
30.50
31.50
32.50
33.50
34.50
= -10.0 DB
60.0DB FOR TOP CURVE
SPECTRAL TIME HISTORY PLOT
9000060020: B727 AEROMEX S/L HARD 10 M

Figure A-L4

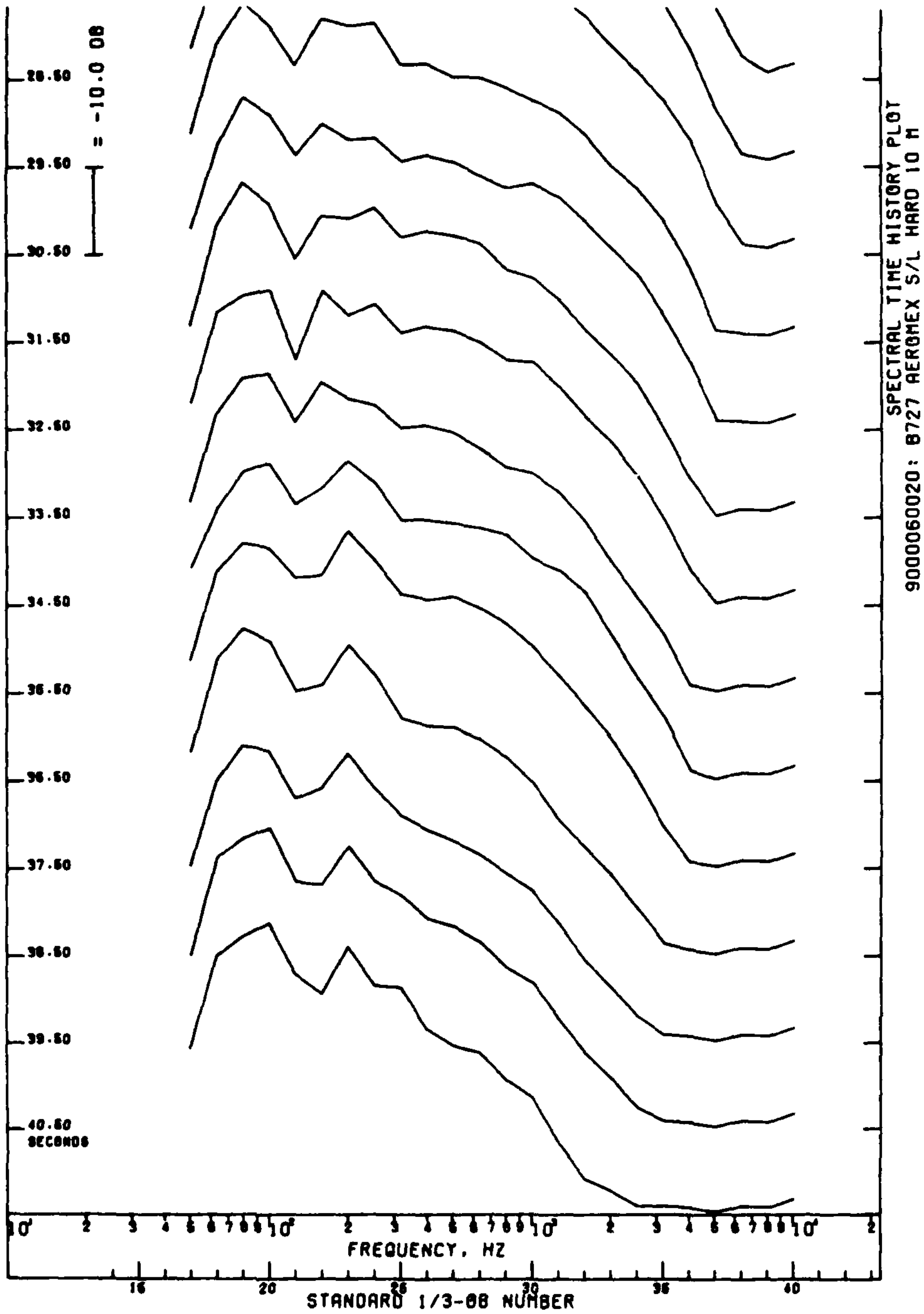

Figure A-L4 (Continued)

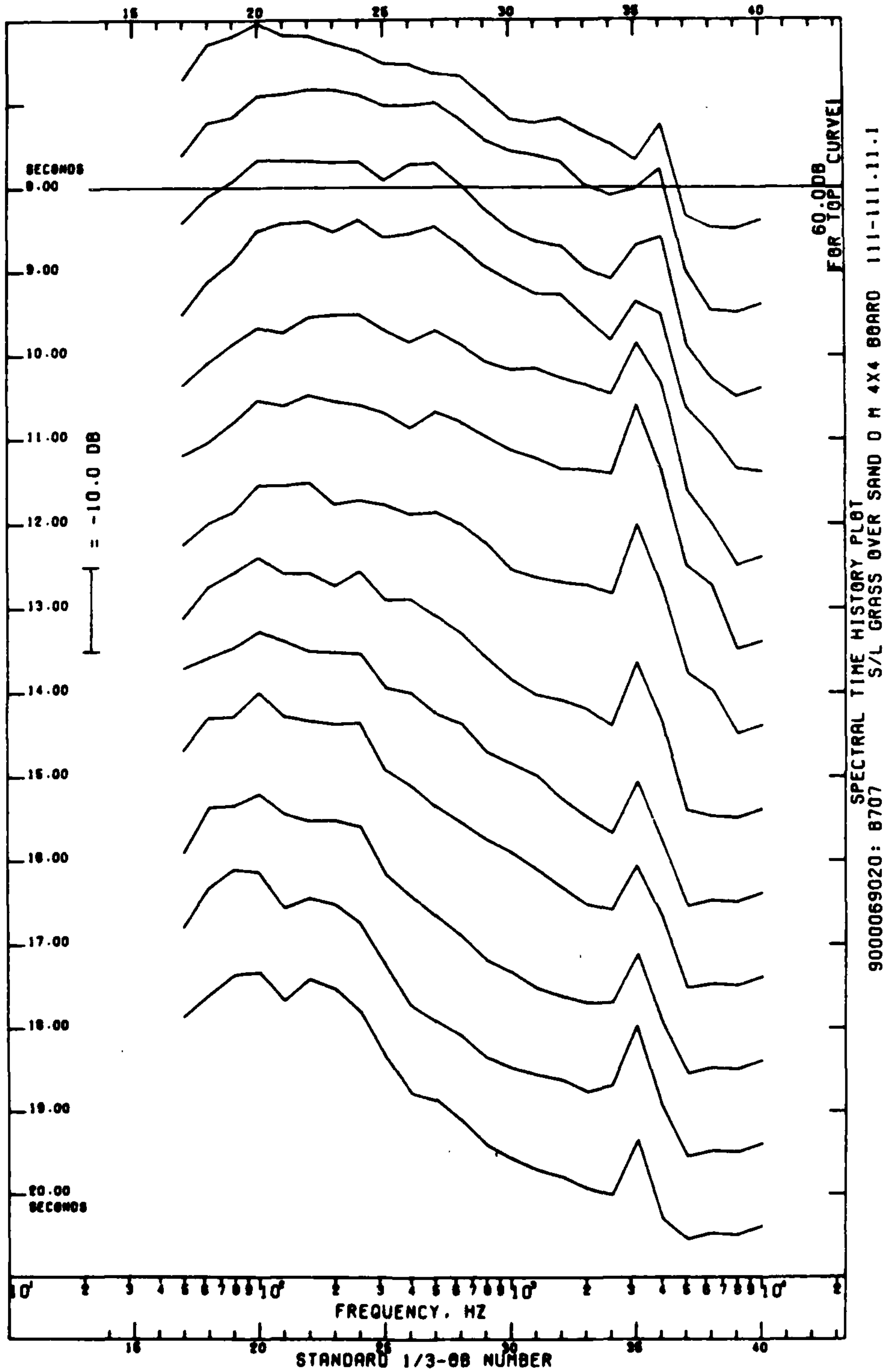
SECONDS
8.00
9.00
10.00
11.00
12.00
13.00
14.00
15.00
16.00
17.00
18.00
19.00
20.00
SECONDS
= -10.0 DB
60.0DB
FOR TOP CURVE
SPECTRAL TIME HISTORY PLOT
S/L GRASS OVER SAND O M 4X4 BOARD 111-111-11.1
9000069020: B707
FREQUENCY, HZ
STANDARD 1/3-OB NUMBER

Figure A-N1

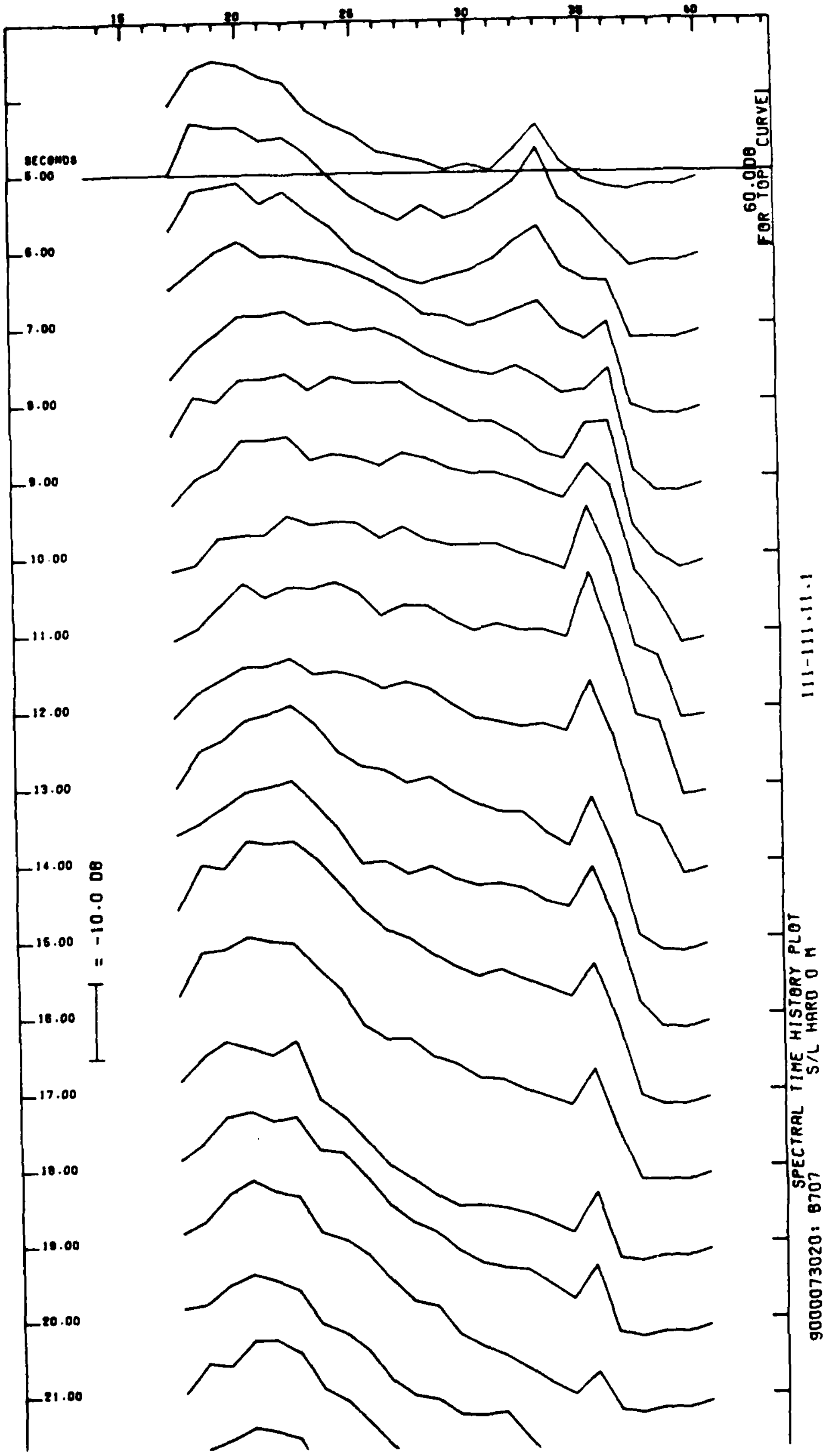
15
20
25
30
35
40
SECONDS
5.00
6.00
7.00
8.00
9.00
10.00
11.00
12.00
13.00
14.00
15.00
16.00
17.00
18.00
19.00
20.00
21.00
= -10.0 DB
60.0DB
FOR TOP CURVE
111-111.11.1
SPECTRAL TIME HISTORY PLOT
S/L HARD 0 M
9000073020: B707

Figure A-N2

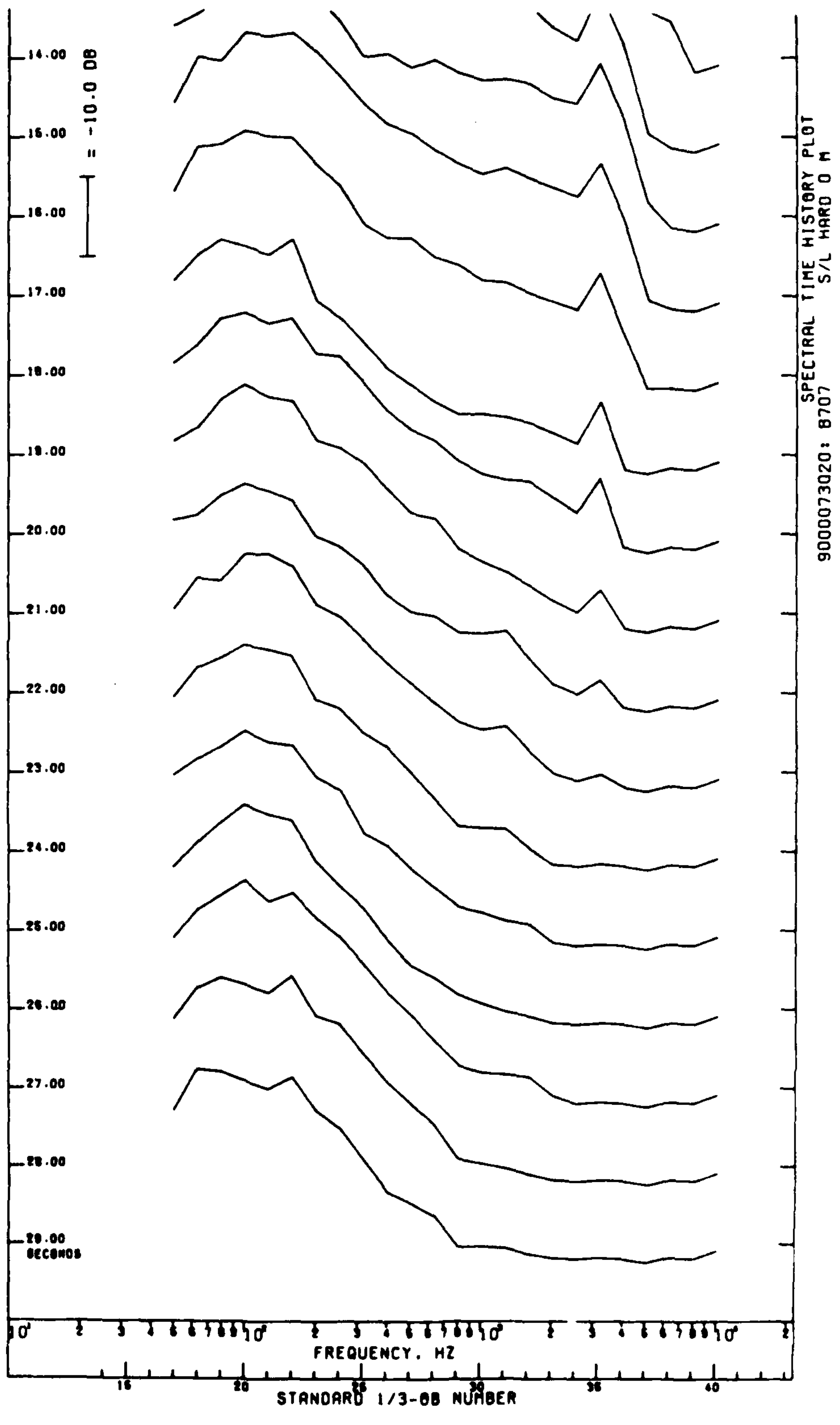

Figure A-N2 (Continued)

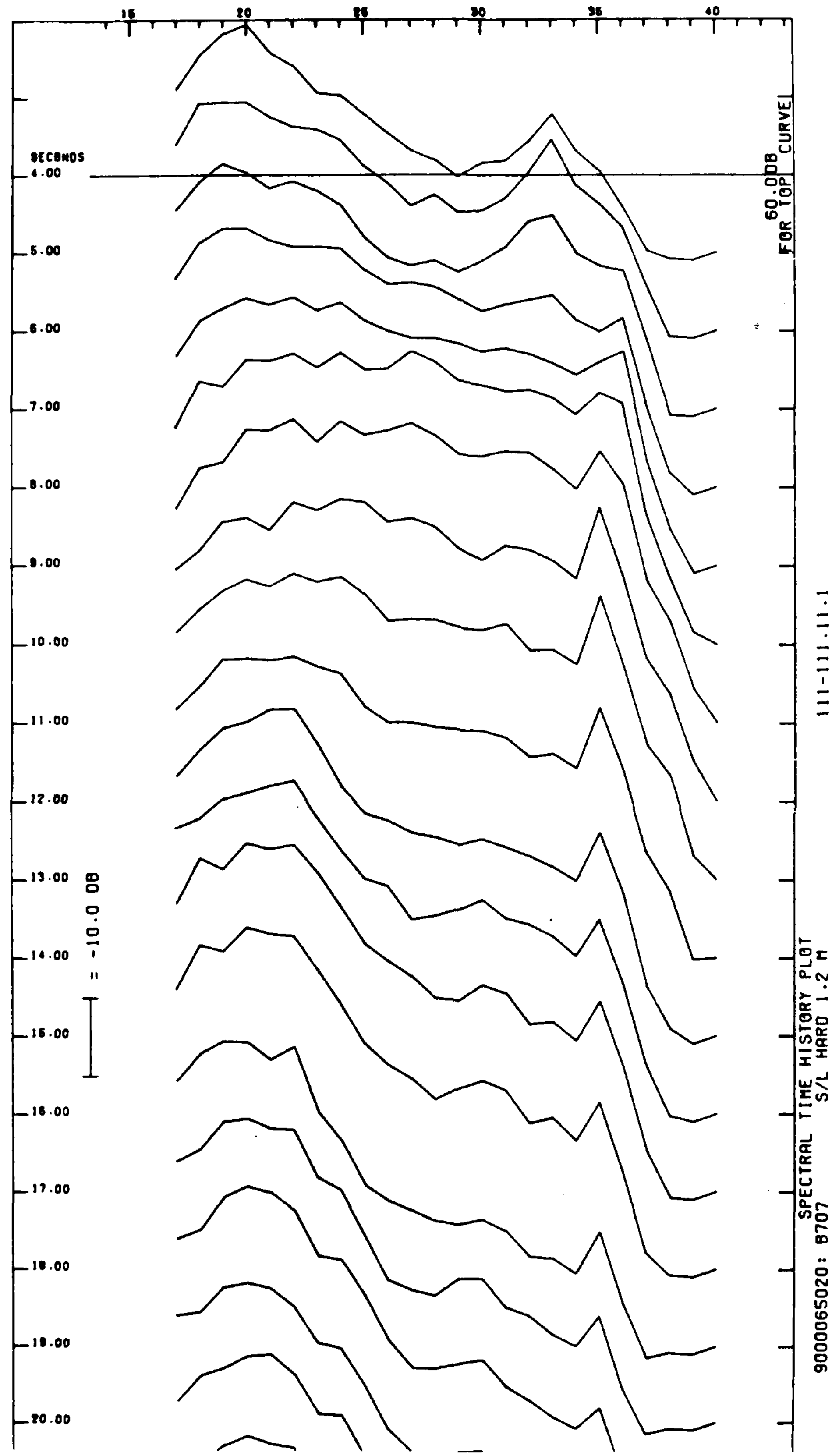
15
20
25
30
35
40
SECONDS
4.00
5.00
6.00
7.00
8.00
9.00
10.00
11.00
12.00
13.00
14.00
15.00
16.00
17.00
18.00
19.00
20.00
= -10.0 DB
60.0DB
FOR TOP CURVE
SPECTRAL TIME HISTORY PLOT
900006502O: B707 S/L HARD 1.2 M
111-111.11.1

Figure A-N3

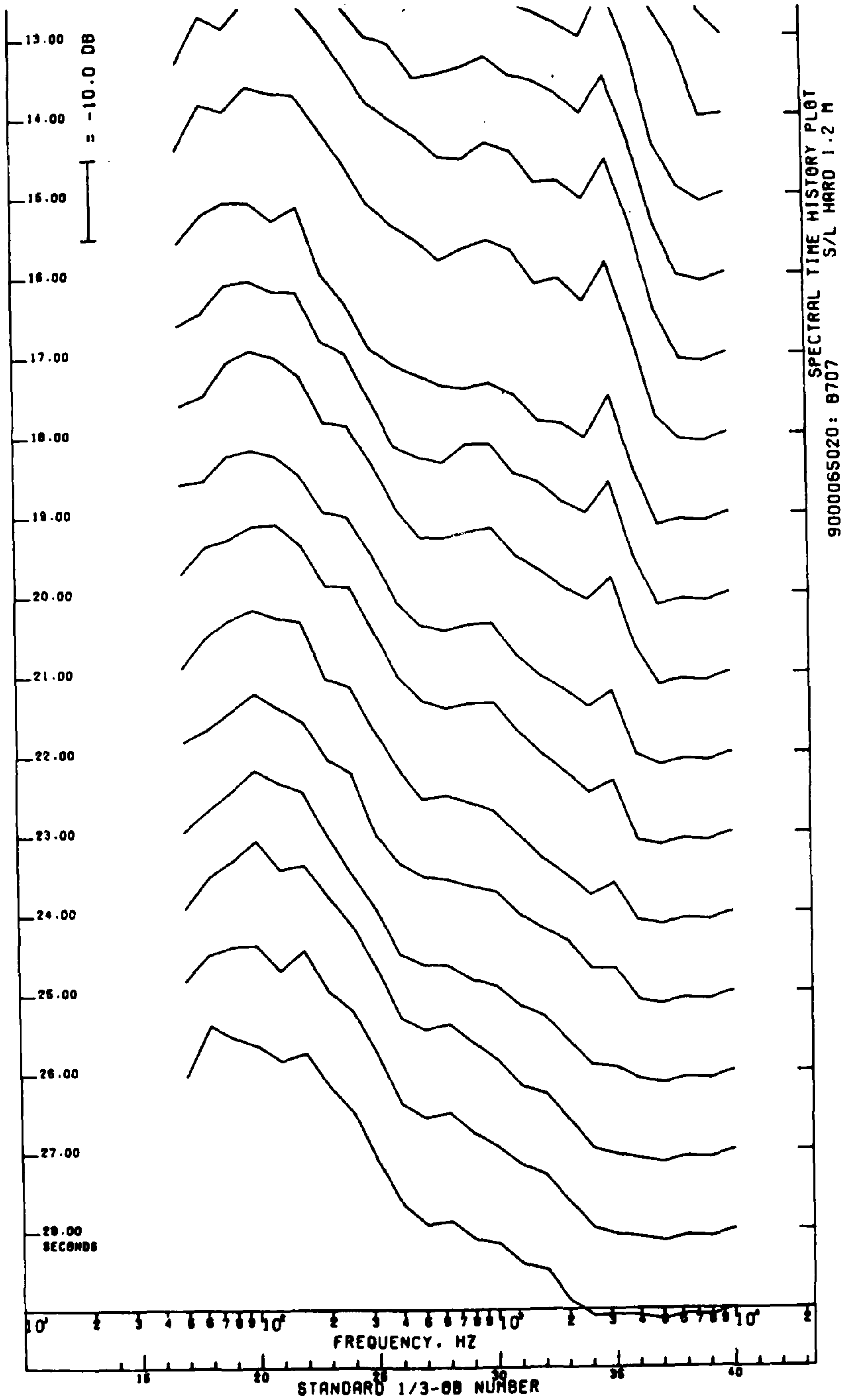

Figure A-N3 (Continued)

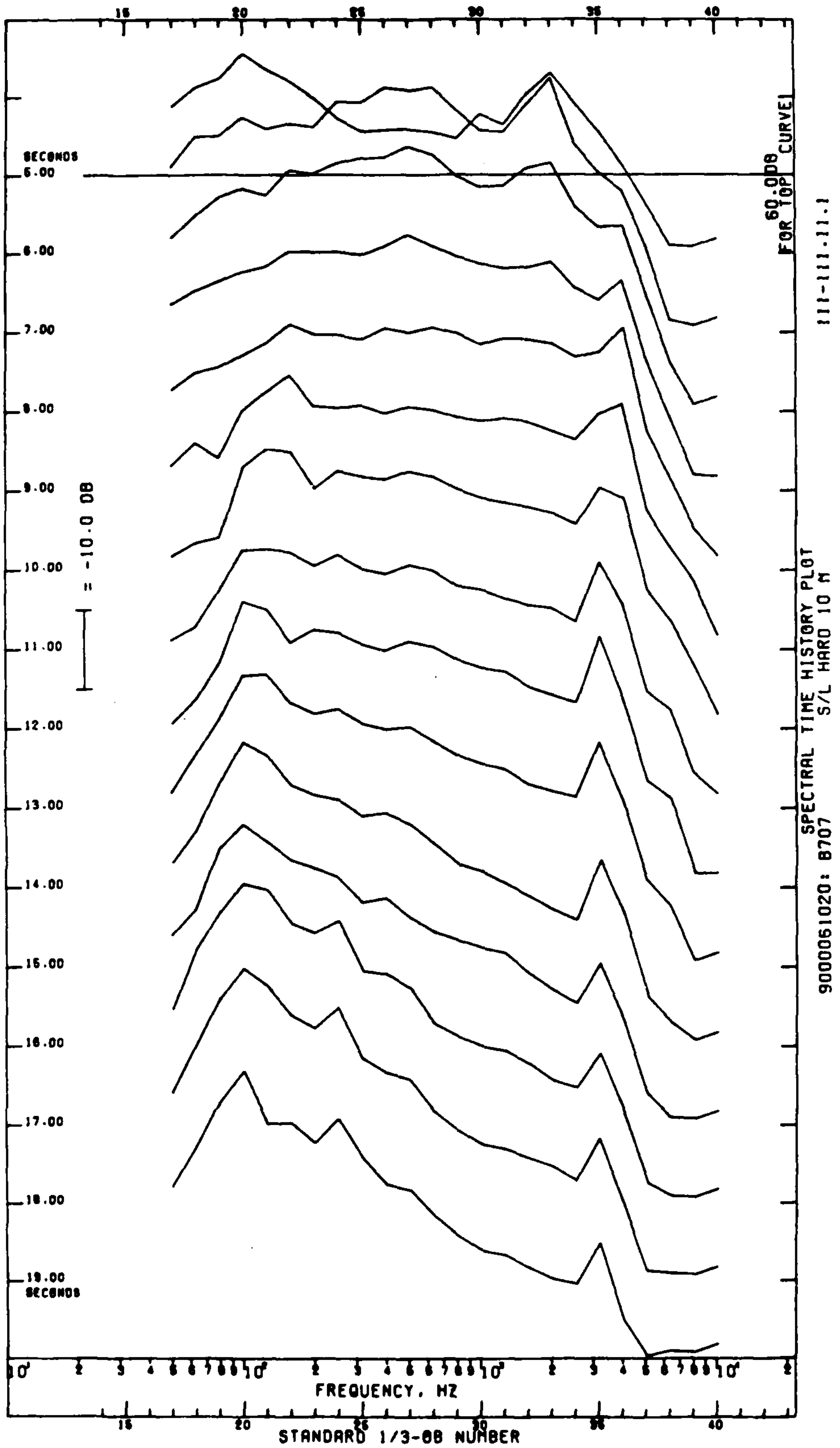

SECONDS
5.00
6.00
7.00
8.00
9.00
10.00
11.00
12.00
13.00
14.00
15.00
16.00
17.00
18.00
19.00
SECONDS
= -10.0 DB
60.0DB
FOR TOP CURVE)
111-111-11-1
SPECTRAL TIME HISTORY PLOT
S/L HARD 10 M
9000061020: B707
FREQUENCY, HZ
STANDARD 1/3-OB NUMBER

Figure A-N4

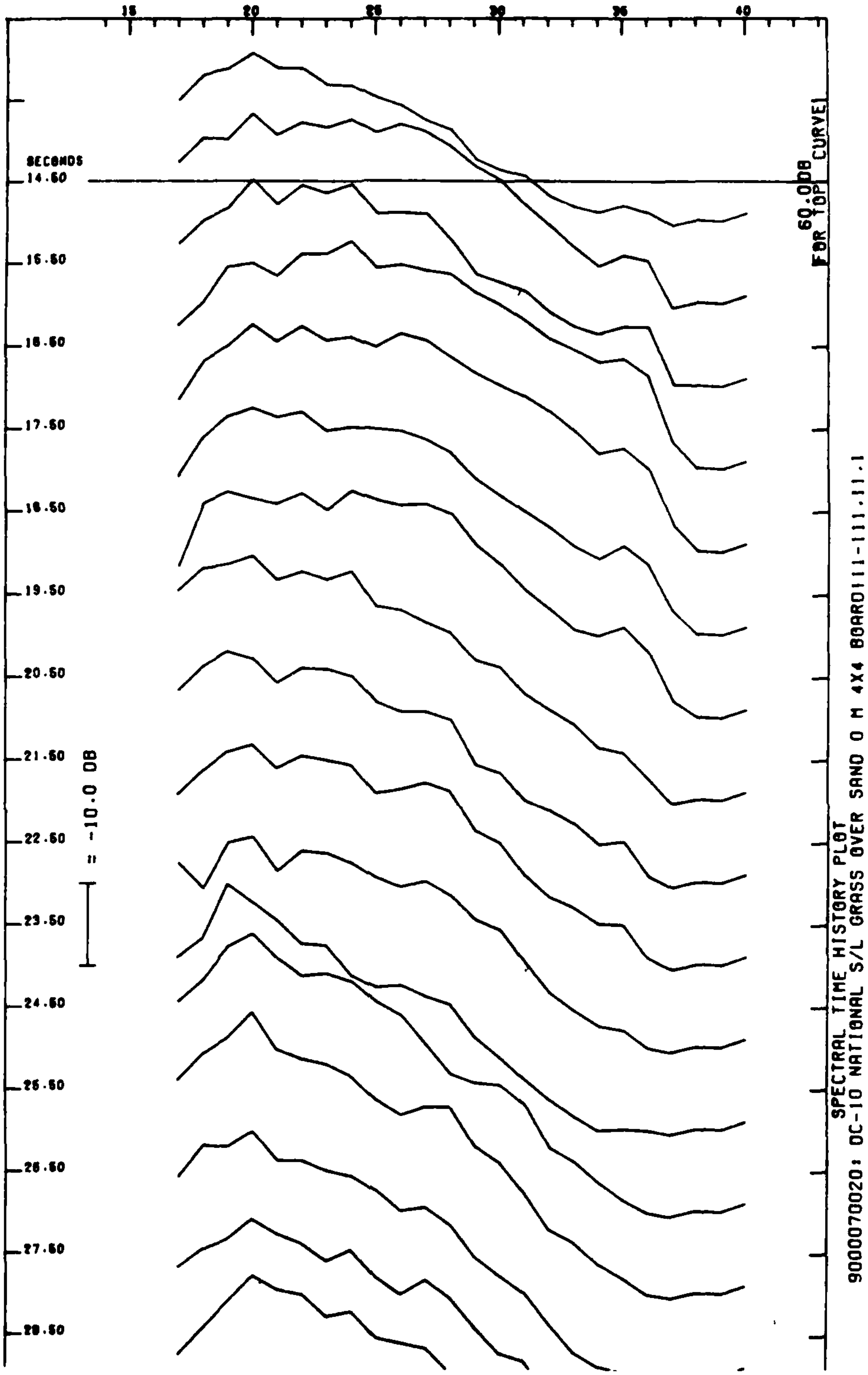
15
20
25
30
35
40
SECONDS
14.50
15.50
16.50
17.50
18.50
19.50
20.50
21.50
22.50
23.50
24.50
25.50
26.50
27.50
28.50
= -10.0 DB
60.0DB
FOR TOP CURVE
SPECTRAL TIME HISTORY PLOT
9000070020: DC-10 NATIONAL S/L GRASS OVER SAND 0 M 4X4 BOARD111-111.11.1

Figure A-Q1

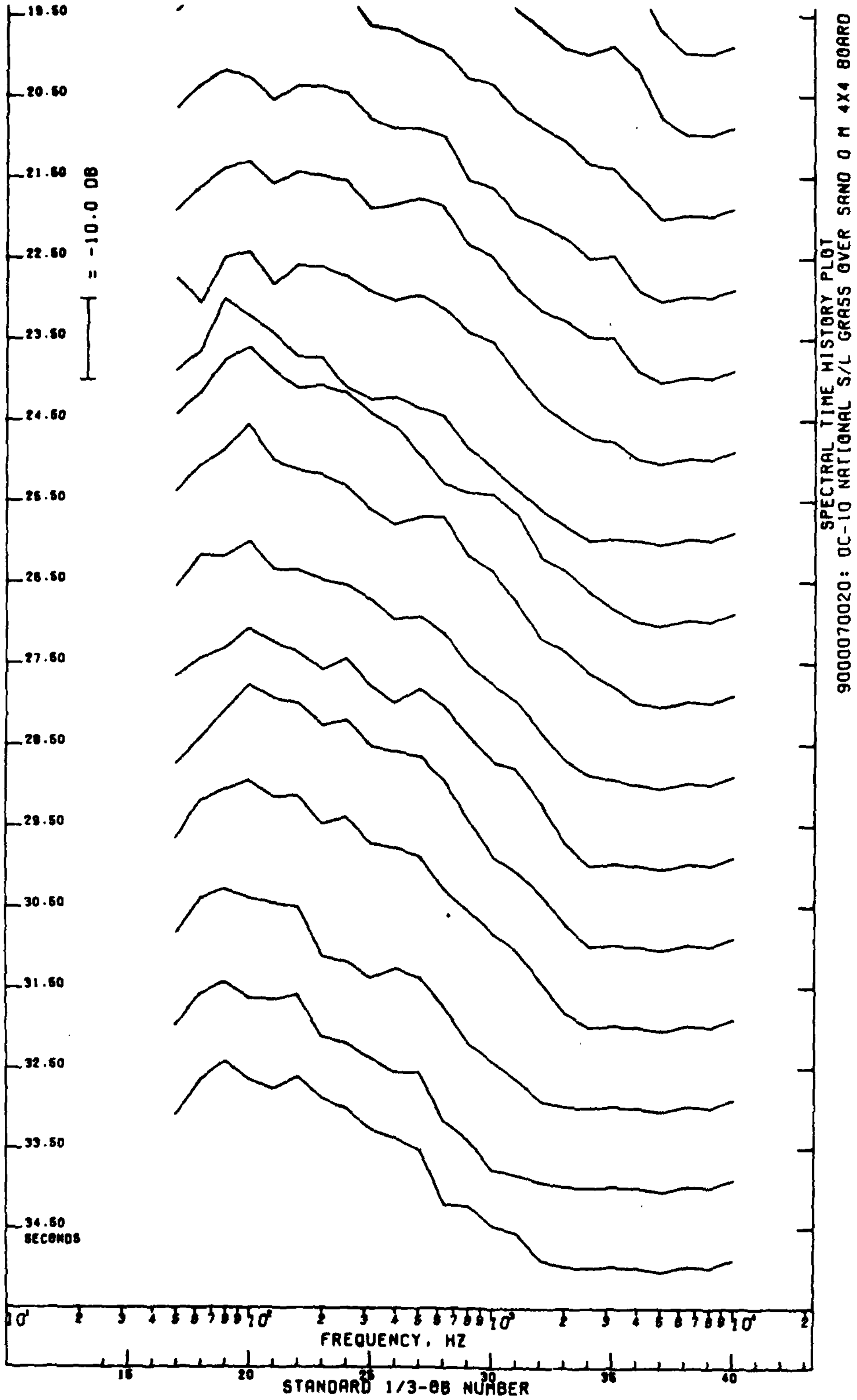

Figure A-Q1 (Continued)

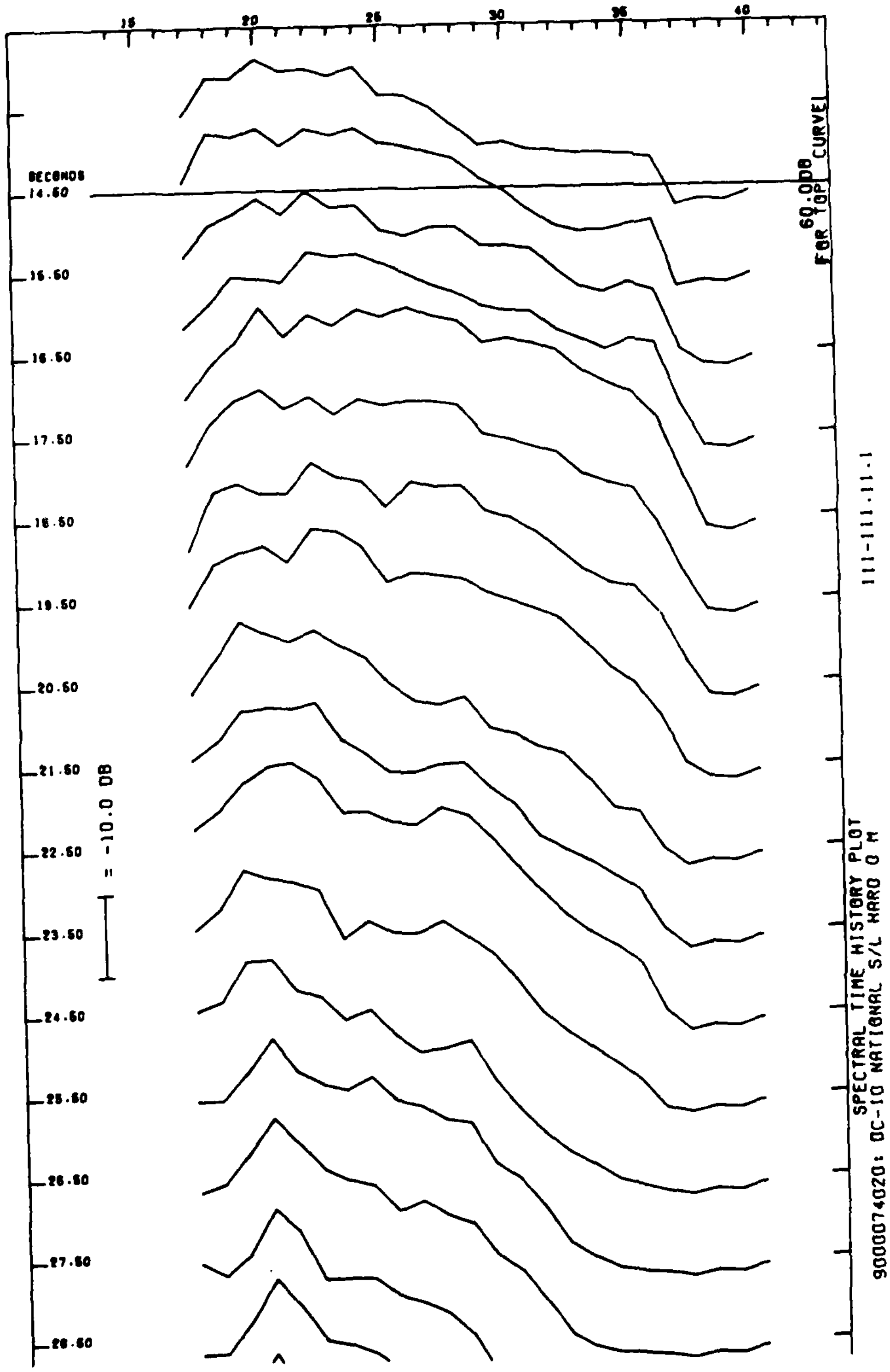
SECONDS
14.50
15.50
16.50
17.50
18.50
19.50
20.50
21.50
22.50
23.50
24.50
25.50
26.50
27.50
28.50
15
20
25
30
35
40
= -10.0 DB
60.0DB
FOR TOP CURVE
111-111.11.1
SPECTRAL TIME HISTORY PLOT
90000074020: DC-10 NATIONAL S/L HARD O M

Figure A-Q2

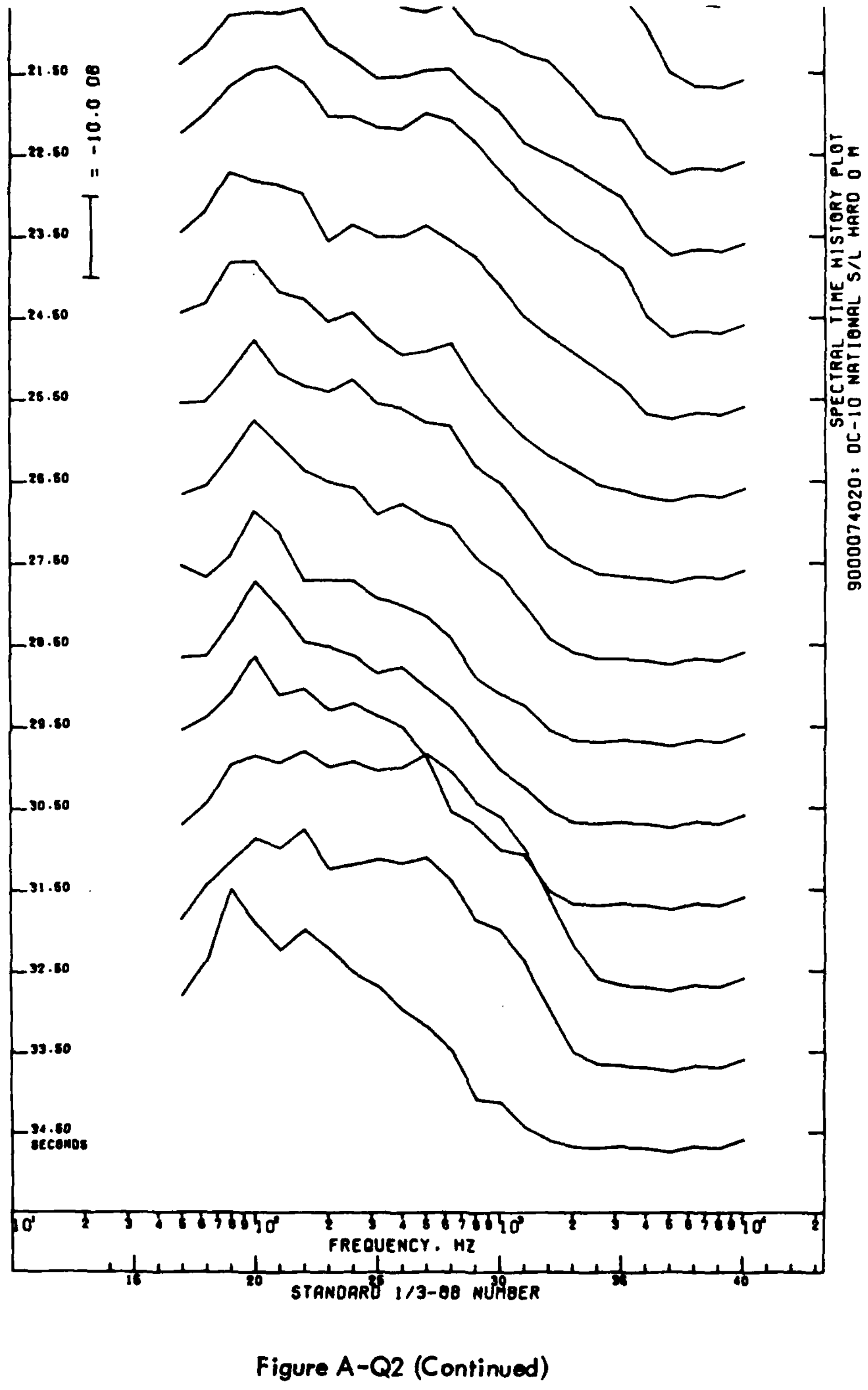

Figure A-Q2 (Continued)

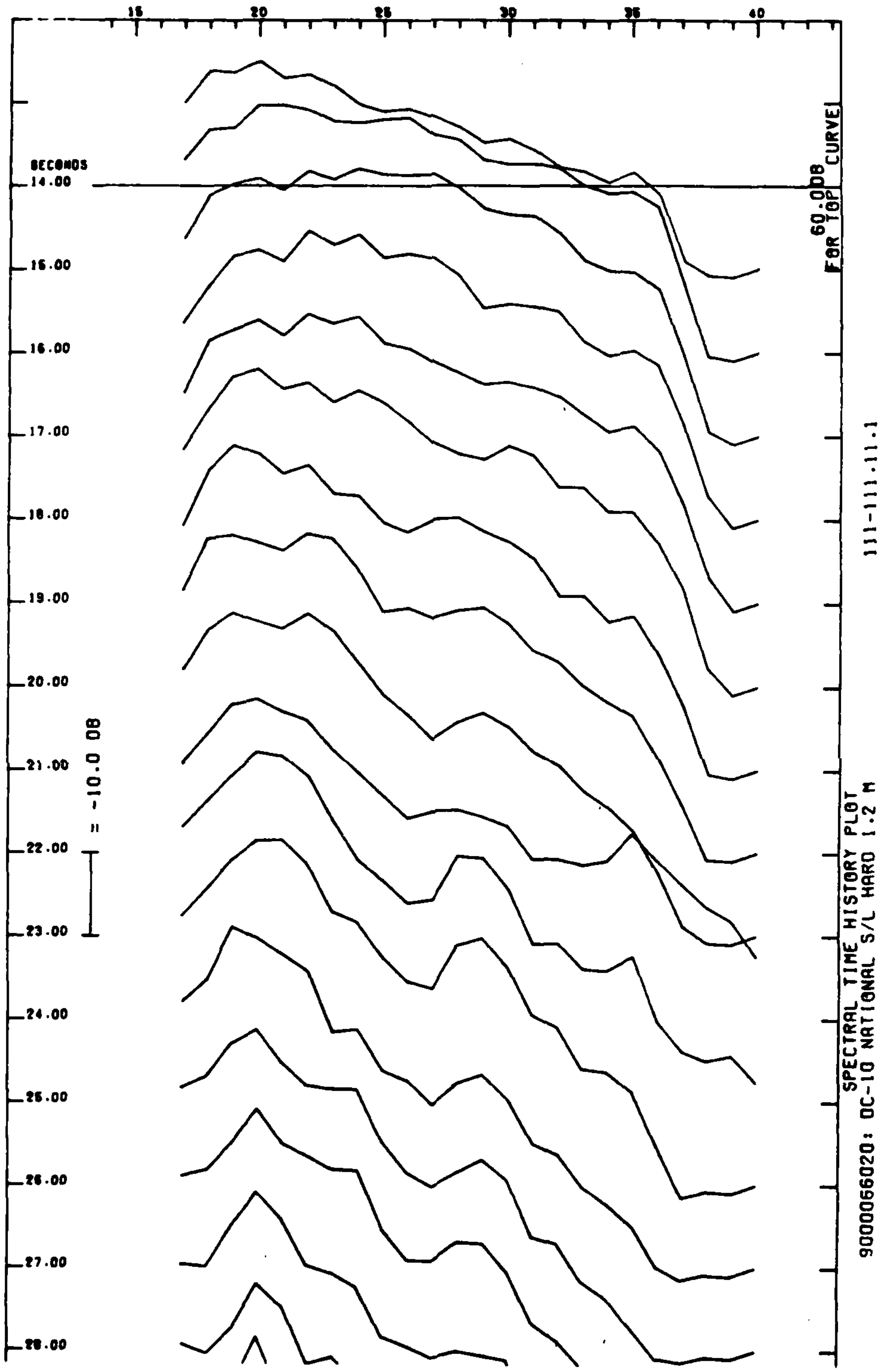
15
20
25
30
35
40
SECONDS
14.00
15.00
16.00
17.00
18.00
19.00
20.00
21.00
22.00
23.00
24.00
25.00
26.00
27.00
28.00
= -10.0 DB
60.0DB
FOR TOP CURVE
111-111.11.1
SPECTRAL TIME HISTORY PLOT
900066020: DC-10 NATIONAL S/L HARD 1.2 M

Figure A-Q3

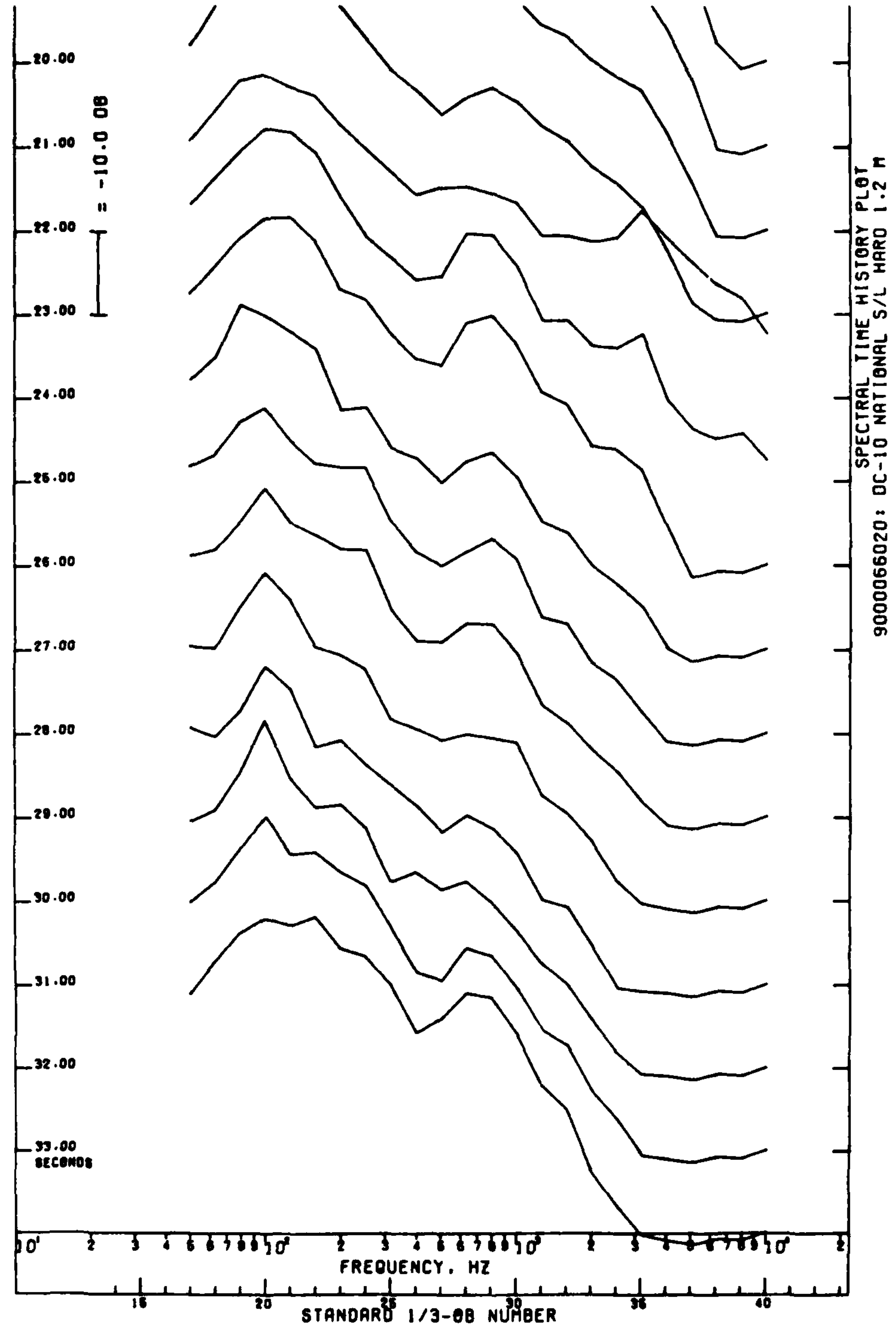

Figure A-Q3 (Continued)

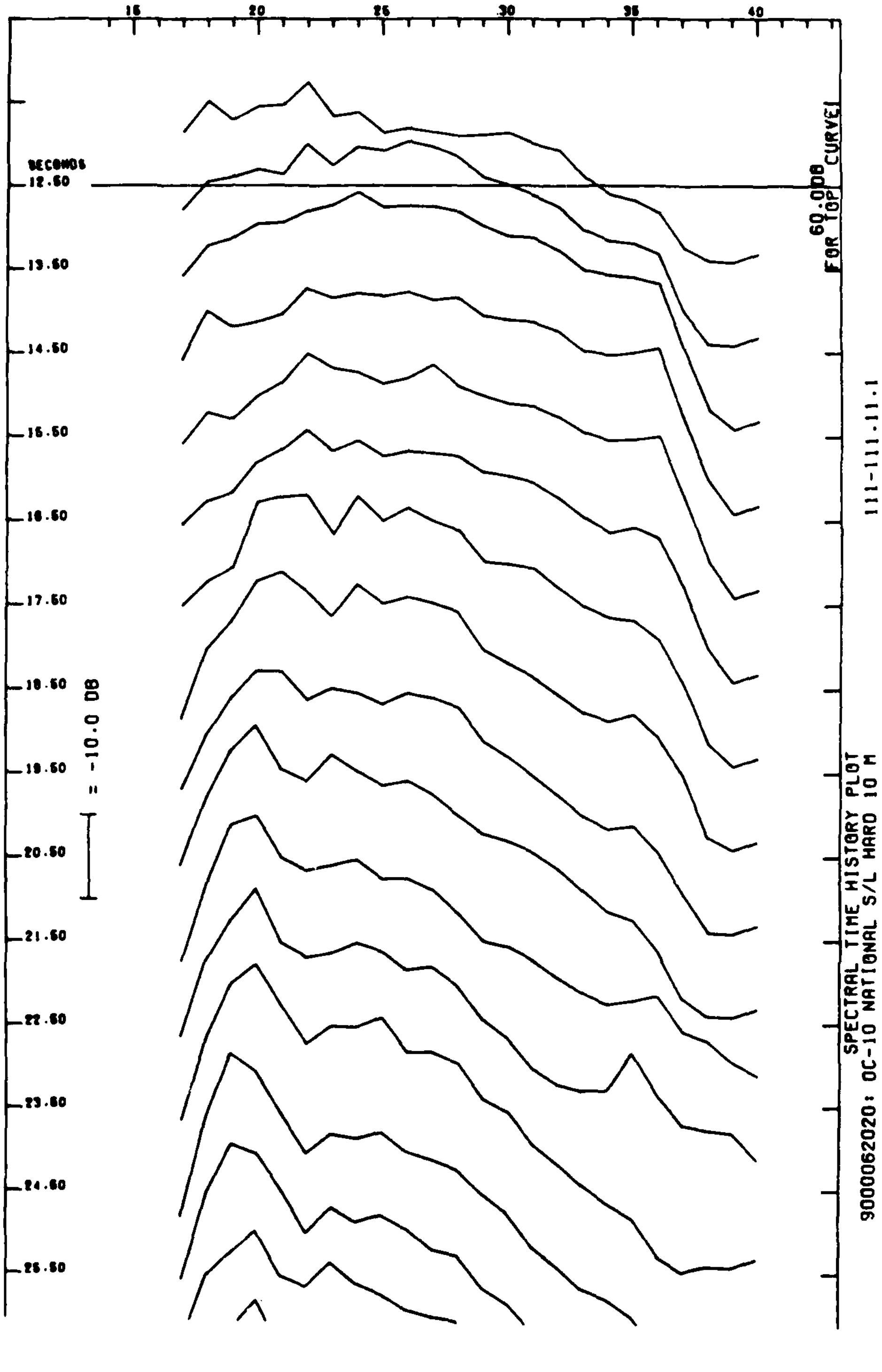

15
20
25
30
35
40
SECONDS
12.50
13.50
14.50
15.50
16.50
17.50
18.50
19.50
20.50
21.50
22.50
23.50
24.50
25.50
= -10.0 DB
60.0DB
FOR TOP CURVE
111-111.11.1
SPECTRAL TIME HISTORY PLOT
900062020: DC-10 NATIONAL S/L HARD 10 M

Figure A-Q4

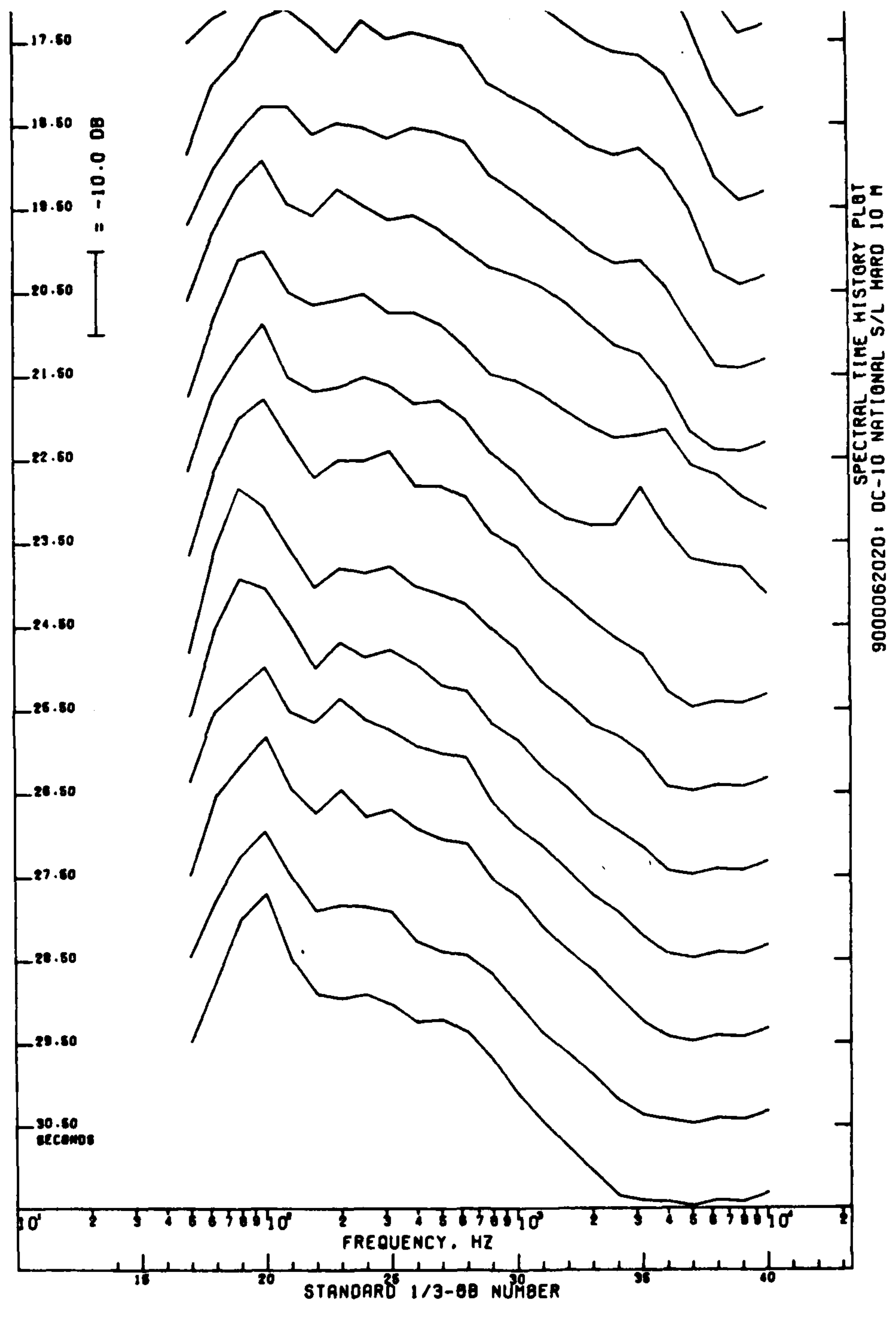

Figure A-Q4 (Continued)

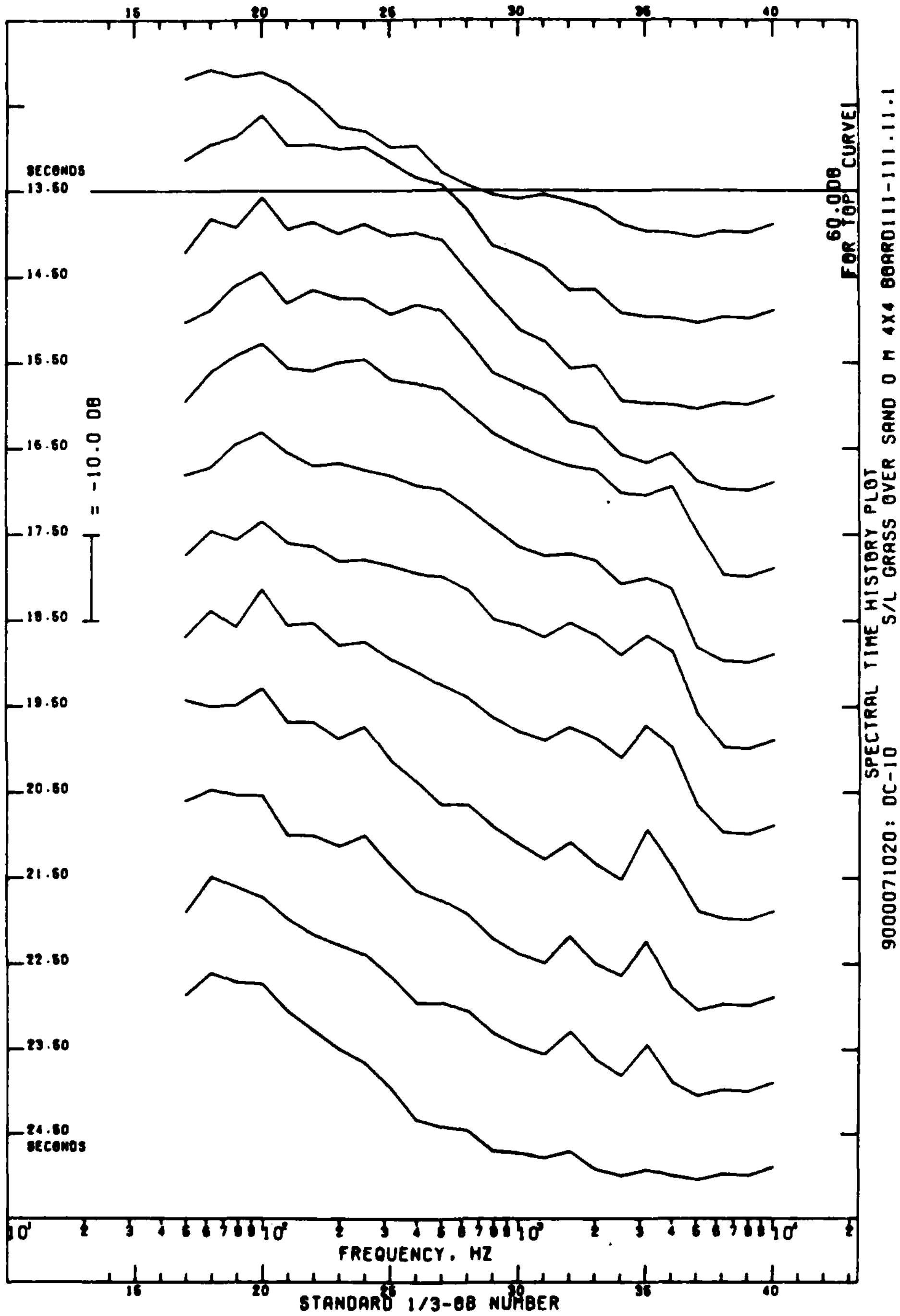

SECONDS
13.50
14.50
15.50
16.50
17.50
18.50
19.50
20.50
21.50
22.50
23.50
24.50
SECONDS
= -10.0 DB
60.0DB
FOR TOP CURVE)
SPECTRAL TIME HISTORY PLOT
S/L GRASS OVER SAND 0 M 4X4 BOARDIII-III.II.1
9000071020: DC-10
FREQUENCY, HZ
STANDARD 1/3-OB NUMBER

Figure A-R1

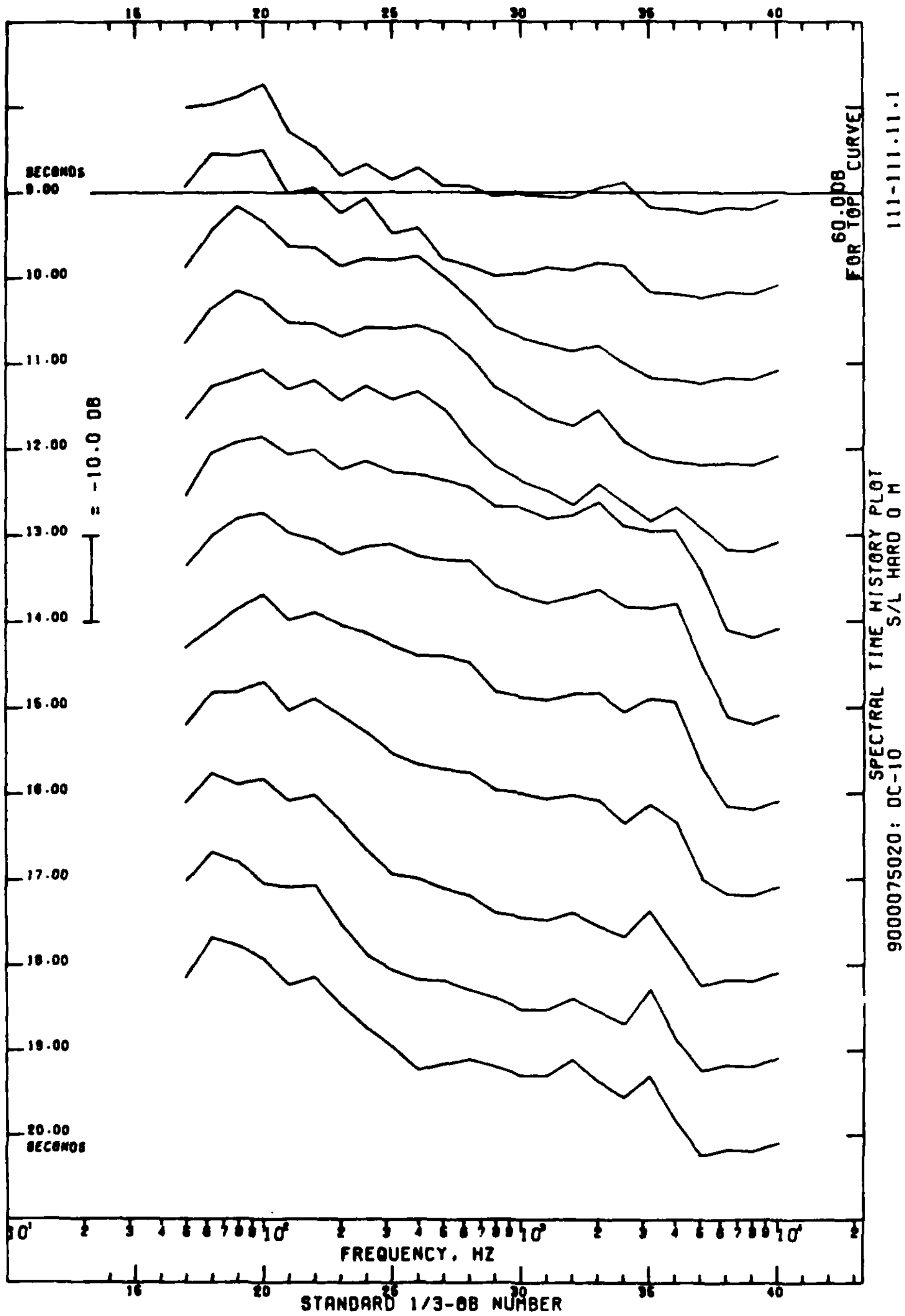
SECONDS
9.00
10.00
11.00
12.00
13.00
14.00
15.00
16.00
17.00
18.00
19.00
20.00
SECONDS
= -10.0 DB
60.0DB
FOR TOP CURVE
111-111.11.1
SPECTRAL TIME HISTORY PLOT
S/L HARD 0 M
9000075020: DC-10
FREQUENCY, HZ
STANDARD 1/3-OB NUMBER

Figure A-R2

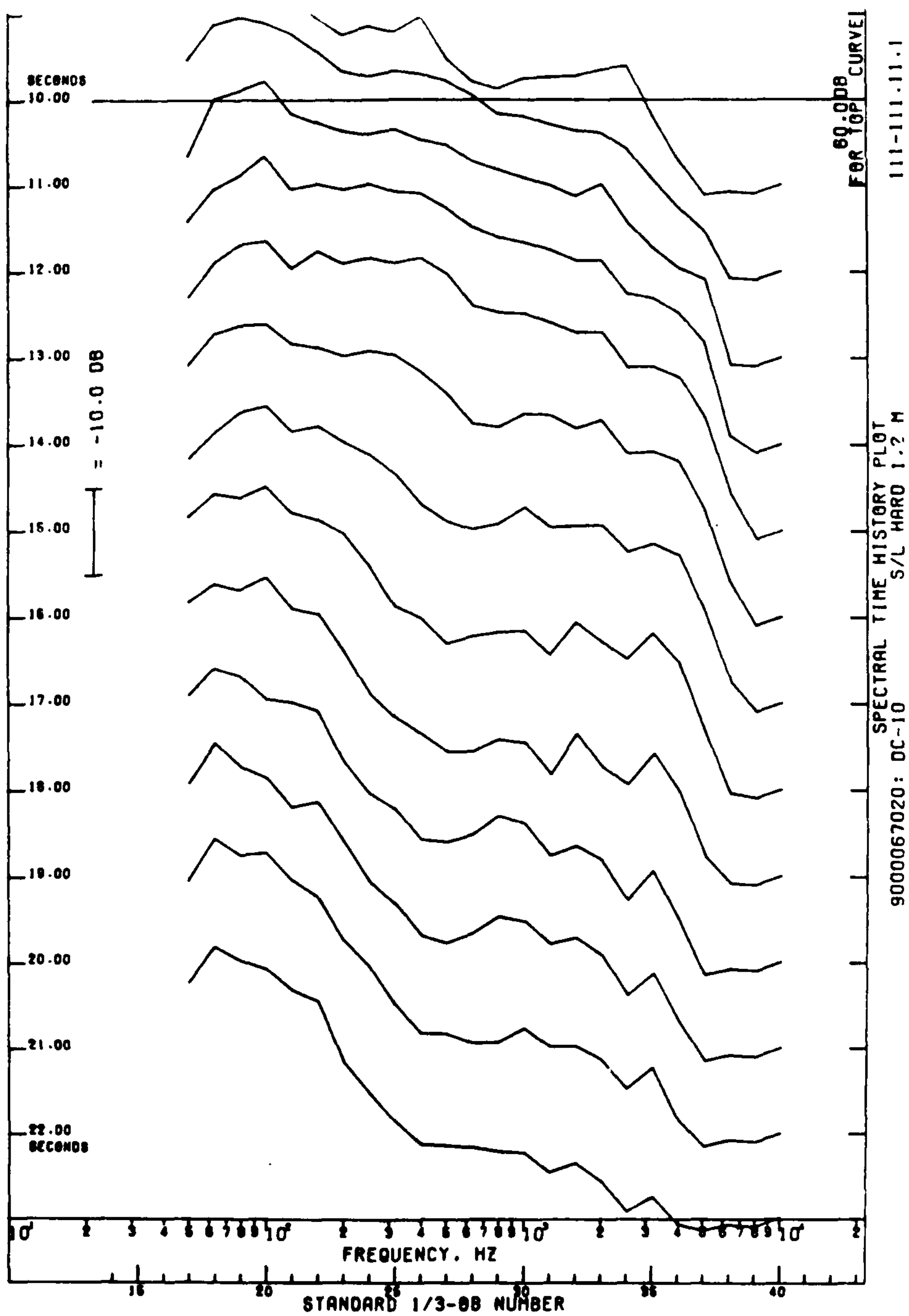
SECONDS
10.00
11.00
12.00
13.00
14.00
15.00
16.00
17.00
18.00
19.00
20.00
21.00
22.00
SECONDS
= -10.0 DB
60.0DB
FOR TOP CURVE
111-111.11.1
SPECTRAL TIME HISTORY PLOT
900006702O: DC-10
S/L HARD 1.2 M
FREQUENCY, HZ
STANDARD 1/3-OB NUMBER
15
20
25
30
35
40

Figure A-R3

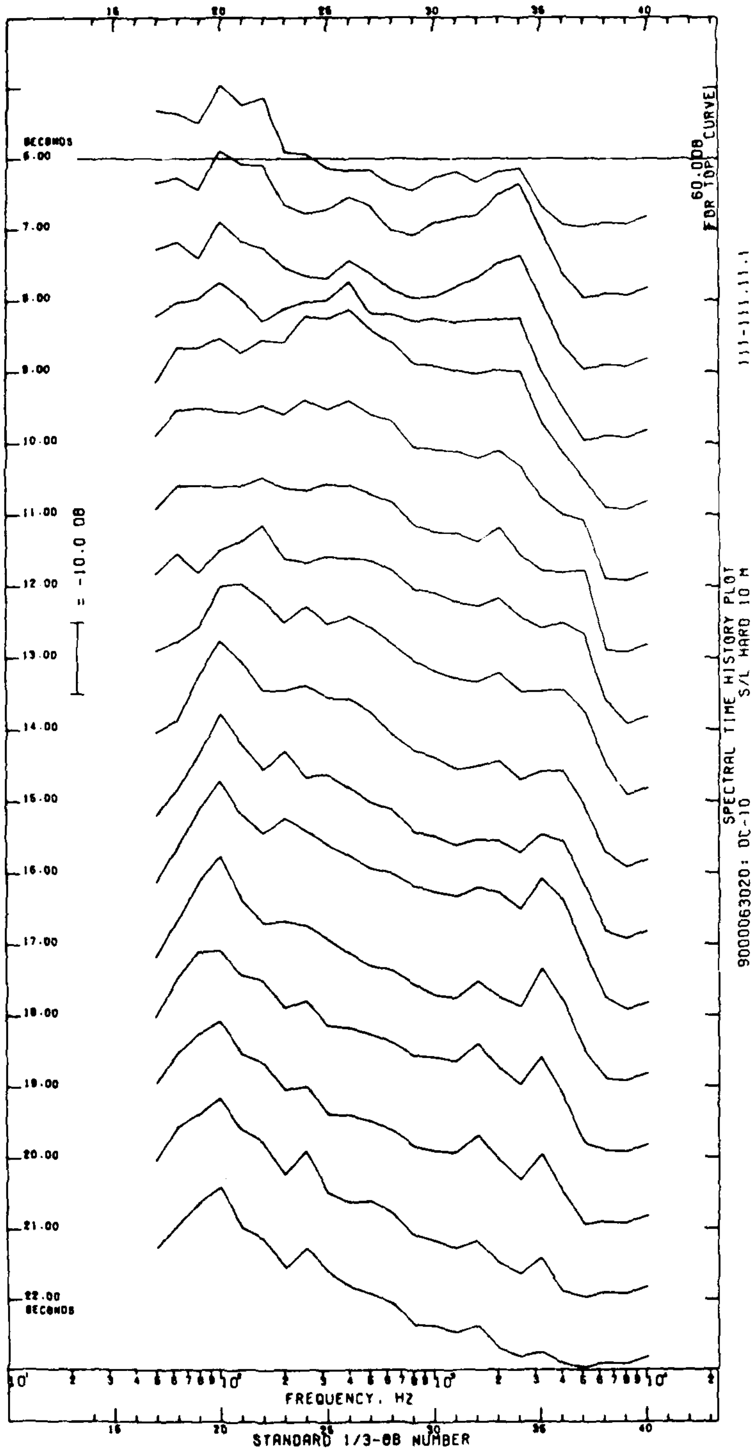
SECONDS
6.00
7.00
8.00
9.00
10.00
11.00
12.00
13.00
14.00
15.00
16.00
17.00
18.00
19.00
20.00
21.00
22.00
SECONDS
= -10.0 DB
60.0DB
FOR TOP CURVE
SPECTRAL TIME HISTORY PLOT
9000063020: DC-10 S/L HARD 10 M
FREQUENCY, HZ
STANDARD 1/3-OB NUMBER

Figure A-R4

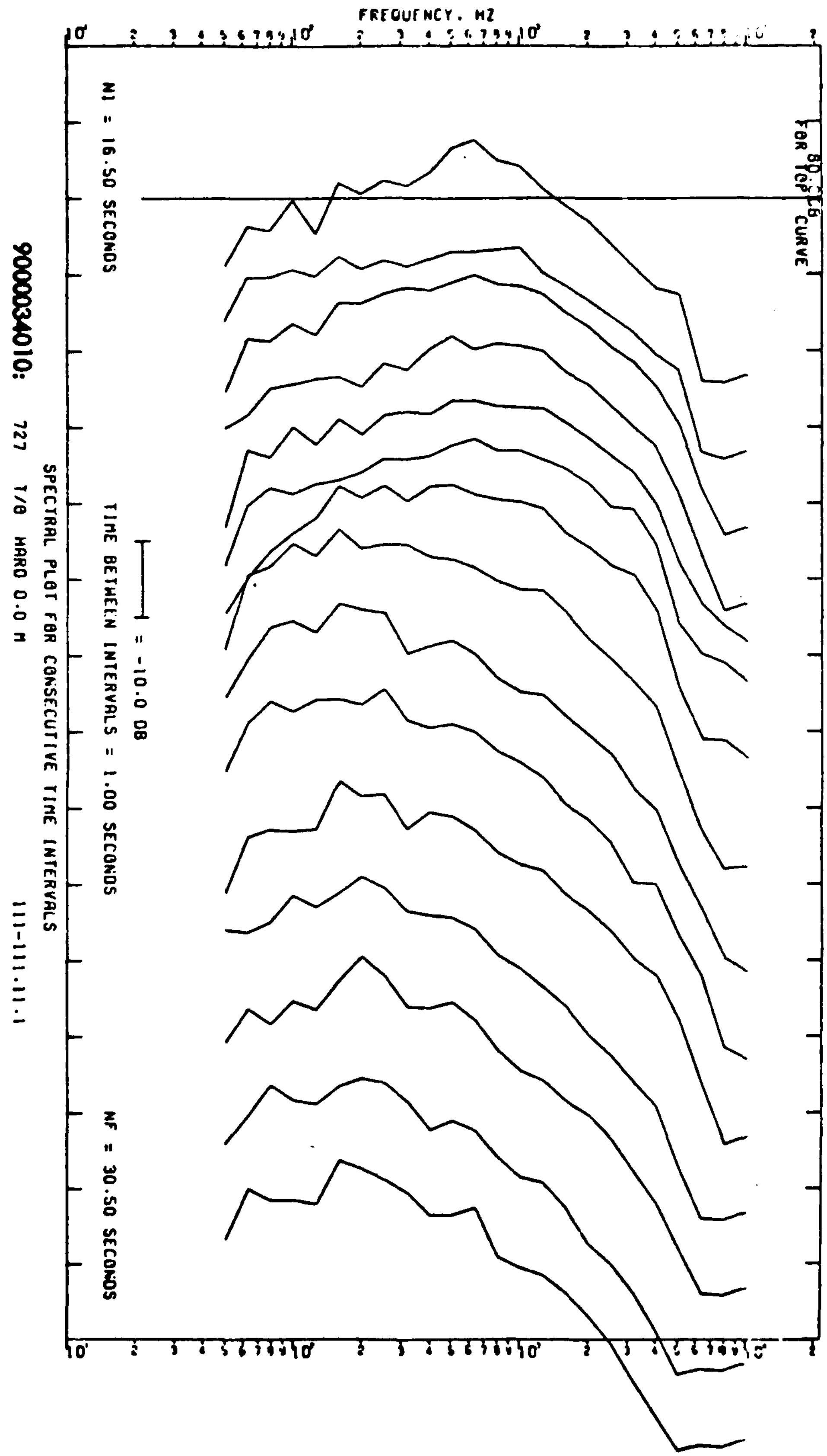
FREQUENCY, HZ
80.0 DB FOR TOP CURVE
NI = 16.50 SECONDS
NF = 30.50 SECONDS
= -10.0 DB
TIME BETWEEN INTERVALS = 1.00 SECONDS
SPECTRAL PLOT FOR CONSECUTIVE TIME INTERVALS
9000034010: 727 T/O HARD 0.0 M
111-111.11.1

Figure A-G1

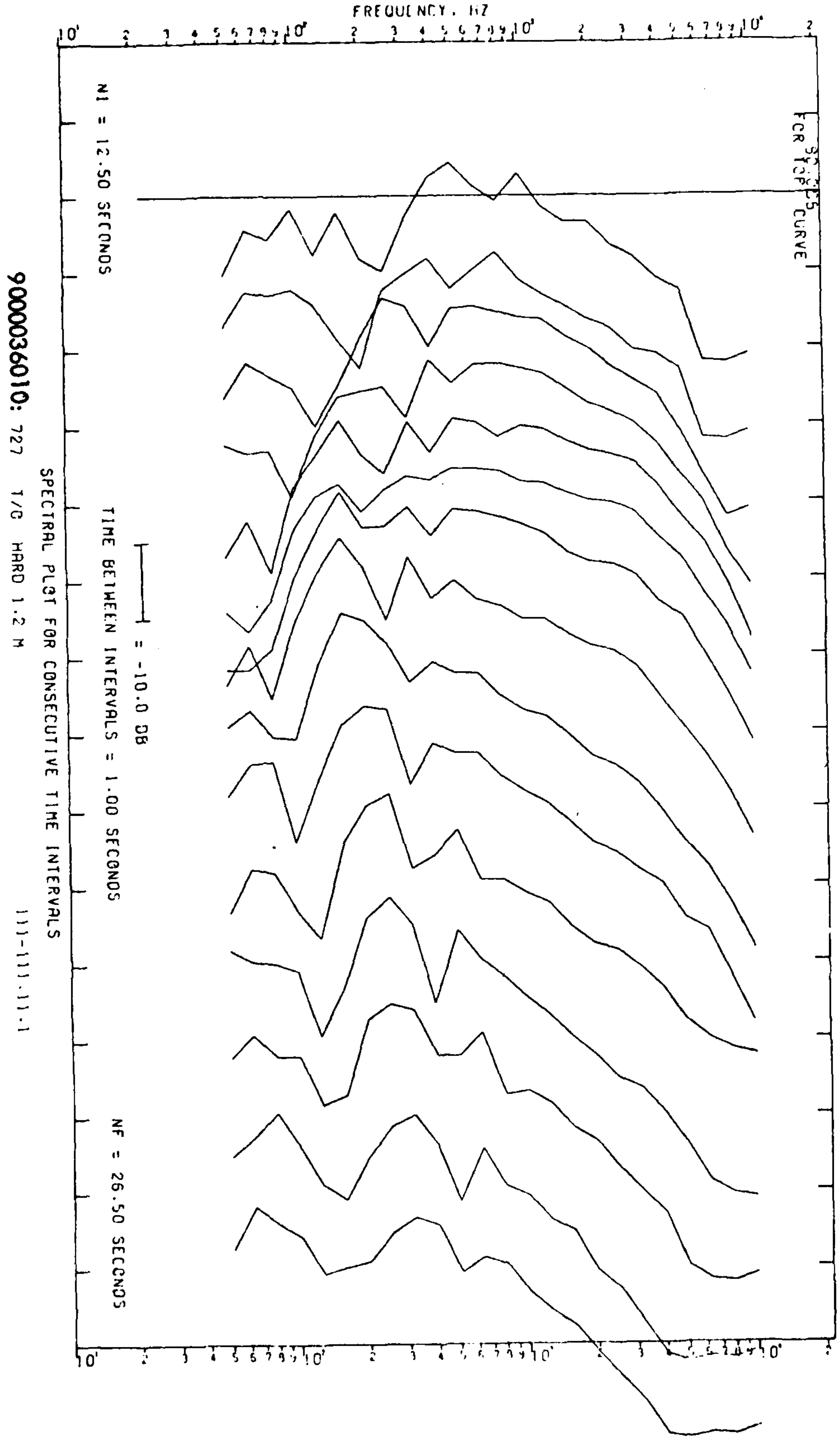
FREQUENCY, HZ
NI = 12.50 SECONDS
FOR TOP CURVE
TIME BETWEEN INTERVALS = 1.00 SECONDS
= -10.0 DB
NF = 26.50 SECONDS
SPECTRAL PLOT FOR CONSECUTIVE TIME INTERVALS
9000036010: 727 T/O HARD 1.2 M

Figure A-G2

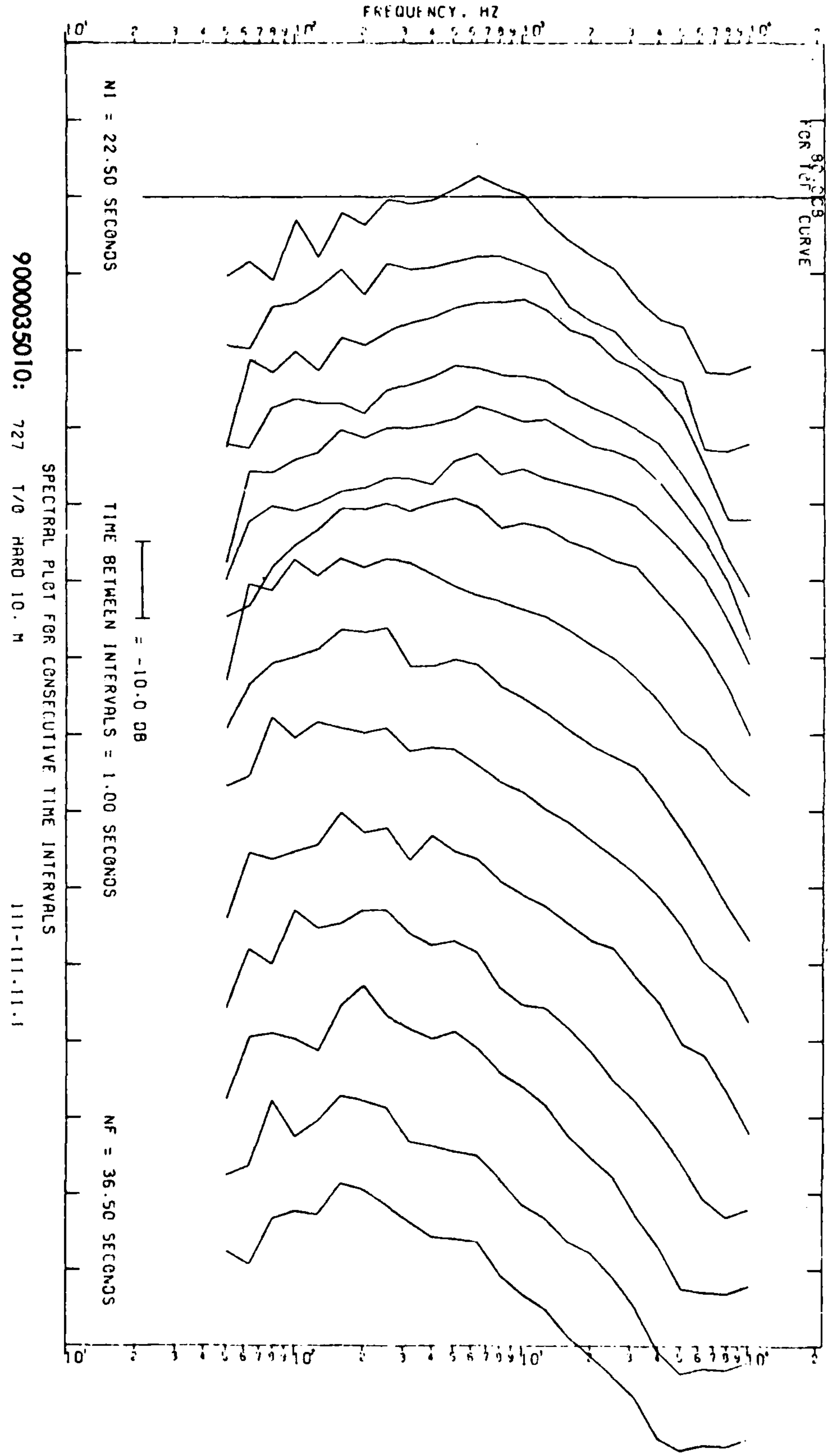
FREQUENCY, HZ
NI = 22.50 SECONDS
TIME BETWEEN INTERVALS = 1.00 SECONDS
= -10.0 DB
NF = 36.50 SECONDS
9000035010: 727 T/O HARD 10. M
SPECTRAL PLOT FOR CONSECUTIVE TIME INTERVALS

Figure A-G3

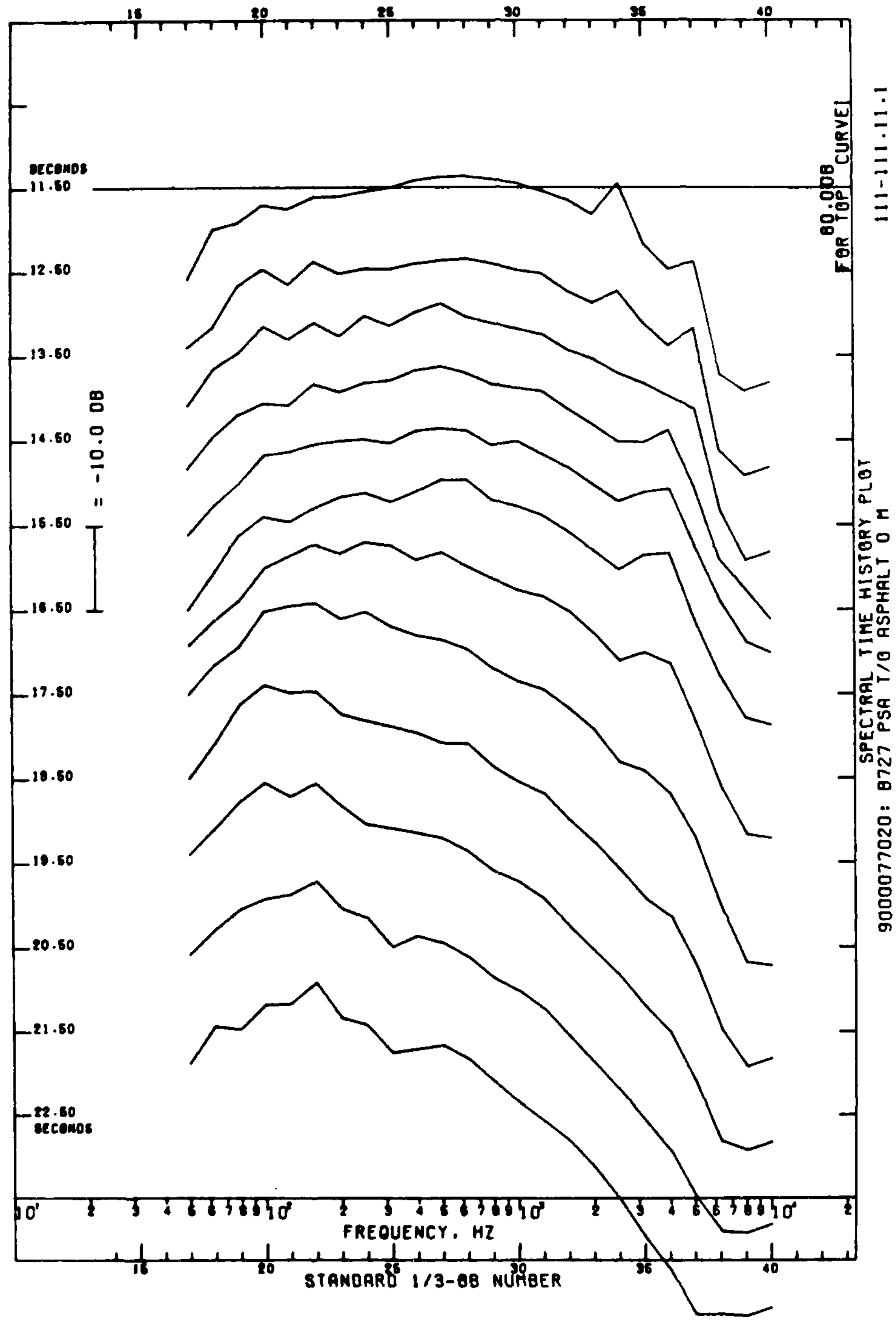

SECONDS
11.50
12.50
13.50
14.50
15.50
16.50
17.50
18.50
19.50
20.50
21.50
22.50
SECONDS
= -10.0 DB
80.0DB
FOR TOP CURVE
111-111.11.1
SPECTRAL TIME HISTORY PLOT
9000077020: B727 PSA T/O ASPHALT 0 M
FREQUENCY, HZ
STANDARD 1/3-OB NUMBER

Figure A-M1

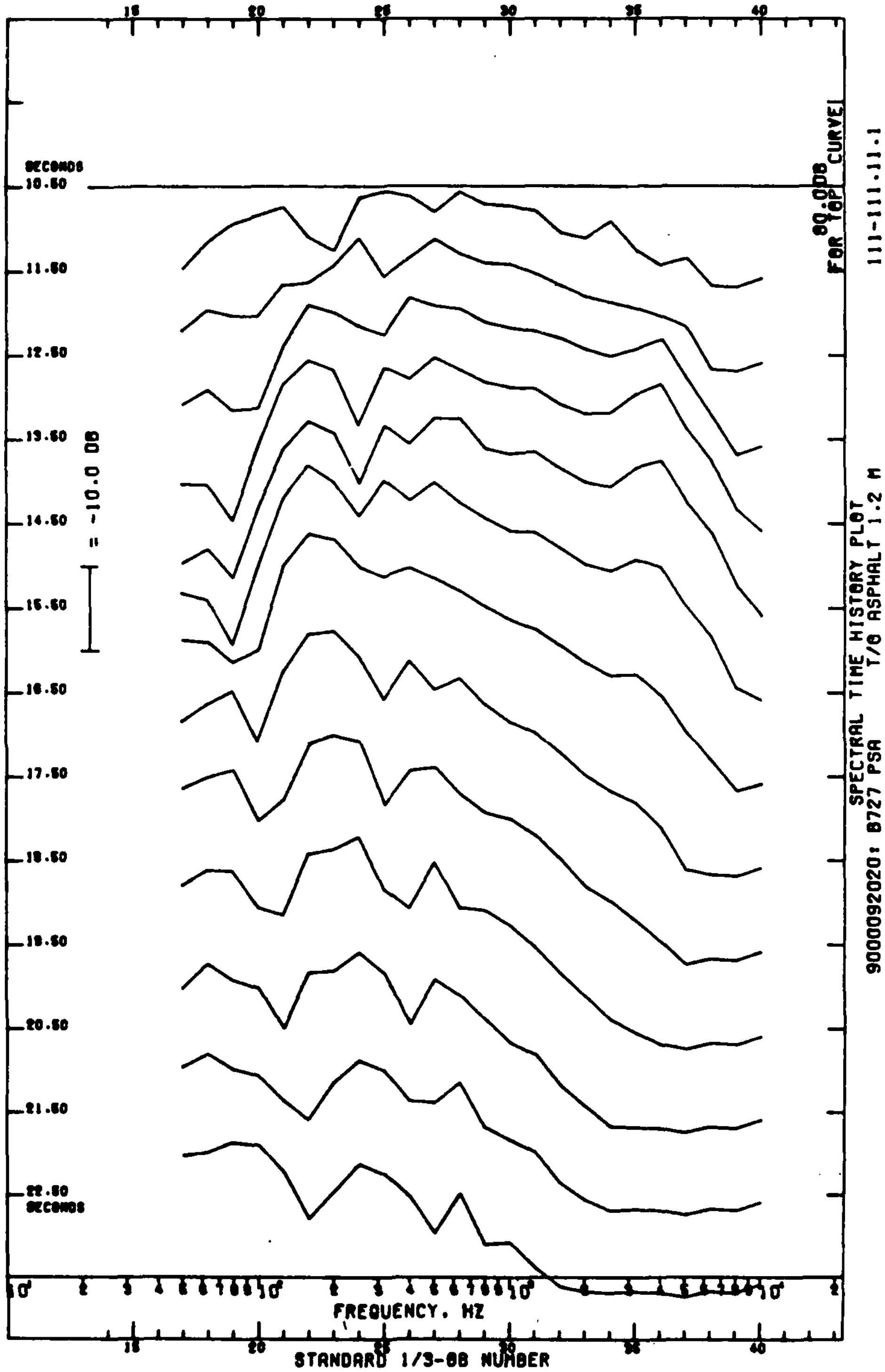
SECONDS
10.50
11.50
12.50
13.50
14.50
15.50
16.50
17.50
18.50
19.50
20.50
21.50
22.50
SECONDS
= -10.0 DB
90.0DB FOR TOP CURVE
111-111.11.1
SPECTRAL TIME HISTORY PLOT
9000092020: B727 PSA T/O ASPHALT 1.2 M
FREQUENCY, HZ
STANDARD 1/3-OB NUMBER

Figure A-M2

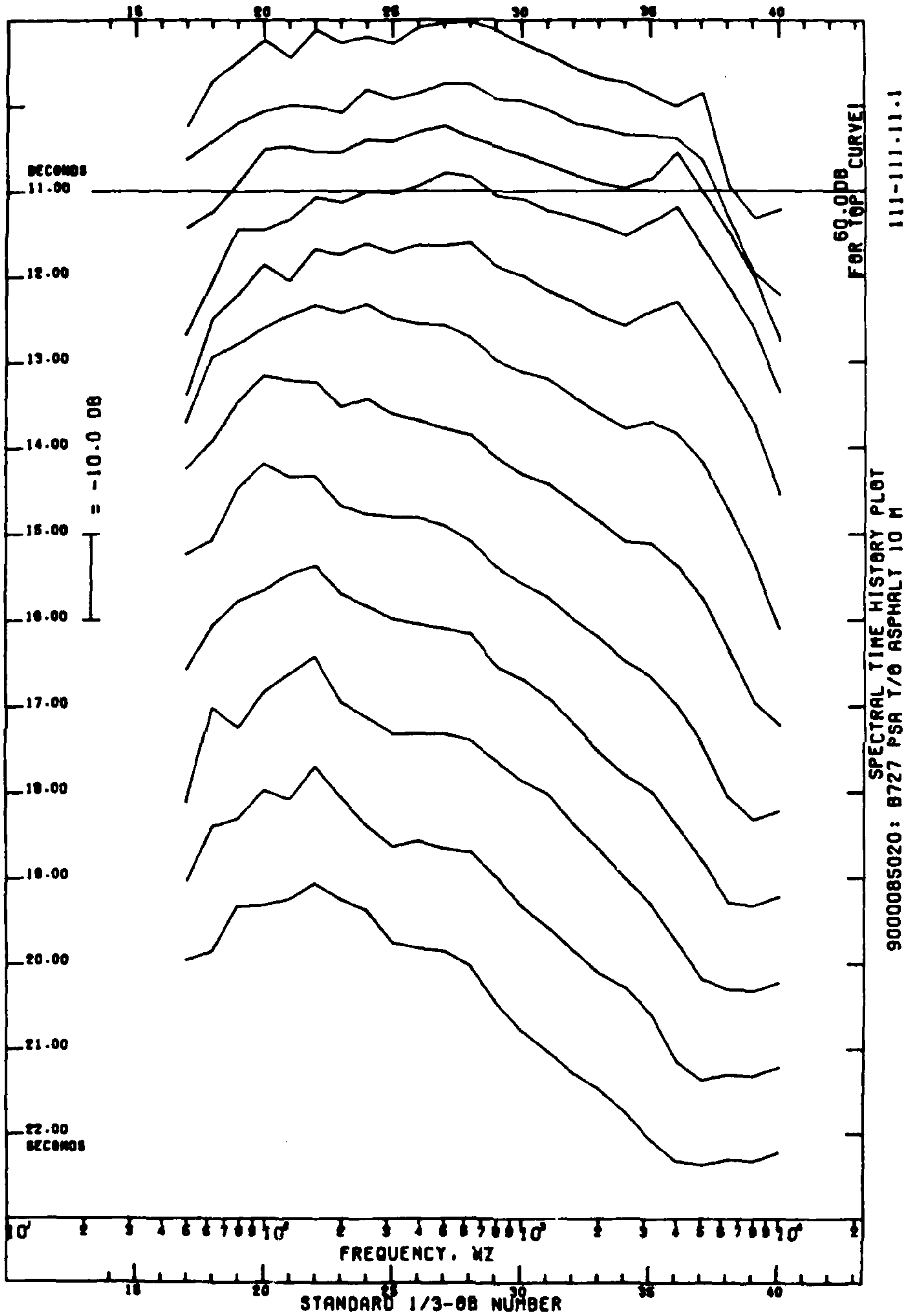
SECONDS
11.00
12.00
13.00
14.00
15.00
16.00
17.00
18.00
19.00
20.00
21.00
22.00
SECONDS
= -10.0 DB
60.0DB
FOR TOP CURVE
111-111-11.1
SPECTRAL TIME HISTORY PLOT
9000085020: B727 PSA T/O ASPHALT 10 M
FREQUENCY, HZ
STANDARD 1/3-OB NUMBER

Figure A-M3

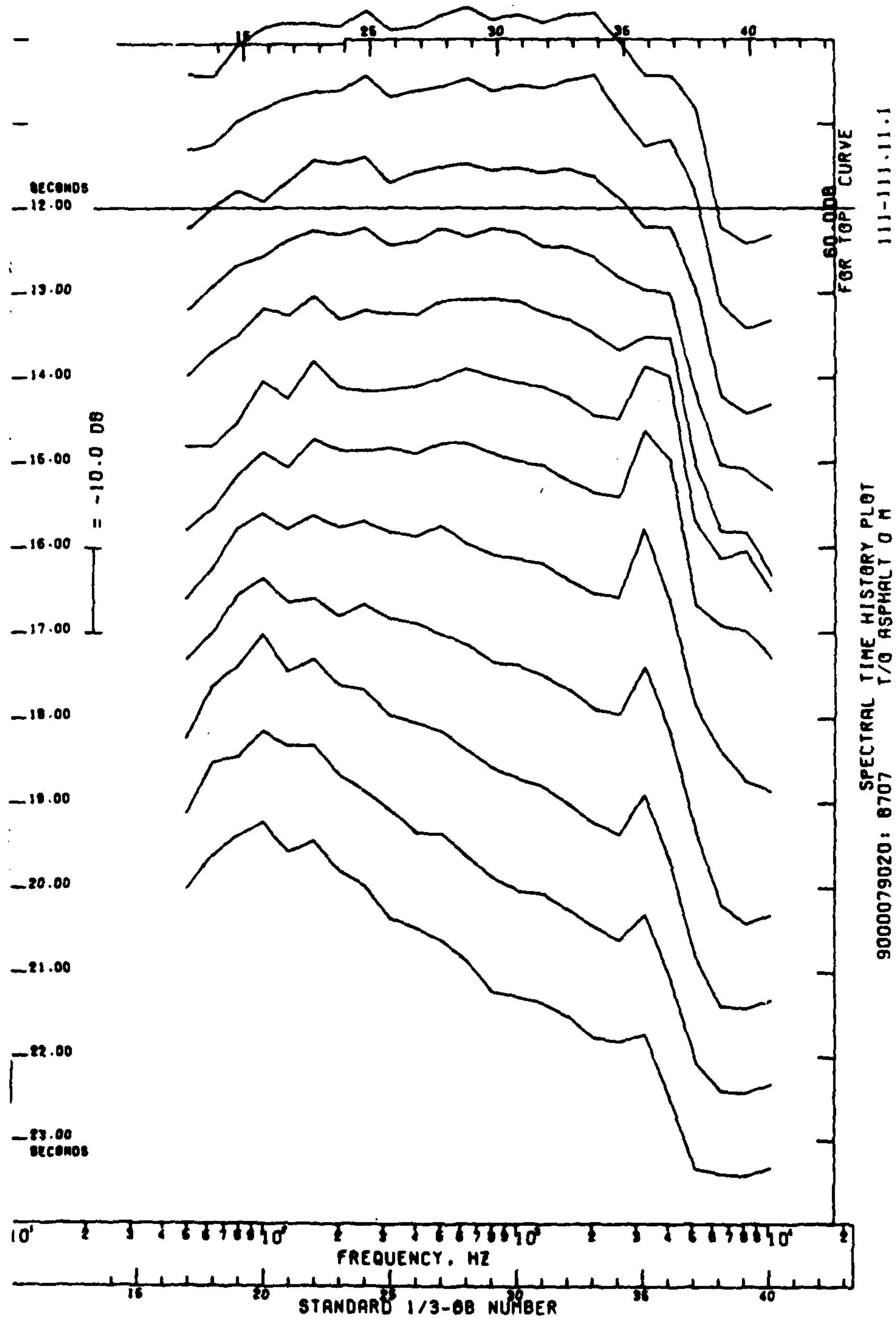
SPECTRAL TIME HISTORY PLOT
9000079020: 8707 T/O ASPHALT O M
60.0DB FOR TOP CURVE
111-111.11.1
= -10.0 DB
SECONDS
12.00
13.00
14.00
15.00
16.00
17.00
18.00
19.00
20.00
21.00
22.00
23.00
SECONDS
FREQUENCY, HZ
STANDARD 1/3-OB NUMBER

Figure A-01

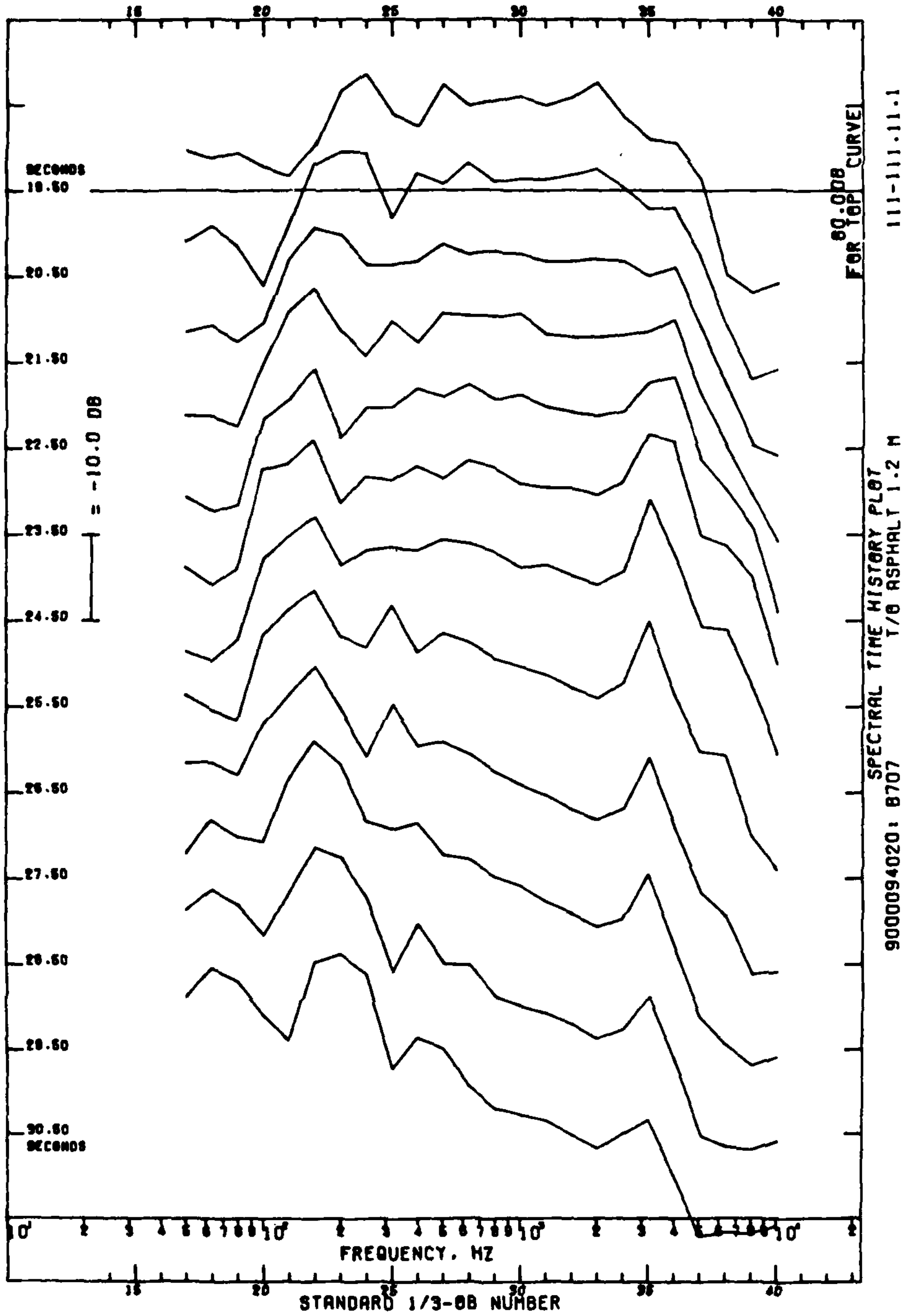
SECONDS
19.50
20.50
21.50
22.50
23.50
24.50
25.50
26.50
27.50
28.50
29.50
30.50
SECONDS
= -10.0 DB
FREQUENCY, HZ
STANDARD 1/3-OB NUMBER
80.0DB
FOR TOP CURVE
111-111.11.1
SPECTRAL TIME HISTORY PLOT
T/8 ASPHALT 1.2 M
900009402O: B707

Figure A-O2

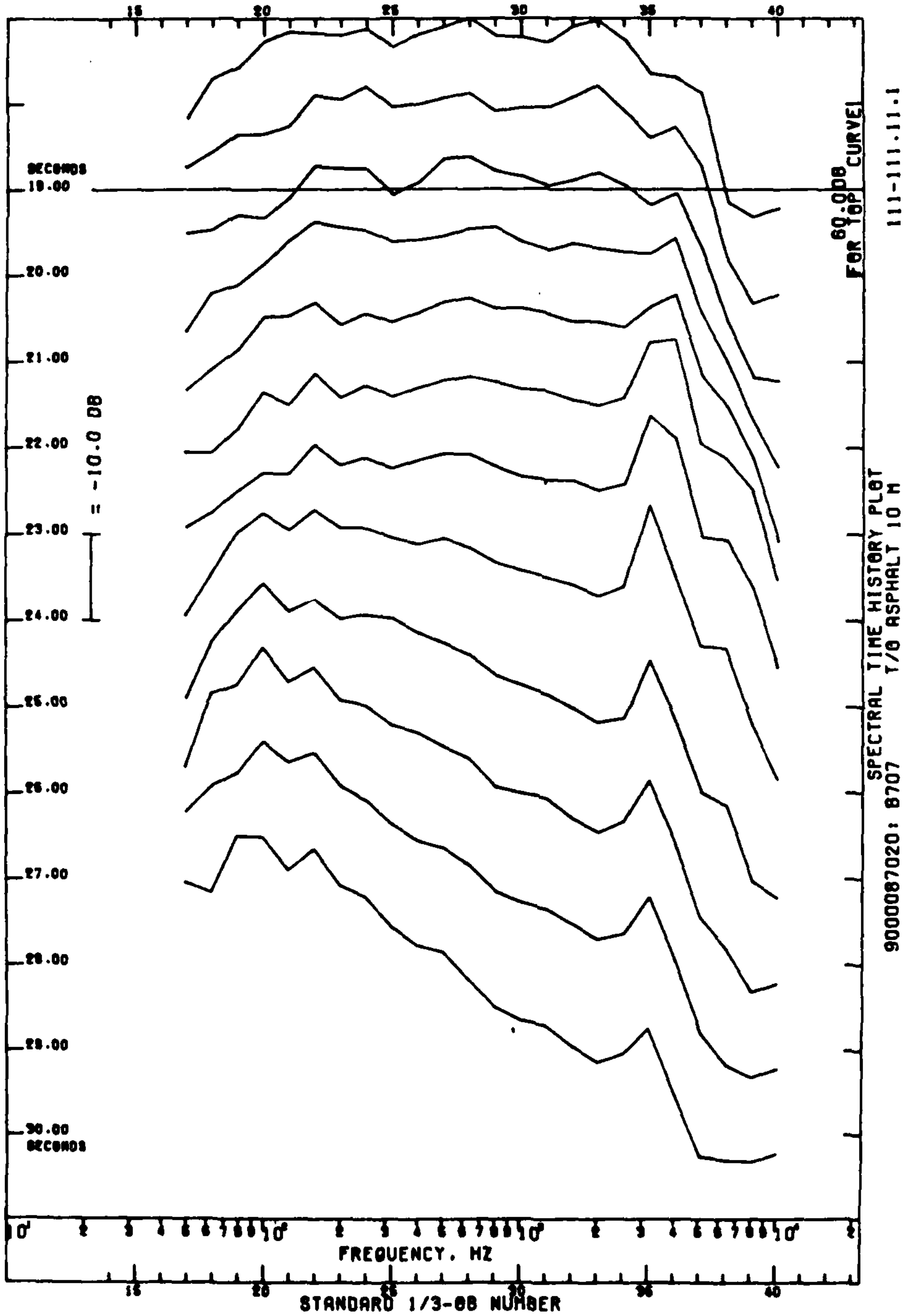
SECONDS
19.00
20.00
21.00
22.00
23.00
24.00
25.00
26.00
27.00
28.00
29.00
30.00
SECONDS
= -10.0 DB
60.0DB
FOR TOP CURVE
SPECTRAL TIME HISTORY PLOT
T/O ASPHALT 10 M
9000087020: B707
FREQUENCY, HZ
STANDARD 1/3-OB NUMBER

Figure A-03

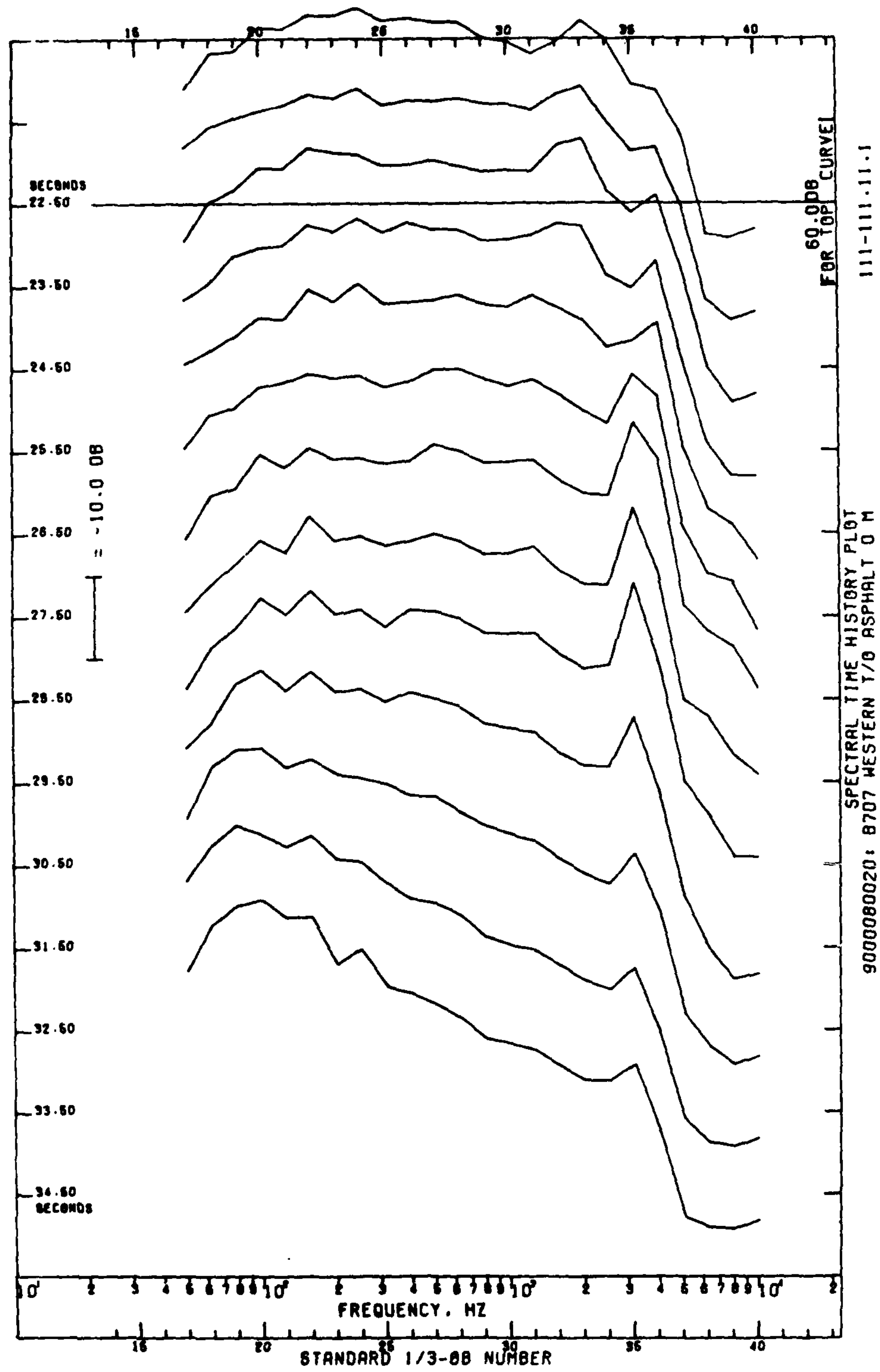

SECONDS
22.60
23.60
24.60
25.60
26.60
27.60
28.60
29.60
30.60
31.60
32.60
33.60
34.60
SECONDS
= -10.0 DB
60.0DB
FOR TOP CURVE
111-111-11.1
SPECTRAL TIME HISTORY PLOT
900080020: B707 WESTERN T/O ASPHALT 0 M
FREQUENCY, HZ
STANDARD 1/3-OB NUMBER

Figure A-P1

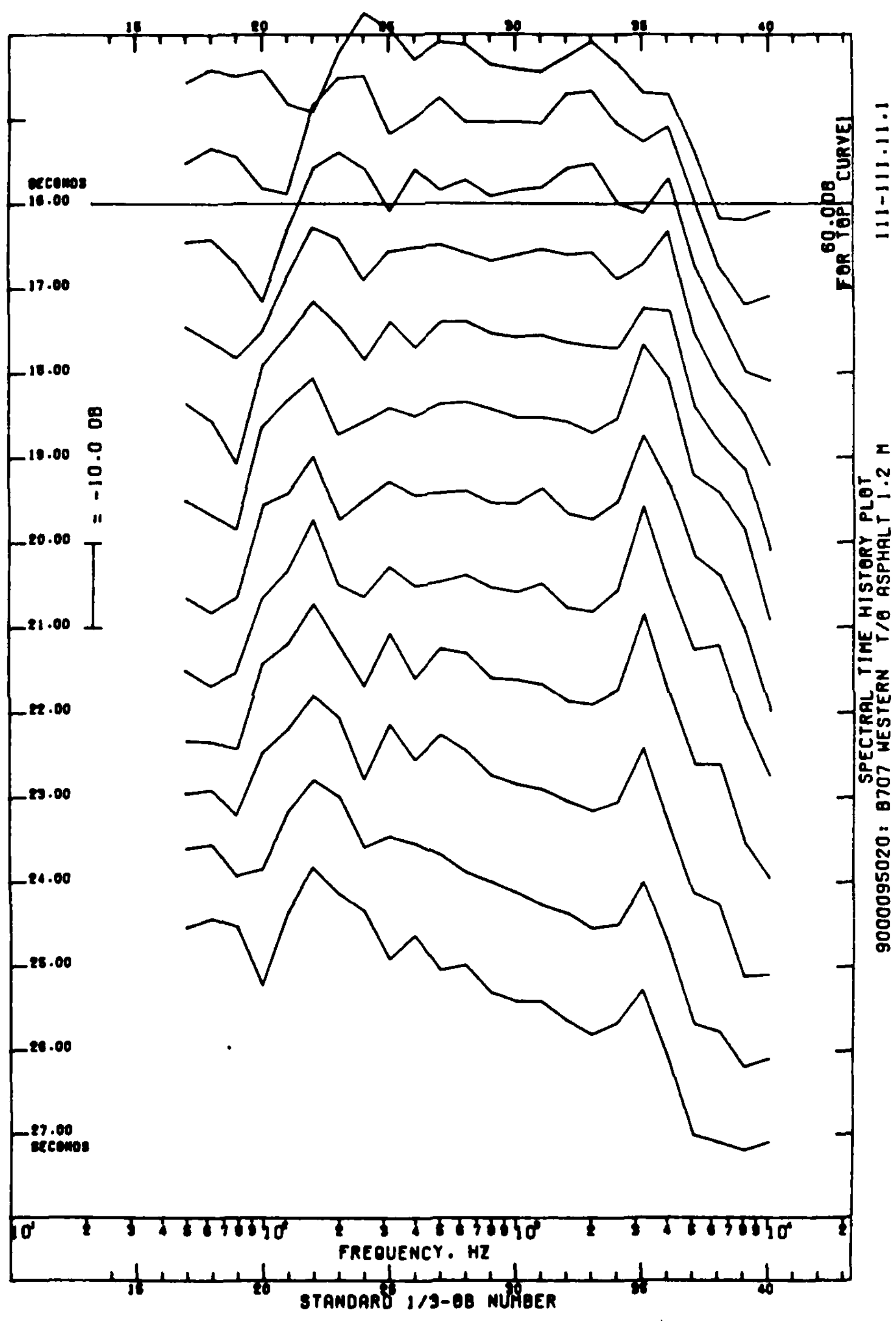
SECONDS
16.00
17.00
18.00
19.00
20.00
21.00
22.00
23.00
24.00
25.00
26.00
27.00
SECONDS
= -10.0 DB
60.0DB
FOR TOP CURVE
111-111.11.1
SPECTRAL TIME HISTORY PLOT
9000095020: B707 WESTERN T/O ASPHALT 1.2 M
FREQUENCY, HZ
STANDARD 1/3-OB NUMBER

Figure A-P2

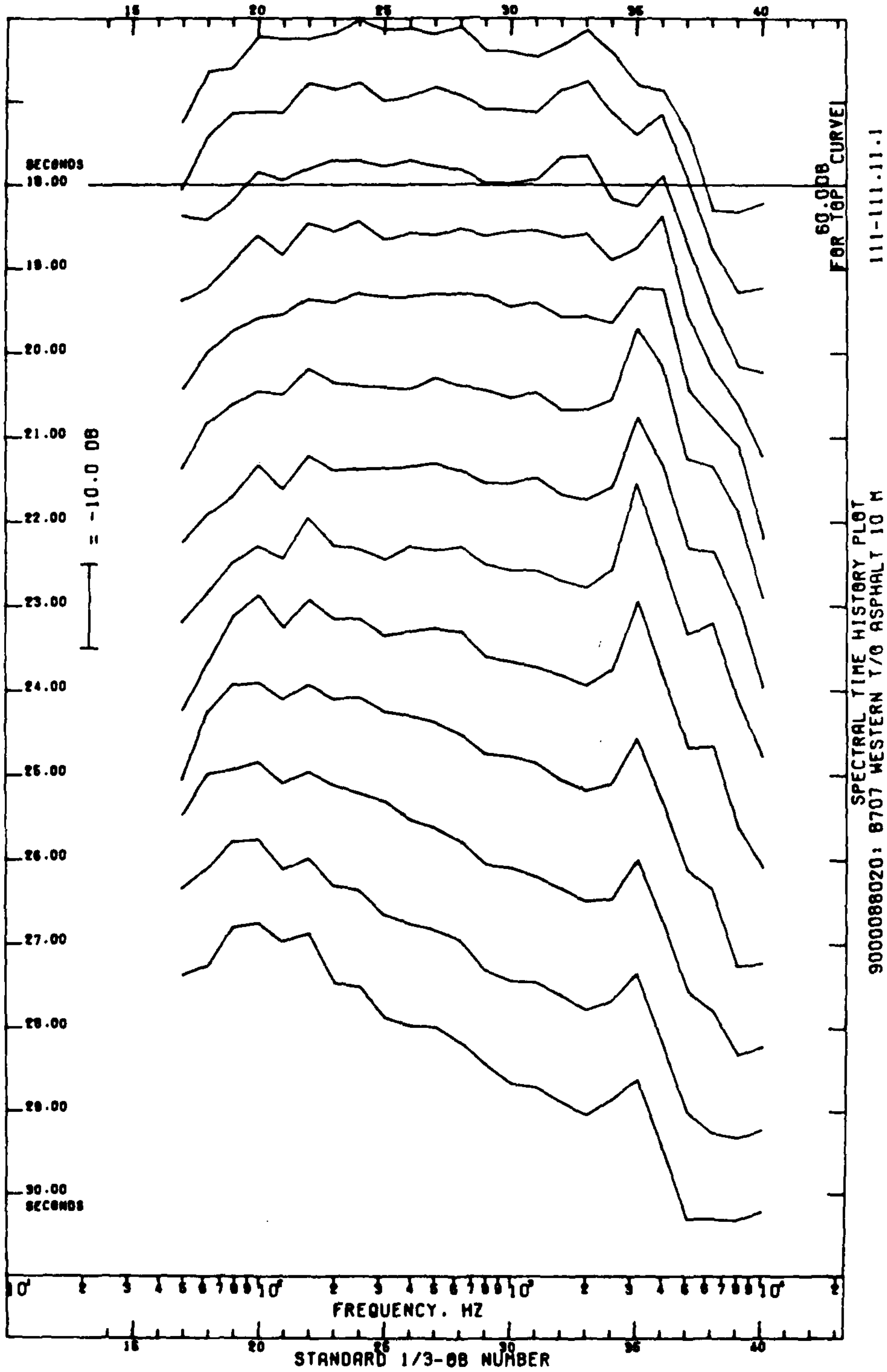

SECONDS
18.00
19.00
20.00
21.00
22.00
23.00
24.00
25.00
26.00
27.00
28.00
29.00
30.00
SECONDS
= -10.0 DB
60.0DB FOR TOP CURVE
111-111.11.1
SPECTRAL TIME HISTORY PLOT
9000088020; B707 WESTERN T/O ASPHALT 10 M
FREQUENCY, HZ
STANDARD 1/3-OB NUMBER

Figure A-P3

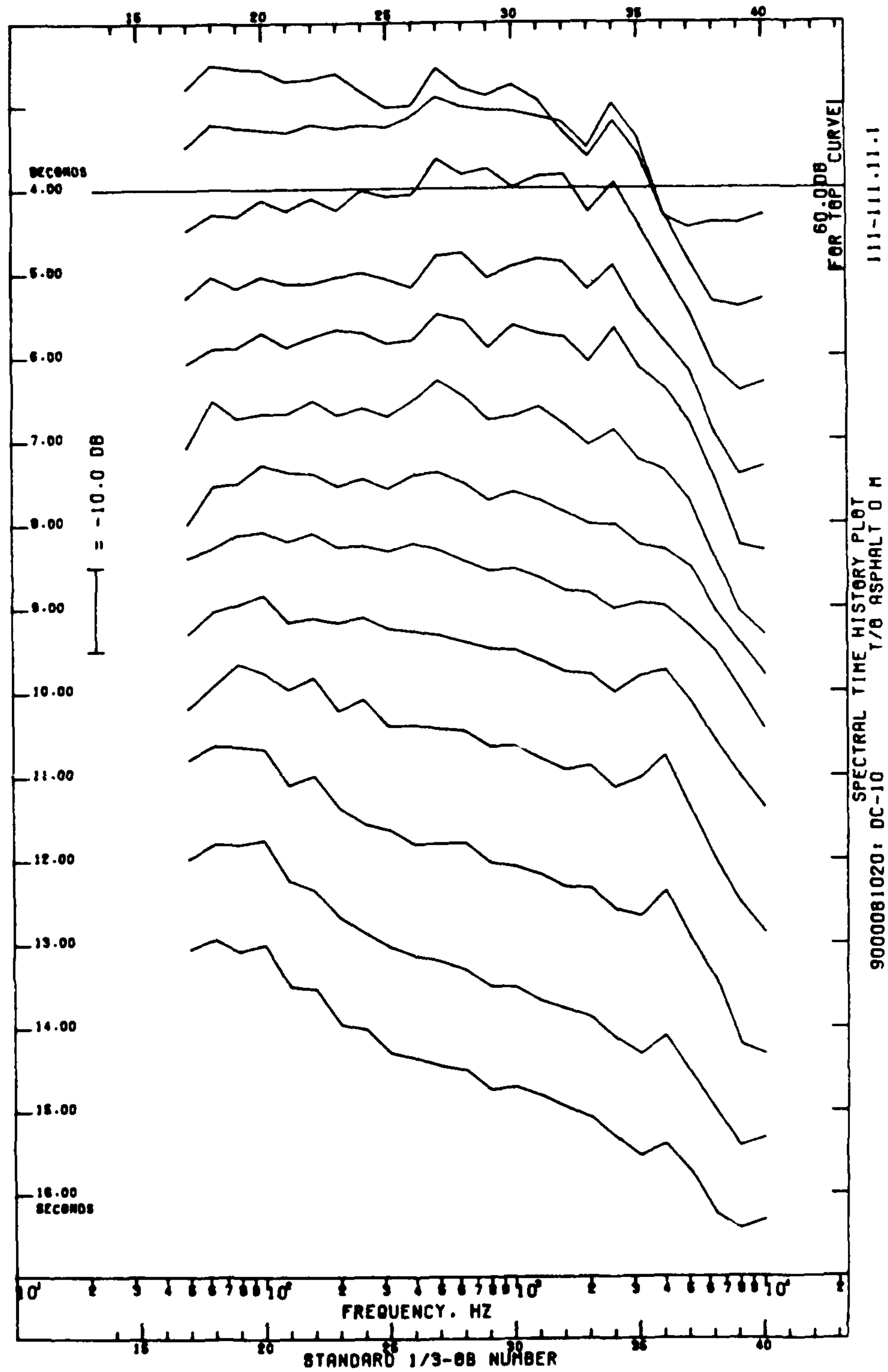
SPECTRAL TIME HISTORY PLOT
900081020: DC-10 T/B ASPHALT 0 M
60.0DB FOR TOP CURVE
111-111.11.1
SECONDS
= -10.0 DB
FREQUENCY, HZ
STANDARD 1/3-OB NUMBER

Figure A-S1

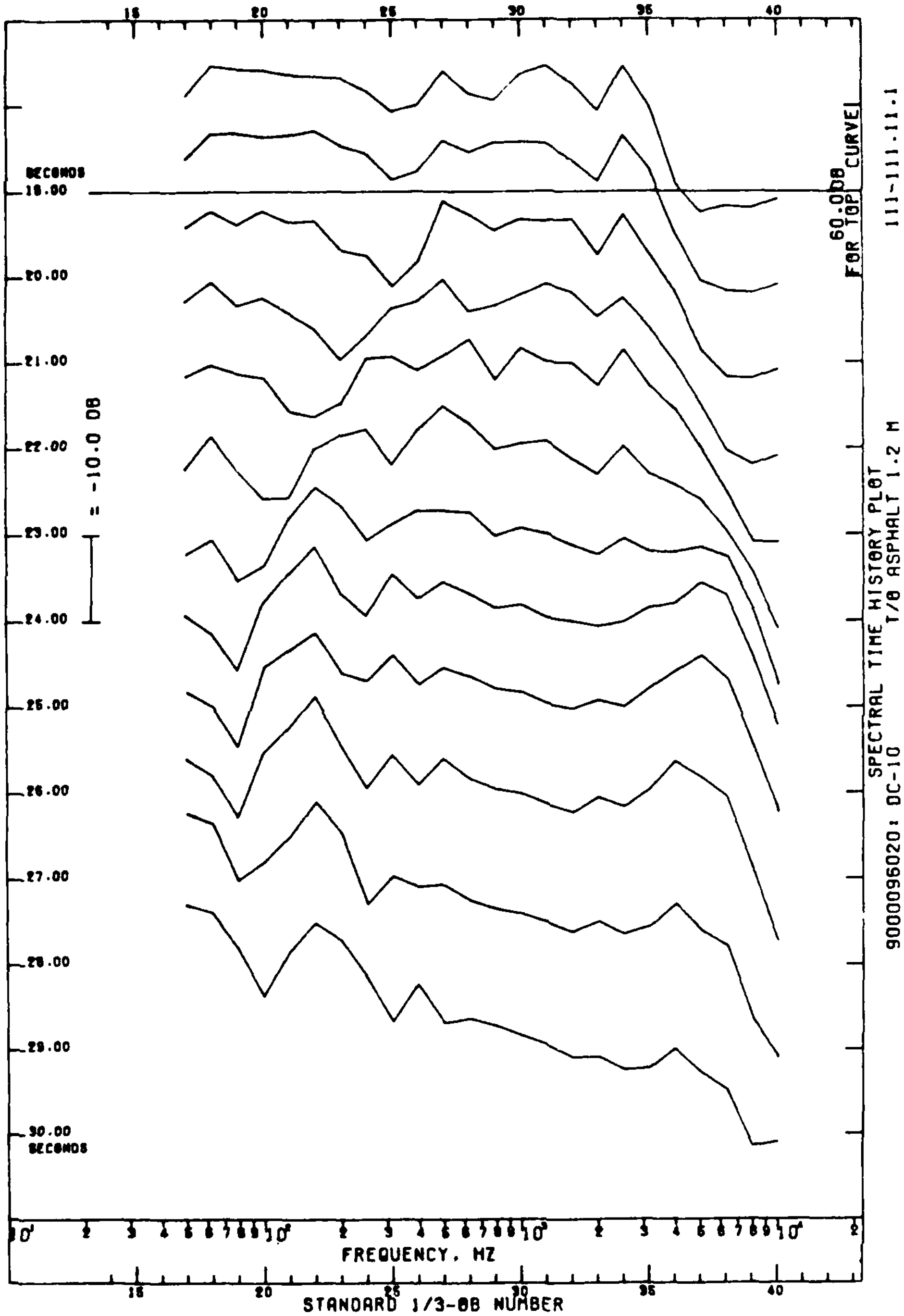
SPECTRAL TIME HISTORY PLOT
9000096020: DC-10
60.0DB
FOR TOP CURVE
= -10.0 DB
SECONDS
FREQUENCY, HZ
STANDARD 1/3-OB NUMBER

Figure A-S2

AD-A081 962 WYLE LABS EL SEGUNDO CALIF F/G 20/1
CORRECTION PROCEDURES FOR AIRCRAFT NOISE DATA. VOLUME I. PSEUDO--ETC(U)
DEC 79 R RACKL DOT-FA78WA-4143
UNCLASSIFIED WR-79-9-VOL-1 FAA/EE-80-1-VOL-1 NL

3 OF 3
AD
A081 962

END
DATE
FILMED
4-80
DTIC

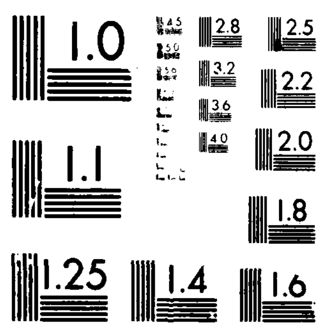

MICROCOPY RESOLUTION TEST CHART
NATIONAL BUREAU OF STANDARDS-1963-A

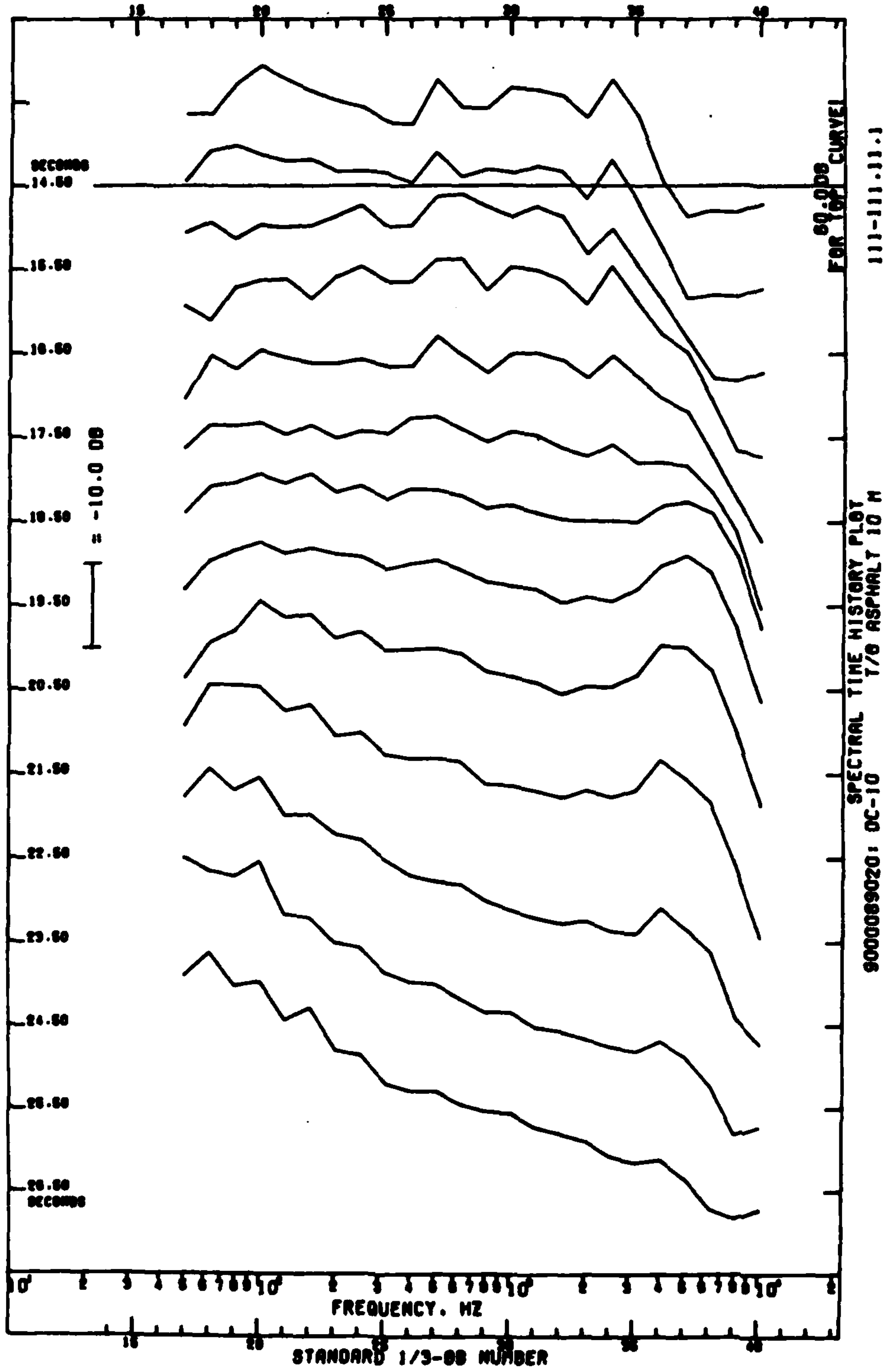

SECONDS
14.50
15.50
16.50
17.50
18.50
19.50
20.50
21.50
22.50
23.50
24.50
25.50
26.50
SECONDS
= -10.0 DB
60.0DB FOR TOP CURVE
SPECTRAL TIME HISTORY PLOT
900008902O: DC-10 T/O ASPHALT 10 M
FREQUENCY, HZ
STANDARD 1/3-OB NUMBER

Figure A-53

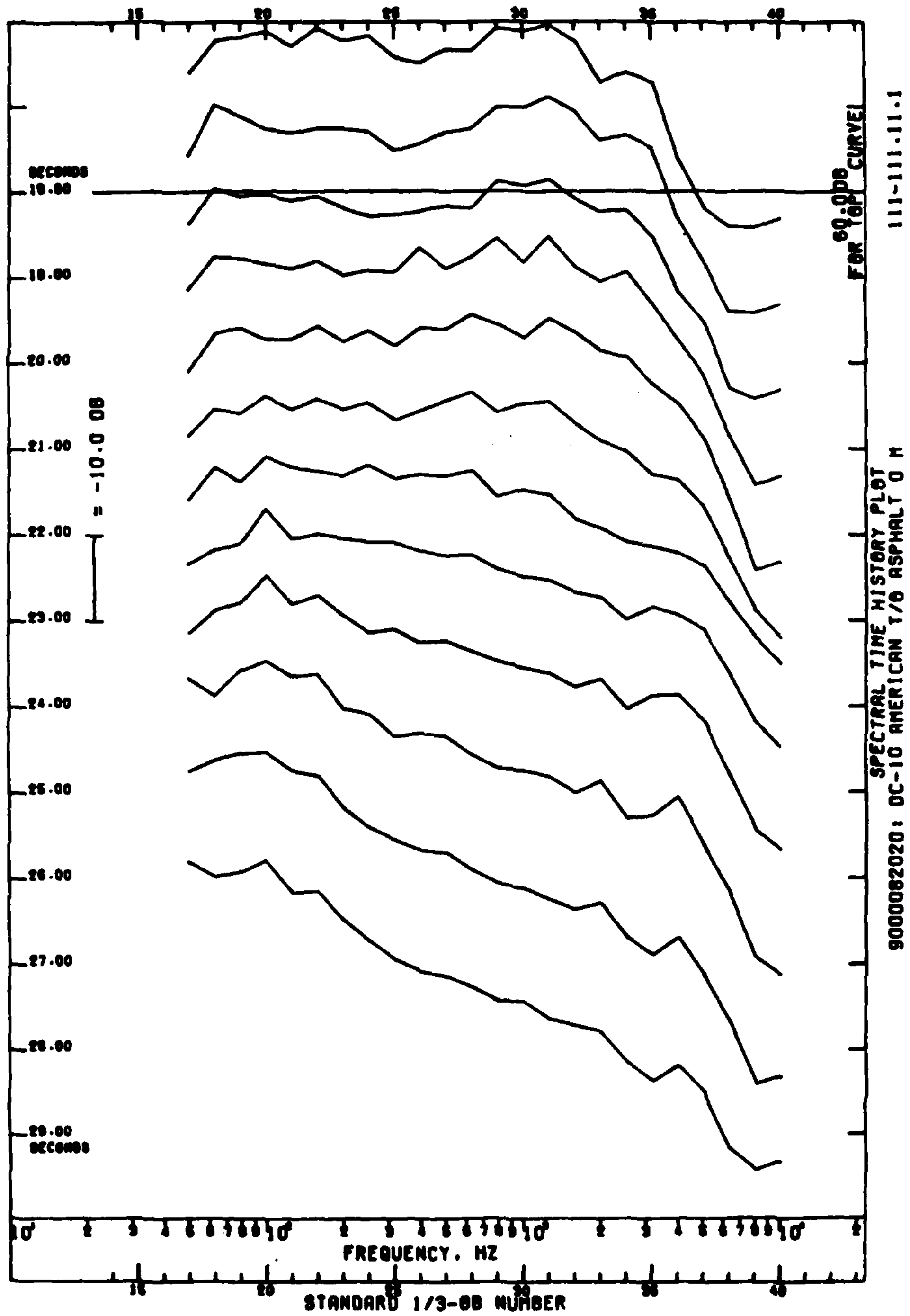
SPECTRAL TIME HISTORY PLOT
9000082020: DC-10 AMERICAN T/O ASPHALT 0 M
60.0DB FOR TOP CURVE
111-111.11-1
SECONDS
19.00
20.00
21.00
22.00
23.00
24.00
25.00
26.00
27.00
28.00
29.00
SECONDS
= -10.0 DB
FREQUENCY, HZ
STANDARD 1/3-OB NUMBER

Figure A-T1

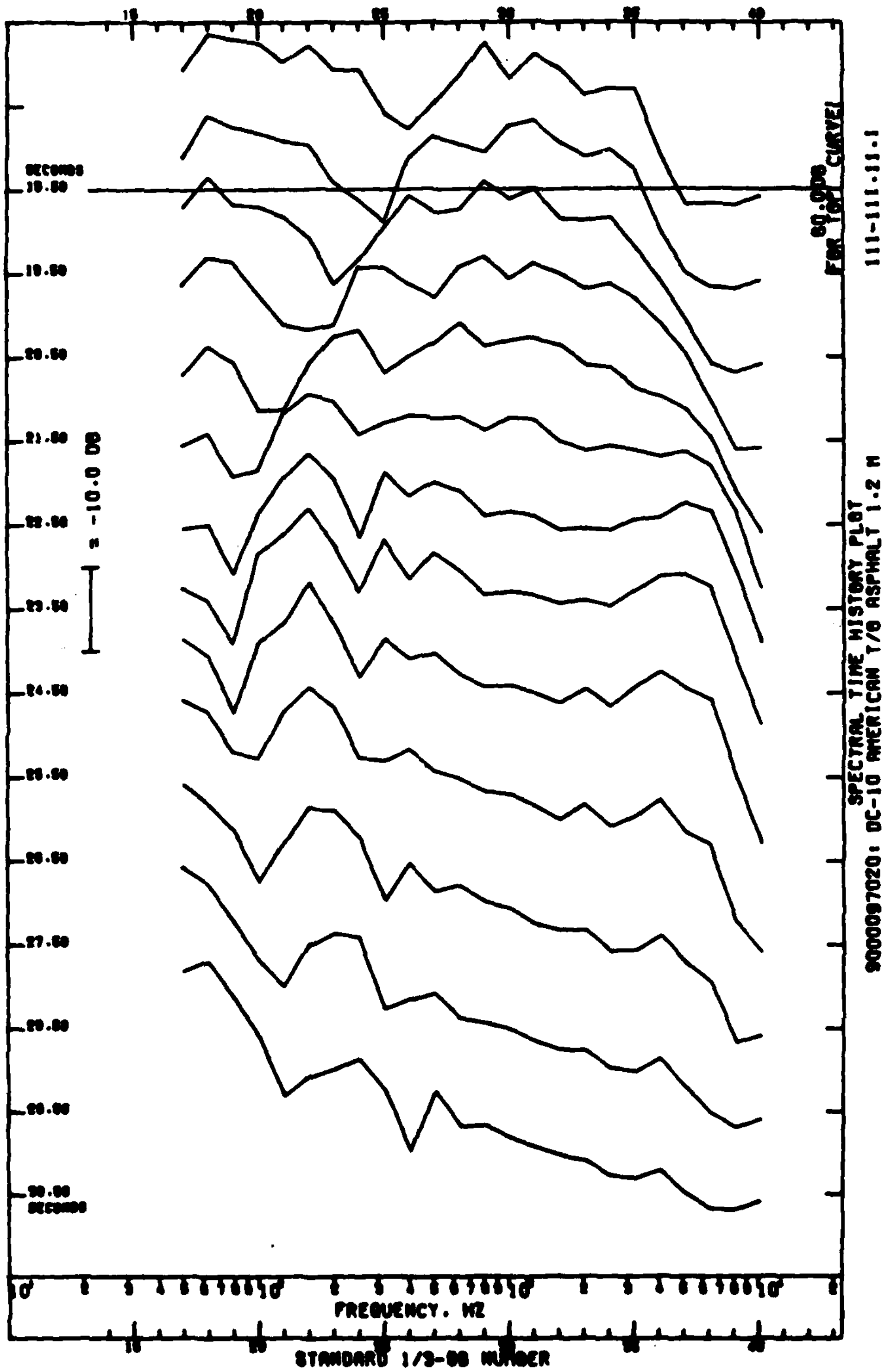
SPECTRAL TIME HISTORY PLOT
DC-10 AMERICAN T/O ASPHALT 1.2 M
90.0DB FOR TOP CURVE
= -10.0 DB
SECONDS
FREQUENCY, HZ
STANDARD 1/3-OB NUMBER

Figure A-T2

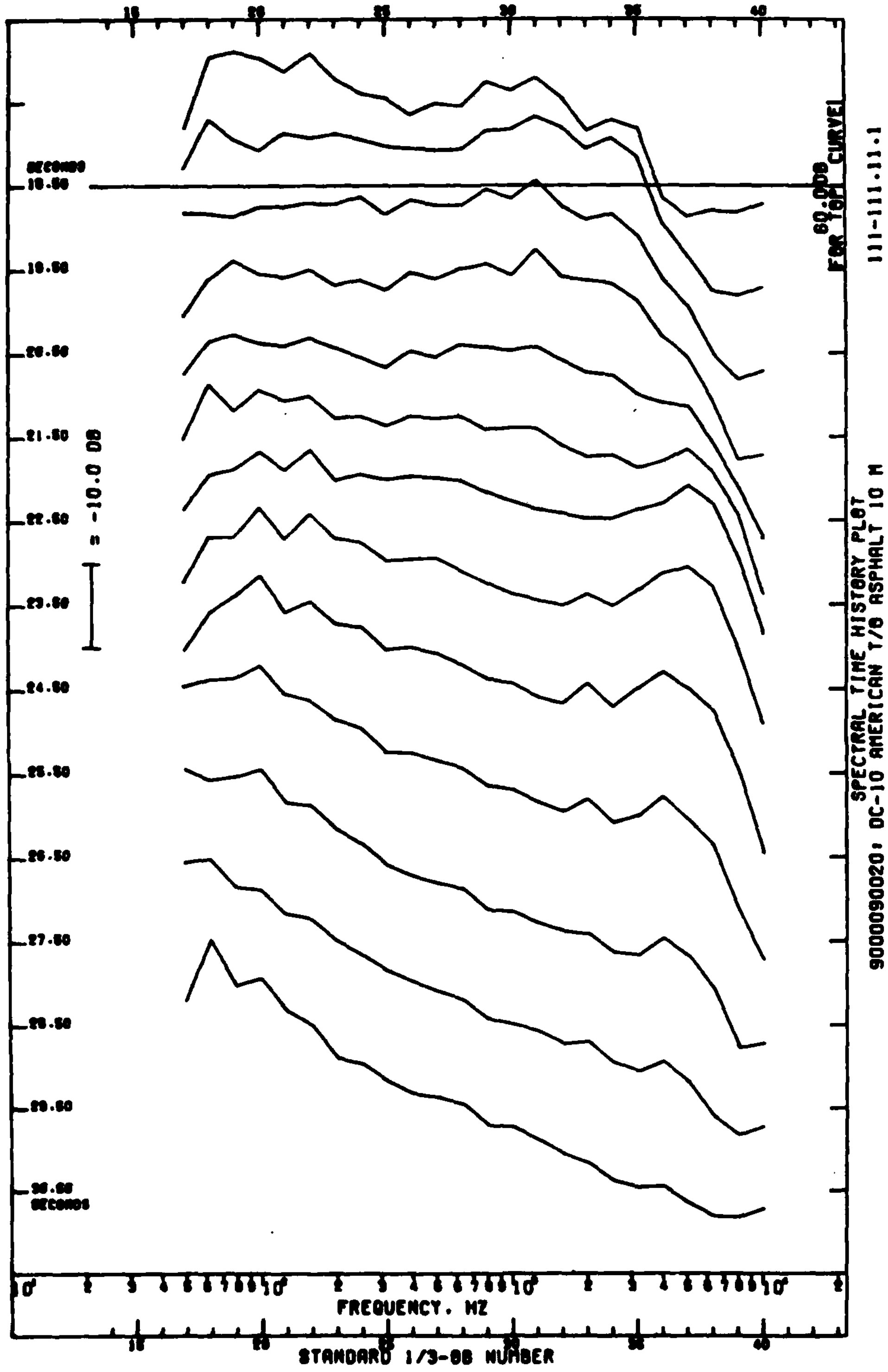
SPECTRAL TIME HISTORY PLOT
9000090020, DC-10 AMERICAN T/O ASPHALT 10 M
111-111-11-1
60.0DB FOR TOP CURVE)
= -10.0 DB
SECONDS
SECONDS
FREQUENCY, HZ
STANDARD 1/3-OB NUMBER

Figure A-T3

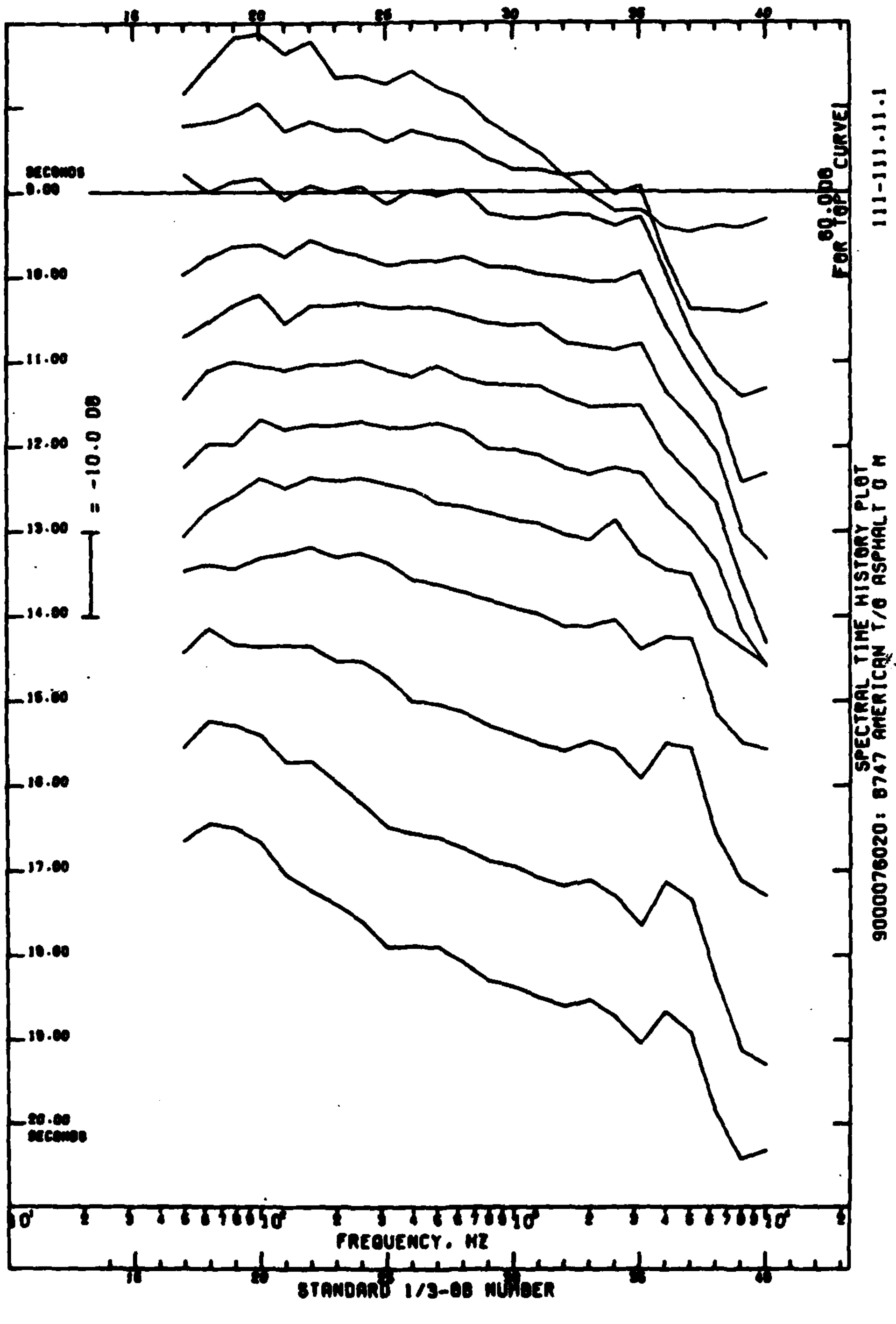

SECONDS
9.00
10.00
11.00
12.00
13.00
14.00
15.00
16.00
17.00
18.00
19.00
20.00
SECONDS
= -10.0 DB
60.0DB
FOR TOP CURVE)
SPECTRAL TIME HISTORY PLOT
9000076020: B747 AMERICAN T/O ASPHALT 0 M
111-111-11-1
FREQUENCY, HZ
STANDARD 1/3-OB NUMBER

Figure A-U1

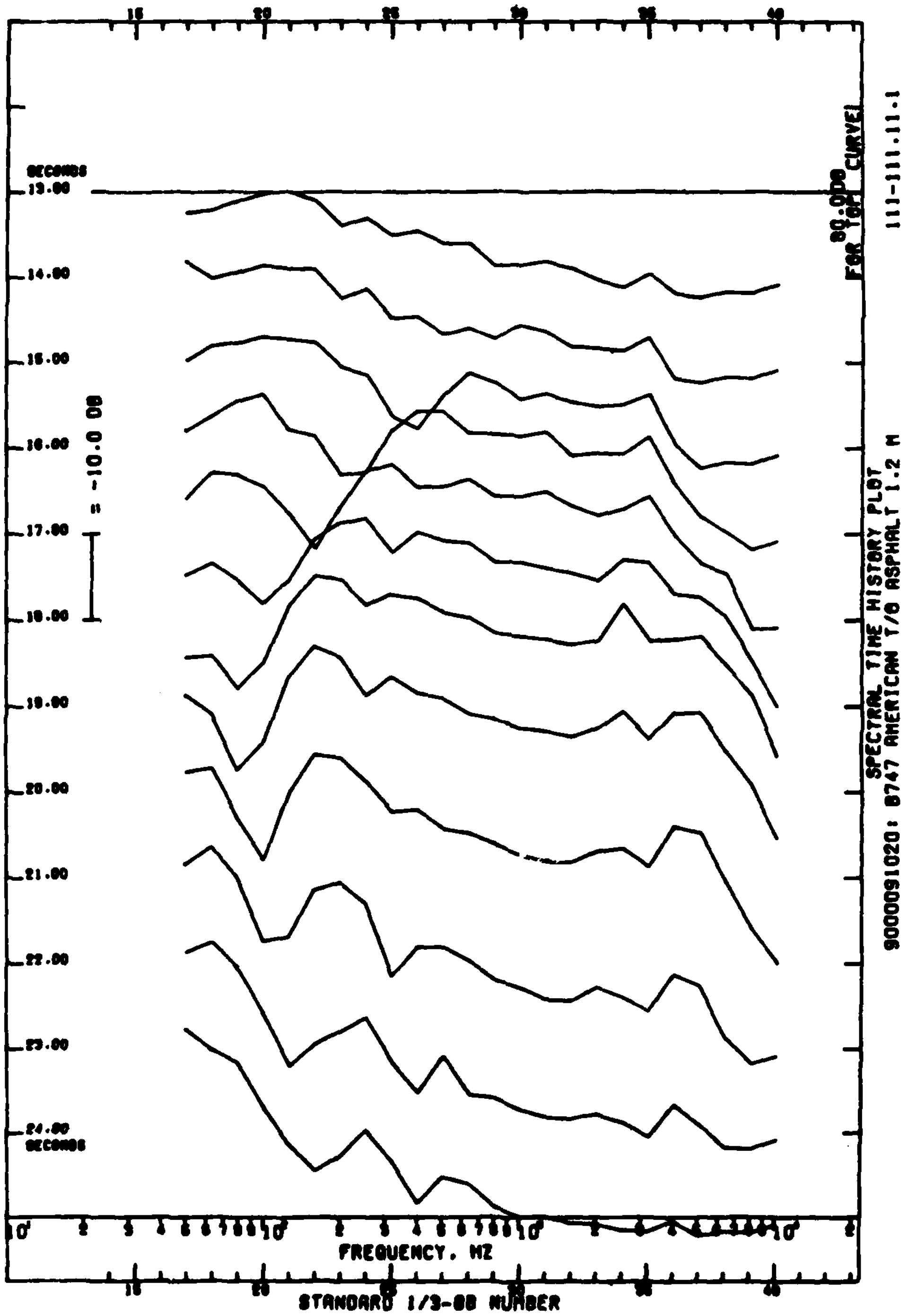
SECONDS
13.00
14.00
15.00
16.00
17.00
18.00
19.00
20.00
21.00
22.00
23.00
24.00
SECONDS
= -10.0 DB
80.0DB
FOR TOP CURVE)
111-111.11.1
SPECTRAL TIME HISTORY PLOT
9000091020: B747 AMERICAN T/O ASPHALT 1.2 M
FREQUENCY, HZ
STANDARD 1/3-OB NUMBER

Figure A-U2

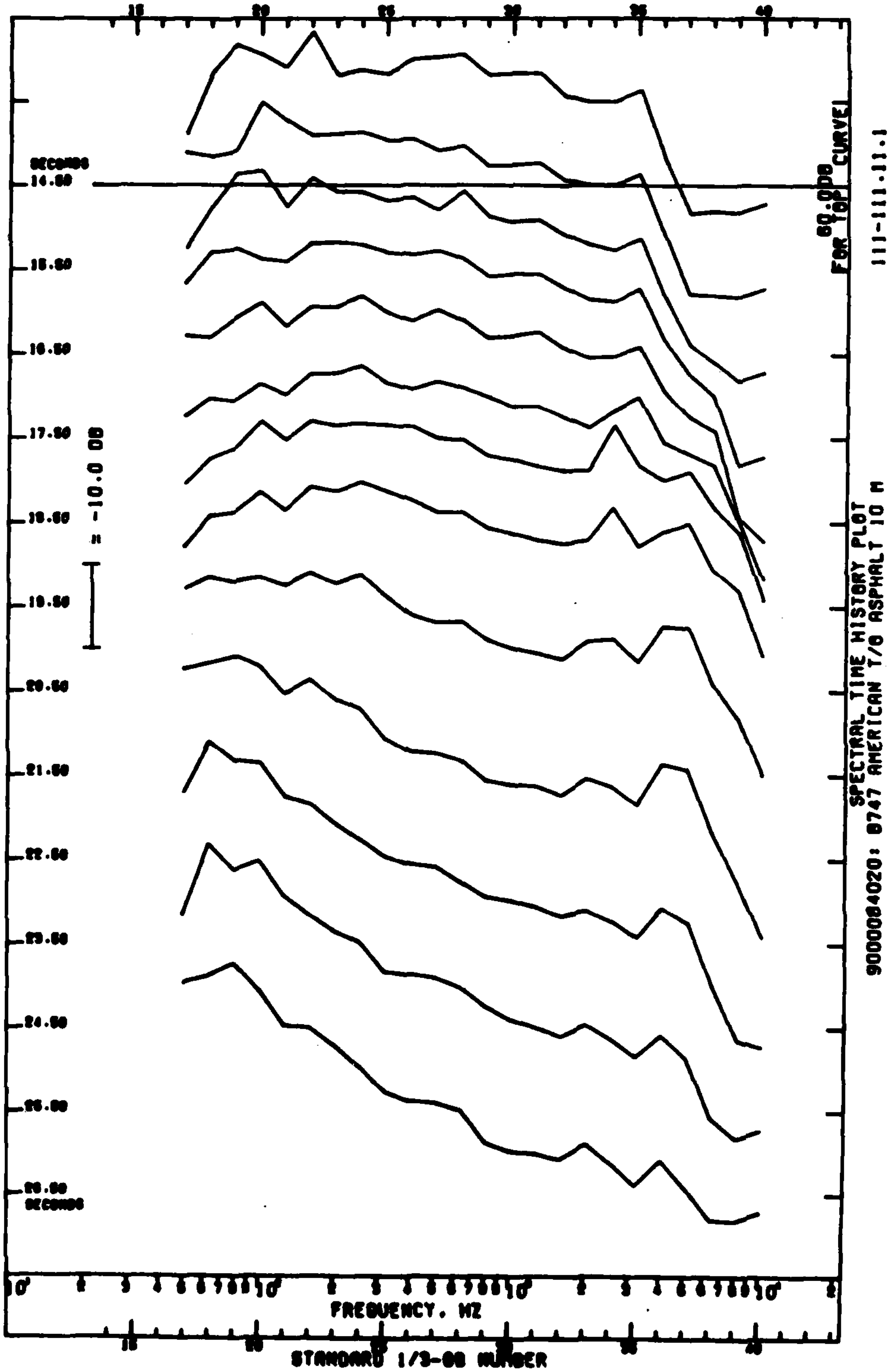

SECONDS
14.50
15.50
16.50
17.50
18.50
19.50
20.50
21.50
22.50
23.50
24.50
25.50
26.50
SECONDS
= -10.0 DB
60.0DB FOR TOP CURVE)
SPECTRAL TIME HISTORY PLOT
9000084020: B747 AMERICAN T/O ASPHALT 10 M
FREQUENCY, HZ
STANDARD 1/3-OB NUMBER

Figure A-U3

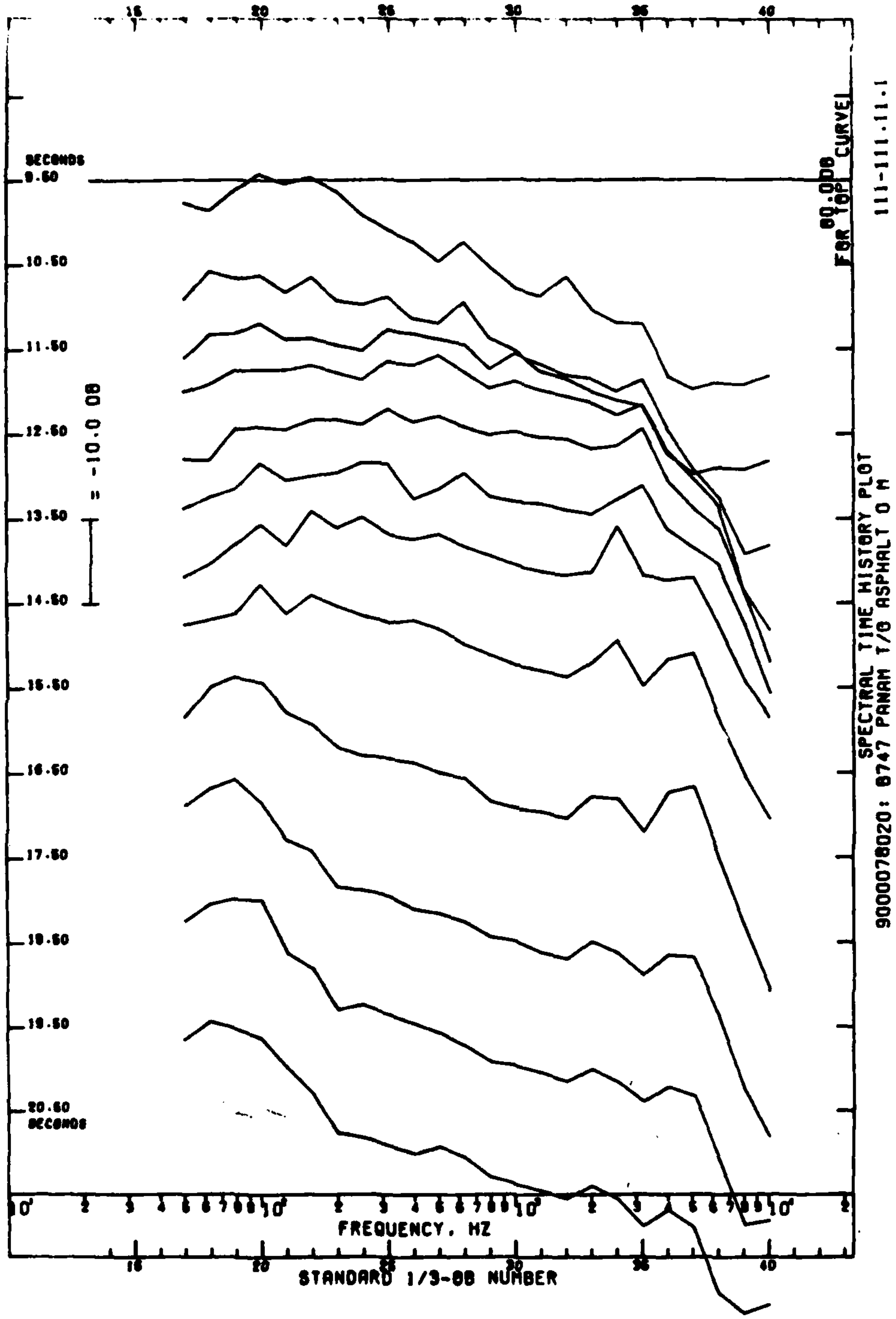
SECONDS
9.50
10.50
11.50
12.50
13.50
14.50
15.50
16.50
17.50
18.50
19.50
20.50
SECONDS
= -10.0 DB
80.0DB
FOR TOP CURVE
111-111.11.1
SPECTRAL TIME HISTORY PLOT
9000078020: B747 PANAM T/O ASPHALT 0 M
FREQUENCY, HZ
STANDARD 1/3-OB NUMBER

Figure A-V1

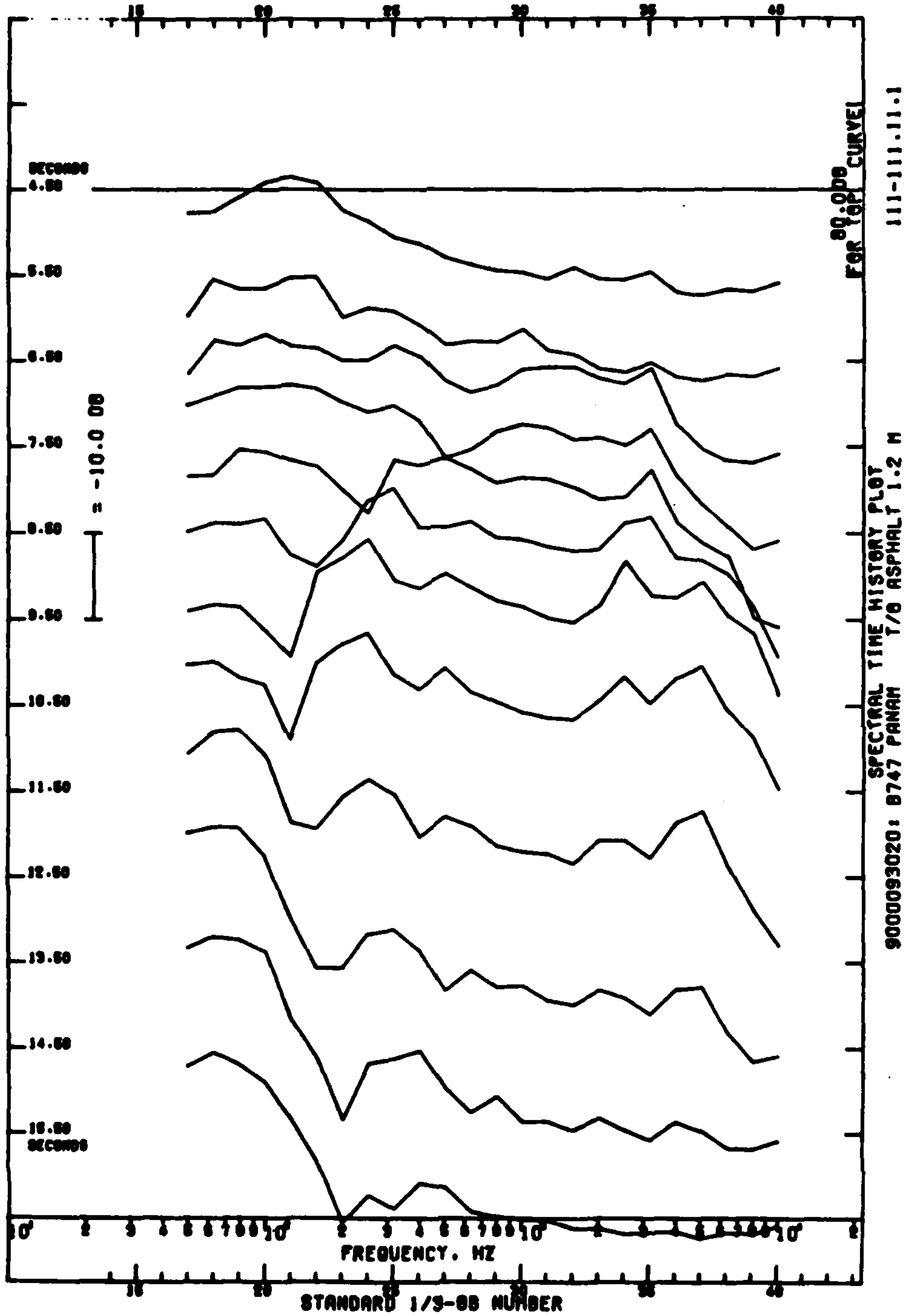

SECONDS
4.50
5.50
6.50
7.50
8.50
9.50
10.50
11.50
12.50
13.50
14.50
15.50
SECONDS
= -10.0 DB
80.0DB
FOR TOP CURVE
111-111.11.1
SPECTRAL TIME HISTORY PLOT
9000093020: B747 PANAM T/O ASPHALT 1.2 M
FREQUENCY, HZ
STANDARD 1/3-OB NUMBER

Figure A-V2

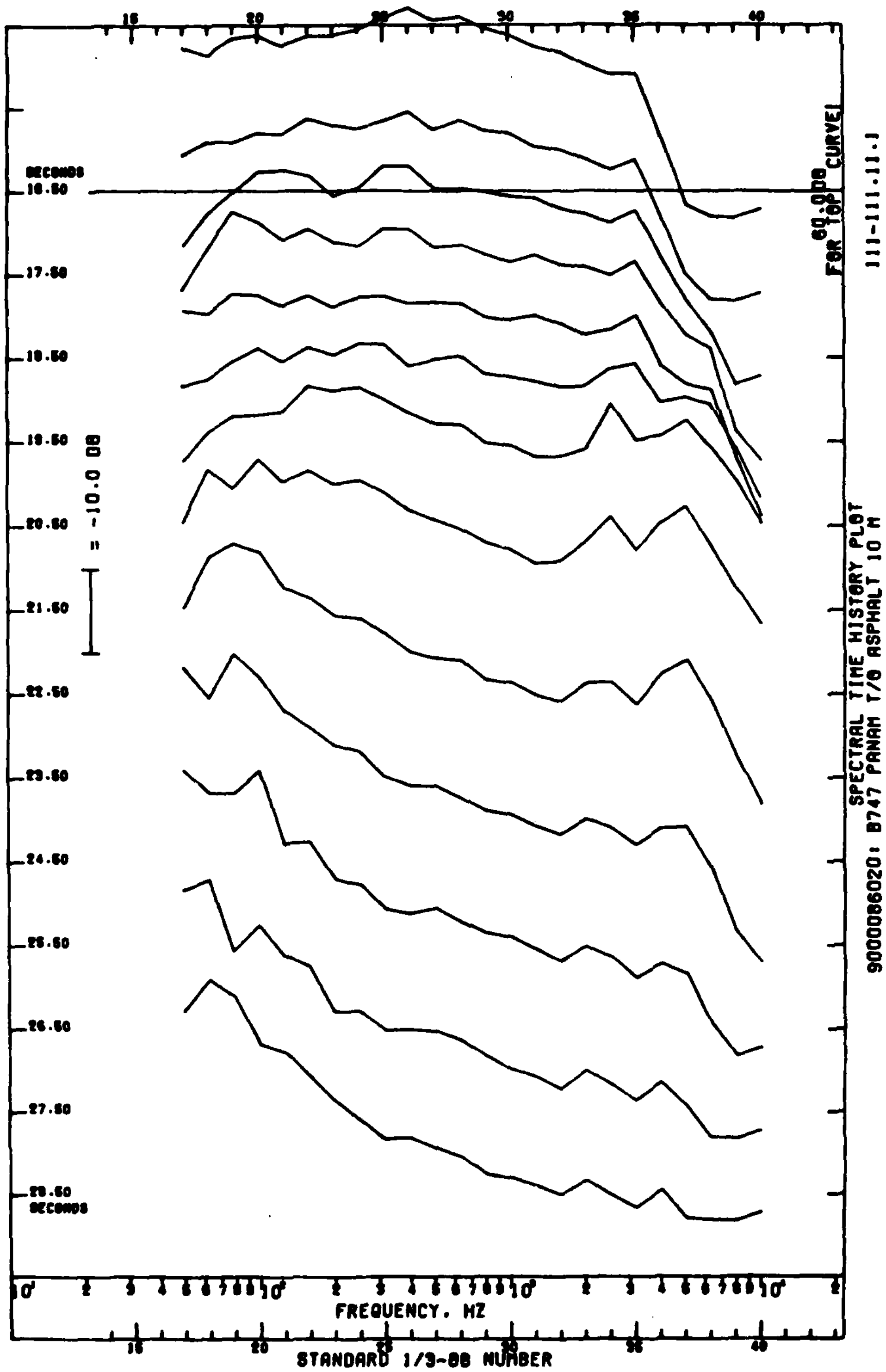
SECONDS
16.50
17.50
18.50
19.50
20.50
21.50
22.50
23.50
24.50
25.50
26.50
27.50
28.50
SECONDS
= -10.0 DB
60.0DB
FOR TOP CURVE)
111-111-11-1
SPECTRAL TIME HISTORY PLOT
9000086020: B747 PANAM T/O ASPHALT 10 M
FREQUENCY, HZ
STANDARD 1/3-OB NUMBER

Figure A-V3

APPENDIX B

SOLUTION OF AIRCRAFT EMISSION LOCATION EQUATION

In Section 2.2.2.1, "Step 3" requires the solution of the following vector equation:

$$\mathbf{A} = \mathbf{E} + \mathbf{u} M \left| \mathbf{E} \right| \tag{B-1}$$

where **E** is the unknown vector. Rewrite eq. (B-1) and decompose:

$$A_1 - E_1 = u_1 M (E_1^2 + E_2^2 + E_3^2)^{1/2} \tag{B-2}$$

$$A_2 - E_2 = u_2 M (E_1^2 + E_2^2 + E_3^2)^{1/2} \tag{B-3}$$

$$A_3 - E_3 = u_3 M (E_1^2 + E_2^2 + E_3^2)^{1/2} \tag{B-4}$$

Divide (B-2) by (B-3) and (B-4), and isolate E_2 and E_3, respectively:

$$E_2 = B_2 + E_1 u_2/u_1 \quad , \quad E_3 = B_3 + E_1 u_3/u_1$$

where:

$$B_2 = A_2 - A_1 u_2/u_1 \quad , \quad B_3 = A_3 - A_1 u_3/u_1$$

Insert this into (B-2):

$$A_1 - E_1 = U_1 M (E_1^2 + (B_2 + E_1 u_2/u_1)^2 + (B_3 + E_1 u_3/u_1)^2)^{1/2}$$

which is solved for E_1 as given in Section 1.3.2.1. In determining which sign of the square root is appropriate we are guided by the fact that the sound emission must occur in time <u>before</u> the aircraft is at the apparent location. Considering the extremely simplified case of $\mathbf{A} = (0, 0, 1)$, $\mathbf{u} = (1, 0, 0)$, then $B_2 = 0$, $B_3 = 1$, $C_1 = 0$, $C_2 = -M^2$, and:

$$E_1 = \pm M/(1-M^2)^{1/2}$$

Clearly, E_1 must be negative here to satisfy the emission precedence conditions. Conversely, had we chosen $\mathbf{u} = (-1, 0, 0)$, E_1 would have to be positive. In general, the root has the opposite sign of u_1.

APPENDIX C

CALCULATION PROCEDURE FOR A COMPLEX FUNCTION REQUIRED IN THE REFLECTION CORRECTION

Reference 24 shows that the following complex function is required in the course of evaluating the reflection effects from a finite impedance surface:

$$F(t) = 1 - \pi^{1/2}\, t\, W(it)$$

where both t and F are complex numbers and W(z) is the complex error function defined by:

$$W(z) = e^{-z^2}\, \mathrm{erfc}(-iz)$$

For small arguments t the following power series expansion for F(t) is used:

$$F(t) = 1 - \pi^{1/2}\, t\, e^{t^2} + 2\, t^2 \sum_{n=0}^{\infty} \frac{(2t^2)^n}{1 \cdot 3 \cdot 5 \ldots (2n+1)}$$

For large arguments t the following asymptotic expansion for F(t) is used:

$$F(t) \doteq -2\pi^{1/2}\, U(-\mathrm{Re}\ t)\, t e^{t^2} + (2t^2)^{-1} - 3(2t^2)^{-2} + 15(2t^2)^{-3} - + \ldots$$

U(s) denotes the unit step function which equals 0 for negative s, equals 0.5 for s = 0, and equals 1 for positive s.

A limited numerical study showed that an appropriate change-over point from the power series to the asymptotic expansion is around $|t| = 2$.

A FORTRAN function subroutine FØFT which calculates F(t) is supplied in Figure C-1. Function values calculated very close to $|t| = 2$ by the two methods described above are only approximately equal, not exactly so. There is a slight numerical discontinuity at $|t| = 2$.

```
      COMPLEX FUNCTION FOFT(*,TAU)
      COMPLEX TAU,TVE,TSQ,DELTA,SUM,T4
      EQUIVALENCE (T4,TVE)
      IF(CABS(TAU).LT.2.) GOTO 914
      TSQ=TAU*TAU
      T4=TSQ
      FOFT=(0.5,0.)/T4
      T4=T4*TSQ
      FOFT=-(0.75,0.)/T4+FOFT
      T4=T4*TSQ
      FOFT=(1.875,0.)/T4+FOFT
      IF(REAL(TAU)) 911,912,913
911   DENOM=1.
      GO TO 915
912   DENOM=0.5
915   FOFT=FOFT-DENOM*3.544908*TAU*CEXP(TSQ)
913   RETURN
914   TVE=1.
      TSQ=2.*TAU*TAU
      DENOM=1
      ODDN=1
      DELTA=TVE
      SUM=0
      ITERAT=0
920   SUM=SUM+DELTA
      ITERAT=ITERAT+1
      TEST=CABS(DELTA/SUM)
      IF(TEST.LT.5.E-5) GOTO 910
      IF(ITERAT.GT.25) GOTO 930
      TVE=TVE*TSQ
      ODDN=ODDN+2
      DENOM=DENOM*ODDN
      DELTA=TVE/DENOM
      GOTO 920
910    TSQ=TAU*TAU
      FOFT=1.-1.772454*TAU*CEXP(TSQ)+2.*TSQ*SUM
      RETURN
930   WRITE(6,940) ITERAT
940   FORMAT(I5,' ITERATION EXCEEDED IN FOFTAU CALCULATION.')
      RETURN 1
      END
```

Figure C-1. FORTRAN Function Subroutine for Calculating Values of a Function Required in the Reflection Correction.

APPENDIX D

DETAILS OF RAW DATA CLEANING PROCEDURES

Prior to calculation of momentary and single event metrics (L_A, L_S, PNL, PNLT, EPNL) the aircraft flyover noise data measured at LAX and digitized as described in Appendix A, was subjected to two processing steps: (1) smoothing each SPL across adjacent half second spectra to provide the required equipment response, and (2) correction for background ambient noise.

The instantaneous 1/2-second spectra were smoothed in the time domain according to FAR Part 36, Section A36.3(5) (Ref.29). The formula used in this study was:

$$SPL_{Smoothed,\ i} = 10 \log_{10} (0.2\ z^{SPL_{i-2}} + 0.35\ z^{SPL_{i-1}} + 0.45\ z^{SPL_i})$$

where SPL is the sound pressure level in dB in any one 1/3-octave band, i indicates the current time step (i - 1 is the previous 1/2 second, i - 2 is the previous 1 second before "i"), and z equals $10^{0.1}$.

FAR Part 36, A36.5(d) (3) (Ref.29), offers a choice of how to account for influences of ambient noise. Either up to 4 bands of any one 1/2-second spectrum may be excluded from EPNL calculations, or, SPL's in bands contaminated by ambient may be corrected under an FAA approved method. Since no formal aircraft noise certification was intended in this study, it was decided to correct the raw data (after smoothing) by a procedure detailed below. We also recognized that there exist two kinds of ambient noise, one of acoustic or electrical origin which adds to the signal of interest on an energy basis (called pre-detection or background noise), and one of instrumentation origin which occurs after the signal detection in the spectrum analyzer and does not add to the signal but simply provides an analyzer threshold below which the signal is masked out (called post-detection noise floor).

In practice, one deals with a mixture of these two different noise floor phenomena. For the LAX data from general examination of many different spectra, it was possible to assume that there exists a particular cutoff band for all

spectra below which the ambient is energy adding (pre-detection) background noise and above which the ambient is post-detection noise floor. Each 1/2-second time-smoothed spectrum ("given") was compared with and corrected for "ambient" in the following way:

- o Below the cutoff band, "ambient" is subtracted from "given" on an energy basis; however, that downward correction is limited to 10 dB.

- o In the region at and above the cutoff band, the upper tail is rolled off at a rate of 3 dB per 1/3-OB if the signal gets too close to the noise floor. "Too close" means that "given" minus "ambient" is less than 2 dB.

A computer program was coded which carries out the above corrections in the following 7-step process.

1. Compute band by band differences (in dB) by subtracting the ambient from the given. Define a band indicator array in the following way:

   a. All indicators are first set to zero;

   b. For those bands where the above calculated difference is less than or equal to a threshold, the indicator is set to one. Below the pre/post-detection cutoff band f_N the threshold is 0.457575 dB (this limits the correction in step (2) to 10 dB). Above the cutoff, the threshold is 2 dB.

2. For frequency bands below the cutoff band, and if the band indicator is 0, "ambient" is subtracted from "given" according to the energy subtraction method in order to arrive at a corrected band level:

$$\text{Corrected Level} = \text{Given} + 10 \log_{10} \left[1 - 10^{-(\text{Difference}/10)}\right]$$

3. If either all indicators are one (given is very close to ambient) or all indicators are zero (little ambient problem), no further corrective action is taken (i.e., skip steps 4 through 7).

4. Starting at the lower end of the spectrum, a search is made for each occurrence of a one indicator for all bands below the cutoff band f_N.

5. Set the band level in each band found in step (4) to 10 dB below the given level.

6. Starting at the upper end of the spectrum and proceeding backwards, a search is made for the first occurrence of a zero indicator. If the highest band already has a zero indicator the next step (7) is skipped.

7. Set the level in the band just above the one found in step (6) to 3 dB below the level of the latter. Repeat this 3 dB per 1/3-octave band rolloff procedure up to the highest band.

Figures D-1 and D-2 show a spectral time history at two steps in the data cleaning process: raw data (D-1), and after smoothing and correcting for ambient (D-2).

In most cases, we were able to use the first spectrum of each flyover noise data set as the ambient as the aircraft was far enough away at that time. When this was not the case, an ambient spectrum from another noise data set was substituted making sure that microphone location (ground, 1.2 m, pole) and data channel and approximate time of day were the same.

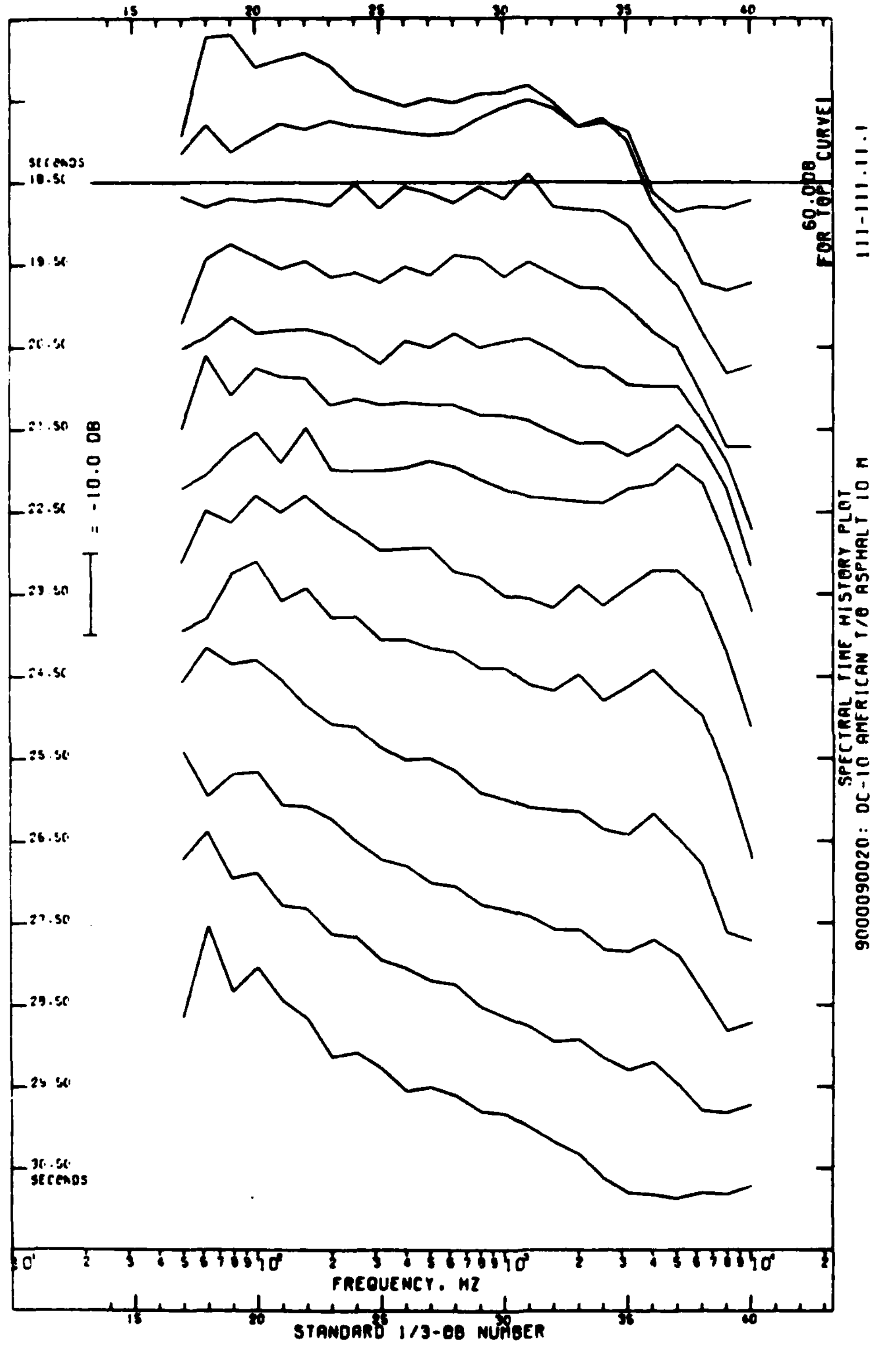

Figure D-1. Spectral Time History of Dataset 9000090020, "Raw" Data.

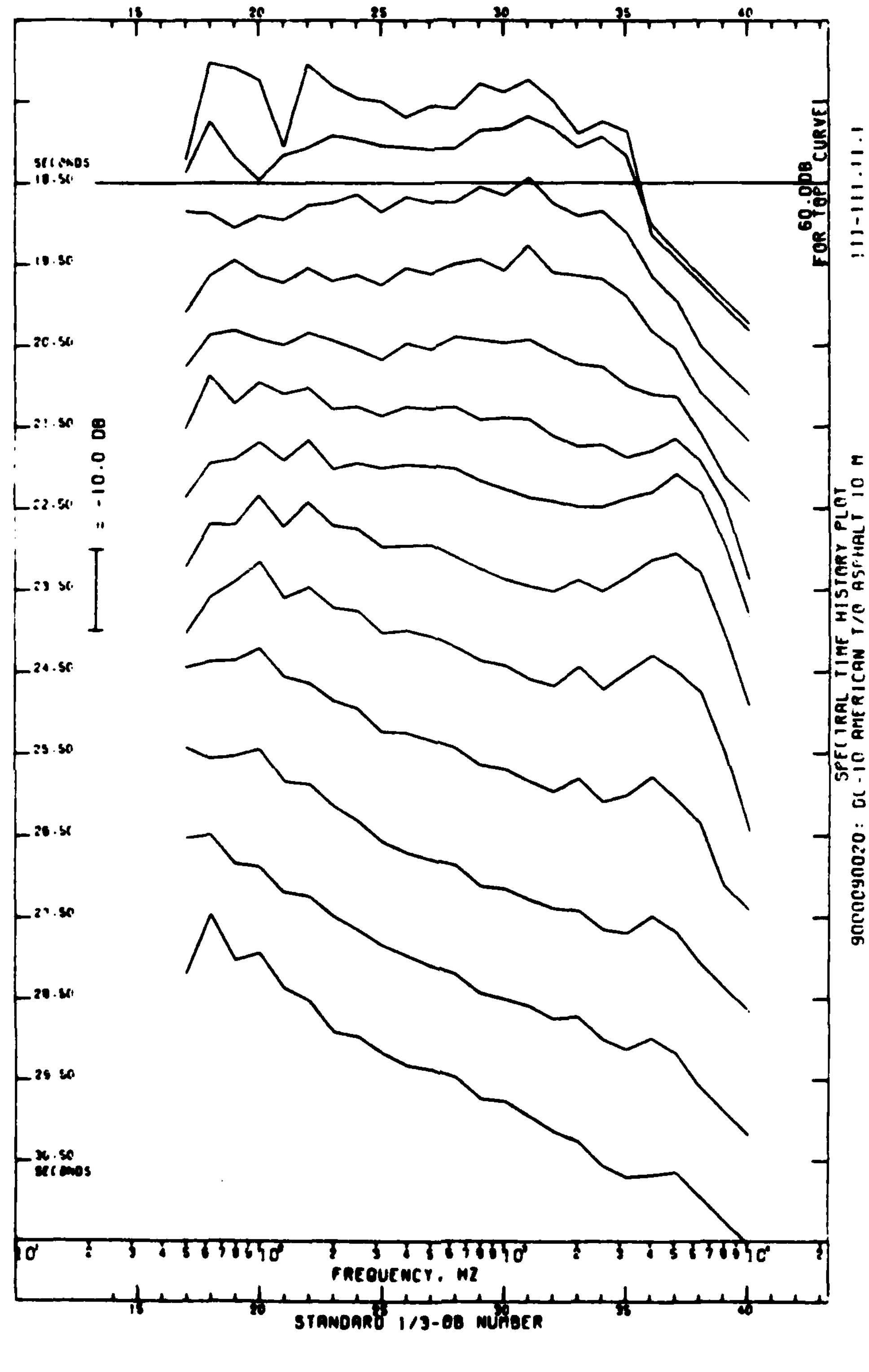

Figure D-2. Spectral Time History of Dataset 9000010020, After Smoothing and Correcting for Ambient.